Building a functional lymphatic network: A novel role for Reelin in collecting lymphatic vessel development

Sophie Clair Fforde Lutter

University College London

and

Cancer Research UK London Research Institute

PhD Supervisor: Taija Mäkinen

A thesis submitted for the degree of

Doctor of Philosophy

University College London

October 2011

Declaration

I Sophie Clair Fforde Lutter confirm that the work presented in this thesis is my own. Where information has been derived from other sources, I confirm that this has been indicated in the thesis.

Abstract

The mature lymphatic vasculature consists of two distinct vessel types, lymphatic capillaries and collecting lymphatic vessels, which have distinct functions in the uptake and transport of lymph respectively. However, despite the functional importance of these two vessel types, much remains unknown about the processes involved in remodelling the initially uniform lymphatic plexus into a functional hierarchy of mature vessels, and particularly the role of smooth muscle cells and the extracellular matrix in this process and in the subsequent function of collecting lymphatic vessels. Here we have identified Reelin, an extracellular matrix protein whose previous characterisation has remained largely confined to the central nervous system, as required for correct development and function of collecting lymphatic vessels. In the absence of Reelin, collecting vessels are enlarged, with a reduction in smooth muscle cell coverage and a concomitant failure to down-regulate expression of the capillary marker, LYVE-1. Unexpectedly, the canonical Reelin receptors ApoER2 and VLDLR were dispensable for normal lymphatic development, suggesting the involvement of alternative receptor(s). We have also uncovered a previously un-described mechanism for activation of Reelin signalling via interactions between smooth muscle cells and lymphatic endothelial cells, and have shown that the latter increase expression of the smooth muscle cell recruitment factor, *MCP1*, upon stimulation by Reelin. This work highlights the largely unexplored importance of the extracellular matrix for correct lymphatic development and function, emphasises the importance of interactions between the lymphatic endothelium and surrounding smooth muscle cells in propagating vessel development and emphasises the hitherto unrecognised importance of smooth muscle cells for lymphatic vessel morphogenesis and function.

Acknowledgement

I am wary of beginning this chapter with a cliché, in case it sounds less than genuine. Unfortunately, I can't think of a better way to express my heartfelt gratitude to the people who have helped me to accomplish this task, so I shall have to take the risk and trust that you will see the truth through the formulaic phrases. There really are a great many people without whom this wouldn't have been possible. Firstly, of course, is Taija. Thank you. Not only for your scientific help, guidance and expertise, which has been constant and invaluable, but also for your continued support and patience and for always seeing a way through, and a way to inspire and motivate even when things have seemed most impossible.

Thank you also to my thesis committee, Holger Gerhardt and Julian Lewis, who have not only provided useful suggestions but also interesting discussion over the years.

Of course, life in the lab hasn't been all about the PhD and everyone in the Lymphatic Development Lab deserves a great deal of thanks, both for the freely given scientific help and advice, and also for creating such a positive and friendly working atmosphere. In particular, Eleni has always been a voice of wisdom and calm amidst the chaos, although I am certain that she won't agree with me about that! Elenita, I have often sought and always valued your advice and friendship throughout these last four years, and I am sure that that will never change.

Throughout our studies, Anna, Caroline, Denise and Vanni have supplied a constant stream of comfort, laughter, gossip and adventure and I am very grateful for all the fun we've had. Vanni, I hope that you will continue to share your secrets and stories with me, safe in the knowledge that the 'colander' will never leak – at least not further than the other members of the 'coven', as you have so charmingly been known to call us! Caroline and Anna, my fellow coven members, although I know none of us are certain what new and exciting directions we will move in from here, I have no doubt that your futures will be bright and glittering. It is odd to imagine that we won't always see each other every day, but I know that our friendship will travel as far as we do. Denise, I was

so sad when you left to return to Germany, and yet am so happy that it hasn't changed a thing. I can't think of anyone I would rather be lost in a forest on top of a mountain in a thunderstorm, or taught to salsa in a stranger's living room in the depths of Cuba with than you! May the adventures long continue!

Just as life in the lab wasn't always about the PhD, so the PhD didn't always seem to stay in the lab! So thank you to Bella, my wonderful housemate, whose love of her cats has kept my own sanity firmly in perspective over the last year or so! In all seriousness, I can't believe that we have lived together for such a long time now. Thank you for introducing me to Jo and Kat and some other truly fabulous friends. Getting to know and love you all has been a brilliant experience and I wouldn't change a thing. Ellie, we have come a long way since the first day of college and although there is in general less fancy dress involved now, nothing has really changed… you have always known when a tub of Ben & Jerry's and a 'Matt Damon Day' has been required! Thank you and also Sian, Laura, Andrea and Daj for being such good friends for so many years.

Finally, thank you to the people I really could not have come so far without; Mum, Dad, Philly and Chris. Your love and support means the world to me. You've always been there with a phone call, a smile and a hug through the laughter and the tears. Knowing that you would be there, no matter what the outcome, has helped more than anything to me keep me pushing forward, and will continue to do so into whatever new adventures await me in the future.

So really, this thesis does not represent my achievement. It has been a truly team effort throughout and I hope that you can all appreciate the contributions you have made to its completion as much as I do.

Table of Contents

Table of figures

List of tables

Abbreviations

4-OHT	4-Hydroxytamoxifen
Ang	Angiopoietin
ApoE	Apolipoprotein E
ApoER2/Lrp8	Apolipoprotein E Receptor 2
αSMA	alpha Smooth Muscle Actin
BEC	Blood vascular Endothelial Cell(s)
BM	Basement Membrane
CCL21	Chemokine (C-C motif) ligand 21
CCR7	C-C Chemokine Receptor type 7
CLEC2	C-type lectin-like receptor 2
Coup-TFII	Coup Transcription Factor 2
Cx	Connexin
Dab1	Disabled 1
DC	Dendritic Cell
E	Embryonic day
EC	Endothelial Cell
ECM	Extracellular Matrix
EGF/EGFR	Epidermal Growth Factor/EGF Receptor

ER	Endoplasmic Reticulum
FITC	Fluorescein isothiocyanate
FoxC2	Forkhead box protein C2
HA	Hyaluronan
HB-EGF	Heparin-binding EGF-like Growth Factor
HSPG	Heparan Sulfate Proteoglycan
IP	Intraperitoneal
Itg	Integrin
LEC	Lymphatic Endothelial Cell(s)
LYVE-1	Lymphatic vessel endothelial hyaluronan receptor
MC	Mural Cell(s)
MCP-1/CCL2	Monocyte Chemotactic Protein 1
MMP	Matrix Metalloproteinase
NG2	Chondroitin Sulfate Proteoglycan 4
NO	Nitric Oxide
Nrp2	Neuropilin 2
P	Postnatal day
PDGF/PDGFR	Platelet Derived Growth Factor/PDGF Receptor
Pdpn	Podoplanin

PECAM-1/CD31	Platelet/Endothelial Cell Adhesion Molecule 1
Prox1	Prospero homeobox protein 1
Reln	Reelin
siRNA	Small interferance Ribonucleic Acid
SFK	Src Family Kinases
SMC/vSMC	Smooth Muscle Cell(s)/Vascular SMC
Slp76	Lymphocyte cytosolic protein 2
Syk	Spleen tyrosine Kinase
TGFβ	Transforming Growth Factor beta
TIMP	Tissue Inhibitor of Metalloproteinase
VE-Cadherin	Vascular Endothelial Cadherin
VEGF/VEGFR	Vascular Endothelial Growth Factor/VEGF Receptor
VLDLR	Very Low Density Lipoprotein Receptor

Chapter 1. Introduction

1.1 Functions and associated pathology of the lymphatic vasculature

1.1.1 Discovery of the lymphatic system

The lymphatic system is a network of vessels and organs that grows alongside the blood vasculature and is found in all vascularised tissue, except the central nervous system and bone marrow (Figure 1.1). The term '*lymphaticus*', derived from the latin meaning 'distracted and confused' was first used to refer to the lymphatic system in the 17th Century, and was an apt description of the understanding of lymphatic biology to date.

The ancient Greeks first described structures filled with colourless fluid, which Hippocrates termed 'white blood', but they were unsure what they were describing, so it wasn't until Gasparo Aselli observed white fluid-filled vessels, which he called '*lacteis venis*' or 'milky veins', in the mesentery of a well-fed dog in 1622 that the lymphatic system was truly discovered. His mistaken belief that lymphatic fluid flowed into the liver where it was converted to blood was not corrected until Jean Pecquet described the entry of the thoracic duct into the veins in 1651 and gave the first correct description of the route of lymphatic fluid into the blood. In 1653, Olaus Rudbeck and Thomas Bartholin independently described the presence of lymphatic vessels throughout the body and hypothesised their involvement in movement of fluid filtered from the blood. It was then nearly another hundred years before William Hunter and his students proposed that the lymphatic vessels acted as absorbing vessels throughout the body (Witte et al., 1997, Skobe and Detmar, 2000).

The first true insight into the fine structure of lymphatic vessels came from von Recklinghausen in 1862, who discovered that lymphatic vessel walls comprised a single

layer of endothelial cells, whose borders stained black with silver nitrate. He was thus able to disprove the prevailing hypothesis that lymph moved into the blood vessels via fine tubular structures and instead proposed that interstitial fluid flowed into 'open-ended' lymphatic capillaries. The major breakthrough in understanding lymph formation and lymphatic flow arose from Earnest Starling in 1896, whose experiments showed that lymph formed from the blood by filtration and that 'transcapillary exchange' depended on the balance of blood capillary and tissue hydrostatic pressure. Starling also made the key observation that oedema was the result of imbalanced lymph formation and absorption (Skobe and Detmar, 2000, Witte et al., 1997). An interesting new insight into regulation of tissue fluid volume and lymphatic function suggests that it is not only the difference in volume, but also in tonicity (ratio of Na^+ and K^+ to water) of interstitial fluid that affects homeostasis (Machnik et al., 2009). Furthermore, macrophages play a key role in this system, by releasing the lymphatic chemokine VEGF-C to act as an osmoprotective protein, maintaining interstitial volume via increased lymphangiogenesis (Machnik et al., 2009).

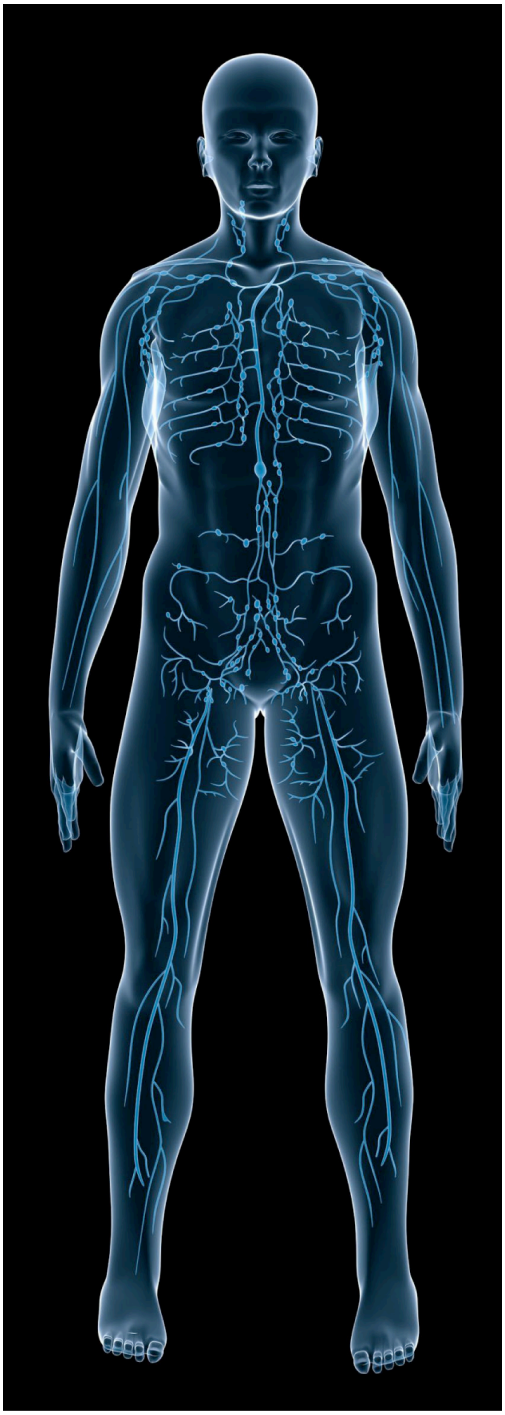

Figure 1.1 The human lymphatic system.
The lymphatic system is a network of vessels and organs that grows into all vascularised tissue, except the central nervous system and bone marrow. Image purchased from www.123rf.com.

1.1.2 Maintenance of tissue homeostasis

Maintenance of the body's tissue fluid balance is an extremely important function of the lymphatic vasculature. Blood pressure causes water, proteins and other macromolecules to escape from the blood capillaries. Over the course of a day, 50% of the circulating protein leaks from the capillaries and cannot be directly reabsorbed (Skobe and Detmar, 2000). The major function of the lymphatic vasculature is to collect this interstitial fluid, part of which is also taken up by post-capillary venules, and return it to the blood vasculature via lympho-venous connections, the main example of which is between the thoracic duct and the junction between the left subclavian and internal jugular veins. This is the drainage route of lymph from the left side of the body, abdomen and lower limbs. The right lymphatic trunk returns lymph from the right upper arm, thorax and head to the right subclavian vein (Tammela and Alitalo, 2010). Additional lympho-venous connections occur in the renal, hepatic and adrenal veins as well as other peripheral locations (Alitalo et al., 2005). Estimates of total post-nodal lymph flow have reached as high as 4 litres/day in humans, which is increased to around 8 litres when the volume of fluid absorbed by lymph node microvessels is also taken into account (Levick and Michel, 2010). This huge fluid turnover is critical for maintenance of plasma volume and to avoid an increase in tissue pressure. Moreover, efficient drainage of interstitial fluid ensures adequate cell nutrition by minimising distances between cells and capillaries (Skobe and Detmar, 2000).

Interestingly, it seems likely that the major function of the lymphatic vasculature can also be a driving force for its formation. A sophisticated tail skin wound model, in which the dermis is removed to arrest lymphatic flow and collagen is injected under a silicon sleeve to act as a bridge for interstitial flow, revealed that directional movement of interstitial fluid precedes lymphangiogenesis and that newly forming lymphatic vessels grow in the direction of flow (Boardman and Swartz, 2003). Furthermore, arresting flow by allowing interstitial fluid to circumvent the wound area prevented lymphangiogenesis, suggesting that flow is in fact necessary for lymphatic vessel formation, at least in adult skin (Rutkowski et al., 2006).

1.1.3 Immune surveillance

Dendritic cells (DCs) act as the 'sentinels' of the immune system. They reside in peripheral tissues and upon encountering foreign antigens, traffic back to the lymph nodes via lymphatic vessels, where they are optimally positioned to encounter naïve or memory T cells and thus activate a specific immune response (Randolph et al., 2005). For a long time, DC entry and passage through the lymphatic vessels was viewed as a passive process, where the lymphatic vasculature was simply a conduit through which dendritic cells travelled. While the presence of erythrocytes and a large number of neutrophils in the afferent lymph following contact elicitation (an inflammatory immune reaction at the site of a second (or subsequent) contact with a sensitizing antigen) suggests that some non-specific or passive uptake into the lymphatic vessels can occur, an increasing body of research has revealed an active role for the lymphatic endothelium in interacting with DCs and mediating their entry into the lymphatic capillaries (Randolph et al., 2005, Jurisic and Detmar, 2009).

The discovery that the chemokine receptor CCR7 is required both in homeostatic and inflammatory conditions for DC entrance to lymphatic vessels was a first indication that DC entry into afferent lymph was not a passive process, consistent with the observation that CCL21, a ligand for CCR7, is expressed in the lymphatic endothelium (Ohl et al., 2004). Shear stress is also an important regulator of DC transmigration, as high transmural flow increased LEC expression of CCL21 as well as the leukocyte adhesion molecules ICAM-1 and E-selectin both *in vitro* and *in vivo*, thus enhancing DC transmigration. In lymphoedema conditions, when flow is greatly decreased, LEC expression of CCL21 (and therefore DC transmigration) is also diminished (Miteva et al., 2010).

Pflicke and colleagues demonstrated through sophisticated explant culture and microscopy techniques that the basement membrane (BM) of the lymphatic capillaries was discontinuous and organised into pre-formed 'portals' through which DCs migrated in an integrin-independent manner. These portals were still present in *CCR7*$^{-/-}$ mice, even though DC were incapable of migrating through, indicating that it is not the DC,

but the lymphatic endothelium itself that mediates organisation of the BM in such a way as to allow transmigration of immune cells (Pflicke and Sixt, 2009). Studies of *Plexin-A1*$^{-/-}$ mice and transplant of wild type DCs into *Sema3A*$^{-/-}$ mice elicited two more molecules indispensable for DC entrance to the lymphatics, and suggested a mechanism by which the lymphatic endothelium actively participates in DC transmigration. LEC-derived Sema 3A interacts with its receptor Plexin-A1, which is expressed on the rear side of the dendritic cell. This promotes acto-myosin contraction by phosphorylation of the myosin light chain, and allows the DC to squeeze through the narrow gap in the lymphatic BM and between the LEC to enter the afferent lymph (Takamatsu et al., 2010).

1.1.4 Dietary fat absorption

Since Aselli discovered the lymphatic vessels in the mesentery of a well-fed dog in the 17th Century, lymphatic function in absorption of dietary fat has been documented. Enterocytes in the small intestine assemble lipid-rich, water-soluble complexes called chylomicrons, which are absorbed by lacteals (intestinal lymphatics) and constitute up to 15% of lymph volume after ingestion of a fat-containing meal (Jurisic and Detmar, 2009, Wang and Oliver, 2010). There is evidence suggesting a link between lymphatic function and fat absorption/deposition, for example the transformation of chronic oedema following breast cancer surgery from accumulation of lymph fluid to excess deposition of subcutaneous adipose tissue (Brorson et al., 2006) and decreased lymphatic function in patients suffering from lipidema (reviewed in (Wang and Oliver, 2010)). However, the role of the lymphatic vasculature in fat metabolism is not yet well understood.

The homeobox transcription factor Prox1 is an essential regulator of lymphatic development, and, as will be discussed in more detail below, its loss is incompatible with life (Wigle and Oliver, 1999). In 2005, Harvey and colleagues showed that surviving *Prox1*$^{+/-}$ mice developed adult-onset obesity, despite no changes in exercise or

eating habits (Harvey et al., 2005). However, *Prox1*$^{+/-}$ mice did display abnormal patterning and function of lymphatic vessels, especially in the mesentery, and the severity of lymphatic abnormalities correlated with the degree of obesity. The authors also went on to show that culturing pre-adipocytes with chyle from the thoracic cavity of *Prox1*$^{+/-}$ newborns increased adipogenesis, thereby suggesting a mechanism by which lymph leaking from malfunctioning lymphatic vessels could promote local adipogenesis and eventually result in obesity (Harvey et al., 2005).

Interestingly, a recent study demonstrated that hypocholesterolemia, resulting from *ApoE* deficiency, causes destruction of previously functioning lymphatic vessels (Lim et al., 2009). This suggests that the link between lymphatic function and fat metabolism is not linear, and leads to the possible conclusion of an increasingly devastating feedback loop in which hypercholesterolemia can cause lymphatic vessel malfunction, and in turn lymph leakage from damaged lymphatic vessels can increase adipogenesis. Further research into the mechanisms of fat absorption into lymphatic vessels and whether lymphatic defects can cause any human obesity syndromes is required to help us further understand the role of the lymphatics in metabolism of dietary fat (Jurisic and Detmar, 2009, Wang and Oliver, 2010).

A summary of lymphatic function is given in Figure 1.2

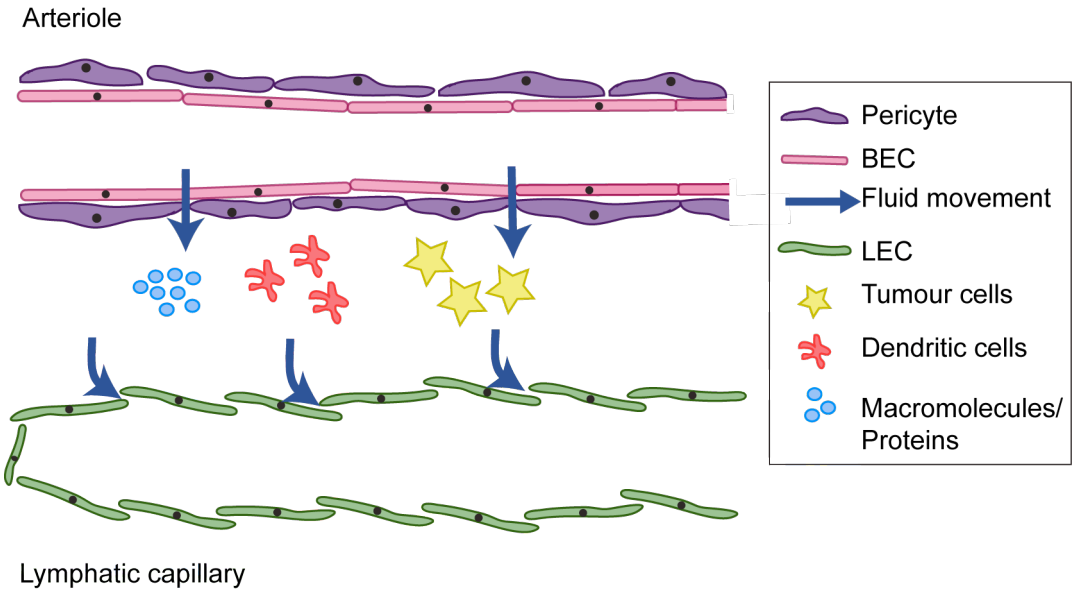

Figure 1.2 Function of the lymphatic vasculature.
Fluid is extravasated from the blood vasculature due to high pressure and accumulates in the interstitium. From here, it enters the lymphatic capillaries through the over-lapping cell-junctions of the blind-ended lymphatic capillaries, along with proteins and other macromolecules, antigen presenting cells and cancer cells undergoing metastasis.

1.1.5 Lymphoedema

Failures in lymphatic development or function can result in lymphoedema, which although rarely life-threatening, is disfiguring and disabling and can lead to social or psychological disorders. Lymphoedema results from an imbalance in lymph formation and absorption and is characterised by swelling of the limbs, tissue fibrosis, accumulation of subcutaneous fat and increased susceptibility to infection (Wang and Oliver, 2010, Jurisic and Detmar, 2009, Rockson, 2001). Lymphoedema can either be inherited (primary lymphoedema) or caused by traumas due to surgery, infection or radiation therapy (secondary lymphoedema) (Alitalo et al., 2005). Although some headway has been made in pre-clinical studies of curative therapies (Karkkainen et al., 2001, Tammela et al., 2007), as yet available treatments still aim to manage the symptoms, rather than solve the problem, for example, by manual drainage, massage,

compression garments, liposuction and dietary modification (Rockson, 2001, Wang and Oliver, 2010, Brorson et al., 2006).

1.1.5.1 Primary Lymphoedema

Primary, or congenital, lymphoedema is a heterogeneous disease that is often seen in conjunction with other problems, as one symptom of a more complex syndrome. Mutations responsible for congenital lymphoedema in a number of human diseases have been identified, and mouse models of these mutations have been essential to understand its underlying causes. However, since many of the genes involved are also important for lymphatic development, these will be discussed in more detail below and this section will concentrate on human disease.

Heterozygous mutations in the tyrosine kinase domain of *VEGFR3* have been found in a number of families with Milroy's disease, in which functional failure and, probably to a lesser extent, hypoplasia of the lymphatic capillaries leads to lymphoedema (Mellor et al., 2010), (Karkkainen et al., 2000), (reviewed in (Wang and Oliver, 2010, Alitalo et al., 2005)).

Mutations in *FOXC2* have also been linked to human lymphatic disease; in this case lymphoedema-distichiasis (LD), which is characterised by a double row of eyelashes (distichiasis) and bilateral lower limb lymphoedema (Fang et al., 2000). Interestingly, skin biopsies of human LD patients revealed that while there was abnormal SMC recruitment to lymphatic capillaries in the skin of the swollen oedematous feet, the vessels of the unaffected forearms remained normal (Petrova et al., 2004). Furthermore, a recent study of lymphatic function in LD patients with a *FOXC2* mutation revealed that lymphatic function in the swollen foot was dependant on gravity, suggesting that a genetic predisposition to lymphatic abnormality might have an anatomical trigger (Mellor et al., 2011).

Other lymphoedema syndromes that have been linked to specific mutations include Hypotrichosis-lymphoedema-telengiectasia (HLTS), a rare disease linked to mutations in the transcription factor SOX18 (Irrthum et al., 2003) and Hennekam syndrome, which is characterised by mental retardation, limb lymphoedema, intestinal lymphangiectasias and facial abnormalities and is caused by mutations in *CCBE1*, which encodes Collagen and Calcium-Binding EGF-domain-1, a secreted protein essential for lymphatic development in zebrafish (Alders et al., 2009), (Hogan et al., 2009). Finally, mutations in *GJC2*, which encodes the gap junction protein Connexin 47 have recently been found in several families with inherited lymphoedema. This may be due to disrupted lymphatic flow, resulting from gap junction abnormalities (Ferrell et al., 2010).

1.1.5.2 Secondary Lymphoedema

The leading cause of secondary lymphoedema in the developing world is filariasis, more commonly known as elephantiasis. This is a parasitic infection of the lymphatic vessels by *Wuchereria bancrofti* or *Brugia malayi* worms, transmitted by mosquito bites (Alitalo et al., 2005). An inflammatory reaction that triggers production of VEGF, VEGF-C and VEGF-D leads to hyperplasia and severe damage to the lymphatic vasculature. This leads to chronic lymphoedema of the lower limbs or genitalia (reviewed in (Wang and Oliver, 2010, Rockson, 2001)). In industrialised nations, the leading cause of secondary lymphoedema is damage to lymphatic vessels and removal of lymph nodes after breast cancer surgery or radiation therapy. It has been estimated that around 20% of women develop the condition after breast cancer surgery (Jurisic and Detmar, 2009, Wang and Oliver, 2010). While some success has been reported in long-term management of post-operative lymphoedema with liposuction (Brorson et al., 2006), treatments aiming to repair the damaged lymphatic vasculature are still a long way from the clinic. Promising pre-clinical data however, suggests that a solution may be on the horizon. Application of VEGF-C after lymph node removal promoted the development of new, functional lymphatic vessels in mice, which lead to a

corresponding reduction in oedema. Furthermore, VEGF-C aided the incorporation of transplanted lymph nodes into the existing vasculature, which again improved lymphatic drainage (Tammela et al., 2007).

Increasing understanding of the underlying causes of congenital lymphoedema and forays into novel treatment strategies means that we can hopefully look forward to the development of curative, rather than management, treatment strategies for lymphoedema in the future.

1.1.6 Inflammation

The role of the lymphatic system in immune surveillance has been discussed above, but the consequences of inflammation-induced lymphangiogenesis are mixed. During inflammation, inflammatory cells and macrophages express VEGF-C, which promotes lymphangiogenesis (Baluk et al., 2005, Kerjaschki et al., 2004). Furthermore, a number of studies have also shown evidence for incorporation of LEC progenitors, believed to be macrophages or other bone-marrow derived cells, into lymphatic vessels under inflammatory or tumour conditions and that these cells are capable of stimulating *de novo* lymphangiogenesis.

Maruyama and colleagues demonstrated direct incorporation of cells co-expressing the macrophage marker CD11b with lymphatic endothelial markers Prox1 and LYVE-1 in the walls of newly generated lymphatic vessels in the inflamed corneal stroma. These vessels were not continuous with the limbal lymphatic vessels, suggesting that innate immune cells contributed to pathological lymphvasculogenesis, rather than incorporating into sprouts growing from existing vessels. Furthermore, macrophage depletion by application of clodronate liposomes prevented $CD11b^+$ macrophage infiltration and lymphangiogenesis in the stroma, providing compelling evidence for the importance of these cells in pathological lymphangiogenesis (Maruyama et al., 2005). Furthermore, in studies of renal transplant rejection, 4.5% of $Prox1^+$ LECs, which

accounted for 12.9% of the lymphatic vessels in female-donor kidney transplants, were found to derive from male recipient LEC progenitors (Kerjaschki et al., 2006). Recent work has aimed to more completely characterise the phenotype of bone marrow derived LEC progenitors and assess their role in lymphangiogenesis. Lee and colleagues demonstrated that culturing bone marrow derived cells with lymphangiogenic cytokines lead to up-regulation of LEC markers including Prox1, LYVE-1, Podoplanin, VEGFR-3 and Foxc2, while still expressing the macrophage marker CD11b (Lee et al., 2010). Over time in culture, these cells lost hematopoietic identity, but maintained expression of LEC markers, and furthermore could contribute to lymphatic neovascularisation *in vivo* under pathological conditions, thus providing important evidence for the involvement of bone marrow derived cells in pathological lymphangiogenesis (Lee et al., 2010). However, it is important to note that bone marrow derived cells do not contribute to lymphangiogenesis in all pathological conditions. For example, studies of tumour-induced lymphangiogenesis found that new vessels sprouted from the preexisting lymphatic endothelium with no contribution from bone marrow derived cells (He et al., 2004).

Increased lymphangiogenesis during infection promotes removal of fluid, chemokines and leukocytes from the site of inflammation, the importance of which was demonstrated by blocking VEGF-C signalling using soluble VEGFR-3-IgG during *Mycoplasma pulmonis* infection, which resulted in accumulation of fluid and leukocytes and mucosal oedema (Baluk et al., 2005). However, increased lymphangiogenesis also promotes immune cell trafficking to the lymph nodes and may support the formation of an inflammatory loop, for example CCL21 on new lymphatic vessels attracts CCR7-positive dendritic cells, which may promote the inflammatory reaction that leads to renal transplant rejection (Kerjaschki et al., 2004, Jurisic and Detmar, 2009). Increased lymphatic vessel density is also a feature of inflammatory bowel disease (Rahier et al., 2011), but whether this is protective or pathological is unclear. While increased lymphatic vessels clear cytokines and immune cells and may act to 'balance' increased inflammatory angiogenesis, increased lymphatic remodelling or obstruction causes a build-up of cytokines and immune cells and can recapitulate the symptoms of inflammatory bowel disease (reviewed in (Alexander et al., 2010)). Likewise, treatment of a mouse model of psoriasis with a VEGFR-3 tyrosine kinase inhibitor resolved

inflammation by reducing the number of inflammation associated blood and lymphatic vessels, suggesting that again in this situation, lymphangiogenesis is pathological, rather than protective (Halin et al., 2008).

1.1.7 Metastasis

The lymphatic vessels provide a crucial route for tumour cell metastasis. Once tumour cells reach the lymph node, they can disseminate to distal sites in the body and become secondary tumours, the prognosis for which is often poor. There is still some question as to the mechanism, or purpose, of lymph node metastasis. The lymph node could be 'trapping' the tumour cells, leading to a lag phase in dissemination, or the presence of tumour cells in the lymph node could simply be evidence of metastatic potential; tumour cells are found in the lymph nodes while in transit around the body. Alternatively, the lymph nodes could be a site for tumour cell amplification, promoting their metastatic spread (Tammela and Alitalo, 2010). Regardless, the extent of lymph node metastasis is an important determinant for the staging and prognosis of most human malignancies, and in some cases determines or guides treatment options (Tobler and Detmar, 2006).

Over-expression of VEGF-C in breast cancer cells increases intratumoural lymphangiogenesis, and the presence of tumour cells within these lymphatic vessels suggests functionality (Skobe et al., 2001), however there is suggestion that intratumoural lymphatic vessels may collapse under the high pressure inside the tumour, so may not be useful for enhanced metastasis (Alitalo et al., 2005). Despite this, Skobe and colleagues found increased lymph node and lung metastases in VEGF-C over-expressing tumours and in the case of lung metastasis, saw strong positive correlation between the density of lymphatic vessels within the tumour, and the lung area covered by metastases (Skobe et al., 2001). Similarly, crossing a mouse line that over-expresses VEGF-C in β cells of the endocrine pancreas with mice that develop non-lymphangiogenic, non-metastatic tumours in the same tissue, induced the onset of both

lymphangiogenesis and metastasis, strongly indicating a causal relationship between VEGF-C, lymphangiogenesis and lymph node metastasis (Mandriota et al., 2001). Increased tumour associated lymphangiogenesis has also been observed in mice that over-express VEGF-C in the skin (Hirakawa et al., 2007). VEGF-C expressing tumours developed enhanced lymphatic vessel networks in the lymph nodes even prior to metastasis, suggesting that the tumour can regulate lymphangiogenesis at a distance, thus paving the way for further tumour cell dissemination. In support of this hypothesis, increased lung and distant lymph node metastasis were observed in mice over-expressing VEGF-C in the skin (Hirakawa et al., 2007). Indeed, VEGF-C and VEGF-D expression can be considered useful prognostic indicators, as clinical data suggests that their expression in a number of tumour types is highly correlated with lymphangiogenesis and lymph node metastasis (Feng et al., 2010, Liu et al., 2008). Furthermore, blocking VEGF-C/VEGF-D signalling by inhibiting VEGFR-3 can prevent increased lymphangiogenesis and also lymph node metastasis in several different tumour models (He et al., 2002, Karpanen et al., 2001, Zhang et al., 2010a, Yang et al., 2011, Padera et al., 2008).

Other studies suggest that the correlation between tumour-expressed VEGF-C and lymphatic metastasis is unlikely to be solely due to increased lymphangiogenesis. Using high resolution imaging, Tammela and colleagues observed that VEGF-C induced lymphatic sprouting resulted in 'leaky' lymphatic vessels that had intercellular gaps in the endothelial monolayer, which could potentially facilitate tumour cell invasion (Tammela et al., 2007). More recently, a series of 3-dimensional cell culture assays demonstrated that VEGF-C over-expression in tumour cells increased their chemoattraction to LEC (Issa et al., 2009). This occurred predominantly via VEGFR-3 dependant up-regulation of CCL21 in LEC, which attracted tumour cells to the lymphatic vessels via its receptor, CCR7. Additionally, autocrine VEGF-C-stimulated VEGFR-3 phosphorylation in tumour cells resulted in increased proteolytic activity and motility through a 3 dimensional matrix, demonstrating increased tumour cell invasiveness (Issa et al., 2009). Notably, while LEC-derived CCL21 promotes tumour cell chemotaxis towards lymphatic vessels, interstitial flow also synergistically enhances tumour cell chemotaxis towards the lymphatic endothelium via autocrine CCL7/CCL21 signalling (Shields et al., 2007). Furthermore, the mode of tumour cell

migration may influence its metastatic spread, for example single cell migration is required for blood-borne metastasis and requires TGFβ signalling, while in the absence of TGFβ tumour cells migrate collectively, in which state they are more likely to spread via the lymphatic vasculature (Giampieri et al., 2009).

1.2 Development of the lymphatic vasculature

Most evidence to date supports the model of mammalian lymphatic development first proposed by Florence Sabin in the early 20th Century. By making detailed anatomical observations after ink injection into pig embryos, she proposed that the lymphatic vasculature sprouted from the cardinal veins (Sabin, 1902). An alternative theory proposed a few years later, following analysis of domestic cat embryos, suggested that the jugular lymphatic sacs arise after the venous network is 'surrounded' in some places by a 'secondary capillary network' and so the lymphatic endothelial cells in fact derive from mesenchymal precursors (Huntington and McClure, 1910). These studies formed the basis of the debate that has existed ever since, as to whether mesodermal progenitors contribute to mammalian developmental lymphangiogenesis.

The development of sophisticated genetic tools has enabled lineage-tracing studies, which have aimed to resolve this controversy. Expressing *Cre* recombinase under the control of *Prox1*, which is expressed only in lymphatic endothelial cells, or *Tie2*, which at the stages examined is expressed only in blood vascular endothelial cells, revealed Prox1-positive prospective LEC in the cardinal vein at E9.5. These cells subsequently sprouted from the vein to form the lymph sacs, and from there the entire lymphatic vasculature. Normal lymph sacs in *Runx1* deficient mice, which lack haematopoietic precursors, lead to the conclusion that murine lymphatics are solely venous derived and include no contribution from haematopoietic-derived cells (Srinivasan et al., 2007).

Nevertheless, the ability of bone marrow derived cells to incorporate into growing lymphatic vessels under pathological conditions in adults, as discussed above, has

contributed to the controversy surrounding the origins of the lymphatic vasculature. Furthermore, grafting quail somites into chick embryos and analysing the lymphatic vasculature using a quail-specific antibody, indicates that the somitic mesoderm of the avian wing bud can differentiate into lymphatic endothelium (Wilting et al., 2000). In addition, $Prox1^{+}$ lymphangioblasts, which share a common origin with angioblasts, have been identified in *Xenopus* tadpoles (Ny et al., 2005), (reviewed in (Karpanen et al., 2006b, Makinen et al., 2007)). However, a contribution of mesenchymal progenitors to the lymphatic endothelium has yet to be identified during normal lymphatic development in mammals and recent lineage-tracing experiments suggest that cells of the myeloid lineage do not transdifferentiate into embryonic LECs and furthermore, are not a significant source of lymphangiogenic cytokines in embryonic skin, contrary to the situation in adult pathological lymphangiogenesis (Gordon et al., 2010).

In summary, the current model of lymphatic development favours the view that lymphatic endothelial specification occurs in a polarised fashion on one side of the cardinal veins at E9.5-10.5 in mouse and embryonic weeks 6-7 in humans (Tammela and Alitalo, 2010). LEC bud from the veins and form the lymph sacs, after which the lymphatic and blood vasculatures separate; only maintaining connections in defined locations for the purpose of returning lymph to venous circulation. Lymphatic vessels sprout from the lymph sacs to form a primary lymphatic plexus, which then undergoes extensive remodelling in late embryonic and early postnatal stages to give rise to the mature lymphatic vasculature, consisting of distinct collecting vessels and capillaries (Schulte-Merker et al., 2011, Tammela and Alitalo, 2010, Jurisic and Detmar, 2009, Makinen et al., 2007, Karpanen et al., 2006b) (Figure 1.3). The molecular regulation of this carefully orchestrated differentiation process is discussed in more detail below.

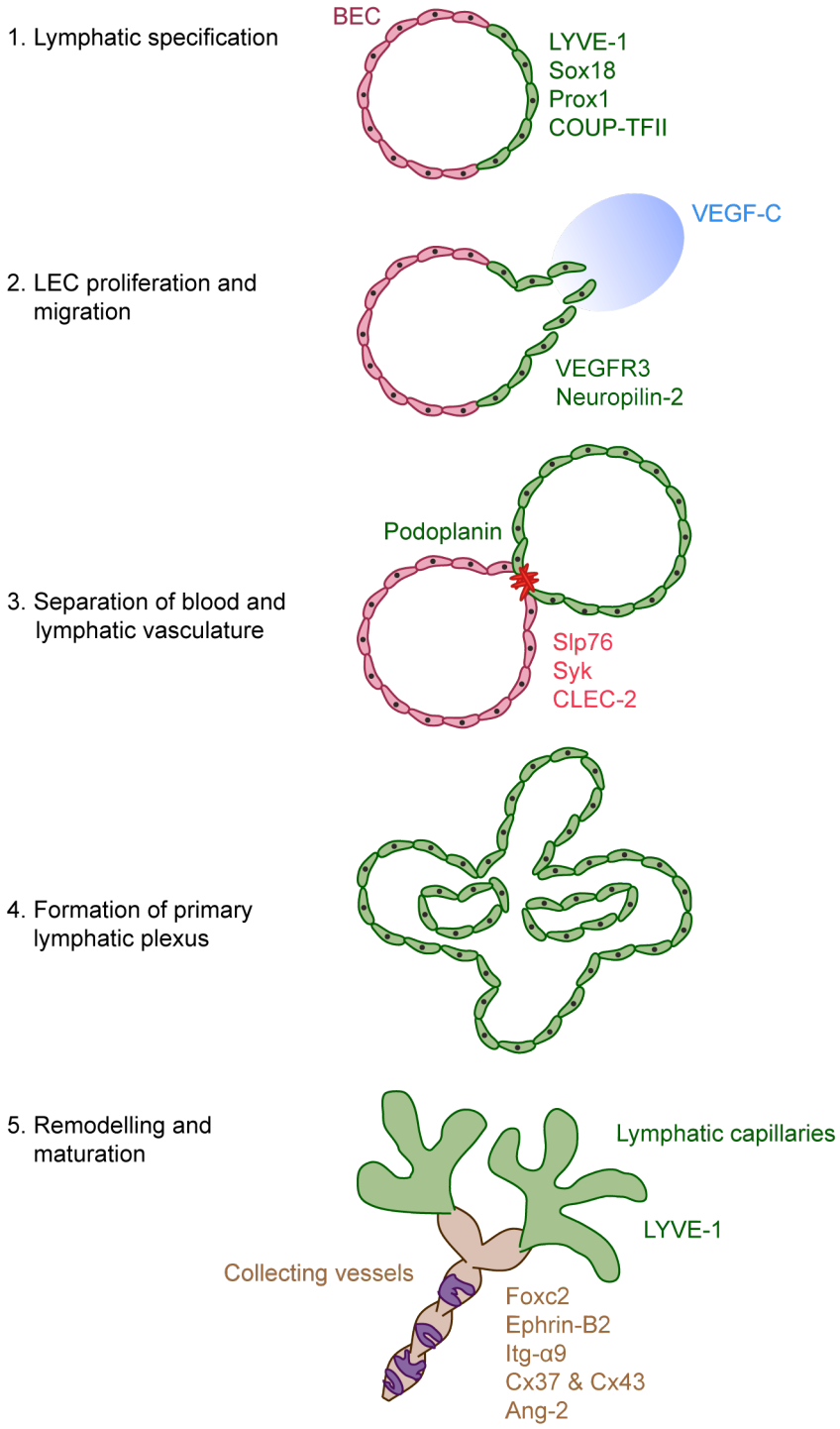

Figure 1.3 Development of the lymphatic system.
Current model of lymphatic development in mice, and the genes involved in regulating each step. Adapted from (Karpanen and Makinen, 2006)

1.2.1 Lymphatic specification

In mice, a number of genes have been identified whose expression marks the onset of lymphatic differentiation, and in many cases, the proteins they encode are essential for lymphatic development.

LYVE-1 was initially identified by its structural homology to CD44 in the Hyaluronan (HA) binding domain (Banerji et al., 1999), and starts to be expressed in the venous endothelium just prior to Prox1, making it one of the earliest markers of prospective lymphatic endothelial cells (Alitalo et al., 2005). However, despite extensive analysis of both physiological and pathological conditions in *Lyve1* null mice, no phenotype could be identified. Therefore, despite its early expression in the prospective lymphatic endothelium - and throughout lymphatic development - until its final down-regulation in mature lymphatic collecting vessels, the function of LYVE-1 is yet to be discovered (Gale et al., 2007, Huang et al., 2006).

The homeobox transcription factor Prox1 has been identified as a master regulator of lymphatic identity, since its over-expression in BEC can to some extent re-programme them to a lymphatic phenotype; suppressing expression of around 40% blood vascular endothelial markers, while up-regulating expression of 19% lymphatic specific genes (Petrova et al., 2002). Sox18 binds to specific sites in the *Prox1* promoter and directly activates *Prox1* expression (Francois et al., 2008). Consistent with this, Sox18 is first detected in EC of the cardinal vein at E9, just prior to Prox1 expression, and continues to be expressed in LEC until E13.5, at which stage it is expressed in almost all cells of the lymph sac. Its expression subsequently subsides and Sox18 is not found in dermal or mesenteric LEC, or in lymphatic vessels in adult tissues, suggesting that it is not required for maintenance of LEC identity after specification (Francois et al., 2008).

Ragged mice have a naturally occurring mutation in *Sox18* and homozygous mouse mutants do not initiate lymphatic differentiation, dying at around E14.5 with gross subcutaneous oedema, thus demonstrating the importance of Sox18 function for

lymphatic development. Mice heterozygous for *Sox18* mutations show defects in lymphatic patterning, which is suspected to contribute to the oedema shown in both *Sox18*$^{-/-}$ mice and HLTS (Francois et al., 2008).

Prox1 expression is first detected at E9.5 in lymphatic endothelial fated cells on one side of the cardinal veins (Wigle and Oliver, 1999), and its expression is maintained in LEC throughout development, although levels of Prox1 are reduced in the collecting lymphatic vessels except in the luminal valves (Norrmen et al., 2009). Prox1 is essential for lymphatic development. In *Prox1*$^{-/-}$ embryos, LEC are initially specified, but fail to bud from the veins and no lymph sacs or lymphatic capillary networks form. These mice display gross subcutaneous oedema at E14.5 and die between E14.5 and E15 (Wigle and Oliver, 1999). *Prox1* haploinsufficient pups also die, with chyle in the mesentery, at or around birth in all but one genetic background. Surviving *Prox1*$^{+/-}$ mice have disorganised and leaky lymphatic vessels, again demonstrating the importance of Prox1 for normal lymphatic development (Harvey et al., 2005). Although the importance of Prox1 for lymphatic development is now well understood, it is also important for development of other tissues, for example the central nervous system and the heart, as evidenced by growth retardation and structural disorganisation of the heart in both *Prox1* null and cardiac-specific mutant embryos (Risebro et al., 2009).

The transcription factor Coup-TFII has also been recently identified as important for LEC specification. *Coup-TFII* deletion at different stages of early lymphatic development revealed that it is required for both specification and maintenance of early LEC identity (up to E13.5) (Lin et al., 2010). However, deletion at E14.5 or E15.5 had no effect, suggesting that after this stage Coup-TFII is no longer required for maintenance of LEC fate (Srinivasan et al., 2010). Consistent with a similar role in specifying, but not maintaining, LEC fate to that of Sox18, Coup-TFII may also be able to directly bind to, and activate, *Prox1* (Srinivasan et al., 2010). Interestingly, while Coup-TFII does not appear to function in quiescent adult lymphatic vessels, inactivation in a tumour model lead to a decrease in tumour lymphatic vessels, suggesting a role for Coup-TFII in neo-lymphangiogenesis (Lin et al., 2010).

1.2.2 Lymphatic Sprouting

In the blood vasculature, sprouting angiogenesis involves the growth of new vessels from pre-existing ones. Angiogenic stimuli activate endothelial cells in the pre-existing vessel, which then secrete proteases to degrade the basement membrane, allowing the EC to migrate and proliferate into the extracellular matrix (Eilken and Adams, 2010). According to the current dogma, during lymphatic development the newly specified LEC must first sprout from the cardinal vein to form the lymph sacs and then from the lymph sacs to form the rest of the lymphatic vasculature. However, less is known about the regulation of this process in lymphatic than blood vasculature, although it seems that some important differences may exist, for example BEC migrate in tandem, while LEC can migrate as single cells and then assemble together into new vessels (Rutkowski et al., 2006).

One major signalling pathway known to be essential for lymphatic sprouting is VEGF-C/VEGFR-3. VEGFR-3 is expressed from about E8.5 in the mouse embryo, where it is initially expressed in all endothelial cells. However, upon initiation of lymphatic specification around E10.5, its expression becomes restricted to LEC (Kaipainen et al., 1995). VEGF-C is expressed in mesenchyme neighbouring the VEGFR-3^{+} jugular veins from which the lymphatic endothelial cells sprout. In the absence of *Vegfc*, LEC are initially specified (as visualised by Prox1 expression) in the jugular vein, but fail to sprout, resulting in absence of the lymph sacs and subsequently the later lymphatic vessels (Karkkainen et al., 2004). Unlike *Vegfc*$^{-/-}$ mice, *Vegfc* happloinsufficient animals survived embryogenesis, but newborn pups transiently accumulated chyle in the abdomen, and even adult mice displayed lymphoedema and hypoplastic, dysfunctional lymphatic vessels, thus emphasising the importance of VEGF-C for lymphatic development (Karkkainen et al., 2004).

An early role for VEGFR-3 in blood vessel remodelling means that *Vegfr3*$^{-/-}$ mice die at E9.5 before the onset of lymphatic development (Dumont et al., 1998). However, *Chy* mice, which have a heterozygous targeted mutation in the tyrosine kinase domain of *Vegfr3* have defective or absent lymphatic vessels, accumulate chyle in the abdomen

and develop lymphoedema (Karkkainen et al., 2001), demonstrating the importance of VEGFR-3 for normal lymphatic development.

VEGFR-3 stimulation protects cultured LEC from starvation-induced apoptosis and promotes cell survival, growth and migration *in vitro*, via activation of p42/p44 MAPK and Akt phosphorylation (Makinen et al., 2001b). The *in vivo* importance of these functions was demonstrated by blocking VEGF-C/VEGFR-3 signalling using a VEGF-C/D trap: a soluble form of VEGFR-3 that competes with the membrane-bound receptor for VEGF-C/D ligand binding. Expressing this construct from E14.5 in the basal epidermis not only prevents foetal lymphangiogenesis, but also causes regression, via apoptosis, of lymphatic capillaries that had already formed in deeper tissues. Interestingly, these mice are still healthy and viable and regressed vessels grow back by about 3 weeks after birth (Makinen et al., 2001a). Blocking VEGFR-3 signalling in postnatal mice prevented lymphatic vessel regeneration in a tail skin model of adult lymphangiogenesis, but had no effect on existing vessels, which still functioned normally (Pytowski et al., 2005). Together, these results suggest that the requirement for VEGF-C/VEGFR-3 signalling for the spouting and survival of new lymphatic vessels is not constant (Karpanen et al., 2006b).

There is some functional redundancy between the two known VEGFR-3 ligands, VEGF-C and VEGF-D, because over-expression of VEGF-D rescues lymphatic hypoplasia in *Vegfc*$^{+/-}$ mice (Haiko et al., 2008), and could also induce a weak LEC migratory response in explant assays (Karkkainen et al., 2004). However, *Vegfc*$^{-/-}$ mice have no lymphatic vessels, suggesting that physiological levels of VEGF-D cannot substitute for the requirement for VEGF-C during lymphatic development and normal lymphatic vasculature in *Vegfd*$^{-/-}$ mice indicates that VEGF-C is sufficient for lymphatic vessel growth (Haiko et al., 2008).

Surprisingly, *Vegfc*$^{-/-}$*;Vegfd*$^{-/-}$ mice do not phenocopy *Vegfr3*$^{-/-}$ mice. The lymphatic defects are as severe as those seen in *Vegfc*$^{-/-}$ mice alone, but the double mutants appeared as wild-type at E11.5, with normal blood vasculature, while *Vegfr3*$^{-/-}$ embryos had already died by this stage (Haiko et al., 2008). These data suggested that there may be ligand independent functions of VEGFR-3 in blood vascular development and

concordant with this hypothesis, disrupting the ligand-binding domain of VEGFR-3 lead to disrupted lymphangiogenesis, but allowed normal blood vessel development (Zhang et al., 2010b). Interestingly, the lymph sacs still formed normally in these mice, although lymphatic vessels subsequently failed to sprout. This suggests that VEGFR-3 can also function in a ligand-independent manner in this context (Zhang et al., 2010b). However, this is in direct contradiction with the lack of lymph sacs in *Vegfc*$^{-/-}$ mice (Karkkainen et al., 2004).

The axon guidance receptor Neuropilin-2 (Nrp2) is a co-receptor for VEGFR-3 (Karpanen et al., 2006a). It is initially expressed in veins and lymphatic vessels, but becomes restricted to the lymphatics after about E13 (Yuan et al., 2002). Mice deficient for *Nrp2* develop normal collecting vessels, but although lymphatic capillaries develop postnatally, they appear to be absent or reduced between E13-P3 (Yuan et al., 2002). Both VEGF-C and VEGF-D bind to Nrp-2, which is internalised with VEGFR-3 upon VEGF-C/D stimulation. Co-immunoprecipitation experiments revealed an interaction between VEGFR-3 and Nrp2, and Nrp2 internalisation upon ligand binding is dependant on VEGFR-3 (Karpanen et al., 2006a). Nrp2 does not have intrinsic enzymatic signalling ability, but Nrp2 cooperation with VEGFR-3 may aid LEC sensing of growth factor gradients and maximise their response to VEGF-C (Tammela and Alitalo, 2010). In line with this hypothesis, Nrp2 blocking antibodies inhibited LEC tip cell sprouting *in vivo*, in a VEGFR-3 dependant manner, resulting in decreased lymphatic vessel branching in the tail and sprouting in the intestinal lymphatics. However, only the induction of sprouting was affected; Nrp2 blockade had no effect on sprout elongation (Xu et al., 2010).

1.2.3 Separation from the blood vasculature

Separation of the primary lymphatic plexus from the blood vasculature is essential for normal lymphatic function. According to the current model of lympho-venous separation, Podoplanin, on the surface of lymphatic endothelial cells, activates platelets

circulating in the blood via its receptor CLEC-2. CLEC-2 signalling, via the haematopoietic signalling proteins Syk, SLP-76 and PLC-γ2, leads to platelet activation and aggregation at the junctions between blood and lymphatic vasculature, thus 'sealing off' the junction and mediating their separation (Schulte-Merker et al., 2011).

Much of this signalling pathway was identified by analysis of mice deficient in one or more of the components. *Pdpn*$^{-/-}$ mice displayed tortuous, blood filled lymphatic vessels, where abnormal connections between the two vascular systems could be identified by intra-venous injection of dye or FITC-dextran and visualisation of the dye in lymphatic vessels (Uhrin et al., 2010, Bertozzi et al., 2010). *Pdpn*$^{-/-}$ mice failed to aggregate platelets at the separation site of the lymph sac and cardinal vein, suggesting the involvement of haematopoietic cells (Uhrin et al., 2010). This was further confirmed by deletion of *Meis1* (which results in ablation of megakaryocytes/platelets and deficiencies in haematopoietic stem cells) and specific deletion of megakaryocytes, which caused a failure of lymphatic-blood separation (Carramolino et al., 2010). Furthermore, a podoplanin fusion protein was found to bind wild type, but not *Clec2*$^{-/-}$ platelets, suggesting that CLEC-2 is the podoplanin receptor on platelets (Bertozzi et al., 2010).

This was further confirmed by studies of *Clec2*$^{-/-}$ mice. CLEC-2 (C-type lectin-like receptor 2) is specifically expressed on the surface of platelets and megakaryocytes and mice deficient for this protein display disorganised and dysfunctional lymphatic vessels, oedema and blood-filled lymphatics (Suzuki-Inoue et al., 2010, Bertozzi et al., 2010). Furthermore, CLEC-2 signals through Syk and SLP-76 (Suzuki-Inoue et al., 2006), suggesting that activation of CLEC-2 on the surface of platelets may lead to lymphatic and blood vascular separation via Syk and SLP-76. This was consistent with previous observations that mice deficient in *Slp76* or *Syk* displayed abnormal connections between the blood and lymphatic vasculatures, resulting in blood in the lymphatic vessels and chyle in the mesenteric blood vessels of these mice (Abtahian et al., 2003). Transplanting *Slp76*$^{-/-}$ bone marrow into irradiated wild type mice was sufficient to induce mixing of the blood and lymphatic vasculature, as was platelet specific deletion of *Slp76*, demonstrating that SLP-76 is required in hematopoietic cells to regulate lympho-venous seperation (Abtahian et al., 2003, Bertozzi et al., 2010).

1.2.4 Lymphatic Remodelling

Several genes have been specifically implicated in the later stages of lymphatic development, such as specification of capillary vs. collecting vessel identity, or formation of luminal valves, and these will be discussed in more detail below.

1.2.4.1 Foxc2

The forkhead transcription factor Foxc2 is an essential regulator of lymphatic remodelling and maturation of the primary lymphatic plexus. However, consistent with its low expression in LEC prior to E15.5, it does not appear to be important for early lymphatic development (Petrova et al., 2004, Norrmen et al., 2009).

In the mesentery, Foxc2 is transiently up-regulated in all LECs at E15.5, before becoming restricted to sites of luminal valve formation in the mature collecting lymphatic vessels (Norrmen et al., 2009). Consistent with this expression pattern, *Foxc2*$^{-/-}$ mice fail to develop luminal valves, which results in abnormal outflow of FITC-Dextran from collecting vessels. Additionally, dermal capillaries of *Foxc2*$^{-/-}$ mice have irregular sized, dilated lumens, deposit ectopic Collagen IV and display abnormal investment of SMC, where there should usually be none. Concomitantly, *Foxc2*$^{-/-}$ capillaries have increased expression of the SMC recruitment factors *PDGFB* and Endoglin (Petrova et al., 2004). Transient up-regulation of Foxc2 at E15.5 is followed by down-regulation of Prox1, VEGFR3 and LYVE-1 in maturing collecting lymphatic vessels, although Prox1 and VEGFR3 continue to be expressed in the luminal valves (Norrmen et al., 2009). These capillary markers fail to down-regulate in *Foxc2*$^{-/-}$ mice, suggesting that Foxc2 is essential for regulating the maturation of the primary lymphatic plexus into collecting vessels and capillaries, as well as for initiating the development of luminal valves and restricting SMC recruitment to lymphatic capillaries (Norrmen et al., 2009) (Petrova et al., 2004).

Aberrant SMC recruitment to dermal capillaries in *Foxc2*$^{-/-}$ mice may be linked to failure to arrest VEGFR-3 signalling in these mice, which leads to a corresponding increase in *Ang2* expression (Norrmen et al., 2009). Ang2 is required for proper lymphatic development and its loss results in impaired SMC migration to the collecting lymphatic vessels (Gale et al., 2002). Conversely, ectopic *Ang2* expression in *Foxc2*$^{-/-}$ capillaries may result in atypical SMC coverage.

Interestingly, a number of Foxc2 binding sites in primary LECs are also enriched with nuclear factor of activated T cells (NFAT) binding sites. Inhibition of NFATc-1 with cyclosporin A results in a similar phenotype to *Foxc2* deficiency, which is enhanced when NFATc-1 is inhibited in *Foxc2*$^{+/-}$ mice. This suggests that Foxc2 may co-operate with NFATc-1 to mediate the regulation of capillary vs. collecting vessel identity (Norrmen et al., 2009).

1.2.4.2 Connexins

A recent study has identified a role for Connexin 37 (Cx37) and Connexin 43 (Cx43) in lymphatic valve development. Mice lacking either one of these proteins show a reduction in the number of lymphatic valves formed, although this is more extreme in the case of *Cx43*$^{-/-}$ than *Cx37*$^{-/-}$. However, loss of both proteins results in a complete absence of lymphatic valves (Kanady et al., 2011). This appears to be a valve-specific defect, rather than a general failure of collecting vessel specification as expression of other lymphatic markers was normal in *Cx37*$^{-/-}$*;Cx43*$^{-/-}$ mice. Foxc2 may be at least partly responsible for regulating connexin-mediated valve formation, since Cx37 expression was reduced in *Foxc2*$^{-/-}$ mice, although expression of Cx43 was unaffected (Kanady et al., 2011). Cx47 was also localised to the luminal valves (Kanady et al., 2011), which is especially interesting given the recent data demonstrating that mutations in *GJC2*, which encodes Connexin 47, cause primary lympoedema (Ferrell et al., 2010).

1.2.4.3 EphrinB2

Eph receptor tyrosine kinases and their binding partners Ephrins are involved in repulsive axon guidance in the nervous system, but are also essential for embryonic angiogenesis. Ephrins are divided into EphrinAs that are attached to the cell surface by a glycosylphosphatidylinisotol anchor or EphrinBs, which possess a transmembrane domain. Ephrins are capable of both ligand-like activity, via activation of their associated Eph receptors (forward signalling) and receptor-like signal transduction activity (reverse signalling) (Adams and Eichmann, 2010). In the case of EphrinBs, reverse signalling involves recruitment of adaptor proteins to phosphotyrosine residues in the cytoplasmic domain or to a PDZ binding motif. Expression of EphrinB2 in arteries and EphB4 in veins suggests a role for EphB4/EphrinB2 in cell sorting or vessel segregation, but this has yet to be definitively proved (Adams and Eichmann, 2010). Due to embryonic lethality, *Efnb2* null mutants cannot be used to examine the role of this protein in the mature vasculature, but a recent endothelial cell specific *Efnb2* deletion ($Efnb2^{i\Delta EC}$) demonstrated that its loss resulted in reduction of endothelial cell proliferation, tip cell number and complexity of the endothelial network in the postnatal retina (Wang et al., 2010). Interestingly, a cell autonomous requirement for EphrinB2 in vascular SMC and pericytes has also been identified. $Efnb2^{-/-}$ pericytes display spreading defects and fail to form focal adhesions, resulting in disassociation from small-diameter blood vessels (Foo et al., 2006).

Surprisingly, neither the intracellular tyrosine residues, nor the PDZ binding domain of EphrinB2 are required for embryonic blood vessel remodelling (Makinen et al., 2005). However, the lymphatic vasculature was severely disturbed upon disruption of the PDZ binding domain, thus revealing a previously unknown requirement for EphrinB2 reverse signalling via the PDZ binding domain for collecting lymphatic vessel maturation (Makinen et al., 2005).

In contrast to the blood vasculature, within the lymphatic vessels, EphrinB2 expression is confined to the lymphatic endothelium and is not expressed in lymphatic SMC.

However it is expressed only in the endothelium of the collecting lymphatic vessels, not the capillaries, and when the EphrinB2 PDZ binding domain is mutated (referred to as *Efnb2*$^{\Delta V/\Delta V}$), the distinction between these two vessel types is lost (Makinen et al., 2005). Although initial formation of the capillary plexus occurs normally, there is failure in sprout extension and the entire network is hyperplastic. Collecting lymphatic vessels fail to down-regulate LYVE-1 or form luminal valves, while there is ectopic SMC recruitment to the capillaries. The lack of luminal valves and failure of capillary remodelling resulted in FITC-Dextran reflux, indicating loss of functionality in the lymphatic vessels of *Efnb2*$^{\Delta V/\Delta V}$ mice (Makinen et al., 2005).

Interestingly, recent work has linked EphrinB2 signalling to the VEGF-C/VEGFR-3 pathway (Wang et al., 2010). Stimulation of LEC with soluble EphrinB2-Fc or EphB4-Fc fusion proteins resulted in VEGFR-3 internalisation, even in the absence of VEGF-C. However, downstream signalling components were not activated, implying that EphrinB2/EphB4 could not replace VEGF-C. Intraperitoneal (IP) injection of VEGF-C in mice caused VEGFR-3 internalisation and accumulation in the perinuclear regions of mesenteric LEC in wild type, but not *Efnb2*$^{i\Delta EC}$ or *Efnb2*$^{\Delta V/\Delta V}$ mice, suggesting that EphrinB2 is also a regulator of VEGFR-3 internalisation and signalling *in vivo* (Wang et al., 2010).

1.2.4.4 Angiopoietin/Tie signalling

Tie1 and Tie2 receptor tyrosine kinases are expressed mainly in endothelial and haematopoietic cells, while the Tie2 ligands Angiopoietin-1 (Ang1) and Angiopoietin-2 (Ang2) are expressed variably. Ang2 is expressed in almost all endothelial cells, while Ang1 is expressed in SMC, pericytes, fibroblasts and other non-vascular normal and tumour cells (Augustin et al., 2009). Ang1 and Ang2 share a binding site on Tie2, but while Ang1 is a Tie2 agonist, Ang2 is a context-dependant antagonist of Tie2 signalling (Augustin et al., 2009). Tie1 and Tie2 are crucial for embryonic blood vascular

remodelling and stabilisation and are also involved in regulation of lymphatic development. Tie1 has an early role in lymphatic development; *Tie1*$^{-/-}$ mice develop oedema and show abnormal lymph sac patterning at E12.5, which defects precede blood vascular deficiencies (D'Amico et al., 2010). In contrast, Ang2 has a later role in stabilisation of the mature lymphatic vasculature and SMC recruitment to collecting lymphatic vessels. One report *of Ang2*$^{-/-}$ mice observed that instead of single, straight collecting lymphatic vessels with a regular, but discontinuous coverage of SMC in wild type mesenteries, *Ang2*$^{-/-}$ mice showed disorganised vessel networks, surrounded by clusters of poorly organised and dissociated SMCs, suggesting that Ang2 might normally induce SMC recruitment to the vessel (Gale et al., 2002). However, in a different genetic background, the lymphatic defects were slightly different. In this case, collecting lymphatic vessels failed to specify correctly. Very few lymphatic valves formed, but those that did appeared normal and SMC were recruited prematurely to the collecting vessels and ectopically to the lymphatic capillaries (Dellinger et al., 2008). Interestingly, while unable to rescue the blood vascular phenotype of *Ang2*$^{-/-}$ mice, over-expression of *Ang1* under the control of the *Ang2* promoter was able to fully rescue the lymphatic phenotype (Gale et al., 2002) (Dellinger et al., 2008). Also, Ang1 over-expression by injection into the mouse ear causes VEGFR-3 dependent lymphatic capillary sprouting and hyperplasia (Tammela et al., 2005), both of which suggest that the requirement for Angiopoietins in the mature lymphatic vasculature may be rather a requirement for Tie2 activation.

1.3 Structure of the mature lymphatic vasculature

The mature lymphatic vasculature consists of two different vessel types: lymphatic capillaries and collecting vessels. These are structurally and molecularly distinct, particularly suiting them to their individual functions (Figure 1.4 A-B).

1.3.1 Lymphatic capillaries

Lymphatic capillaries are highly permeable, blind-ended structures, with thin walls, wide lumens and a discontinuous basement membrane. Oak-leaf shaped capillary endothelial cells are anchored at the sides and base by VE-cadherin 'button' junctions (Baluk et al., 2007), while the free tips of the cells interdigitate with and loosely overlap their neighbours, forming 'flap junctions' through which dendritic cells and interstitial fluid can pass (Tammela and Alitalo, 2010, Schulte-Merker et al., 2011)(Figure 1.4 A). Sprouting capillaries have 'zipper' junctions, as are found in the collecting lymphatic vessels, which indicates that button junctions are a feature of mature and quiescent capillary endothelium. However, it is interesting to note that both button and zipper junctions have the same protein composition, indicating that specialised junctions form by reorganisation of tight junction proteins, rather than by changes in protein expression (Baluk et al., 2007).

Capillary endothelial cells are anchored to the extracellular matrix by anchoring filaments, which are primarily composed of Emilin-1 and fibrillin (Danussi et al., 2008). An increase in interstitial pressure due to fluid accumulation or movements in the surrounding tissue that put strain on the extracellular matrix causes extension of the anchoring filaments and opening of the capillaries. This leads to an increase in luminal volume and a transient pressure decrease inside the vessel causing an influx of fluid. As the capillary fills, the overlapping junctions close and the pressure returns to normal,

preventing leakage of lymph back into the interstitium (Tammela and Alitalo, 2010, Randolph et al., 2005). Capillary fluid uptake is also sensitive to transmural flow. Increased flow causes disorganisation of VE-cadherin and PECAM-1 in the LEC junctions, increased permeability to Dextran and expression of Aquasporin-2, a component of channels controlling water flux (Miteva et al., 2010).

1.3.2 Lymphatic collecting vessels

Following absorption from the capillaries, fluid drains first into pre-collecting vessels, which share features of both capillary and collecting vessels. For example, the cells are oak-leaf shaped and continue to express LYVE-1 as in the capillaries, but they develop luminal valves and acquire a very sparse coverage of SMC, reminiscent of the collecting vessels (Schulte-Merker et al., 2011, Randolph et al., 2005).

Endothelial cells of the collecting lymphatic vessels are spindle shaped and tightly linked by continuous 'zipper' junctions. Together with a more extensive basement membrane and SMC coverage, this prevents fluid leakage from the vessel (Figure 1.4 B). Collecting vessels are organised into a series of lymphangions, which are separated by luminal valves. The intrinsic pumping action of the lymphatic system is a unique requirement of the lymphatic vasculature, because unlike the blood vasculature the lymphatic system does not have the heart; a central pump to regulate blood flow. Lymph propulsion occurs via both intrinsic pumping action due to lymphatic smooth muscle cell contractions and by passive pressure changes caused by contractions of surrounding skeletal muscle or arterial pulsations. The lymphangions contract sequentially as high pressure on the 'upstream' side of the valve forces it open, while reverse flow closes the valve, thus preventing lymph backflow, as will be discussed in more detail in section 1.4.5 (Randolph et al., 2005, Tammela and Alitalo, 2010, Schulte-Merker et al., 2011). Interestingly, a recent study has identified the capacity for solute exchange from the collecting lymphatic vessels, challenging the current belief that lymphatic vessels absorb fluid without ever leaking it back into the interstitium

(Scallan and Huxley, 2010). This work demonstrated that solute does move from the vessel lumen into the interstitium, thus increasing the protein concentration of lymph in prenodal collecting lymphatic vessels; an observation that has important implications for lymphatic function and maintenance of tissue fluid balance (Scallan and Huxley, 2010).

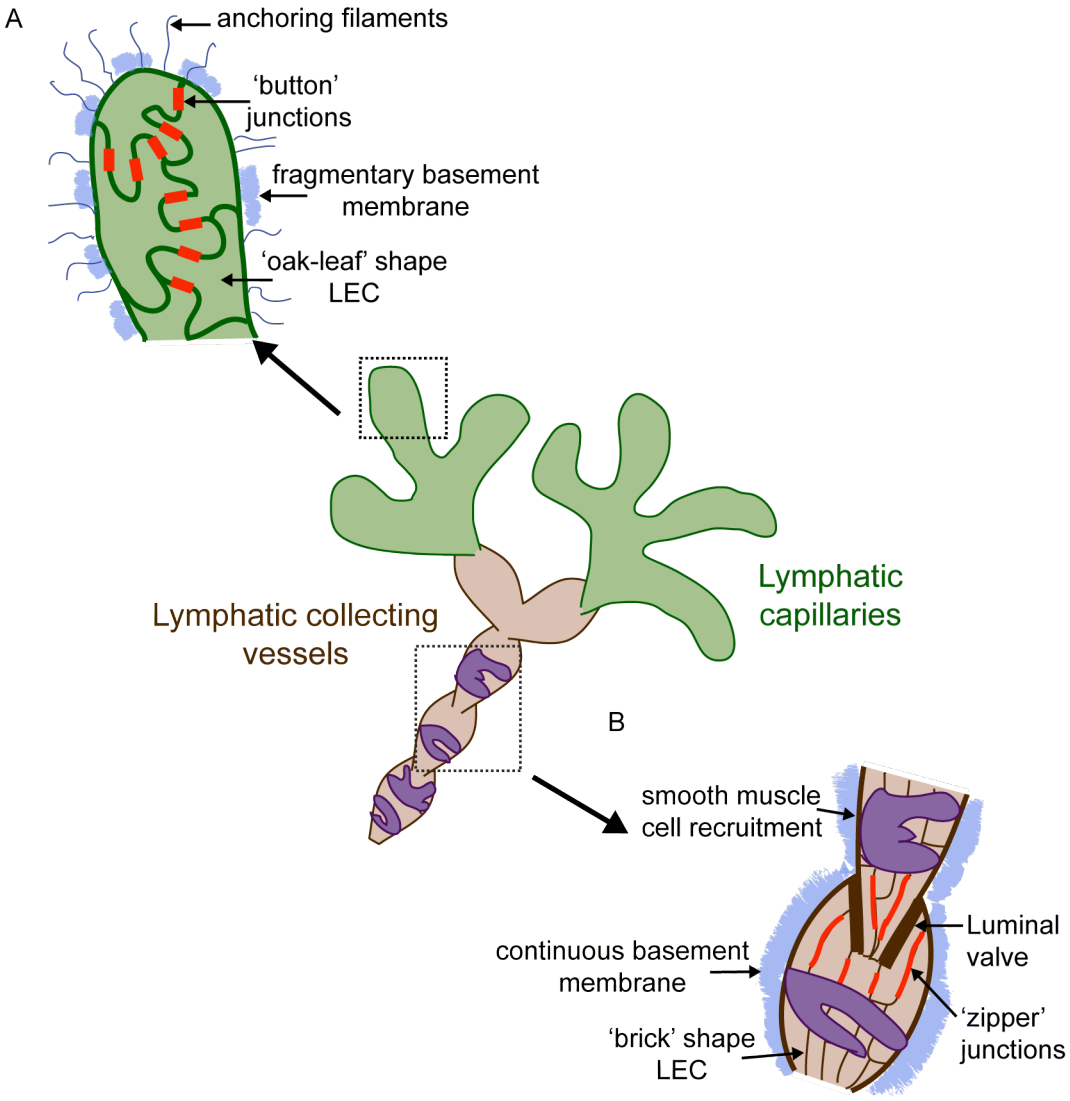

Figure 1.4 Organisation of the mature lymphatic vasculature.
Details of the structural organisation of (A) lymphatic capillaries and (B) lymphatic collecting vessels

1.4 Smooth muscle cells in blood vascular and lymphatic function

1.4.1 Pericytes and Smooth Muscle Cells

The majority of our understanding of the importance of smooth muscle cells and pericytes, commonly referred to as mural cells (MC), comes from studies of the blood vascular system. The distinction between smooth muscle cells and pericytes is fluid and often hazy. Attempts have been made to distinguish the two cell types by marker gene expression, for example αSMA is commonly used to identify SMC, while Desmin, NG2 and RGS5 are often used to distinguish pericytes. However none of these markers are exclusive to pericytes and their expression is dynamic; they may all be expressed in both pericytes and smooth muscle cells in different tissues, developmental stages and species. For example, αSMA does not identify pericytes in the mouse retina, but does in the chicken (Gerhardt and Betsholtz, 2003, Armulik et al., 2005). Another way to differentiate between the two cell types is by defining them based on contacts with endothelial cells and the extracellular matrix. By this definition, pericytes contact endothelial cells directly through holes in their shared basement membrane, while SMC are separated from the endothelium by the basement membrane (Gerhardt and Betsholtz, 2003). However, this distinction also fails during developmental and even postnatal angiogenesis, when the basement membrane is not yet complete. For this reason, the distinctions between pericytes and smooth muscle cells are unclear and it seems probable that rather than representing two distinct cell types, they instead represent two ends of a continuum from the same lineage, where the larger blood vessels are surrounded by αSMA positive SMC, capillaries are covered with a pericyte layer and intermediate vessels may be covered by cells that take on the characteristics of both. In accord with this is the ability of pericytes to differentiate into SMC and vice versa (Armulik et al., 2005).

The density of pericyte coverage and pericyte morphology varies between different organs and may reflect specialised functions of different vascular beds, for example pericyte coverage is high in the legs and lower torso in humans, where increased blood pressure is necessary to pump blood against gravitational force (Armulik et al., 2005, Bergers and Song, 2005, Gerhardt and Betsholtz, 2003).

1.4.2 Vascular SMC / Pericyte ontogeny

Vascular smooth muscle cells (vSMC) and pericytes have a complex ontogeny that has not yet been fully resolved. Most evidence suggests multiple origins for vSMC and pericytes, including transdifferentiation from mesenchymal progenitors (Hirschi et al., 1998, Hellstrom et al., 1999), and derivation from neural crest cells (Etchevers et al., 2001). It is also unclear whether vSMC and pericytes derive from the same, or different origins. However, work in quail-chick chimeras demonstrated that cranial neural crest cells could derive into αSMA-expressing pericytes in capillaries and vSMC in arteries, and furthermore that much of the vasculature of the face and jaw contained cells that had derived from quail cranial neural crest (Etchevers et al., 2001). Together with the phenotypic plasticity of SMC and pericytes, this suggests that they share a common origin (Armulik et al., 2005). However, SMC in different vascular beds have been demonstrated to derive from distinct origins. Apart from neural crest and mesenchymal cells previously mentioned, somites, the proepicardium and the secondary heart field have all been implicated as sources of SMC progenitors and incredibly, the aorta has been shown to have SMC from different origins along its length, for example the neural crest, somites and mesoepithelium (Majesky, 2007). SMC progenitors, termed 'mesoangioblsts' capable of differentiating into skeletal or smooth muscle cells or fibroblasts, also reside in the arterial wall and are postulated to be able to differentiate into SMC during vessel remodelling or repair (Majesky, 2007, Majesky et al., 2011). However, despite the large volume of research involved in characterising vascular SMC ontogeny, the molecular regulation of SMC differentiation has not yet been fully elucidated and what it is that controls the fate determination of such an ontologically

diverse range of progenitors to finally express the same proteins and function in a similar manner are unclear (Majesky et al., 2011).

1.4.3 Vascular SMC / Pericyte recruitment to the endothelium

1.4.3.1 PDGFB/PDGFRβ

Paracrine signalling between PDGF-B, expressed in angiogenic sprouts and PDGFR-β in developing pericytes is crucial for proper pericyte recruitment to newly formed blood vessels. Mice deficient for PDGF-B die embryonically, due to haemorrhage and oedema caused by lack of pericytes (Lindahl et al., 1997). The same phenotype is seen in mice lacking PDGFR-β, which also show decreased vSMC coverage of the large arteries, although this is more severe in superficial than deeper vessels (Hellstrom et al., 1999). *Pdgfb*$^{ret/ret}$ mice have a mutation in the C terminal retention motif that allows PDGF-B binding to proteoglycans in the extracellular matrix, which results in impaired pericyte recruitment in many vascularised tissues (Abramsson et al., 2003). Tumours transplanted into these mice have reduced pericyte coverage and weaker pericyte adhesion to the vessel wall than those in wild-type mice. Applying exogenous PDGF-B by injecting tumour cells that over-express it, rescued the density of pericytes recruited to the vessel, but not their attachment, demonstrating that PDGF-B must be retained close to the endothelial surface for proper integration of pericytes into the vessel wall (Abramsson et al., 2003). Numerous other studies have confirmed the importance of PDGF-B/PDGFR-β signalling for pericyte migration and proliferation both *in vitro* and *in vivo*, by demonstrating enhanced SMC migration and proliferation after PDGF-BB stimulation, or by preventing pericyte recruitment by blocking PDGF-B/PDGFR-β signalling (Benjamin et al., 1998, Stratman et al., 2010, Fuxe et al., 2011).

1.4.3.2 Ang1/Tie2

Mice lacking either Tie2 or Ang1 show very similar embryonic lethal phenotypes, including failure of vascular remodelling and pericyte recruitment, suggesting a role for this signalling pathway in this process. This hypothesis is consistent with the generally held view that Tie2 is expressed in the endothelium, while Ang1 is expressed initially in mesenchymal tissues surrounding the vessels, and is later restricted to SMC/pericytes (Sato et al., 1995, Suri et al., 1996, Augustin et al., 2009). However, recent data is contradicting these conclusions and is likely to reopen the debate over the function of Angiopoietin/Tie signalling in the vasculature. A study of cultured retinal pericytes identified Tie2 expression in these cells and showed that Ang1 acts directly on pericytes to promote survival and migration (Cai et al., 2008), while recently published work using a conditional *Ang1* knock-out mouse showed that either global or cardiac specific *Ang1* deletion gives the same phenotype as previously reported, except that pericyte recruitment is completely unaffected. Pericyte coverage continues to be normal at any stage of *Ang1* deletion despite severe vascular defects that occur when deletion occurs prior to E13.5, arguing against any role for Ang1 in pericyte recruitment (Jeansson et al., 2011). It is possible that the vascular deficiencies observed in the original $Ang1^{-/-}$ are secondary to cardiac failure and therefore pericyte loss could result from endothelial cell death (Gaengel et al., 2009). However, this is not consistent with normal pericyte recruitment even when *Ang1* is deleted very early in the conditional mutant, leaving the reason for the discrepancies between these results unclear.

To add to the confusion over Ang1 involvement in pericyte recruitment, in human venous malformation a mutation causes constitutive activation of Tie2, and smooth muscle cell coverage is uneven or absent on certain veins (reviewed in (Gaengel et al., 2009)). Likewise, over-expression of Ang1 is known to cause a reduction in the number of pericytes, while also reducing vessel leakage in inflammatory conditions (Fuxe et al., 2011). This may be consistent with the findings of Jeansson et al, who reported no phenotype in normal, quiescent vasculature of *Ang1* deficient mice, if

deletion occurred after E13.5, but enhanced angiogenesis and fibrosis during wound healing in *Ang1* deficient mice (Jeansson et al., 2011).

Overall, it seems that Ang1 is necessary for proper cardiac and vascular development, but its role in pericyte recruitment remains unclear. In the adult vasculature, it is possible that Ang1/Tie2 signalling is not functional, except in pathological conditions such as wound healing or inflammation, where it may constrain angiogenesis and promote vessel stability. The complex functions of Ang1 in the vasculature may rely on a fine balance between Ang1-mediated Tie2 activation, and Ang2-mediated antagonism.

1.4.4 vSMC / Pericyte function

The contractile behaviour of vSMC and pericytes has been widely documented (eg (Bastin and Heximer, 2011, Rucker et al., 2000)), and allows performance of one of the major functions of vascular smooth muscle; regulating vessel tone and blood flow by calcium dependant tonic contractions. Briefly, Myosin Light Chain Kinase (MLCK) is activated upon Ca^{2+} binding to calmodulin. MLCK then phosphorylates Regulatory Myosin Light Chain (RMLC), which leads to activation of Myosin ATPase and interaction between Myosin and Actin that then initiates smooth muscle contractions (Bastin and Heximer, 2011, Muthuchamy and Zawieja, 2008). When Ca^{2+} is reduced, inactivation of MLCK leads to Myosin Light Chain Phosphatase (MLCP) mediated dephosphorylation of RMLC that then deactivates ATPase and the smooth muscle relaxes (Muthuchamy and Zawieja, 2008). However, this is only one function of vSMC/Pericytes. In large blood vessels, the thick coating of vSMC also provides structural support (Gerhardt and Betsholtz, 2003), and a further essential role for pericytes in maintaining vessel stability by either limiting endothelial cell proliferation or depositing extracellular matrix (or both) is discussed in more detail below.

Deletion of *Pdgfb* or *Pdgfrβ* resulted in a 25% increase in capillary diameter, although this was highly variable and irregular along the vessel length, in contrast to the wild-

type state (Hellstrom et al., 2001). This corresponded to a 60% increase in the number of EC nuclei, despite a shortening of junction length (ie vessels were dilated, but the endothelial cells were densely packed), and a lack of pericytes from E11.5 onwards, indicating that pericytes regulate vessel stability, at least in part, by limiting endothelial cell proliferation. There was also a reduction in the junction proteins VE-cadherin and Occludin at E18.5 in *Pdgfb*$^{-/-}$ and *Pdgfrβ*$^{-/-}$ mice, suggesting that pericytes may also regulate junctional, and therefore vessel, stability (Hellstrom et al., 2001). However, since VE-cadherin and Occludin levels are normal at E12.5, despite there already being a lack of pericytes at this stage, this defect may be secondary to the earlier endothelial abnormalities. Recently, it has been shown that reducing pericyte recruitment to endothelial tubes by blocking PDGF-B/PDGFR-β or HB-EGF/EGFR signalling by soluble receptor trap, ligand blocking antibodies, or siRNA knockdown of the receptors in SMC, results in increased endothelial tube diameter, although in this case not due to increased proliferation, and a decrease in basement membrane deposition (Stratman et al., 2010). This suggests that, as previously hypothesised, pericyte regulation of vascular stability is also in part due to basement membrane deposition (von Tell et al., 2006). However, it is surprising that given the apparent importance of pericytes for vascular stability, pericyte loss of up to 90% can be tolerated (Enge et al., 2002).

Pericyte regulation of vascular stability is also important in pathological conditions. *Pdgfb*$^{ret/ret}$ mice survive to adulthood despite impaired pericyte recruitment and attachment to the vessels. However, the vasculature of tumours grown in *Pdgfb*$^{ret/ret}$ mice is unstable, with a greater vessel diameter (Abramsson et al., 2003). A recent study demonstrated that pericyte ablation decreased vessel stability and increased vessel remodelling in conditions of sustained inflammation, but not in uninfected controls. This perhaps suggests that pericytes are required to regulate vessel stability in actively remodelling vessels, such as occurs in development or chronic inflammation, but not in the quiescent, adult vasculature (Fuxe et al., 2011). However, the potential for increased vessel deterioration following PDGF-B blockade beyond the 7 day duration of the study cannot be ruled out, as vessel stability at later timepoints was not examined. Some research suggests that pericytes can maintain vessel integrity even in conditions such as hyperoxia, which is detrimental to the vasculature and leads to vessel regression in immature vessels that are not yet fully protected by pericyte coverage (Benjamin et

al., 1998). This is supported by work in 3D collagen matrices, which showed that addition of 20-30% pericytes relative to endothelial cells into the culture completely inhibited Matrix Metalloproteinase-1 (MMP)-1 and MMP-10 mediated vessel regression by delivering Tissue Inhibitor of Metalloproteinase -3 (TIMP)-3, whose expression by pericytes is strongly up-regulated upon EC-Pericyte co-culture (Saunders et al., 2006). However, other work suggests that the presence of pericytes is not enough on its own to protect vessels from regression. Treatment of tumours with VEGF-targeting angiogenesis inhibitors lead to a decrease in pericyte marker expression and basement membrane immunoreactivity in tumour vessels. Despite this reduction being only half as extensive as the reduction in endothelial cell marker expression, it demonstrated that vessel regression occurred even in vessels associated with pericytes (Inai et al., 2004), so the suggestion that pericytes act as a protective mechanism and marker of vessel maturity remains controversial. However, the discrepancy between these two results may be resolved by consideration of pericyte organisation around the vessels investigated. While pericyte association with the endothelium in the mature vasculature is close, with the SMC wrapping around the endothelial cells of larger vessels and tightly associated with the endothelium even in small-calibre blood vessels, pericyte investiture of tumour vessels is much looser, perhaps rendering pericytes a less effective protection against regression in this situation (Inai et al., 2004, von Tell et al., 2006).

1.4.5 Lymphatic smooth muscle

Despite major advances in understanding of vascular smooth muscle, our knowledge of lymphatic smooth muscle is limited, for example it is not known whether lymphatic smooth muscle derives from the same lineage as vascular smooth muscle. While one study has suggested that lymphatic smooth muscle is of mesenchymal origin (Ohtani and Ohtani, 2001), nothing else is known of its ontogeny and differences in protein expression profiles and contractile functions of lymphatic and blood vascular smooth muscle may cast doubt on the shared lineage hypothesis. On the other hand, blood

vessels display specialised functions in different organs that are subjected to different metabolic demands (Gerhardt and Betsholtz, 2003), and it is possible that vSMC/pericyte function varies accordingly, which may be consistent with the 'continuum' of perictye phenotypes observed in the blood vasculature. Therefore, the same may be true of lymphatic smooth muscle, and functional specialisation may occur *in situ*. Consistent with this is the observation that, like blood vascular smooth muscle, there are differences in the SMC density around lymphatic vessels in different tissues, which have different contractile properties. This is reflected in a change of contractile protein expression, for example between smooth muscle cells from mesenteric lymphatics and the thoracic duct (Muthuchamy et al., 2003).

The poor survival of mice mutant in the pathways responsible for vascular SMC/ pericyte recruitment to blood vessels means that these mice often die before any potential role in lymphatic smooth muscle recruitment can be determined. However, as discussed previously, we know that Ang2 acts as a Tie2 agonist in the lymphatic system, contrary to the case in the blood vasculature and *Ang2*$^{-/-}$ mice display lymphatic defects suggestive of a role in SMC organisation (Gale et al., 2002) (Dellinger et al., 2008). We can also infer by over-expression of PDGF-B in the mesenchyme and resulting SMC dissociation from the lymphatic vessels (Tammela et al., 2007), and up-regulation of PDGF-B expression in capillaries of *Foxc2*$^{-/-}$ mice that recruit ectopic SMC (Petrova et al., 2004) that lymphatic endothelial/smooth muscle cells are responsive to PDGF-B/PDGFR-β signalling. However, a lack of mouse mutants with specific defects in lymphatic smooth muscle means that in general we have less opportunity to study this process in lymphatic than blood vascular development.

The major difference between blood vascular and lymphatic smooth muscle is in their contractile functions. As is reflected by their contractile protein expression profiles (Muthuchamy et al., 2003), lymphatic smooth muscle is capable of both slow, tonic contractions to control flow resistance, such as is seen in blood vessels, and also brisk, phasic contractions more reminiscent of cardiac muscle (von der Weid and Zawieja, 2004, Muthuchamy and Zawieja, 2008, Zawieja, 2009).

In steady state conditions, prevailing pressure gradients usually act against the passive flow of lymph through the system; therefore energy must be provided to allow the central transport of lymph against a hydrostatic pressure gradient. Energy comes from either intrinsic, or extrinsic lymph pumps. Extrinsic pumps combine all the forces outside the lymphatics, for example respiration, skeletal muscle contraction and heartbeat that can compress the lymphatics and move fluid centrally (Muthuchamy and Zawieja, 2008). This mechanism is thought to be particularly important in heart, skeletal muscle, thorax and gut wall lymphatics, which are exposed to strong external forces, while most other lymphatic networks rely on the intrinsic pump (Zawieja, 2009). This is supported by experimental evidence demonstrating a difference between the intrinsic pumping capability of lymphatic vessels from different tissues, for example a comparison of the lymphatic pump in mesenteric, cervical, femoral and thoracic duct lymphatics revealed that mesenteric lymphatics had the most and the thoracic duct the least effective intrinsic pumps (Gashev et al., 2004). This is almost certainly due to anatomical location and the greater exposure of the thoracic duct to extrinsic pumping forces generated by respiration and heartbeat and therefore reduced requirement for intrinsic pumping activity.

In the absence of the heart, which pumps blood through the vascular system, or 'lymph hearts' that pump lymph in lower vertebrates, each lymphangion in the mammalian lymphatics must be capable of acting as an intrinsic pump. This relies on strong, co-ordinated phasic contractions of lymphatic smooth muscle, which result in rapid decrease of lymphatic diameter, increase in local lymph pressure, closure of the upstream valve, opening of the downstream valve and ejection of lymph downstream (Muthuchamy and Zawieja, 2008, Zawieja, 2009) (Figure 1.5). Phasic lymphatic contractions are initiated by action potentials generated by pacemaker cells in the muscle wall. These cells are capable of generating a rhythm even when the vessels are empty, and while their exact nature is yet to be defined, they have been identified by their electron dense nature and expression of c-Kit and vimentin, which are widely used as markers of pacemaker cells in the gastrointestinal tract, just underneath the muscle layer in the sheep lymphatic vessel wall (McCloskey et al., 2002). Earlier studies in guinea pig mesenteric lymphatics suggested that the mechanism of pacemaking activity might be related to calcium-dependant spontaneous transient depolarisations (STDs).

These transient depolarisations precede and underlie action potentials, and are correlated with the pumping activity of the lymphangion; increasing lymphatic pumping increases STD activity and vice versa, supporting the hypothesis that STDs of sufficient amplitude may give rise to action potentials and therefore muscle contractions (Van Helden, 1993, von der Weid and Zawieja, 2004).

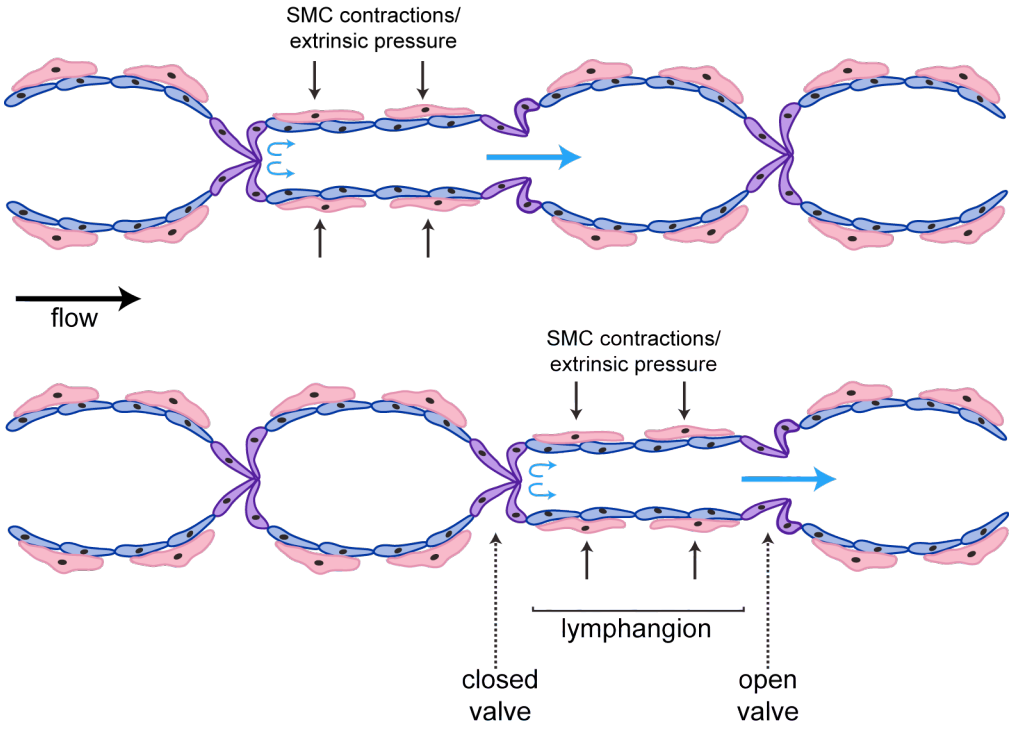

Figure 1.5 The lymphatic pump.
Collecting lymphatic vessels are organised into lymphangions, separated by luminal valves. Direction of flow is indicated with an arrow. Pressure from SMC contractions or extrinsic forces, causes the lymphangion to contract, rapidly narrowing its diameter and opening the downstream luminal valve. Lymph then fills the downstream lymphangion, whose contraction propels the lymph further through the vessel. Closure of the upstream luminal valve prevents backflow of lymph.

Physical factors such as transmural pressure (stretch) and flow (shear) exert strong effects on the lymphatic pump. Initial increases in transmural pressure led to increased pump activity, but further pressure increases then caused a decrease in lymphatic pumping (Gashev et al., 2004). As expected, optimal pump function occurred at different pressures for lymphatics from different tissues; the mesenteric lymphatic pump

functioned optimally at a higher transmural pressure than thoracic duct, cervical or femoral lymphatics, indicating that these lymphatic vessels are better able to withstand high pressure and pressure changes, since significant pumping activity could still be maintained at high transmural pressures (Gashev et al., 2004).

Increasing flow, while transmural pressure remained constant, caused an immediate decrease in lymphatic pump activity in all tissues. This was measured by increased systolic lymphatic diameter, a corresponding decrease in the amplitude of contractions, reduced contraction frequency, ejection fraction (the proportion of lymph released from the lymphangion during each contraction) and fractional pump flow (a measure of overall pump activity taking into account all the above parameters) (Gashev et al., 2004, Gashev et al., 2002). Sophisticated high speed video microscopy and mathematical techniques to measure fluid velocity (by lymphocyte tracking), volume flow rate, wall shear stress, and retrograde flow developed later, confirmed the physiological relevance of the transmural pressure and flow rates imposed during these studies (Dixon et al., 2006). Therefore, decreased phasic smooth muscle contractions when flow increased was not simply an artifact caused by imposing physiologically abnormal pressure gradients on the vessel.

This phenomenon can be explained by the unique requirement of the lymphatic vessels to function as both pump and conduit. Usually, inlet pressure is lower than outlet pressure and lymph movement requires active pumping. However, in cases when the pressure is reversed and inlet pressure exceeds outlet pressure, the lymphatic vessel must switch from pump to conduit. In this case, the pressure gradient itself becomes the main source of energy to drive lymph, which then flows in a passive manner through the vessel and flow can even be reduced, or inhibited, by muscle contraction (Quick et al., 2009). This pressure reversal can occur in a number of situations. Particularly in humans, elevating limbs above the level of the great veins can cause a reversal of the pressure gradient, as can oedema if it causes a rise in interstitial pressure, for example when due to venous hypertension. Finally, external compression of an upstream lymphangion may cause a transient increase in inlet pressure that could lead to a switch from pump to conduit behaviour (Quick et al., 2009, Quick et al., 2007).

There is evidence that flow induced inhibition of lymphatic pumping may be regulated by nitric oxide (NO), as this effect could be recapitulated by addition of NO in the absence of flow, and abolished even in the presence of flow by NO synthase inhibition (Gashev et al., 2002). This perhaps gives some insight into a mechanism by which the lymphatic vessel may switch from pump to conduit: when flow imposes a positive pressure gradient, the lymphatic endothelium is stimulated to release NO, which acts on the lymphatic smooth muscle to reduce contractions and allow the passive flow of lymph.

1.5 The extracellular matrix and vascular basement membrane

The extracellular matrix (ECM) is a complex meshwork of proteins and sugars, which surrounds and supports cells, tissues, and organs providing a protective and structural scaffold. Different organs and tissues express distinct ECM components, which partly helps them to perform their individual functions (Cox and Erler, 2011). One such specialised extracellular matrix is the basement membrane. This was originally identified by electron microscopy as an acellular, sheet-like structure, about 50-100 nm thick, which is always associated with cells (Sasaki et al., 2004, Kalluri, 2003). Similarly to the case with SMC and pericytes, far more is known about the composition, structure and function of blood vascular than lymphatic basement membranes.

1.5.1 Vascular basement membrane function

Vascular basement membranes consist predominantly of Collagen IV, Fibronectin, Nidogen/Entactin, Laminin and heparan sulfate proteoglycans (HSPGs) and the importance and distinct functions of individual matrix components can be assessed by studies of mouse knock-out models (reviewed in (Aszodi et al., 2006)).

For example, loss of Laminin β1 or γ1 leads to early embryonic lethality and the failure to assemble any basement membrane, while *Lama1*$^{-/-}$ mice survive slightly longer, due to partial compensation from Laminin-α5, which is expressed in many of the same tissues. However, this rescue is incomplete, and Laminin-α1 deficient mice still die by E7.5 (Miner et al., 2004). Collagen IV and Perlecan deficient mice assemble basement membranes, but these are weaker and prone to rupture in areas of mechanical stress, indicating that Collagen IV and Perlecan are necessary to maintain basement membrane integrity (Poschl et al., 2004, Costell et al., 1999). The phenotype of *Col4a1/2*$^{-/-}$ mice is the more severe of the two and while the blood vasculature develops and recruits pericytes in the absence of Collagen IV, there are spatial irregularities and the capillaries are dilated, suggesting that Collagen IV is required for the proper organisation of local capillary networks and demonstrating the importance of an intact basement membrane for vascular stability (Poschl et al., 2004). This is confirmed by studies of other vascular basement membrane components. Embryonic lethality of Laminin-α5 deficient mice is probably attributable in part to defects in placental vascularisation. Although there is BM associated with the endothelium of these embryos, it is discontinuous and of variable width. The vessels themselves display increased diameters and reduced branching compared to controls, thus reducing the surface area available for gas and nutrient exchange and indicating that Laminin-α5 has an essential role in development of the placental vasculature (Miner et al., 1998). Laminin α4 is another laminin isoform widely distributed in vascular basement membranes and *Lama4* deletion leads to disorganisation and collapse of microvessels, both embryonically and in the adult, due to deficient formation and stability of capillary basement membranes (Thyboll et al., 2002). Contrary to the case of laminin isoforms, where blood vessels can still form in their absence, although their stability may be compromised (Davis and Senger, 2008), deletion of Fibronectin results in loss, or severe deformity of the dorsal aorta and the embryonic vasculature is severely deficient (George et al., 1993).

1.5.2 Regulation of cell behaviour by the vascular basement membrane

It is well established that the vascular basement membrane is vitally important for providing structural support and stability to the vessels. However, it is also involved in regulating cell behaviour, such as migration, differentiation, survival and proliferation and can mediate efficient communication between endothelial cells, without the need for direct cell-cell contact (reviewed in (Davis and Senger, 2005, Aszodi et al., 2006)(Kruegel and Miosge, 2010).

One important way in which the vascular basement membrane regulates cellular behaviour is by binding to and influencing growth factor signalling. VEGF is a powerful pro-angiogenic growth factor that promotes endothelial cell migration and proliferation. It is alternatively spliced to give rise to 4 different isoforms, which bind variously to Heparan Sulfate Proteoglycans (HSPGs) in the ECM. The longest forms of VEGF, $VEGF_{206}$ and $VEGF_{189}$ are almost entirely matrix-bound, while the shortest form, $VEGF_{121}$ is always soluble. $VEGF_{165}$ behaves in an intermediate manner: 50-70% $VEGF_{165}$ can be released from the matrix upon heparin treatment (Houck et al., 1992). Matrix-bound VEGF can be released by proteolytic processing by either the serine protease Plasmin, or by MMPs 3, 7, 9 and 19 (Houck et al., 1992, Lee et al., 2005). Both bound and soluble VEGF are capable of activating VEGFR2, but they elicit different signalling responses (Lee et al., 2005). It is possible that in the quiescent vasculature, cross-linking of the ECM, or HSPG conformation, may mean that matrix-bound VEGF is not freely available for receptor binding, and VEGF is therefore sequestered by the matrix and can be released upon pro-angiogenic stimulus (Kalluri, 2003). Or, alternative splicing of VEGF may enable efficient formation of growth factor gradients, since the shorter forms would diffuse further, and activate endothelial cells via VEGF receptor binding at a distance to the angiogenic site, thus providing spatially regulated angiogenic cues to direct vascular morphogenesis (Ruhrberg et al., 2002). However, because the longer forms of VEGF are more mitogenic than the short forms, the angiogenic signal would be weaker at this distal site than closer to the matrix-bound VEGF (Ferrara, 2010). VEGF can also bind the heparan II binding

domain of Fibronectin and activate endothelial cell proliferation, migration and Erk activation, but only when the VEGF-binding and cell-binding sites are in the same molecule, suggesting that both VEGFR2 and Integrin-α5β1, a Fibronectin cell-surface receptor, must be side by side to potentiate this response (Wijelath et al., 2006). Another example of ECM positively regulating growth factor signalling is PDGF-B binding to Heparan Sulfate. The Heparan Sulfate binding domain on PDGF-BB is required for pericyte recruitment and PDGF-BB retention at the cell surface (Abramsson et al., 2003). Similarly, reduced Heparan Sulfate N-sulfation in *Ndst1*$^{-/-}$ mice, which lack a N-deacetylase/N-sulfotransferase enzyme, resulted in reduced PDGF-BB binding *in vitro* and delayed pericyte migration towards and retention on the endothelium *in vivo*, thereby demonstrating a requirement for Heparan Sulfate binding for efficient PDGF-BB signalling (Abramsson et al., 2007). On the other hand, HSPG sequestration of HB-EGF prevents proteolytic processing of the transmembrane form of the protein and release of the soluble form of HB-EGF, which induces cell proliferation and migration responses. Instead, sequestration promotes juxtacrine HB-EGF signaling, which leads to growth inhibition (Prince et al., 2010).

1.5.3 Contribution of EC and SMC to the vascular basement membrane

The vascular basement membrane is produced by, and shared between endothelial and smooth muscle cells / pericytes. Co-culturing endothelial cells with smooth muscle cells increases the amount of basement membrane proteins produced by both cell types, compared to that produced in single cell-type cultures, and the onset of basement membrane deposition in the quail embryo coincides with SMC recruitment to the blood vessels (Stratman et al., 2009a). Although most work has concentrated on the function of basement membrane proteins in regulating endothelial cell behaviour, the basement membrane is also important for regulating smooth muscle cell behaviour and function. ECM derived from either SMC, macrophages or EC can induce SMC proliferation, but interestingly only ECM derived from SMC or macrophages can enhance SMC production of proteoglycans (Figueroa et al., 2004). The *in vivo* effect of basement

membrane components on SMC behaviour and function has been investigated recently. For example, when Heparan-sulfate (HS) is deleted specifically from mural cells (MC) *in vivo*, it results in reduced pericyte recruitment and an increase in both sprouting and regression of nascent blood vessels. Interestingly, the requirement for HS in mural cells seems to be spatially dependant; MC that are already in contact with the endothelium can still attach to the vessel; ie the deficiency can be rescued by deposition of endothelial-derived HS in the BM, whereas MC further from the endothelium require HS cell-autonomously in order to polarise and migrate to the nascent blood vessels (Stenzel et al., 2009). Also, when a dominant negative missense mutation is inserted into the *Col4a1* chain, which results in a highly conserved lysine residue being replaced by a glutamic acid, it leads to age dependent defects in both endothelial and smooth muscle cell function. These defects include reduced contractile strength, impaired response to Nor-epinephrine in mice over 6 months old, and increased sensitivity to NO at 11 months old. From this age endothelial cells also showed increase vasodilation responses to acetylcholine, suggesting an overall upregulation of the NO-cAMP pathway in $Col4a1^{+/raw}$ mice, which results in maintenance of the low blood pressure that is caused by a reduced red blood cell count in these mice (Van Agtmael et al., 2010).

1.5.4 Lymphatic basement membrane

In contrast to the blood vasculature, very little is known about the composition of the lymphatic basement membrane and knowledge about the function of individual basement membrane components is fragmentary at best. Although for a long time it was believed that lymphatic vessels were devoid of basement membranes, recent studies have identified an irregular basement membrane around lymphatic capillaries (Pflicke and Sixt, 2009, Vainionpaa et al., 2007). However, although Pflicke and colleagues noted that the basement membranes around collecting vessels did not contain the same discontinuities that were observed in the capillaries, there has been little investigation of

the difference between basement membranes in collecting vessels vs. capillaries and how this might influence their individual vessel function.

However, interactions of the lymphatic vessels with their extracellular environment are starting to be recognised as a potentially important modulator of lymphatic function (Ji, 2006, Avraamides et al., 2008, Wiig et al., 2010, Paupert et al., 2011).

One ECM protein known to be important for lymphatic function is Emilin-1, a major component of the anchoring filaments attaching lymphatic capillaries to the interstitial matrix. *Emilin-1* deficiency leads to a defect in lymph formation and the lymphatic capillaries become hyperplastic, vessel density increases and they fail to respond to changes in interstitial pressure (Danussi et al., 2008).

Another well-characterised role for the ECM in lymphatic function is that of Integrin-α9 and its ECM ligand, Fibronectin (FN) EIIIA. *Itga9* deficient mice develop chylothorax and die within 6-12 days of birth (Huang et al., 2000), and it was subsequently shown that Integrin-α9 could be up-regulated by Prox-1 (Mishima et al., 2007), suggesting a role in lymphatic development. Within the lymphatic vessels, Integrin-α9 is highly expressed in lymphatic valves and loss of *Itga9* (in either a full mutant or endothelial-cell specific knock-out) leads to a failure to form functional valve leaflets (Bazigou et al., 2009). Instead, ring-like constrictions develop, which do not have an organised matrix core between the valve leaflets and are incapable of preventing lymph backflow. *In vitro*, Integrin-α9 binds to Fibronectin containing the EIIIA domain (FNEIIIA), Tenascin-C (TNC) and Osteopontin, but failure to form normal valves in *FNEIIIA* mutants and disorganisation of the FNEIIIA matrix core in *Itg-α9*$^{-/-}$ mice identified FNEIIIA as the physiologically relevant Integrin-α9 ligand in lymphatic valve morphogenesis, and identified a functional role for this extracellular matrix component in lymphatic development (Bazigou et al., 2009). More recent work has also implicated tumour-derived FNEIIIA in enhancing LEC tubulogenesis and branching *in vitro*, suggesting another potential role for this ECM protein in tumour induced lymphangiogenesis (Ou et al., 2010).

Other integrins have also been implicated in lymphangiogenesis, although their role is less well characterised. For example, Integrin-α5 small molecule inhibitors reduced lymphangiogenesis *in vivo* in a model of inflammatory corneal lymphangiogenesis. Interestingly, BECs were less sensitive to Integrin-α5 inhibition and at small inhibitor doses lymphangiogenesis could be selectively inhibited, without affecting angiogenesis (Dietrich et al., 2007). Integrin-α4β1, another FN receptor, has also been implicated in both growth factor and tumour induced lymphangiogenesis. It is expressed only on proliferative LECs and lymphatic vessels, and promoted LEC adhesion and migration on cellular FN *in vitro.* *In vivo,* VEGF-C induced lymphangiogenesis was inhibited by Integrin-α4β1 antagonists or in mice lacking Integrin-α4 in endothelial cells (Garmy-Susini et al., 2010).

The role of other ECM proteins such as collagen and laminin in lymphatic development is even less well defined. Clavin et al. (2008) showed that lymphatic regeneration after skin wounding was enhanced when a Collagen I gel was used to cover the wound. This lead to down-regulation of TGFβ1, and a corresponding increase in infiltration and proliferation of LECs, alongside decreased inflammation and lymphoedema compared to mice lacking the Collagen I gel, which still expressed high levels of TGFβ1 in the ECM. Over-expression of TGFβ1 in Collagen treated mice negated all the beneficial effects, demonstrating that Collagen I acted via regulation of TGFβ1 expression to enhance wound healing and lymphatic regeneration (Clavin et al., 2008). Anti-lymphangiogenic properties have also been suggested for Collagen XVIII and its proteolytic cleavage product, Neostatin-7, as is already known in the blood vasculature (Kojima et al., 2008).

Evidence of a lymphatic function for laminin is sparse, and slightly spurious. LEC medium was demonstrated to be chemotactic for melanoma cells, and this could be blocked with an anti-laminin 1 antibody. Immunoprecipitating the LEC conditioned medium revealed the presence of laminin α4, β2 and γ1 chains, suggesting that this laminin isoform is secreted by the lymphatic endothelium and facilitates melanoma metastasis to the lymphatics (Saito et al., 2009).

Finally, the role of matrix mellatoproteinases (MMPs) in lymphangiogenesis is yet to be clearly defined. In the blood vasculature, as well as processing individual BM proteins to release soluble or active fragments, degradation of the ECM by MMPs is an important first step in the induction of angiogenesis, allowing the EC greater mobility to sprout from the existing vessel (reviewed in (Arroyo and Iruela-Arispe, 2010)). For example, *Mmp1*$^{-/-}$ mice displayed no angiogenic response to FGF stimulation in a corneal angiogenesis model, compared to the efficient sprouting induced in wild type mice (Zhou et al., 2000). In addition, MT1-MMP is required for the formation of vascular guidance tunnels during EC lumenogenesis and tube formation in 3D collagen matrices. Once these tunnels have formed, they allow free movement of EC within them, without the need for further proteolysis (Stratman et al., 2009b). MMP inhibitors, such as Tissue Inhibitor of Metalloproteinase -2 (TIMP)-2 and TIMP3 can block EC migration and invasion into a 3D collagen, and TIMP3 treatment also prevents vasculogenesis and angiogenesis in the mouse embryo, further highlighting the importance of MMPs for angiogenesis (Saunders et al., 2006).

Within the lymphatic vasculature, MMP-9 was strongly up-regulated in the vicinity of lymphatic regeneration in a skin wound model, although its expression levels declined before the onset of lymphangiogenesis. Additionally, lymphatic regeneration was indistinguishable between wild-type and *Mmp9*$^{-/-}$ mice, suggesting that this protease is probably not involved in lymphangiogenesis (Rutkowski et al., 2006). However, MMP-2 was also up-regulated in the area of lymphatic regeneration, and its expression peaked at the onset of lymphangiogenesis. The potential role for MMP-2 in lymphangiogenesis suggested by this study was further supported by 3D lymphatic ring cultures, where TIMP-2 and an inhibitor of MMP-2, MMP-9 and MMP-14 strongly inhibited lymphatic sprouting and network formation. In addition to this, lymphangiomas grew less efficiently in *Mmp2*$^{-/-}$ than wild-type mice, suggesting that MMP-2 might be functionally important for lymphangiogenesis (Bruyere et al., 2008).

Although the importance of ECM proteins in lymphatic development and function is starting to be recognised, there is still much more work to do to fully understand the composition and function of the lymphatic basement membrane, how this may differ

between lymphatic capillaries and collecting vessels and how the basement membrane can affect lymphatic vessel development and function.

1.6 Reelin

Reelin is an extracellular matrix protein that was found to be upregulated in cultured LEC compared to BEC in microarray analyses (Petrova et al., 2002), however its potential function in lymphatic vasculature is not known. The full-length protein is 3461 amino acids (aa) long, with an N-terminus consisting of 500aa that shares 25% homology with the N-terminus of F-spondin. This is followed by eight 350-390aa repeats, each composed of two subdomains flanking a 30aa EGF motif. After the eighth repeat, there is a stretch of basic amino acids, comprising the C-terminus (D'Arcangelo et al., 1995, Tissir and Goffinet, 2003)(Figure 1.6). Two Reelin processing sites have been identified, one within the N-terminus, between repeats 2 and 3, and one at the C-terminus, between repeats 6 and 7 (Jossin et al., 2004), which give rise to five smaller Reelin fragments (Figure 1.6). A growing body of research has demonstrated that these proteolytic processing events are important for Reelin function (Jossin et al., 2007, Tinnes et al., 2011).

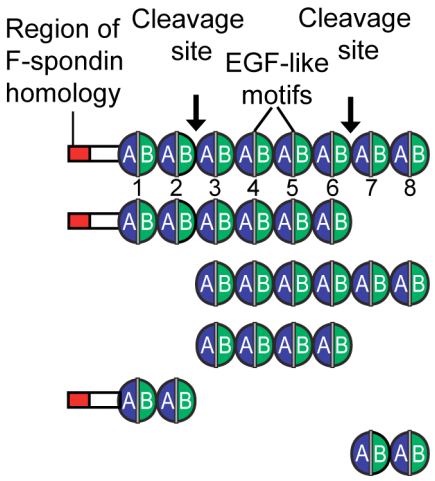

Figure 1.6 Schematic of Reelin structure and cleavage products
Adapted from Jossin et al., 2007.

The function and mechanism of Reelin signalling has been best characterised in the central nervous system, where it is involved in the development of laminar structures in the neocortex, hippocampus, cerebellum and spinal cord (Frotscher, 2010). In fact, a recent report identifying Reelin involvement in mammary gland morphogenesis (Khialeeva et al., 2011), and data from the lymphatic system described herein are the only reports of Reelin function outside the nervous system to date. The failure of correct cortical lamination is the primary, and most studied, defect in *Reln* deficient mice. During normal development, the cortex forms by a closely regulated program of sequential neurogenesis. Progenitor cells are located in the ventricular zone (VZ) and a thin primordium layer forms the pre-plate, just above it. After exiting the cell-cycle, the first waves of post-mitotic neurons migrate from the VZ into the middle of the pre-plate, thus splitting it into three layers; the marginal zone (MZ) on the surface, which remains cell-sparse throughout development and into adulthood, the cortical plate (CP), in which the newly migrated neurons reside, and the sub-plate (SP) underneath. Each successive wave of newborn neurons migrates along radial glial fibres, through the sub-plate and into the cortical plate, passing earlier-born neurons to reach their final position. Thus, early-born neurons are pushed into deeper layers by the migrating late-born neurons, which end up in the more superficial cortical layers – an 'inside out' pattern of cortical lamination (Dhavan and Tsai, 2001, Rice and Curran, 2001). There are six neuronal layers in the adult cortex, where layer I is the most superficial, the marginal zone, and layer VI the deepest (Figure 1.7)

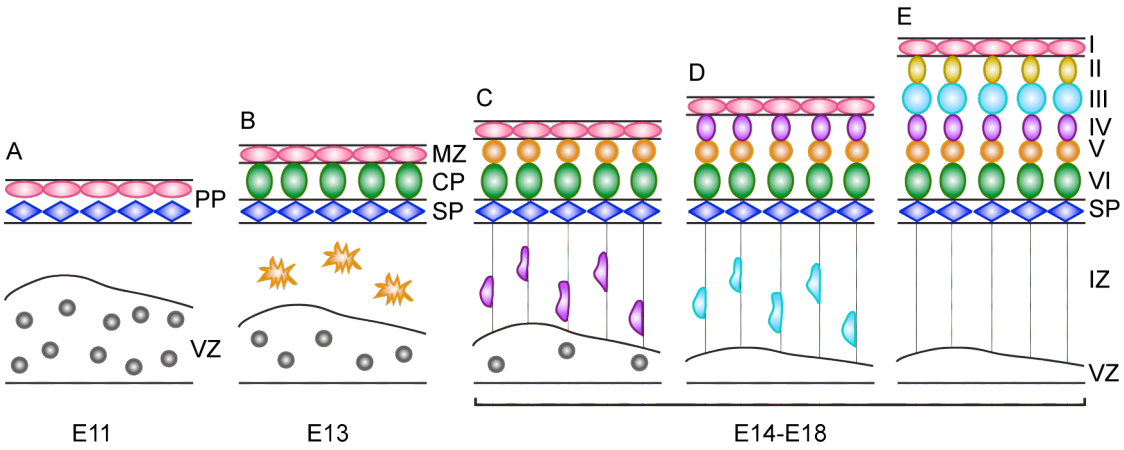

Figure 1.7 Normal cortical development.
The laminar structure of the cortex develops by a series of orchestrated neurogenesis and migration events. (A) During early embryogenesis, dividing neuronal progenitors occupy the ventricular zone (VZ), while a thin primordium layer makes up the pre-plate (PP). (B) The first neurons exit the cell cycle and migrate from the VZ through the intermediate zone (IZ), eventually resting within the pre-plate. This 'splits' the pre-plate into three layers, the marginal zone (MZ) at the top, nearest the pial surface, the cortical plate (CP) in the middle and the sub-plate (SP) underneath. (C-E) Later-born neurons migrate by glia-guided locomotion past earlier-born neurons, to rest in a more superficial layer of the cortical plate, thus giving rise to the 'inside out' pattern of cortical lamination. (E) The cortex is characterised by six distinct layers of neurons (I-VI), with the earliest born neurons in deeper layers, and those born later more superficial. Adapted from (Dhavan and Tsai, 2001).

During development, Reelin is predominantly expressed by a layer of Cajal-Retzius neurons in the MZ of the cortex and in deeper layers of the hippocampus and olfactory bulb (D'Arcangelo et al., 1995), while in the adult brain it is expressed by a population of GABAergic interneurons (Weeber et al., 2002).

In *Reln* deficient mice, post-mitotic neurons fail to split the pre-plate, which shifts towards the pial surface. Later born neurons cannot migrate past their predecessors and so accumulate in an ectopic 'super-plate' – the shifted pre-plate - in an inverted manner, such that later born neurons stay within deeper layers, while early-born neurons remain superficial. Furthermore, there is an ectopic accumulation of cells in the usually cell-free MZ (Forster et al., 2002) (Figure 1.8). Reelin mutation results in Norman-Roberts type Lissencephaly in humans, and deficiencies in Reelin function have also been

implicated in Alzheimer's disease, schizophrenia, autism, bipolar disorder, depression and epilepsy (reviewed in (Herz and Chen, 2006)).

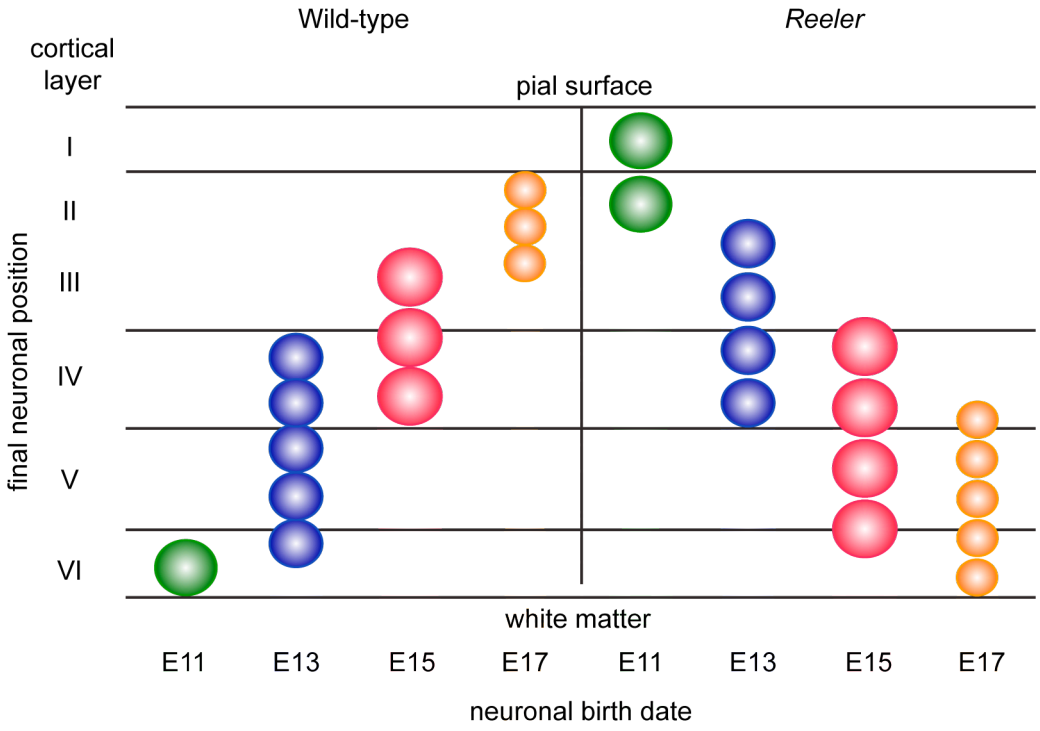

Figure 1.8 Inverted neuronal positions in *Reln* deficient mice.
Later born neurons in the *Reeler* mouse are born and specified correctly, but are unable to migrate past their earlier-born predecessors. This results in an inversion of normal cortical lamination, with early born neurons accumulating ectopically in layer I and in layer II, while late-born neurons stay in deeper layers. Adapted from (Rice and Curran, 2001).

The literature surrounding the mechanism of Reelin function in both the developing and adult central nervous system is both prolific and contradictory. Despite years of research, the complex actions of this protein are yet to be definitively elucidated and many conflicting models and hypotheses have been proposed (reviewed in (Zhao and Frotscher, 2010)). In order to discuss them, an understanding of the canonical signalling pathway is required first.

1.6.1 The canonical Reelin signalling pathway

1.6.1.1 ApoER2, VLDLR and Dab1

The major Reelin receptors are lipoprotein receptors ApoER2 and VLDLR, which are expressed in cortical and cerebellar layers adjacent to sources of Reelin signal. ApoER2 and VLDLR are expressed in somewhat different patterns and mutations in either receptor alone result in slightly different neuronal phenotypes, but overall the mice are grossly normal (Trommsdorff et al., 1999). However *Apoer2*$^{-/-}$*;Vldlr* $^{-/-}$ double mutants develop ataxia, wide-gait, tremors and falling from P13 and display an identical neurological phenotype to *Reln*$^{-/-}$, suggesting a high degree of redundancy in this pathway (Trommsdorff et al., 1999). Reelin binding to ApoER2 and VLDLR results in phosphorylation of the intracellular adaptor protein Dab1, which is necessary for the transmission of Reelin signal (Howell et al., 1999, Howell et al., 2000) (Hiesberger et al., 1999). *Scrambler* mice (*Dab1*^{Scm}), which have a spontaneous mutation in *Dab1*, develop an identical phenotype to that of *Reeler* mice, thus defining Dab1 as a critical downstream component of the canonical Reelin signalling pathway (Howell et al., 1997) (Sheldon et al., 1997). ApoER2 and VLDLR have no intrinsic enzymatic activity, but Dab1 is phosphorylated by members of the Src family of kinases (SFK) and SFK activity is in turn increased by Phospho-Dab1 in a positive feedback loop, which may be achieved by ligand clustering at the membrane (Bock and Herz, 2003). It is unknown how SFK are recruited to the Reelin signalling pathway, but a recent paper has suggested the involvement of EphrinBs (Senturk et al., 2011). Lack of *Fyn*, a SFK member, results in accumulation of total Dab1 protein and mild neuronal defects reminiscent of, but less severe than, those in *Reln*$^{-/-}$ mice. This suggests that Fyn is a likely candidate for the major mediator of Dab1 phosphorylation, but normal Phospho-Dab1 in *Fyn*$^{-/-}$ mice suggests compensation by other SFKs, probably Src (Bock and Herz, 2003, Arnaud et al., 2003). Reelin signalling also appears to be negatively regulated by Dab1 degradation, as stimulating primary neuronal cultures with Reelin for 3-5 days lead to a 30% decrease in over-expressed Dab1 and an 80% reduction in

endogenous Dab1 (Feng et al., 2007). Further experiments revealed that Reelin-induced Dab1 phosphorylation at a specific YXQI motif leads to recruitment of SOCS (Suppressor Of Cytokine Signalling) proteins, which target Dab1 for ubiquitination and degradation. Electroporation of Cullin (Cul)5 shRNA *in vivo* and *in vitro* protected Dab1 from degradation and *Cul5*$^{-/-}$ mice had increased levels of phospho-Dab1, suggesting that Cul5, an E3 ubiquitin ligase was ultimately responsible for Dab1 degradation (Feng et al., 2007).

ApoER2/VLDLR binding and Dab1 phosphorylation have been clearly identified as upstream components of the Reelin signalling pathway through which the majority of Reelin signalling appears to be transmitted (Figure 1.9). However, the downstream signalling pathway is more complex and consists of multiple strands.

1.6.1.2 Regulation of Tau phosphorylation

Tau proteins bind to and stabilise microtubules when in a hypophosphorylated state. Reelin inhibits Tau phosphorylation, thereby promoting stabilisation of microtubules, via activation of PI3K (Phosphatidylinositol 3-Kinase). Recruitment of the p85α subdomain of PI3K to phospho-Dab1 allows PI3K activation, which is dependent on SFK (Bock et al., 2003). PI3K activation stimulates Protein Kinase B (PKB), the main cellular kinase responsible for inhibition of Glycogen synthase kinase 3β, which phosphorylates Tau (Beffert et al., 2002). *Reeler, Apoer2*$^{-/-}$*;Vldlr*$^{-/-}$ and *Dab1*^{Scm} brains show accumulation of hyperphosphorylated Tau, which leads to its dissociation from microtubules and disruption of the actin cytoskeleton, thus indicating a requirement for all upstream components of the canonical Reelin signalling pathway in regulation of Tau phosphorylation and microtubule stability (Hiesberger et al., 1999, Beffert et al., 2002) (Figure 1.9).

1.6.1.3 C3G/Akt phosphorylation

Another strand of the Reelin signalling pathway was elucidated by creation of a neuronal specific *Crk/CrkL* deficient mouse with defects strikingly similar to those of the *Reeler* mouse, including in the cortex, where there was a failure to split the cortical pre-plate, accumulation of neurons with no lamina structure in a super-plate below the pial surface and the presence of cells in the cell-free MZ. Normal Dab1 phosphorylation and turnover in these mice placed Crk and CrkL downstream of Dab1. Additionally, C3G and Akt, which regulate neuronal adhesion and migration, were not phosphorylated in *Crk/CrkL* deficient mice (Park and Curran, 2008). Recently, migration defects in *Dab1* mutant mice were recapitulated by interfering with Rap1 signalling, which is controlled by C3G. The same phenotype was also observed by expression of a dominant negative Cadherin construct, or Cadherin 2 shRNA in migrating neurons, suggesting that cadherins are required cell autonomously to stabilise the leading edge of migrating neurons. Rescue of Rap1 disruption by cadherin overexpression placed cadherins, such as Cadherin 2, downstream of Rap1 (Franco et al., 2011) (Figure 1.9).

1.6.1.4 N-cofilin-serine3 phosphorylation

Finally, N-cofilin is an actin depolymerising protein that promotes disassembly of F-actin, but when it is phosphorylated at Serine 3, it is no longer able to depolymerise F-actin, thereby stabilising the cytoskeleton. Reelin increases N-cofilin phosphorylation at Serine 3, and LIMK1 activity (which is the major N-cofilin phosphorylating kinase) both *in vivo* and *in vitro*. This effect was abolished when cortical slices were treated with PI3K inhibitors and in mice lacking *Dab1*, placing LIMK1 and N-cofilin downstream of Dab1 and PI3K (Chai et al., 2009).

Although complex, all strands of the signalling pathway elucidated thus far seem to link Reelin to regulation of cytoskeletal organisation and stability (Figure 1.9), although it is not known whether Reelin acts through all pathways simultaneously, or mediates different functions through different pathways; in which case it is unclear how one pathway is selected over another. Combined with the migration defects visible in *Reln*$^{-/-}$ mice, there seems to be a clear involvement of Reelin in correct migration and cytoskeletal organisation of neurons and glia. However, it is less clear whether this involvement involves regulation of migration initiation, continuation or termination.

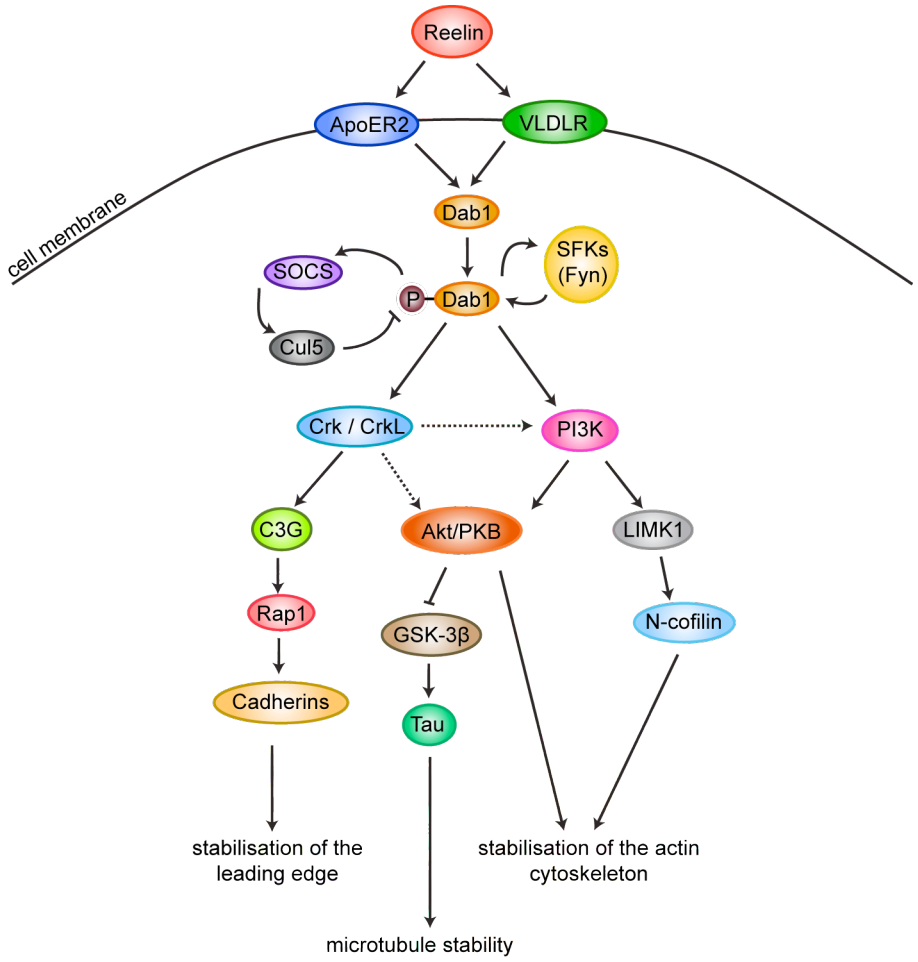

Figure 1.9 Reelin signalling pathway.
Reelin canonical signalling pathways and downstream effectors. Dashed arrows: AKT phosphorylation at serine 473 is positively regulated by Crk/CrkL(Park and Curran, 2008), which suggests that these proteins may be upstream of the PI3K/Akt signalling pathway.

The following discussion of Reelin functions during development, concentrating on its roles in the cortex and hippocampus, as well as functions in the adult, will highlight some of these controversies and identify some possible models of Reelin function.

1.6.2 Reelin as a pro-migratory signal

There are two main mechanisms by which newborn post-mitotic neurons exit the ventricular zone. Early-born neurons migrate via somal translocation, when distances are short, and the neuronal leading processes can reach from the VZ to the pre-plate. As sequential waves of neurons are born and begin to migrate, the distance from the VZ to the superficial layers gets longer, and the leading processes no longer reach the entire distance. In this case, neurons traverse the intermediate zone (IZ) and cortical plate via glia-dependant locomotion, which involves using radial glial fibres as a guiding scaffold. These late-born neurons revert to somal translocation during their terminal migratory phase, when their leading process has reached the marginal zone and they have detached from the glia. Both means of migration involve extension and stabilisation of the neuronal leading process, movement of the nucleus towards it, and retraction of the trailing edge (reviewed in (Frotscher, 2010).

A requirement for Reelin for somal translocation has recently been identified. It was previously established that, like *Reeler* mice, *Dab1*^{Scm} neurons fail to extend processes into, or migrate into the pre-plate, suggesting that Reelin transmits a permissive signal to initiate migration (Sanada et al., 2004). Detailed studies of a conditional *Dab1* knock-out mouse, in which *Dab1* was deleted specifically in post-mitotic, but pre-migratory neurons at varying developmental stages, determined that Dab1 was required for both initial and terminal neuronal somal translocation, which depends upon stabilisation of the leading edge by cadherins, via Rap1 (Franco et al., 2011). However, in the absence of Dab1, late born neurons could still extend processes, polarise and migrate past early-born neurons normally, so Dab1 is not required for glia-guided

migration (Franco et al., 2011). While this study suggested that Dab1 is not required for glial dependant migration, injection of *Dab1* RNAi at E16, when glia-guided migration is underway, and analysis at E20 or E21 showed that *Dab1* deficient neurons lagged behind their wild-type counterparts, suggesting that Reelin signalling does promote migration of late-born neurons in their glial-guided locomotion stage (Olson et al., 2006). However, this study used RNAi injection, rather than neuronal specific *Dab1* deletion, so concomitant deletion of *Dab1* in glial cells and an effect of Reelin on glial-guided locomotion by directly affecting glial cells cannot be ruled out.

In fact, Reelin is also required for correct formation of the radial glial scaffold in both the cortex and the hippocampus. Fewer glial cells extend long processes in *Reeler* mice, frequently failing to reach the MZ. Culturing glial cells from *Reeler* mice in Reelin-containing medium induced process formation, thereby demonstrating that this is a direct effect of Reelin signalling on the glial cells (Hartfuss et al., 2003). Furthermore, stripe choice assays on hippocampal slice cultures revealed that while neurons and their processes showed no preference for Reelin or control stripes, $GFAP^{+}$ radial glial cells strongly preferred Reelin stripes, and Reelin promoted branching of glial processes, similar to what is observed in the Reelin positive wild-type MZ (Forster et al., 2002).

Additional evidence for a pro-migratory function for Reelin in cortical development comes from rescue experiments, where it was demonstrated that exogenous Reelin either applied globally to *Reeler* cortical slice cultures, or expressed ectopically in the VZ (where it is not usually expressed), were able to rescue initial migration defects, including splitting the pre-plate. Global application of Reelin to cortical slice cultures was also able to rescue neuronal layer formation (Jossin et al., 2004), although ectopic Reelin expression in the VZ did not rescue cortical lamination and cell layers were even more mixed than in $Reln^{-/-}$ mice (Magdaleno et al., 2002). This suggests that while Reelin might be initially performing a pro-migratory function, it may also be acting to promote cell-cell interaction to mediate proper migration and layer formation. Another explanation as to why cortical lamination could not be completely rescued by ectopic Reelin expression in the VZ is that perhaps Reelin needs to be expressed in its normal location in order to fully rescue the *Reeler* phenotype. This was observed in the

hippocampus, where addition of exogenous Reelin could rescue $GFAP^+$ glial fibre length, but not orientation or granule cell (GC) lamination. This could only be rescued by Reelin expression in its normotropic location, by wild-type co-culture with the Reelin-expressing dentate gyrus in close apposition to the *Reeler* granule cell layer (Zhao et al., 2004).

1.6.3 Reelin as a stop signal

While there is plenty of evidence for a pro-migratory function for Reelin during development, there is also evidence suggesting the opposite. Firstly, the over-migration of neurons into the MZ in *Reeler* mice suggests that Reelin normally provides a 'stop' signal telling neurons that they have reached the correct destination (Frotscher et al., 2009). This is also observed in mutations in components of the signalling pathway, such as $Apoer2^{-/-};Vldlr^{-/-}$ and $Cul5^{-/-}$ (Trommsdorff et al., 1999, Feng et al., 2007). $Dab1^{Scm}$ neurons were shown by GFP electroporation and subsequent clonal analysis of radial glia and their neuronal progeny to be significantly closer apposed to the glial cells than wild-type neurons, which could suggest a failure to detach properly from the glial cell - an essential part of migration termination (Sanada et al., 2004). Reelin-induced inhibition of neuronal migration and detachment from the radial glial scaffold was shown by timelapse photography *in vitro* and by addition of Reelin coated fluorescent microspheres to the cerebral wall *in vivo*. This lead to a neuron-free area around the bead, suggesting either cessation of neuronal migration, avoidance of the Reelin coated bead, or premature neuronal detachment from the glia (Dulabon et al., 2000). Stabilisation of the actin cytoskeleton could also be indicative of a role for Reelin in terminating or preventing migration. All the known downstream effectors of Reelin signalling are involved in maintenance of cytoskeletal stability. For example, while hippocampal neurons extended processes equally onto Reelin or control substrate in a stripe choice assay, those processes on the Reelin stripes showed reduced filopodia and increased serine-3-phosphorylation of N-cofilin. Time-lapse microscopy confirmed this

and showed continued growth of neuronal processes on control substrate, while those on Reelin stopped (Chai et al., 2009).

1.6.4 Reelin in the adult brain

Some Reelin functions in the adult may also give an insight into the mechanisms of Reelin function during development. For example, temporal lobe epilepsy is accompanied by granule cell dispersion (GCD). Kainate (KA) injection, which induces focal epileptic regions and is a mouse model for temporal lobe epilepsy, also induces GCD and a decrease in Reelin expression. Since GCD is also observed in *Reln* deficient mice, and when Reelin function is blocked by injection of the CR-50 function-blocking antibody, it was hypothesised that the Reelin deficiency observed after KA injection might be the cause of GCD in models of temporal lobe epilepsy (Heinrich et al., 2006). This was further demonstrated by the rescue of GCD (although not other cellular changes, such as KA-induced cell death, loss of neurogenesis or hypertrophy of the glial scaffold) by perfusion of exogenous Reelin (Muller et al., 2009). Therefore, Reelin might play a role in maintaining the stability of the adult cyto-architecture by preventing further migration of mature neurons.

Neurogenesis and neuronal migration continue after birth in the forebrain, where neurons migrate from their birthplace in the subventricular zone (SVZ) to the olfactory bulb, their final destination. The mechanism of neuronal migration in this system is distinctive, with the neurons moving as a co-ordinated chain, and forming a well-defined pathway called the rostral migratory stream (RMS) (Hack et al., 2002). In the postnatal olfactory bulb, Reelin is not required for the initiation or early stages of migration, as this occurs normally in *Reeler* mice, however individual cells fail to detach from the RMS, giving rise to a disorganised distribution of neurons over the entire granule cell layer, instead of forming organised layers (Hack et al., 2002). This is supported by *in vitro* data, which showed Reelin promoting detachment of individual cells from tangentially migrating chains of neurons growing from subventricular zone

explants, thus suggesting a role for Reelin in mediating neuronal detachment from the RMS, which is an essential step for terminating migration and finally differentiating. These findings have recently been corroborated by experiments with a transgenic mouse line that over-expresses Reelin in the postnatal and adult forebrain, causing increased detachment of neuronal precursors from the RMS (Courtes et al., 2011). However, contrary to detachment as a means to terminate migration, this study emphasises the potential for further migration of neuronal precursors detached from the RMS by ectopic Reelin, as evidenced by their increased dispersal. This is given functional relevance by the observation that Reelin is up-regulated around lesions in the adult brain and that when Reelin is over-expressed, there is an increase in progenitor cell recruitment to the lesion, and a corresponding reduction in the number of progenitors around lesions in *Reln* deficient mice, potentially implicating Reelin as a therapeutic target in treatment of adult brain lesions (Courtes et al., 2011).

1.6.4.1 Synapatic plasticity

Studies of *Apoer2*$^{-/-}$ and *Vldlr*$^{-/-}$ single mutant mice identified a role for Reelin in modulating synaptic plasticity in the adult. A widely used indicator of synaptic plasticity is measurement of long term potentiation (LTP), which is a long-term enhancement of signal transmission between two synapses and is believed to be a major cellular mechanism underlying learning and memory. Both *Apoer2*$^{-/-}$ and *Vldlr*$^{-/-}$ mice show defects in fear conditioning and induction of LTPs, although this is much more severe in *Apoer2* deficient mice. Enhancement of LTPs after perfusing hippocampal slices with Reelin demonstrated that Reelin might induce LTPs, and the abrogation of Reelin induced LTP enhancement in either *Apoer2*$^{-/-}$ or *Vldlr*$^{-/-}$ mice suggested that these two receptors act in a non-redundant manner in this system (Weeber et al., 2002). The stronger LTP inhibition in *Apoer2* deficient mice suggested a key role for this receptor in modulation of Reelin induced synaptic plasticity, which was subsequently demonstrated to rely upon an alternatively spliced domain in the intracellular region (Beffert et al., 2005). The mechanism by which Reelin modulates synaptic plasticity

has now been described. Reelin signalling, which in this system is still dependant on ApoER2, VLDLR, Dab1 and SFKs, increases synaptic responses to glutamate, by tyrosine phosphorylating and increasing Ca^{2+} flux through the NMDA receptor; a glutamate receptor that is thought to be the primary molecular device for modulating synaptic plasticity (Chen et al., 2005). These studies all used addition of exogenous Reelin to elucidate its function at the synapse, but close analysis of *Reln* haploinsufficient mice also revealed a role for endogenous Reelin. An extensive array of behavioural tests showed that *Reln*$^{+/-}$ mice showed hippocampus specific impairment in acquiring or retaining long-term associative fear conditioned memory. This is coupled to reduced short and long-term synaptic plasticity, measured by reduced LTPs and paired pulse facilitation (PFF; an increase in post-synaptic potential evoked by a second impulse. This is a widely used measure of short-term synaptic plasticity) (Qiu et al., 2006). Molecularly, the reduction in synaptic plasticity of *Reln* haploinsufficient mice is accompanied by significant reductions in the post-synaptic proteins Postsynaptic density protein 95 (PSD-95), the NMDA receptor subunits NR2A and NR2B and the phosphatase PTEN, which were all shown by co-immunoprecipitation of the whole brain synaptosome to interact at the synapse, perhaps suggesting that Reelin not only regulates phosphorylation and Ca^{2+} flux through the NMDA receptors, but also expression of these essential post-synaptic proteins (Ventruti et al., 2011).

In summary, the cellular functions and mechanisms of Reelin signalling are highly complex. Reelin appears to be able to both initiate and terminate migration; both by modulating cytoskeletal stability, and to carry out different functions in different tissues. Furthermore, within the same tissue Reelin appears to be able to mediate opposite effects on different cell types, for example increasing branching of glial processes (Forster et al., 2002), but inhibiting growth and branching of neuronal processes (Chai et al., 2009). Some of this complex functionality may be regulated by signalling via different intracellular signalling pathways, or by interacting with (and moderating the function of) other signalling pathways, for example the NMDA receptors at the synapse. Alternatively, some different Reelin functionality may be explained by differential signalling through either ApoER2 or VLDLR.

1.6.5 Differential roles of ApoER2 and VLDLR

The expression patterns of ApoER2 and VLDLR are slightly different, for example *Vldlr* is abundant on the intermediate zone and cortical plate immediately adjacent to Reelin expressing cells, whereas *Apoer2* is expressed in post-mitotic neurons en route to, or at their final destination (Trommsdorff et al., 1999). Fate mapping studies of individual neurons in the single receptor mutants revealed divergent functions for each receptor. In the absence of *Apoer2*, early-born layer V and some layer IV neurons migrate normally, but late-born layer IV and layer II-III neurons fail to migrate and stay close to the VZ (Hack et al., 2007). This suggests a role for ApoER2 in facilitating proper migration of late-born neurons. Conversely, VLDLR appears to mediate the Reelin 'stop' signal. Mice lacking *Vldlr* show ectopic invasion of interneurons and pyramid cells, some of which are misoriented, into the usually cell-sparse MZ, recapitulating the over-migration phenotype in the *Reeler* cortex and suggesting the absence of a proper 'stop' signal (Hack et al., 2007). Part of these different receptor functions may be dependant on their distinct membrane localisation and subcellular properties. For example, ApoER2 is localised to lipid rafts domains of the cell membrane, while VLDLR is not, which gives rise to different endocytosis properties. Reelin is endocytosed rapidly upon binding to VLDLR, but Reelin bound to ApoER2 is stable (Duit et al., 2010). Other differences include ApoER2 cleavage upon Reelin binding, which is also dependant on lipid raft localisation and ApoER2, but not VLDLR, degradation in lysosomes after endocytosis. These specific subcellular properties of the Reelin receptors may influence their function – perhaps triggering activation of different intracellular signalling pathways, or determining the outcome of Reelin signalling (Duit et al., 2010).

1.6.6 Aims of this work

The divergent functions of lymphatic capillaries and collecting lymphatic vessels in uptake and transport of lymph have been well characterised, but the process by which these two distinct vessel types develop from the uniform primary plexus and how the differences between them help to mediate their specific functions is less clear.

The overall aim of my project was to investigate how defining features of collecting lymphatic vessels, such as SMC coverage and an intact BM, contribute to collecting vessel development and function.

To accomplish this, the specific objectives in this project were:

1) Characterisation of the events leading up to differentiation of dermal collecting vessels, such as SMC recruitment and BM deposition, by whole-mount immunofluorescence of mouse ear skin
2) Identification of lymphatic-specific extracellular matrix proteins by microarray analysis of blood and lymphatic vessels

From this, we identified Reelin as an ECM protein that was specifically expressed in the lymphatic vessels. The subsequent objectives of my project then became:

3) Characterisation of Reelin expression in the developing and mature vasculature
4) Determination of the function of Reelin in lymphatic development *in vivo*
5) Investigation of the mechanisms of Reelin signalling in lymphatic vasculature

Chapter 2. Materials and Methods

2.1 Mice

Reeler (D'Arcangelo et al., 1995), *Dab1*^{Scm} (Ware et al., 1997), *Lyve1* (Gale et al., 2007) and *R26-mTmG* (Muzumdar et al., 2007) mice were obtained from the Jackson Laboratory. *Apoer2*$^{-/-}$ (Trommsdorff et al., 1999), *Vldlr*$^{-/-}$ (Frykman et al., 1995), *Efnb2*^{lx} mice (Grunwald et al., 2004) and *Efnb2*^{GFP} (Davy and Soriano, 2007) have been described previously and were obtained from their originators. The *Prox1-creER*^{T2} line was generated by Taija Makinen as described in Bazigou et al., 2011. To induce Cre recombination, a single dose of 0.5mg 4-OHT dissolved in Peanut Oil was administered by intraperitoneal injection at P7 or P12, as indicated. *Dab1*^{Scm} mice were maintained in a C3HeB/FeJ * DC/Le background and *Efnb2*$^{lx/lx}$*;Prox1-creER*^{T2} mice were maintained in a mixed 129Sv/BL6 background. All other strains were maintained in a C57Bl/6 background.

Animal care and husbandry was provided by Cancer Research UK Biological Resources Unit (BRU).

I performed all experimental procedures myself. All maintenance, breeding and experimental procedures were carried out in accordance with UK legal and ethical standards and in accordance with the UK Coordination Committee on Cancer Research UK guidelines and Home Office regulation.

2.2 Genotyping

Ear and tail biopsies of mice, taken by members of the BRU or myself, were boiled at 95°C for 45 minutes in 'Hotshot' Buffer (25mM NaOH, 0.2mM disodium EDTA. pH 12). Immediately afterwards, samples were placed on ice and neutralised with an equal volume of 40mM Tris-HCL pH 5. Samples were stored at -20°C prior to commencing polymerase chain reaction (PCR).

PCR was performed using DreamTaq (Fermentas), DreamTaq Buffer (Fermentas) and 0.8mM dNTPs (Invitrogen). 1μL DNA sample was added to a total volume of 25μL PCR reaction. Details of primers, annealing temperatures and PCR conditions for each primer set are listed in Table 2.1.

The PCR reactions were run on a 1.5-2% agarose gel (Invitrogen), diluted in TAE buffer (40mM Tris, 20mM Glacial Acetic Acid, 1mM EDTA) containing 0.01-0.03mg/mL ethidium bromide (Sigma).

Efnb2^{GFP} mice were genotyped by visual examination of ear, tail or eye tissue to identify GFP-positive signal.

Dab1^{Scm}, *Apoer2*$^{-/-}$*;Vldlr*$^{-/-}$ and *Reln*$^{-/-}$ mice were identified by visual observation of phenotype (smaller size than wild type littermates, trembling, falling and unsteady gait). *Dab1* genotyping primers were designed against the insert responsible for the mutation, therefore the PCR reaction is not capable of distinguishing between mutant and heterozygous mice; identification of *Dab1*^{Scm} mice relies on visual examination of the phenotype.

Gene	Primers	Cycling conditions	Product size
Reln	(S): CTGCTACACAGTTGACATACCTTAATCTAC (AS): AGAGCCTAGAGGTTAGGGACACAACTCTTC (AS): TAAGGGAGTCCTGGTCTCTTTCTGTCTTTA	95°C 5min 30 cycles: 95°C 30 sec 63°C 30 sec 72°C 30 sec 72°C 5 min	WT: 150bp Mut: 300bp
ApoER2	(S): GATTGGGAAGACAATAGCAGGCATGC (AS): GCTTGTTGGAATTCAGCCAGTTACC (S): CCACAGTGTCACACAGGTAATGTG (AS): ACGATGACCCCAATGACAGCAGCG	94°C 1.5 min 38 cycles: 94°C 30 sec 56°C 45 sec 72°C 45 sec 72°C 2 min	WT: 520bp Mut: 420bp
VLDLR WT	(S): CAGTCTGCGTCATCATCACA (AS): CCCTGGAGAAAATCTGCGGGTTAAATA	94°C 3 min 36 cycles: 95°C 30 sec 62°C 1 min 72°C 1 min 72°C 5 min	WT: 400bp
VLDLR MUT	(S): CAGTCTGCGTCATCATCACA (AS): CCTCGTGCTTTACGGTATCGCCGCTC	95°C 3 min 36 cycles: 95°C 30 sec 62°C 30 sec 72°C 1 min 72°C 5 min	Mut: 200bp

Dab1	(S): CCCTGGGATAATGGGGTAAG (AS): AAGAATAAAGCTTTGTCGCAGAA	95°C 5 min 36 cycles: 95°C 40 sec 60°C 30 sec 72°C 1.5 min 72°C 5 min	110bp
Cre	(S): GCCTGCATTACCGGTCGATGCAACGA (AS): GTGGCAGATGGCGCGGCAACACCATT	95°C 5 min 35 cycles: 95°C 30 sec 63°C 30 sec 72°C 30 sec 72°C 5 min	800bp
LYVE-1 WT	(S): GACACCTTTGCCATTCCCACACC (AS): GCATCTAACCCAGCGAGCAGTCCGGTG	94°C 4 min 35 cycles: 94°C 30 sec 62°C 1 min 72°C 1 min 72°C 2 min	500bp
LYVE-1 MUT	(S): GCAGAGAGAGGGAGGAGG (AS): GCATCTAACCCAGCGAGCAGTCCGGTG	94°C 4 min 35 cycles: 94°C 30 sec 62°C 1 min 72°C 1 min 72°C 2 min	400bp

Table 2.1 PCR conditions used to genotype all mouse strains used in this thesis
S = sense, AS = anti-sense

2.3 Cell Culture

All cell lines were cultured at 37°C in 5% CO_2. 1% Penicillin/Streptomycin (Pen/Strep), 1% Glutamine and 0.1% Fungizone/Amphoterycin B (Sigma) was added to all growth media, unless otherwise stated.

Human lymphatic endothelial cells (LEC) were isolated from primary dermal microvascular endothelial cell cultures (PromoCell) using rat antibody to human Podoplanin (NZ-1, Angiobio) and Mini/MidiMACS magnetic separation system (Miltenyi Biotech), by Sherry Xie as previously described (Makinen et al., 2001b). The cells were cultured on 2μg/ml Fibronectin (FN; Sigma) coated plates in Endothelial Cell Growth Medium Kit MV (Promocell) in the presence of 50ng/ml VEGF-C (R&D systems). Human venous smooth muscle cells (HUVSMC; Cellworks), or Human aortic smooth muscle cells (HAoSMC; Promocell) were cultured in Smooth Muscle Cell Growth Medium (Promocell) and used at passages 3-6. For co-culturing of LEC and HUVSMC, LEC were plated on FN coated plates at 80% confluency at least 4 hours before plating HUVSMC.

For immunoprecipitation of cell medium, both LEC and SMC were plated as above, but incubated in endothelial cell growth medium with 5% IgG-stripped FBS (PAA), plus supplements (Promocell). For culture of SMC in LEC-conditioned medium, LEC were cultured in IgG-stripped Endothelial Cell growth medium (as above) for two days. The medium was then collected and centrifuged to remove cellular debris, before being re-incubated on SMC, 50% pre-conditioned medium and 50% fresh IgG stripped medium. The same procedure was followed for incubation of LEC in SMC-conditioned medium.

2.3.1 Creating a fibroblast matrix

To create a fibroblast matrix, NIH-3T3 cells were grown in DMEM + 10% FBS. 4mL 0.2% gelatin was added to a 10cm dish and incubated for 1hr at 37°C, before washing with PBS. NIH-3T3 cells were collected in matrix medium (growth medium + 50μg/ml L-ascorbic acid, sodium salt (Sigma), from a freshly prepared and filter purified 50mg/ml stock solution) and $1x10^6$ cells were seeded in the 10cm dish. After 24 hours, the medium was changed to fresh matrix medium. This was repeated every 48 hours for 9 days, after which the medium was aspirated and the cells rinsed with PBS. 3ml of pre-warmed (37°C) extraction buffer (PBS + 0.5% Triton X-100 and 20mM NH_4OH) was added to lyse the cells and incubated at room temperature until no intact cells could be seen. 2-3ml PBS was added to dilute the cell debris, which was removed gently using a pipette. This step was repeated, then 10U/mL DNAse was added for 30 minutes at 37°C to minimize DNA debris, then washed twice with PBS, before covering the matrix-coated plates with PBS supplemented with 1% Penicillin/Streptomycin (Pen/Strep), 1% Glutamine and 0.1% Fungizone/Amphoterycin B. Plates were sealed with Parafilm and stored at 4°C for no more than 2-3 weeks before use. This protocol was obtained from Current Protocols in Cell Biology (2002).

2.3.2 Generation of full-length Reelin

Reelin expression and secretion after pCrl transfection into HEK 293 cells is a well-established method for collecting full-length Reelin and all its cleavage products to use in subsequent cell treatments (Jossin et al., 2004, 2007), (Feng et al., 2007), (Chai et al., 2009). Briefly, HEK 293 cells, cultured in DMEM (Invitrogen) plus 10% FBS, were transfected with pCrl (full-length Reelin cDNA; obtained from Tom Curran, St Jude), using Lipofectamine 2000 (Invitrogen). After two days, the transfected cells and untransfected control cells were counted and plated in equal numbers. After settling, the medium was changed to 0% serum DMEM for two days and then collected and

centrifuged to remove cellular debris. For chemotaxis and cell-stimulation experiments, supernatant from Reelin-transfected or untransfected control cells was concentrated approximately 25x using an Amicon ultra-15 centrifugal filter unit, 50kDa (Sigma), thus also removing any proteins smaller than 50kDa from the supernatant.

2.4 Antibodies

A full list of antibodies used for immunofluorescence experiments throughout this thesis can be found in Table 2.2 (primary antibodies) and Table 2.3 (secondary antibodies). A full list of antibodies used for Western Blotting experiments within this thesis can be found in Table 2.4 (primary antibodies) and Table 2.5 (secondary antibodies).

Antibody	Source	Dilution
Rabbit anti-mouse LYVE1	Reliatech	1:1000
Rabbit anti-mouse Desmin	Abcam	1:100
Rabbit anti-mouse Collagen IV	Serotec	1:100
Rabbit anti-mouse Laminin-α5	(Ringelmann et al.)	1:400
Rabbit anti-mouse GFP	Invitrogen	1:200
Rabbit anti-mouse Erp57	Abcam	1:100
Rabbit anti-mouse Golph4	Abcam	1:200
Rabbit anti-mouse Efemp1	Abcam	1:100
Rabbit anti-mouse NG2	Chemicon	1:100
Rabbit anti-mouse Fibronectin	Abcam	1:200
Rat anti-mouse PECAM-1	BectonDickinson	1:250
Rat anti-mouse VE-Cadherin	(Gotsch et al.)	1:100
Rat anti-mouse LYVE-1	R&D Systems	1:500
Goat anti-mouse Reelin	R&D Systems	1:200
Goat anti-mouse VLDLR	R&D Systems	1:100
Goat anti-mouse Integrin-α9	R&D systems	1:200
Mouse anti-mouse acetylated αTubulin*	Abcam	1:100
Hamster anti-mouse Podoplanin (8.1.1)	Developmental Studies Hybridoma Bank	1:200
Hamster anti-mouse PECAM-1	Chemicon	1:500
Rat anti-human Podoplanin NZ1	AngioBio	1:50
Rabbit anti-human LYVE-1	Reliatech	1:50
Cy3-conjugated mouse anti-αSmooth Muscle Actin	Sigma	1:500 (wholemount) or 1:50 (cells)

Table 2.2 Primary antibodies used for immunofluorescence experiments in this thesis

Mouse anti-mouse acetylated αTubulin antibody was used together with Vector M.O.M. Blocking reagent. After one hour blocking in PBS plus 3% milk, ears were

then blocked in PBS plus M.O.M blocking reagent (1 drop in 1.25mL PBS) for at least a further hour.

Secondary Antibody	Source	Dilution
Donkey anti-rat cy2, cy3 or cy5	Jackson ImmunoResearch	1:300
Donkey anti-rabbit cy2, cy3 or cy5	Jackson ImmunoResearch	1:300
Donkey anti-goat cy2 or cy3	Jackson ImmunoResearch	1:300
Goat anti-syrian Hamster cy2, cy3 or cy5	Jackson ImmunoResearch	1:300
Biotin Donkey anti-goat	Jackson ImmunoResearch	1:300

Table 2.3 Secondary antibodies used for immunofluorescence experiments in this thesis

Antibody	Source	Dilution
Mouse anti-human Reelin	Calbiochem	1:500
Mouse anti-human CD31	Dako	1:1000
Mouse anti-human α-tubulin	Sigma	1:8000
Cy3-conjugated mouse anti-αSmooth Muscle Actin	Sigma	1:1000
Rabbit anti-human Spock3	Abcam	1:1000
Rabbit anti-human Efemp1	Abcam	1:1000
Rabbit anti-human Nidogen2	Immundiagnostik	1:1000

Table 2.4 Primary antibodies used for Western blotting in this thesis

Secondary Antibody	Source	Dilution
Goat anti-mouse HRP	Jackson Immunoresearch	1:5000
Goat anti-rabbit HRP	Jackson Immunoresearch	1:5000

Table 2.5 Secondary antibodies used for Western blotting in this Thesis

2.5 Immunofluorescence staining

Mice were killed by schedule 1 methods: CO_2 and cervical dislocation, or cervical dislocation alone. The outer ears were removed by cutting along the base of the ear, closest to the head. These were opened by teasing apart the dorsal layer of the ear skin from the base using forceps, being careful to leave all the cartilage on the ventral side of the ear. The opened dorsal ear skin was then fixed.

To obtain embryos for embryonic skin samples, the mother was killed by cervical dislocation, the abdominal space opened and the embryos removed into PBS. The embryos were removed from the amniotic sac using forceps and culled by decapitation. The skin was carefully dissected, using microscissors to cut around the dorsal edges of the skin and then pulled away using forceps. The skin was pinned flat and then fixed.

2.5.1 Immunofluorescence staining of whole-mount ears and embryonic skin

For whole-mount staining of ears and embryonic skin, tissues were fixed in 4% PFA (Paraformaldehyde) overnight at 4°C, washed several times in PBS, permeabilised in 0.3% Triton X-100 (Acros Organics) in PBS (PBSTx) and then blocked in 3% milk or BSA (Bovine Serum Albumin, Sigma) in PBS for at least 2 hours. Primary antibodies (Table 2.2) were added to the blocking buffer and incubated at 4°C overnight. After 2 hours washing in PBSTx, the tissue was incubated with fluorochrome-conjugated secondary antibodies (Table 2.3) in 1% milk or 3% BSA in PBS for 2 hours at room temperature (RT), washed for 2 hours in PBSTx and mounted in Mowiol mountant (25% w/v glycerol, 1% w/v Mowiol, 100mM Tris (final concentration) and 2% w/v N-propyl-gallate to a final volume of 24mL in H_20).

For NG2 staining (Figure 3.3 A-B'), ears were blocked overnight in PBLEC (1% Tween-20, 0.1mM $CaCl_2$, 0.1mM $MgCl_2$, 0.1mM $MnCl_2$ in PBS, pH 6.8) at 4°C, before incubation with rabbit anti-mouse NG2 antibody, diluted in PBLEC overnight at 4°C. After 2 hours washing and a further 1 hour blocking in PBSTx + 3% milk, other primary antibodies were added and the normal immunofluorescence protocol was resumed.

2.5.2 Signal amplification

Alternatively, for signal amplification using the TSA Fluorescein Tyramide Reagent Pack (Perkin Elmer), the primary antibody (Table 2.2) was incubated in PBSTx +3% milk overnight at 4°C, washed for two hours and then incubated with biotin-conjugated secondary antibodies (Table 2.3), diluted in TNB buffer (0.1M Tris-HCl pH7.5, 0.15M NaCl, 0.5% blocking buffer (supplied in kit)) overnight at 4°C. Samples were then washed for two hours in PBSTx, incubated with SA-HRP (used at 1:750 in TNB buffer) for 30 minutes at RT, washed for 1 hour, incubated with Biotinyl Tyramide-FITC (used at 1:1000 in amplification diluent) for 10 minutes at RT, washed for another hour and then incubated with other (non amplified) primary antibodies in PBSTx + 3% milk, before resuming normal immunofluorescence protocol.

For VLDLR staining (Figure 6.1 C-D'), goat anti-mouse VLDLR antibody (R&D systems) was preabsorbed with a *Vldlr*$^{-/-}$ ear in TNB buffer overnight, before resuming normal amplification and immunofluorescence protocol.

For immunofluorescence staining of unpermeabilised tissue, all steps were carried out in the absence of Triton X-100.

2.5.3 Image Acquisition

All samples were analysed using a Zeiss LSM 510 scanning confocal microscope, except for *Apoer2*$^{-/-}$*;Vldlr*$^{-/-}$ and *Dab1*^{Scm} mice and their wild type controls, which were analysed using a Zeiss LSM 710 scanning confocal microscope. All confocal images, unless otherwise stated, represent 3D projections of Z-stacks.

2.5.4 Immunofluorescence staining of cells on coverslips

For immunofluorescence staining of cells on coverslips, samples were fixed in 4% PFA for 10 minutes at RT, permeabilised with 0.5% Tween-20 (Acros Organics) in PBS (PBST) and then incubated with primary antibodies (Table 2.2) in 5% normal goat serum (NGS) in PBS for 30 minutes at RT. After 30 minutes washing in PBST, the samples were incubated with fluorochrome-conjugated secondary antibodies (Table 2.3) in 5% NGS/PBS for 30 minutes at RT, washed and mounted in Mowiol, or incubated for 5 minutes with DAPI (Invitrogen; 1:1000 in dH_2O), dipped in dH_2O and mounted in Mowiol, before imaging with a Zeiss Axio Observer inverted microscope.

2.6 Relative Quantitative PCR

2.6.1 RNA extraction

For *RELN, APOER2, VLDLR* and *EFNB2* gene expression analysis, RNA was extracted from 2 or 3 independent samples (as indicated in figure legends) of Lymphatic Endothelial Cells (LEC), Blood vascular Endothelial Cells (BEC) Human Aortic (HAo)

and Human Venous Smooth Muscle Cells (HUVSMC), using the RNEasy Mini kit (Qiagen) according to the manufacturer's protocol.

For *LYVE1* mRNA analysis, LEC were cultured alone or together with SMC for 48 hours before RNA extraction, using RNeasy Mini kit, as above.

For Reelin stimulation, LEC were starved overnight in serum free Endothelial Cell Growth Medium (Promocell), supplemented with 0.2% BSA, hEGF-5 and HC-500. The next morning, cells were stimulated with full-length Reelin supernatant, diluted 1:20, control supernatant, diluted 1:20, 1ug/mL recombinant mouse Reelin (R&D), or left untreated for 4, 8 or 24 hours. RNA was extracted at the end of each timepoint using RNeasy Mini kit, as above.

2.6.2 Reverse Transcription

RNA was reverse transcribed using Superscript III Reverse Transcriptase (Invitrogen). Briefly, 500ng RNA, diluted up to 10µl in RNAse-free dH_2O, was incubated with 2.5µM OligoDT and 2mM dNTPs (all Invitrogen) per reaction, and put at 65°C for 5 minutes. After 1 minute on ice, 4µl 5x first strand buffer, 1µl 0.1mM DTT, 40 units (U) RNAse out and 200U Superscript III RT (all Invitrogen) was added to each reaction and put at 50°C for 60 minutes and 70°C for 15 minutes. The RT reactions were then put on ice while 2U RNAse H was added, before being incubated at 37°C for 20 minutes. cDNA samples were kept on ice for immediate use or at -20°C for short-term storage.

2.6.3 Relative quantitative PCR

For *RELN, APOER2, VLDLR, LYVE1* and *EFNB2* gene expression analysis, Platinum SYBR Green qPCR super mix-UDG with ROX (Qiagen) detection system was used.

Each reaction mixture was made up as follows: 12.5μl SYBR Green, 1μl forward primer (10μM), 1μl reverse primer (10μM) and 9.5μl RNAse-free dH_20 and 1μl cDNA.

For *MCP1, PDGFB, HBEGF, ANGPT2* and *TGFβ1* gene expression analysis, Taqman probes (Applied Biosystems) were used and each reaction mixture was made up as follows: 10μl Taqman mastermix, 8μl RNAse-free dH_20, 1μl Taqman probe and 1μl cDNA.

cDNA was amplified in duplicate by quantitative real-time PCR (ABI 7900HT), with cycling conditions as follows: step 1, 2 minutes at 50°C; step 2, 10 minutes at 95°C; step 3, 15 seconds at 95°C and step 4, 1 minute at 60°C. Steps 3 and 4 were repeated 35-40 times. Ct values were exported and ΔΔCT was calculated using either the complementary computer software or in Excel. In all cases, except *LYVE1* expression in LEC/SMC co-cultures compared to LEC alone, relative quantifications of gene expression were normalised to expression of the endogenous gene, *GAPDH*. In the case of *LYVE1*, expression was normalised to *PECAM1*.

The primers used were: *RELN*: 5'-GTTTTGCAAATTGGGAGCAT-3' and 5'-CCGTTGTTGACGCTGTATTG-3', *APOER2*: 5'- GCGGAACTATTCACGCCTCA-3' and 5'-TGCGATTGGTGGCAACTTC-3', *VLDLR*: 5'-CATTGCTGTTGATTGGGTGT-3' and 5'- CCAGTAAACAAAGCCAGACAGTG-3'; *PECAM1*: 5'-GAGAGGACATTGTGCTGCAA-3' and 5'-GGGTTTGCCCTCTTTTTCTC-3', *LYVE1*: 5'-GCTTTCCATCCAGGTGTCAT-3' and 5'-AGCCTACAGGCCTCCTTAGC-3', *EFNB2:* 5'-CTGCTGGATCAACCAGGAAT-3' and 5'-GATGTTGTTCCCCGAATGTC-3' and *GAPDH*: 5'-GAAGGTGAAGGTCGGAGTC-3' and 5'-GACAAGCTTCCCGTTCTCAG-3' (All custom made from Sigma).

Taqman probes (Applied Biosystems) were: *PDGFB*; Hs00966522_m1, *ANGPT2*; Hs01048042_m1, *TGFβ1*; Hs00998133_m1, *HBEGF*; Hs00181813_m1, *CCL2/MCP1*; Hs00234140_m1 and *GAPDH*; Hs99999905_m1.

2.7 Vessel Dissection and Microarray

2.7.1 Vessel Dissection and RNA extraction

For RNA extraction from murine lymphatic vessels, arteries and veins, dissection plates were first incubated overnight in RNAse away solution, washed several times in DEPC treated H_2O and then incubated for a further hour in 70% EtOH. Dissection tools were also incubated overnight in 70% EtOH.

P6 or P7 wild type (C57Bl/6) pups were culled by cervical dislocation, then the whole mesenteries were dissected using sterile scissors and forceps and taken straight into DMEM plus 10% FBS. Although our previous analysis of lymphatic collecting vessel differentiation had been done in the dermal lymphatic vasculature, we used mesenteric vessels for our array, due to the accessibility of this tissue for dissection. P6 and P7 mice were chosen for vessel dissection for practical reasons. At this stage, the vessels are large enough to make dissection possible, but the perivascular adipose tissue that obstructs the vessels, making clean dissection impossible, has yet to be deposited. Regional gene expression changes between mesenteric and dermal lymphatic vessels need not affect the usefulness of data gained from this array since, as with any screen, specific expression of the gene of interest must be validated by further expression studies, as was performed for Efemp1, Nidogen 2 and Spock 3 (Figure 3.12) and Reelin (Figure 4.1 A-A'). All the mice used in this array were in a C57Bl/6 background, and so possible strain specific differences must be taken into account if applying data from this array to mice bred into a different genetic background. It should also be noted that the pups were not starved prior to sacrifice. Mesenteric lymphatics are only visible when full of chyle, so clean dissection of lymphatic vessels would be extremely difficult in starved pups. However, the importance of the lymphatics in fat absorption means that recent feeding may affect gene expression, again highlighting the need for further validation of microarray data.

Samples waiting to be dissected were kept on ice. The mesenteries were put onto the dissection plate in DEPC-PBS. Lymphatic vessels were dissected by gently holding the vessel at the end nearest the mesenteric root using forceps and then gently pulling away, carefully tweezing excess fibrous tissue from the mesenteric membrane away from the vessel. The other end of the vessel was then cut using micro-scissors. The vessels were placed in a drop of lysis buffer RLT, plus β-Mercaptoethanol (1:100) from the RNeasy Micro kit (QIAGEN) while the remaining vessels were excised. Arteries and veins were dissected using a similar technique, but were first separated from each other using forceps, and as much fibrous tissue pulled away from the vessel as possible. Once all the vessels from one mesentery had been dissected, they were cut into small pieces, to assist efficient lysis and put into ~100µl buffer RLT plus β-Mercaptoethanol.

When all the mesenteries had been dissected, and tissue lysed, the lysis buffer containing the vessel segments was heated at 37°C for 10-15 minutes, and vortexed to increase the eventual RNA yield, before storage at -80°C. Upon removal from -80°C, samples were heated at 37°C for 5-10minutes then RNA was extracted using the RNeasy micro kit (QIAGEN), according to the manufacturer's instructions. Samples from 9 pups (all the pups from two litters) were pooled prior to RNA extraction.

2.7.2 Microarray and analysis

100ng RNA from two independent samples of lymphatic vessels, arteries and veins were sent on dry ice to the Cancer Research UK Paterson Institute, where the Paterson Institute Microarray Service amplified the RNA using WT-Ovation Pico RNA Amplification System (NuGEN) and used it for expression profiling using the Mouse exon 1.0 ST Array (Affymetrix), according to manufacturer's instructions. The Affymetrix exon array is comprised of 25-mer probes synthesised *in situ* on the GeneChip. The probes are grouped into 'probe sets' of 4 probes, all directed against the same exon, although there can be more than one probe set per exon. Analysis can be carried out at this level to give 'exon level' data, including information on alternative

splicing events. Alternatively, the probe sets can be grouped again into 'transcript clusters', which are grouped by mapping the probe sets to mRNA sequences collated from various databases (eg RefSeq and Ensembl) to give 'core level' analysis at gene level. This level of analysis was used in our project. Quantification was run using apt-1.10.0 from Affymetrix. The read-out from each probe is a measure of signal intensity, which was processed using RMA (robust multichip average) (Irizarry et al., 2003). This algorithm calculates the average signal intensity from all the probes across a transcript cluster, simultaneously looking for consistency in the rank of signal intensity between probes and probe sets on all chips to weight against less robust readings, whose signal intensity ranking is not maintained across all samples. The algorithm also includes quantile normalisation, which assumes similar signal distribution across all chips and corrects for differences in RNA concentrations and reaction efficiencies between chips to ensure that they are comparable. Gene changes were selected using a linear model and multiple testing correction, and a false discovery rate (fdr) of <0.05, was applied to correct for errors generated in a large dataset. Lymphatic specific transcriptional changes were selected for. All annotation was taken from Affymetrix and all analysis carried out in Bioconductor (Gentleman et al., 2004) using Limma by Phil East in the Cancer Research UK Bioinformatics and Biostatistics department.

2.7.3 Identification of extra-cellular matrix related genes

Genes that were expressed at least 2-fold higher in lymphatic vessels compared to arteries or veins, and in arteries and veins compared to lymphatic vessels were identified. All the genes in this list were searched in Uniprot (www.uniprot.org) and those where the subcellular localisation was identified as extracellular matrix were selected to give a list of all genes that encode proteins involved in extracellular matrix structure, assembly or degradation and are expressed at least 2-fold higher in lymphatic vessels, arteries or veins.

2.8 Western Blot Analysis and Immunoprecipitation

Whole cell lysate for Western Blot analysis was collected by washing cells in cold PBS then lysing in Triton X-100 lysis buffer (50 mM Tris [pH 7.5], 120 mM NaCl, 10% glycerol, 1% Triton X-100), supplemented with Complete Protease inhibitors (Roche). All samples (cells and medium) were kept on ice or at 4°C.

2.8.1 Measuring protein concentration

For LEC/BEC analysis, a BCA protein assay (Pierce) was performed to measure total protein concentration, according to manufacturers instructions. An equal amount of protein was then added to each lane of a 7.5% SDS-PAGE gel.

For LEC/LEC-SMC co-culture, equal volumes of lysate were added to the gel, and a loading control was used to confirm that equal numbers of cells were used.

2.8.2 SDS gel electrophoresis and immunoblotting

Gels were run at 0.02A in 1x SDS-PAGE running buffer (25mM Tris, 0.2M Glycine, 3.5mM SDS). The gel was run until the blue dye ran out the bottom of the gel. Protein separation was visualized using Full-Range Rainbow Molecular Weight Marker (Amersham) loaded in the gel.

All gels were transferred onto a polyvinyidene difluoride (PVDF) membrane (Amersham) using the X Cell II Blot Module (Invitrogen) in 1x Tris-Glycine-Methanol transfer buffer (25mM Tris, 0.2M Glycine, 20% Methanol). Efficient transfer was achieved at 30V for one hour (one gel) or 60V for one hour (2 gels). After transfer, the

membrane was rinsed in TBST (1x TBS plus 0.1% Tween-20) then blocked in TBST plus 5% milk. 1x TBS is 20mM Tris, 0.14M NaCl, pH 7.6.

Membranes were incubated with primary antibodies (Table 2.4) in TBST plus 5% BSA overnight at 4°C, washed for one hour in TBST, incubated with HRP-conjugated secondary antibodies (Table 2.5) in TBST plus 5% BSA for 2 hours at RT, washed for a further hour and then developed using the ECL chemiluminescence detection system (Amersham) with exposure on autoradiography film (Amersham).

2.8.3 Immunoprecipitation

For analysis of secreted Reelin, IgG-stripped medium was collected after 2 days culture from LEC, HUVSMC and LEC/HUVSMC co-culture and centrifuged at 4°C to remove dead cells.

For Reelin immunoprecipitation, samples were pre-cleared with Protein G beads (Sigma) for 2 hours at 4°C then centrifuged at 4°C. The supernatant was incubated with 1µl mouse anti-human Reelin antibody (Calbiochem) at 4°C overnight with gentle rocking. Protein G beads were then incubated with the sample for 2 hours at 4°C, centrifuged and the supernatant removed. 20µl of 2x Laemmli Sample Buffer (LSB) was added to the beads, which were then washed gently in PBS, vortexed, boiled at 95°C for 5 minutes, vortexed again and centrifuged briefly, before running equal volumes in a pre-cast NuPAGE Novex 7% Tris-Acetate gel (Invitrogen) with 1x NuPAGE Tris-Acetate SDS running buffer (Invitrogen). The gel was run at 120V, until the blue dye ran out the bottom of the gel. HiMark pre-stained protein standard (Invitrogen) loaded in the gel was used to visualize protein separation. The rest of the protocol was completed as for a Western Blot (above).

Quantification of the signal intensity of Reelin bands in the medium and lysate of LEC cultured alone compared to those co-cultured with SMC was carried out using ImageJ. The Reelin signal in LEC and LEC/SMC co-cultures was normalized to CD31 by

dividing the Reelin value by its respective CD31 value. A ratio of Reelin in LEC to LEC/SMC co-cultures was then calculated by dividing both values by the LEC value.

2.9 Whole Vessel Imaging and analysis

Images were captured using the x20 objective on the Zeiss 510 Scanning confocal microscope (*Reln*$^{-/-}$ and wild-type controls, *Efnb2*$^{lx/lx}$*;Prox1-creER*^{T2}*,* and *R26-mTmg; Prox1-creER*^{T2}), or the Zeiss 710 Scanning confocal microscope (*Apoer2*$^{-/-}$*;Vldlr*$^{-/-}$*, Dab1*^{Scm} and wild-type controls). Pictures were taken along the length of 3 randomly chosen collecting lymphatic vessels from the ears of each of 5 *Reln*$^{-/-}$ mice and 4 wild-type controls, 3 *Apoer2*$^{-/-}$*;Vldlr*$^{-/-}$ mice, *Dab1*^{Scm} mice and 3 of each of their respective wild-type controls and 3 *Efnb2*$^{lx/lx}$*;Prox1-creER*^{T2} mice.

The images were aligned and processed using Adobe Photoshop CS3 and CS4.

Thresholding and quantification were performed using MetaMorph Imaging software (Molecular Devices) (Figure 2.1 A-A'). Briefly, the colour channels of the image were separated and an exclusive threshold applied to the red (αSMA) channel, so that the background was captured by, while all SMC were excluded from, the threshold (Figure 2.1 A'). The length of the vessel was measured and divided into quarters (*Apoer2*$^{-/-}$*;Vldlr*$^{-/-}$, *Dab1*^{Scm} and their wild-type controls) or 500 pixel regions (*Reln*$^{-/-}$ and wild-type controls), using the line tool. A region of interest (ROI) was drawn around each vessel segment in the original, non-colour separated image (ROIs excluded any overlapping blood vessels, which had a high SMC coverage and would skew the results)(Arrows, Figure 2.1 A') and copied onto the red, thresholded channel. SMC coverage was calculated by measuring the percentage thresholded area of the ROI and subtracting this from 100%. In the case of the *Reln*$^{-/-}$ and wild-type control vessels, the total number of 500 pixel regions in each vessel was calculated and divided by 4 to represent a quarter of the vessel.

The mean SMC coverage for each vessel quarter was calculated and plotted and an unpaired Student's T-test used to calculate the significance of the difference between wild-type and mutant mice.

A similar thresholding technique, but including the whole vessel, was used to quantify the percentage of LVYE-1 immunofluorescence. The line tool in MetaMorph was used to measure the width of the widest and narrowest vessel points.

All graphs, calculations and statistics were performed using Prism 5 software.

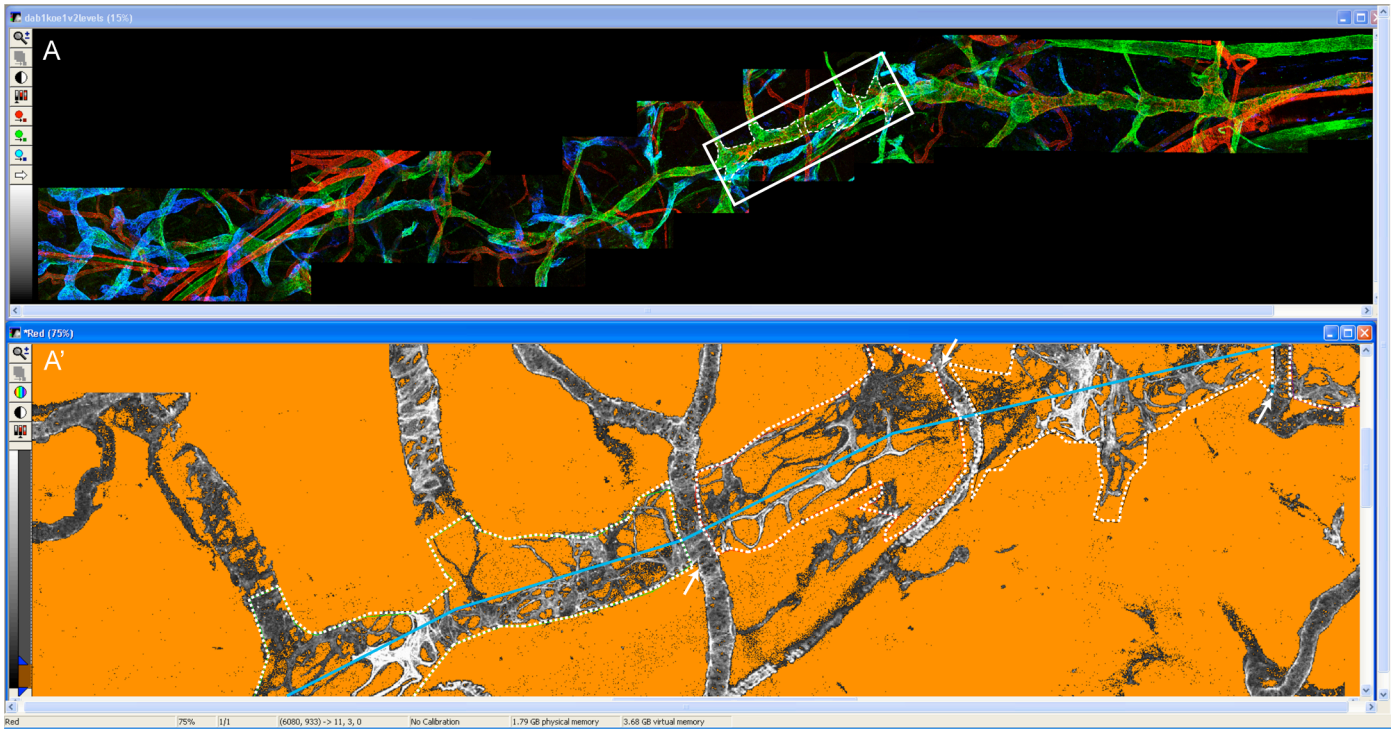

Figure 2.1 Quantification of SMC coverage.
Whole vessel image (A) was opened and channels separated. White box details approximate area magnified in (A'). Red channel (A') shows SMC coverage and was set to monochrome. Line tool (blue line; A') was used to calculate the total length of the vessel and divide it into quarters. A region of interest (ROI) was drawn around each vessel quarter (dashed line), excluding overlapping blood vessels (arrows; A'). All regions of interest and lines were drawn on whole vessel image (A) and copied to red channel (A'), but are only shown on magnified A' for clarity. An exclusive threshold was applied to the red channel (orange, in A') such that only SMC were excluded. The percentage thresholded area was measured for each region, and then total percentage thresholded area was calculated for each vessel quarter and subtracted from 100 to leave % area covered by SMC.

2.10 Visualisation and quantification of lymphatic vessel function

2.10.1 FITC Dextran injection

For FITC-Dextran injection, 3-week old mice were anaesthetised by IP injection of 75-100μL Hypnorm (VitaPharma)/Hypnovel (Roche)/PBS mixed in the ratio 1:1:2, using a 25G needle. Once the mice were deeply asleep (assessed by lack of reaction to a slight pressure from forceps on the foot, or no ability to right themselves when turned on their side), a minimal volume of FITC-Dextran (Sigma, 8mg/mL in PBS) was injected into the hindlimb footpads (n = 5 each wild-type and *Reln*$^{-/-}$), or intra-dermally into the ears (n = 7 each wild-type and *Reln*$^{-/-}$). The mice were culled after 15 minutes by cervical dislocation. The skin was removed by using scissors to make an incision around the waist of the animal and then gently peeling it away. The hindlimb lymphatic vessels were imaged using a Leica stereomicroscope and the Planapo 0.63x objective at 100x magnification. The images were acquired using the complementary computer software (Leica). Ears were processed as for immunofluorescence.

2.10.2 Whole body imaging

The back legs and hindquarters of 3-week old mice were shaved and the remaining hair removed by application of Veet hair removal cream one day prior to the procedure.

To image the lymphatic flow, the mice (n = 4 each wild-type and *Reln*$^{-/-}$) were first anaesthetised using Isofluorane-Vet 100% Inhalation Vapour (Merial) in the chamber of a Xenogen XGI-8 Gas Anaesthesia System. Once deeply asleep, the mice were transferred to the IVIS Spectrum Whole Body Imaging Chamber (Caliper Life

Sciences) and positioned so that their noses were inside the anaesthesia nose cone. 2μL of ICG dye (Sigma, 1% in dH_2O) was injected into the footpad. The injection site was covered with black tape and the door to the chamber shut. Image acquisition was started immediately, using Living Image 3.0 software (Caliper Life Sciences). The settings were as follows: Exposure: 2, Binning: 8, F/stop: 2, Excitation wavelength: 745, Emission wavelength: 840, Field of View (FOV): B, Height: 0.3cm. The dynamic distribution of the ICG was monitored over time by sequential acquisition of 70 images, with a 0 second delay between acquisitions resulting in one image every 5-6 seconds. This is the maximum speed of the system.

For qualitative analysis, the accumulation / lack of accumulation of fluorescence within the lymph node at the end of imaging provides a first readout. In order to quantify the efficiency of lymphatic function, a small region of interest (ROI) was drawn around the vessel, approximately half way between the knee and the lymph node. The ROI was copied to all images in the sequence and fluorescence intensity measurements taken using the 'ROI measurements' tool. For a given animal the same ROI was used for all measurements, although between mice, the position of the ROI varied depending on their positioning within the image frame. Fluorescence intensity was expressed in 'Efficiency' units, as recommended by the manufacturer of the imaging system. This is the ratio between the number of photons used for excitation over the number of emitted photons, expressed as a percentage. It gives a measurement of signal intensity that is independent of the acquisition parameters (exposure, binning and F-stop) and is related to the local concentration of dye, so can thus be used as a quantitative measurement of lymphatic function.

2.10.3 Evans Blue injection

After IVIS spectrum imaging, the mice were kept anaesthetised for a further 5 minutes, while 2μL Evan's Blue dye (2%; Sigma) was injected into the other footpad (n = 4 wild-type and n = 5 *Reln*$^{-/-}$). After 5 minutes, the mice were culled by cervical

dislocation. The lymph nodes were dissected out, by first removing the skin, then using forceps to hold one end of the lymph node and pulling gently to remove it. Any excess tissue was removed, and the lymph nodes put in an Eppendorf tube with 5μL formamide at 60°C overnight. The following morning, the absorbance of the formamide was measured at 620nm, using a nanodrop.

2.11 Human phospho-kinase array

To identify novel downstream components of the Reelin signalling pathway, the Proteome Profiler Human Phospho-Kinase Array Kit (R&D Systems) was used.

LEC and HUVSMC were cultured as above. Prior to protein stimulation, cells were washed with PBS, serum starved overnight in serum free Endothelial Cell Growth Medium plus 0.2% BSA plus supplements (LEC) or serum free DMEM + 0.2% BSA (HUVSMC), then washed twice in starvation medium and incubated for a further 2 hours. To stimulate the cells, either Full-Length Reelin, Control DMEM (both 50% total medium), 1μg/ml mouse recombinant Reelin fragment (R&D systems), 50ng/ml VEGF-C (LEC; R&D systems) or 50ng/ml recombinant rat PDGF-BB (HUVSMC; R&D systems) was added to the culture medium for 20 minutes at 37°C.

The phosphoarray was carried out as per the manufacturer's instructions. Briefly, after protein stimulation, LEC or HUVSMC were rinsed with PBS and then solubilised with Lysis Buffer 6 at 1 x 10^7 cells/mL. The membranes were blocked for one hour at RT and then incubated with cell lysate, diluted in Array Buffer 1, overnight at 4°C on a rocking platform. The membranes were then washed for 3 x 10 minutes in Wash Buffer, incubated with Detection Antibody A or B for 2 hours at RT then washed for a further 3 x 10 minutes. The membranes were then incubated with Streptavidin-HRP for 30 minutes at RT, before another 3 x 10 minutes washes, and development using the ECL chemiluminescence detection system (Amersham) with exposure on

autoradiography film (Amersham). The key provided with the kit (appendix, Figure 8.1) allowed identification of protein kinases with increased phosphorylation levels.

2.12 Timelapse analysis of Reelin effect on HUVSMC motility

A 24-well plate was coated with either PBS, 2μg/mL FN (Sigma), 9μg/mL recombinant mouse Reelin, 1μg/mL recombinant mouse Reelin, Full length Reelin or control DMEM (3 wells per treatment condition) and left on the shaker at 4°C overnight. The next day, the wells were washed with PBS and then $7.5x10^4$ HUVSMC were plated per well, in SMC culture medium. After 6 hours, when the cells had attached to the plate, they were washed twice with DMEM plus 0.5% FBS and then incubated with 500μL DMEM plus 0.5% FBS. The cells were imaged using a Zeiss Axio Observer Inverted microscope every 4 minutes for 4 hours, using a x10 objective and imaging one field of view for each well. Following acquisition of the data, 20 cells from each well were tracked using Metamorph software. Briefly, gridlines were drawn over the image stack, so as to divide the picture into 20 regions. From each region, the cell closest to the centre that did not migrate out of the field of view over the course of the timelapse was selected for tracking (Figure 2.2). Each cell was tracked manually using the 'track point' tool and the data exported to an Excel file. The total distance each cell migrated was calculated in Excel, and the final data was copied into Prism for statistical analysis.

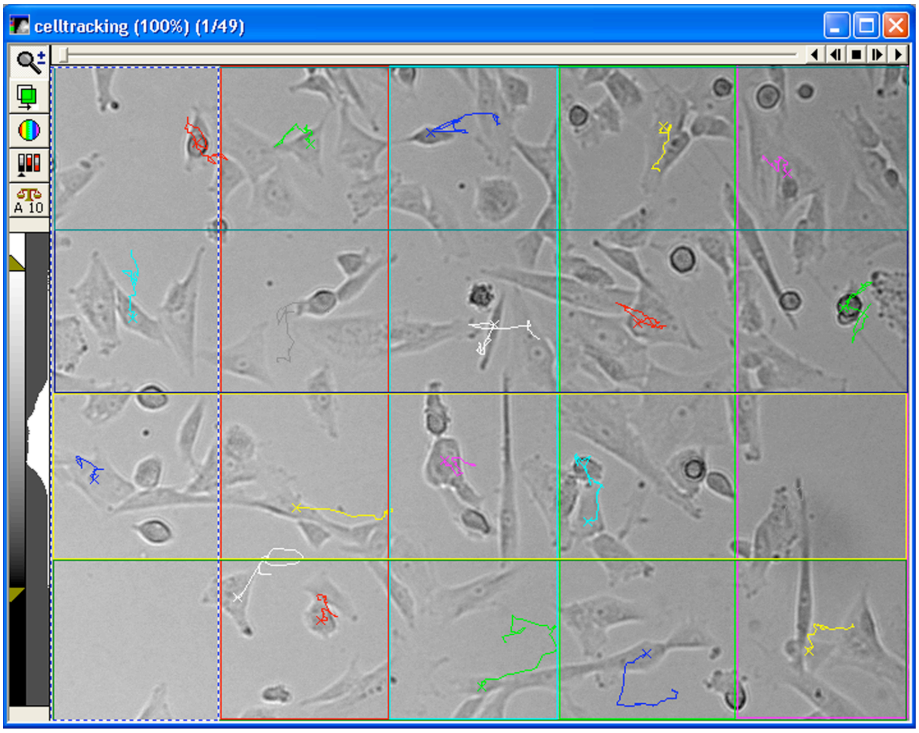

Figure 2.2 Cell tracking.
Time-lapse aquisitions were opened in Metamorph as 'stack' files. A grid was drawn over the image using the region tool, identifying 20 equal sized squares. The cell closest to the centre of each square (that didn't leave the frame over the course of the acquisition) was tracked manually, using the 'track point' tool (tracks shown by coloured lines). Data was exported to excel and the total distance travelled by each cell calculated.

2.13 Adhesion assay of Reelin effect on SMC adhesion

Wells of a non-tissue culture treated 96 well plate were coated with either PBS, 2µg/mL FN (Sigma), 9µg/mL or 10µg/mL recombinant mouse Reelin, 1µg/mL recombinant mouse Reelin, Full length Reelin or control DMEM and left on the shaker at 4°C overnight. The next day, the plate was washed with PBS, then $5X10^4$ HUVSMC were plated in each well in DMEM plus 2% FBS. After 3-4 hours, the medium was removed, the cells washed once in PBS and then fixed with 0.5% crystal violet solution (2.5g crystal violet (Sigma) in 500ml 25% methanol) for 8 minutes on a shaker. After this, the plate was washed thoroughly in tap water and air-dried overnight. Next, the

cells were solubilised in 100μL 0.1M sodium citrate solution (14.705g sodium citrate (Sigma) in 500mL 50% ethanol) and the absorbance was read at OD550nm. This experiment was carried out once with 9μg/mL Reelin (3 wells per treatment condition) and once with 10μg/mL Reelin (3 wells per treatment condition). No difference was observed between the two Reelin concentrations.

2.14 Chemotaxis assay of Reelin effect on SMC directional migration

0.75 x10^5 Smooth muscle cells were seeded in 100μl serum depleted endothelial cell growth medium (1% FCS, supplemented with HC500 and hEGF-5) in the top well of a 6.5mm Transwell with 8μm pore polycarbonate membrane insert (Corning) in a 24 well plate. 600μl untreated serum depleted endothelial cell growth medium, serum depleted medium supplemented with Full-length Reelin (1:20) or Control supernatant (1:20) or 48hr LEC-conditioned serum depleted medium was added to the lower chamber and the assay was incubated for 8-8.5 hours at 37°C. After this time, the medium was aspirated from the inserts and they were transferred to clean wells containing 400μl Cell Stain Solution (Cell Biolabs) and incubated for 10 minutes on a rocker at room temperature. Inserts were then washed several times with water and cells removed from the inside of the insert by wiping with a damp cotton swab. After air-drying, the inserts were imaged using a Leica stereomicroscope and the Planapo 0.63x objective at 16x magnification. Images were opened in Metamorph and 5 regions of interest drawn in the well. An exclusive threshold was applied to capture everything except the migrated cells and the thresholded area was measured. The threshold was set individually for each ROI to compensate for uneven light distribution over the image; ie an accurate threshold for ROI 1 may not have been accurate for ROI 5 (Figure 2.3). The mean thresholded area from all five ROIs was calculated and subtracted from 100% to give the area covered by migrated SMCs, representing SMC density.

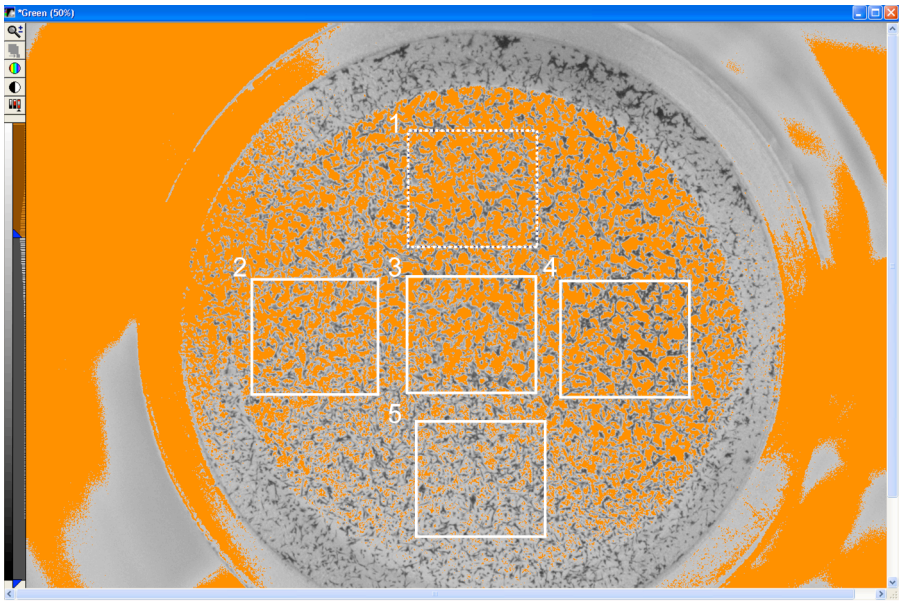

Figure 2.3 Quantification of SMC density after chemotaxis assay.
The image was colour separated the green channel was set to monochrome. 5 equally spaced regions of interest (ROI; white boxes) were drawn around the insert. An exclusive threshold (orange) was applied individually to each ROI to compensate for unequal light distribution. Here, the threshold is set for ROI 1 (dashed box), and is inaccurate for ROI 2, 3 and 5, whose thresholds were set independently. Percentage thresholded area was measured for each ROI and the mean was calculated and subtracted from 100, to leave % coverage by SMC, representing SMC density.

2.15 Statistical Analysis

P values for experiments shown in Figures 4.8 D, 5.1 C-D, 5.2 C, 5.6 B, 6.2 D-E, 6.4 D, 6.8 A-B and 6.9 were calculated using unpaired two-tailed Student's T-test.

Chapter 3. Characterisation of dermal collecting lymphatic vessel differentiation events

3.1 Smooth Muscle Cell Recruitment and LYVE-1 Downregulation

Upon sprouting from the blood vasculature, lymphatic vessels form a LYVE-1 positive primary plexus, which is then remodelled into a hierarchical network of collecting lymphatic vessels and capillaries. One of the earliest steps in the remodelling of the lymphatic vasculature is the formation of luminal valves in the collecting lymphatic vessels, a process that requires Integrin-α9 and its extracellular matrix ligand, Fibronectin EIIIA (Bazigou et al., 2009), EphrinB2 (Makinen et al., 2005) and FoxC2 (Petrova et al., 2004). The events and gene expression changes involved in the early steps of mesenteric lymphatic collecting vessel differentiation have recently been described (Norrmen et al., 2009). However, the timing of these events is temporally distinct in different tissues and the sequence of later events in dermal lymphatic collecting vessel maturation, such as LYVE-1 down-regulation, SMC recruitment and extracellular matrix deposition have yet to be described.

3.1.1 Smooth Muscle Cell recruitment to prospective lymphatic collecting vessels

Mouse ear-skin allows clear visualisation of the lymphatic network in whole-mount tissue, and is thus a useful model for studying postnatal lymphatic remodelling. To investigate the timing of SMC recruitment to lymphatic collecting vessels we used antibodies against α-smooth muscle actin (αSMA) and desmin, markers of SMC and

pericytes respectively. In the ear, the dermal lymphatic plexus develops by sprouting and is initially uniformly LYVE-1 positive. This continues throughout the first weeks of postnatal life. By postnatal day (P)12 LYVE-1 was starting to be down-regulated in the lymphatic plexus, often with no corresponding SMC recruitment (arrows, Figure 3.1 A-A'''), although sometimes SMC could be found loosely attached to the vessels at this stage (data not shown). At P14 the developing collecting vessels acquired SMCs, which became established around the vessels predominantly in areas of low/no LYVE-1 expression (Figure 3.1 B-B'''), and by P16 lymphatic collecting vessels were easily identified by low levels of LYVE-1 expression and the regular, but discontinuous coverage of SMC that characterises mature collecting vessels (Figure 3.1 C-C''').

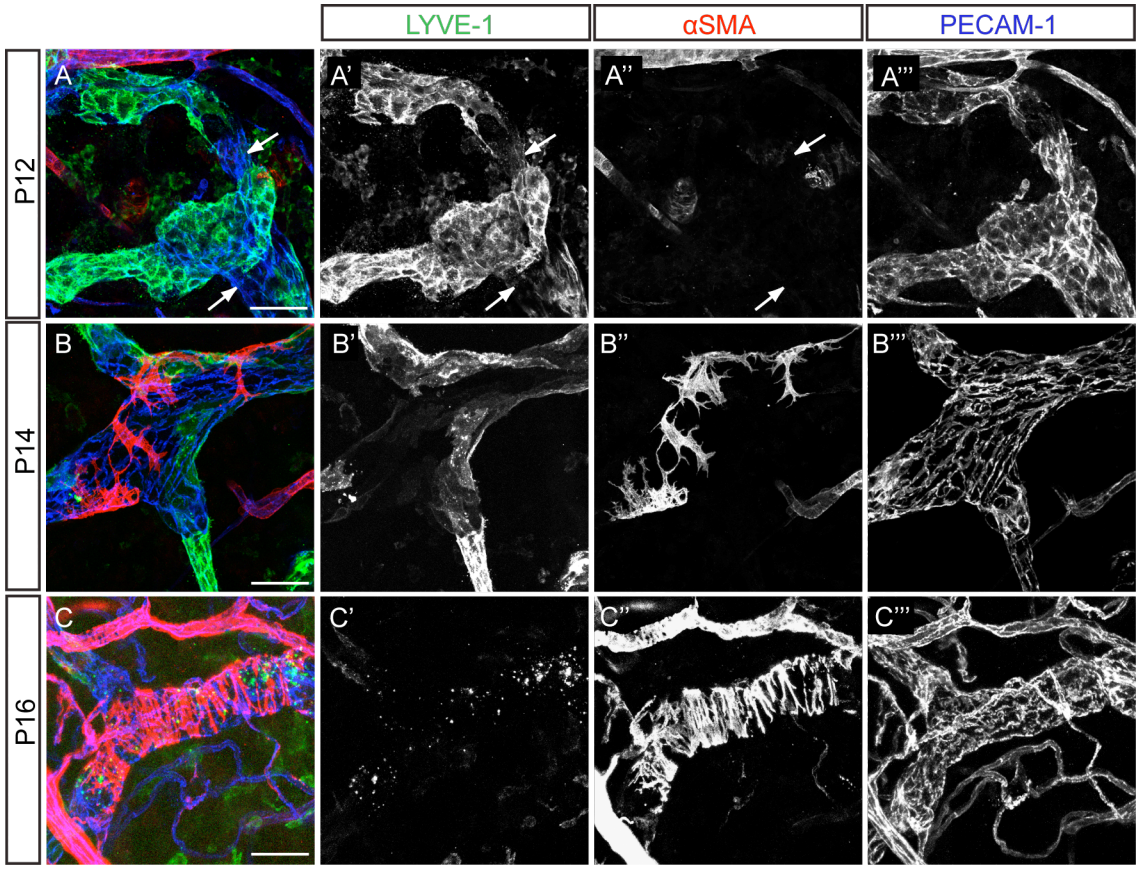

Figure 3.1 Smooth muscle actin as a marker of SMC recruitment to lymphatic collecting vessels.
(A-C''') Immunofluorescence of whole-mount ear-skin at indicated developmental stages with antibodies against LYVE-1 (green), αSMA (red) and PECAM-1 (green). Arrows in A indicate areas of LYVE-1 downregulation prior to SMC recruitment. Scale bars = 50μm.

3.1.2 Differential expression of smooth muscle cell / pericyte markers in blood and lymphatic vessels

To ensure that we were visualising all lymphatic SMC and to control for the possibility that not all lymphatic smooth muscle cells would be α-smooth muscle actin positive, we repeated the time-course using antibodies against the vascular pericyte markers desmin and NG2. In the blood vasculature, desmin has been published as an early marker of differentiating SMC, whereas αSMA is a late marker (Hughes and Chan-Ling, 2004), although there are differences in vascular pericyte marker expression between different tissues (Armulik et al., 2005). However, we found that while the number of desmin positive SMC increased from P12 to P16 (Figure 3.2 A-C'''), there were always fewer desmin positive SMC around the vessel than at the corresponding stage of the αSMA time-course, suggesting that in contrast to the blood vascular system, desmin is not a marker of early differentiating lymphatic SMC.

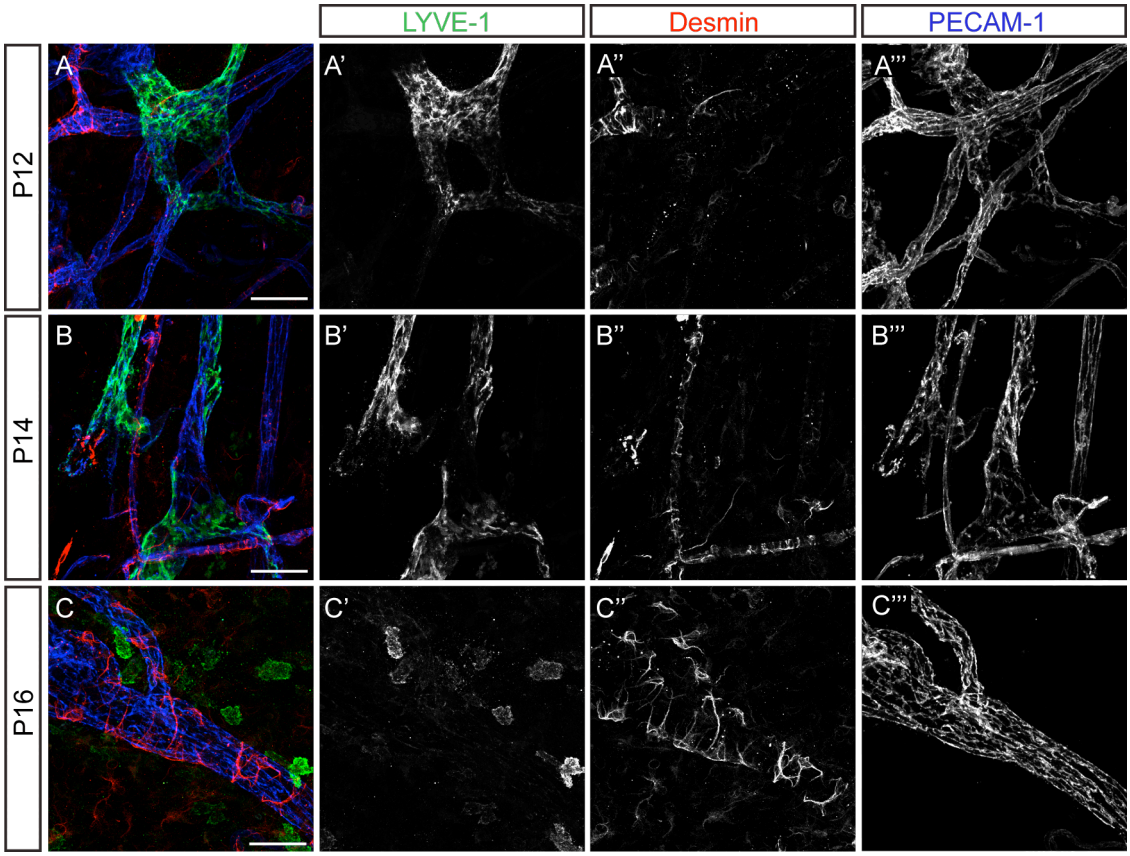

Figure 3.2 Desmin is not a marker of early lymphatic SMC.
(A-C''') Immunofluorescence of whole-mount ear-skin at indicated developmental stages with antibodies against LYVE-1 (green), Desmin (red) and PECAM-1 (blue). Scale bars = 50μm.

We also looked at the vascular pericyte marker NG2 (Gerhardt and Betsholtz, 2003), in both the immature and mature lymphatic vasculature but found that while staining could be seen around the blood vessels at both P15 and P21 (Arrows Figure 3.3 A-B'), none was visible around the lymphatic vessels (Arrowhead, Figure 3.3 A-B'), suggesting that NG2 is not expressed in lymphatic smooth muscle. However, we cannot rule out the possibility of low expression that this antibody is not sensitive enough to detect, since extra permeabilisation steps (see Materials and Methods) were necessary to enable detection even in the blood vasculature using this antibody.

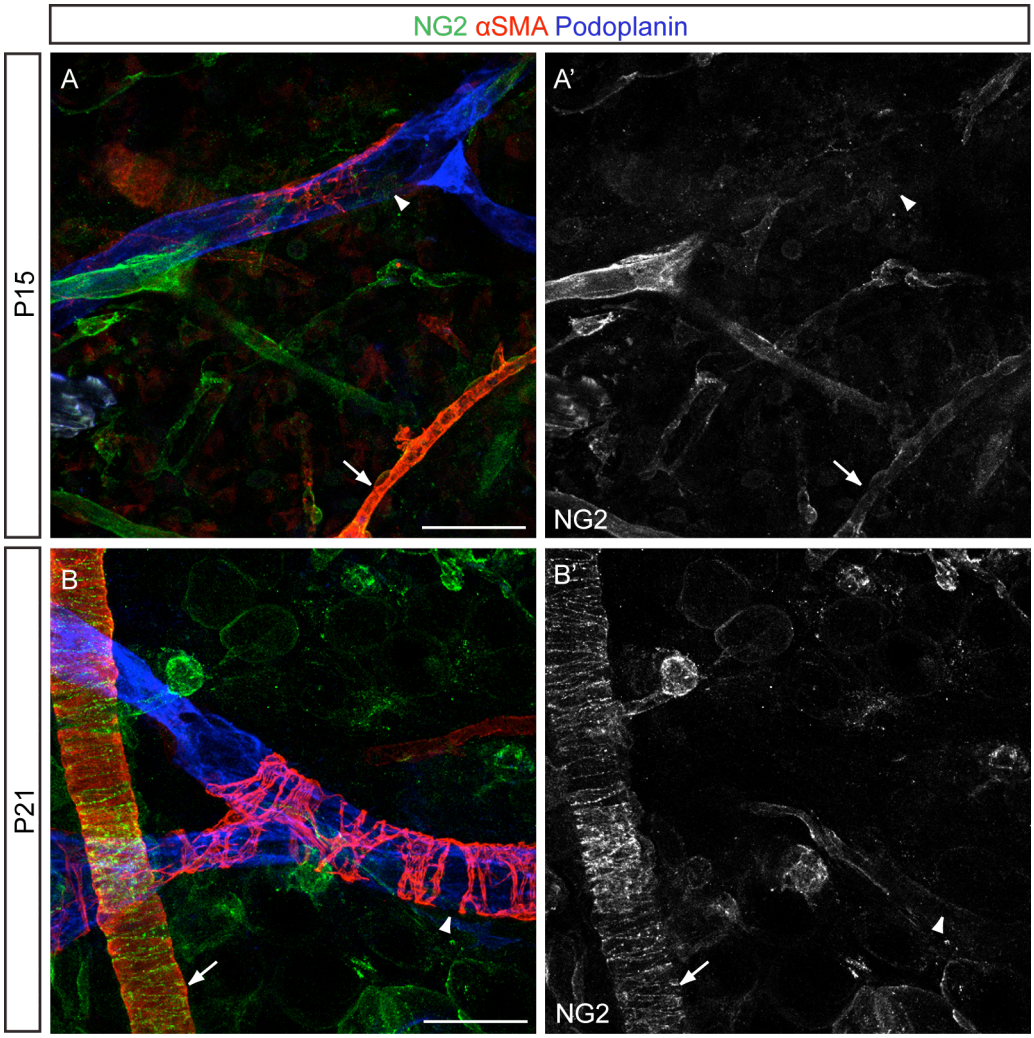

Figure 3.3 NG2 is not expressed in lymphatic SMC.
(A-B') Immunofluorescence of whole-mount ear-skin at indicated developmental stages, using antibodies against NG2 (green), αSMA (red) and podoplanin (blue). Scale bars = 50μm.

3.1.3 LYVE-1 down-regulation is associated with SMC recruitment

In agreement with previous expression data suggesting that SMC recruitment plays a direct role in LYVE-1 down-regulation (Tammela et al., 2007), we found that *LYVE1* mRNA was down-regulated in dermal LEC that had been co-cultured with venous SMC for 48 hours (Figure 3.4 A). However, our expression data suggests that LYVE-1 down-regulation occurs prior to SMC recruitment *in vivo* (Figure 3.1 A-A'''), and we

also readily observed LYVE-1 positive LEC in direct contact with SMC, even after 72 hours in culture, with no obvious decrease in LYVE-1 expression compared to LEC cultured alone (Figure 3.4 B-C). Together these data suggest that while it is likely that LYVE-1 down-regulation is associated with the presence of SMC, it may not be a direct consequence of SMC contact.

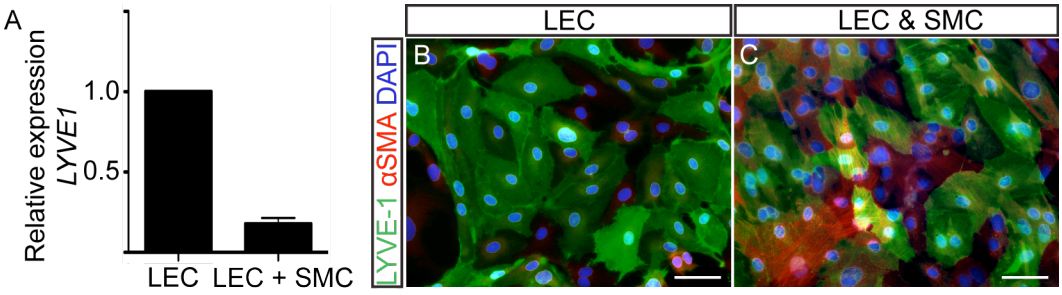

Figure 3.4 Co-culture of LEC and SMC does not reduce LYVE-1 protein levels, but *LYVE1* mRNA is reduced.
(A) RT-PCR data showing *LYVE1* mRNA levels normalised to *PECAM1* in LEC co-cultured with SMC for 48 hours, relative to LEC cultured alone. Mean fold change of 2 experiments ± SEM is shown. Immunofluorescence of LEC (B) and LEC and SMC (C) cultured for 72 hours with antibodies against LYVE-1 (green) and αSMA (red) and DAPI staining. Scale bars = 60µm

3.1.4 Loss of LYVE-1 does not affect collecting lymphatic vessel development

Despite being one of the most commonly used lymphatic markers and the earliest marker of lymphatic commitment (Tammela and Alitalo, 2010), the function of LYVE-1 in the lymphatic system is unknown. Beginning with polarised expression in the venous endothelium at E9, earlier even than induction of Prox1 expression (Alitalo et al., 2005), LYVE-1 continues to be expressed in the lymphatic plexus, until its eventual down-regulation in differentiated collecting vessels, suggesting a possible role in specification or maintenance of lymphatic fate.

Previously published studies of *Lyve1*$^{-/-}$ mice (Huang et al., 2006, Gale et al., 2007) concentrated on analysis of the lymphatic capillary network and function. However, since we had observed that SMC were preferentially recruited to areas of low/no LYVE-1 expression in prospective collecting lymphatic vessels, we investigated the possibility that LYVE-1 could act as a negative regulator of lymphatic remodelling and SMC recruitment.

To test this hypothesis, we stained *Lyve1*$^{-/-}$ and heterozygous mice for PECAM-1, αSMA and VE-cadherin. With this set of markers, we could see not only the smooth muscle cell coverage of the collecting lymphatic vessels, but also the overall vessel morphology, luminal valve morphology and the individual cell shape, since both PECAM-1 and VE-cadherin stain endothelial cell junctions (Baluk et al., 2007) and PECAM-1 also clearly delineates the leaflets of the luminal valves (Bazigou et al., 2009).

We chose to look initially at P21 mice, because at this stage the collecting lymphatic vessels are fully developed and any changes to SMC coverage or cell morphology would be visible. However, we saw no striking defects (data not shown). Since *Lyve1*$^{-/-}$ mice are viable, we made preliminary observations in 6 week old adult mice, in which the dermal lymphatic vasculature is fully matured, so that we could detect any defect that may have become increasingly severe with age. However, even at 6 weeks we could still see no obvious phenotype in the collecting vessel network of the *Lyve1*$^{-/-}$ mice. The overall vessel morphology appeared normal (Figure 3.5 A-D), and we could observe no difference in the SMC coverage of *Lyve1*$^{-/-}$ and heterozygous mice (Figure 3.5 A and C). It was possible that LYVE-1 could have been involved in the change of endothelial cell morphology between oak-leaf shaped cells in lymphatic capillaries, to brick shaped cells in the collecting lymphatic vessels. However, staining with both VE-cadherin and PECAM-1 revealed no defects in cell morphology in the lymphatic capillaries or collecting vessels of *Lyve1*$^{-/-}$ mice (Figure 3.5 A-D). Finally, the luminal valves also appeared normal in *Lyve1*$^{-/-}$ mice (data not shown).

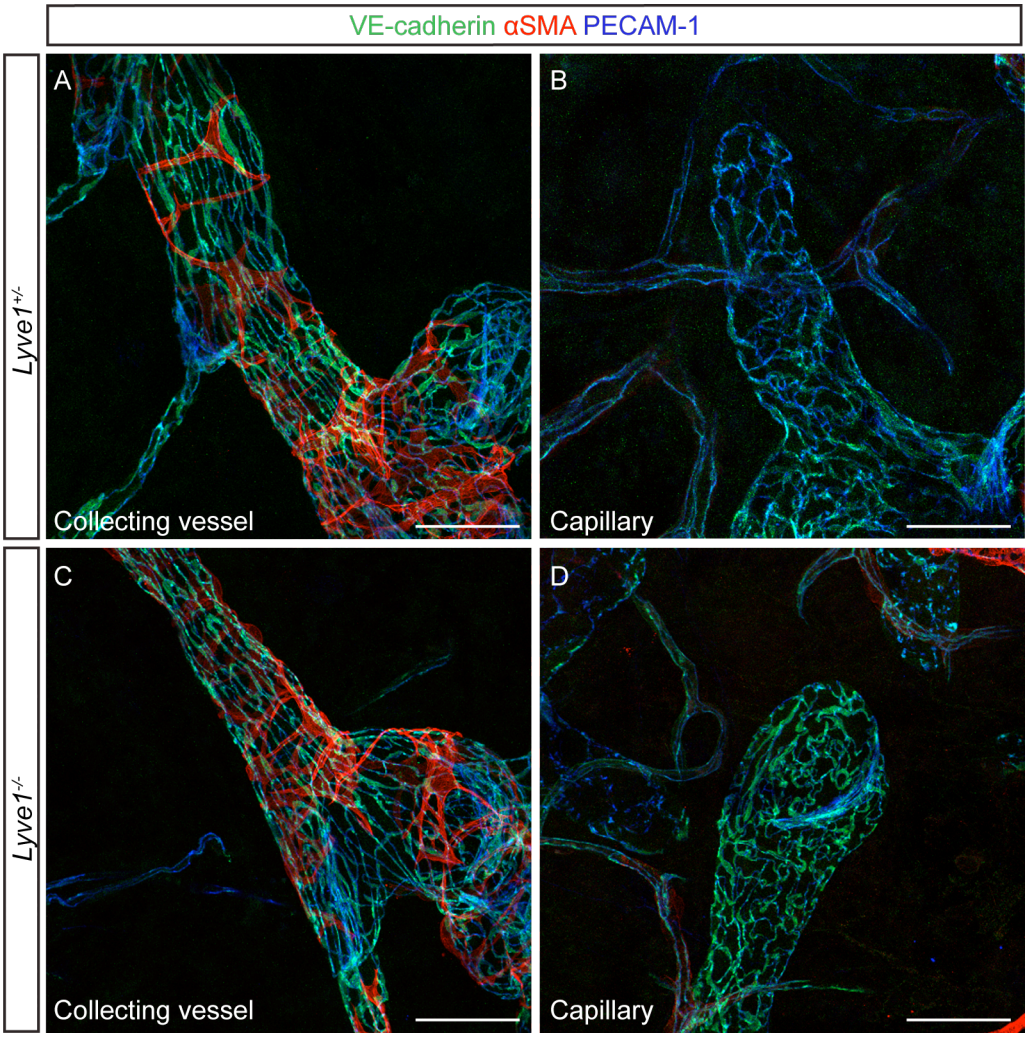

Figure 3.5 *Lyve1* mutant mice have no detectable phenotype
Immunofluorescence of *Lyve1* heterozygous (A-B) or mutant (C-D) mice at 6 weeks, with antibodies against VE-cadherin (green), αSMA (red) and PECAM-1 (blue). Scale bars = 50μm.

In the absence of any striking phenotype in the lymphatic collecting vessels, we did not follow up these preliminary observations for a more thorough characterisation of the phenotype of collecting vessels in *Lyve1*$^{-/-}$ mice, so we cannot rule out the possibility of more subtle deficiencies or age-dependant defects occurring in older mice. At least from these preliminary experiments, it does not seem that LYVE-1 is a negative regulator of SMC recruitment, or involved in the regulation of lymphatic endothelial cell morphology.

3.2 Extracellular matrix deposition

In contrast to the original dogma that lymphatic vessels, particularly lymphatic capillaries, have no or very rudimentary basement membranes (BMs), recent studies have identified a discontinuous basement membrane around dermal lymphatic capillaries, comprising Laminin (but not Laminin-α5), Perlecan, Collagen IV, Collagen XVIII and Nidogen (Vainionpaa et al., 2007, Pflicke and Sixt, 2009). Pflicke et al. also describe a difference between the basement membrane of lymphatic capillaries and collecting vessels: while the BM of lymphatic capillaries is perforated to allow entry of dendritic cells into lymphatic vessels independently of integrin-mediated adhesion, the basement membrane of collecting vessels is continuous and more extensive (Pflicke and Sixt, 2009).

To establish whether we could use the deposition of basement membrane proteins around prospective collecting lymphatic vessels as a marker of collecting vessel differentiation, we examined the expression of Collagen IV, Laminin-α5 and Fibronectin in ear-skin between P12 and P18.

3.2.1 Collagen IV is deposited by LEC, prior to SMC recruitment

Interestingly, the expression patterns and timing of deposition of Collagen IV and Laminin-α5 were very different. Collagen IV started to be deposited around prospective collecting lymphatic vessels prior to LYVE-1 down-regulation and SMC recruitment (arrows, Figure 3.6 A-B’’’), suggesting that Collagen IV was predominantly expressed by LEC, and expression remained high throughout collecting lymphatic vessel development (Figure 3.6 C-C’’’).

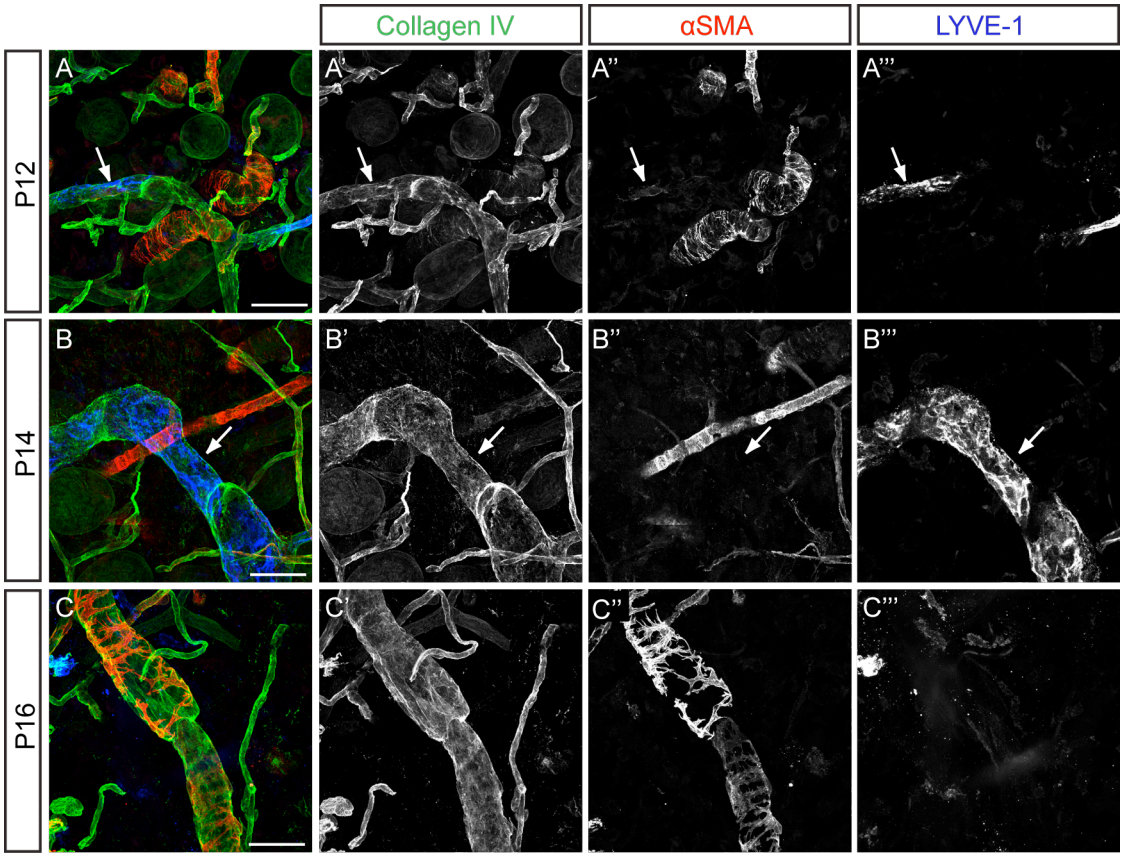

Figure 3.6 Collagen IV deposition around prospective lymphatic collecting vessels. (A-C''') Immunofluorescence of whole-mount ear-skin at indicated developmental stages using antibodies against Collagen IV (green), αSMA (red) and LYVE-1 (blue). Arrows in A-B show collagen IV deposition in LYVE-1 positive vessels, prior to LYVE-1 down-regulation and SMC recruitment. Scale bars = 50μm.

In the adult, we could see Collagen IV expression in the lymphatic capillaries, but it was expressed to a much lower level than in the collecting lymphatic vessels (Figure 3.7 A-B'). This result is in line with those of Pflicke et al. and gives rise to the possibility that either the SMC also contribute directly to Collagen IV deposition in adult collecting lymphatic vessels or that SMC increase Collagen IV deposition by LEC. The latter hypothesis is supported by a recent study demonstrating both *in vitro* and *in vivo* that pericyte recruitment to developing blood vessels can increase ECM (including Collagen IV) deposition by endothelial cells (Stratman et al., 2009a). We observed what looks like the outline of a Collagen IV-positive SMC in the adult collecting vessel (Figure 3.7 A-A'), suggesting that both LEC and SMC contribute to Collagen IV expression in the mature collecting lymphatic vessels.

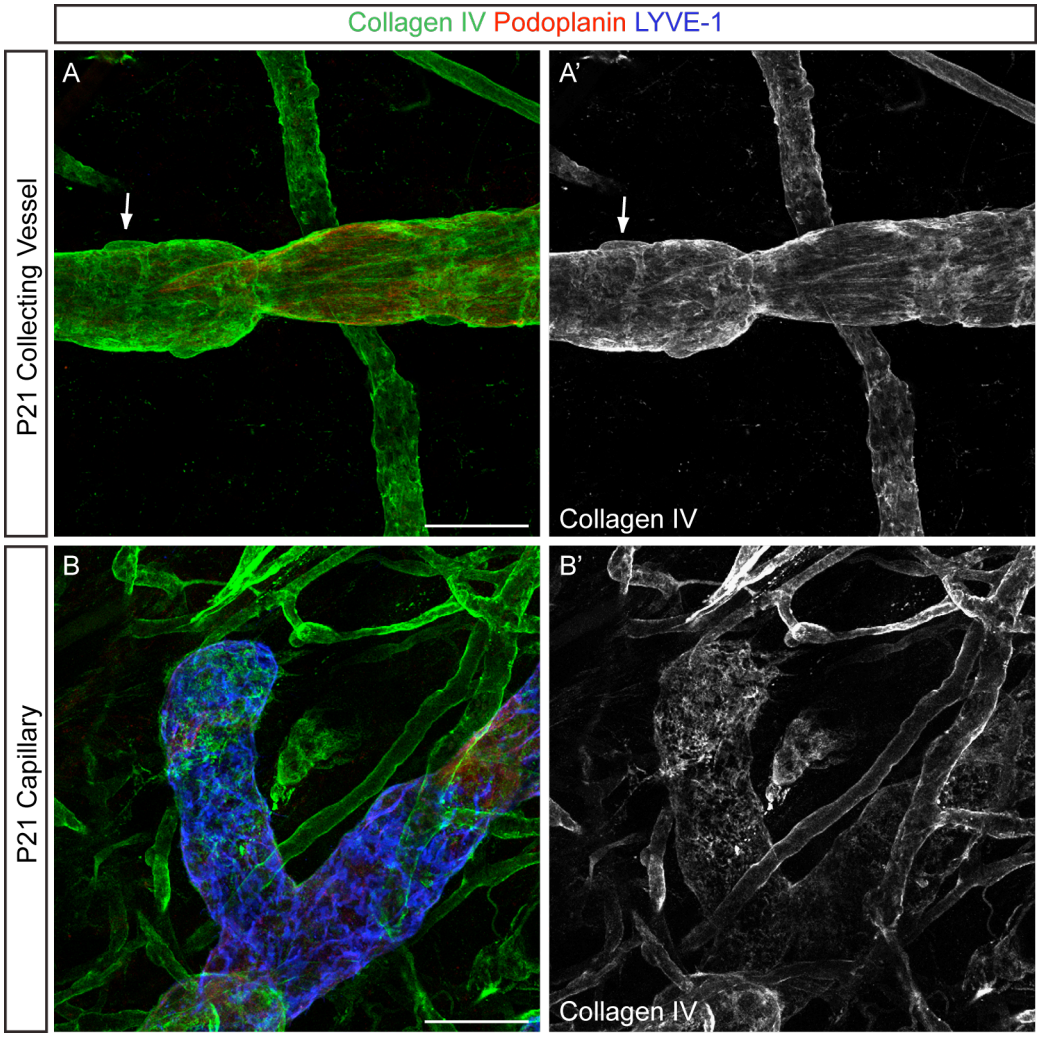

Figure 3.7 Collagen IV expression in the mature lymphatic vasculature.
(A-B') Immunofluorescence of whole-mount ear-skin at P21 in collecting vessels (A-A') and capillaries (B-B') with antibodies against Collagen IV (green), podoplanin (red) and LYVE-1 (blue). Arrow in A indicates Collagen IV positive SMC. Scale bars = 50μm.

3.2.2 Laminin-α5 is predominantly deposited by SMC, except in luminal valves

In contrast to Collagen IV, no Laminin-α5 expression could be detected in the prospective collecting lymphatic vessels until SMC were recruited and established around the vessel (Figure 3.8 A-C'''; asterisk, Figure 3.8 A-A'). However, in line with previously published results, we detected Laminin-α5 expression in luminal valves

(arrows, Figure 3.8 A-A', B-B') (Bazigou et al., 2009). In mature collecting lymphatic vessels, Laminin-α5 staining highlighted the SMC (arrowheads, Figure 3.8 C-C''), a strong indication that, excepting LEC in the luminal valves, these cells are its main source.

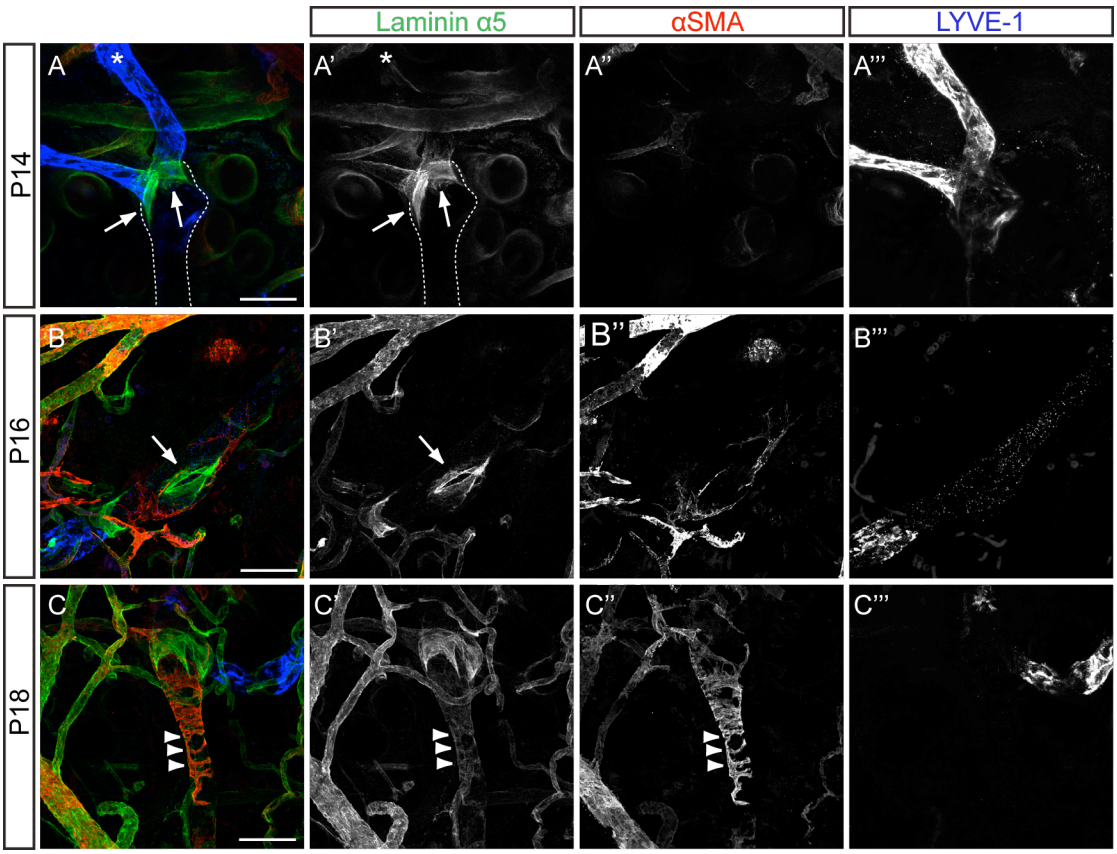

Figure 3.8 Laminin α5 expression in the developing lymphatic system.
(A-C''') Immunofluorence of whole-mount ear-skin at indicated developmental stages with antibodes against Laminin-α5 (green), αSMA (red) and LYVE-1 (blue). Arrow in A indicates Laminin-α5 expression in the luminal valves, asterisk indicates LYVE-1 positive, Laminin-α5 negative immature lymphatic vessel. Arrowheads in C show Laminin-α5 positive collecting lymphatic vessels. Scale bars = 50μm.

3.2.3 Fibronectin is not a specific marker of ECM deposition in the lymphatic vasculature

Fibronectin is a major component of the vascular basement membrane. We examined its expression in the developing and mature lymphatic vasculature, in order to establish whether we could gain any new insights into lymphatic vessel maturation. We observed a dense network of Fibronectin fibrils in the vasculature and surrounding tissues, but could not detect any change in expression between the developing and mature lymphatic vasculature (Figure 3.9 A-B'). Since no specific collecting lymphatic vessel maturation events could be related to changes in Fibronectin expression, we concluded that Fibronectin is not a useful marker of lymphatic collecting vessel differentiation. However, it should be noted that a specific isoform of Fibronectin containing the EIIIA domain is expressed specifically in the matrix core of luminal valves at the onset of Integrin-α9 expression and is required for proper formation of the valve leaflets (Bazigou et al., 2009).

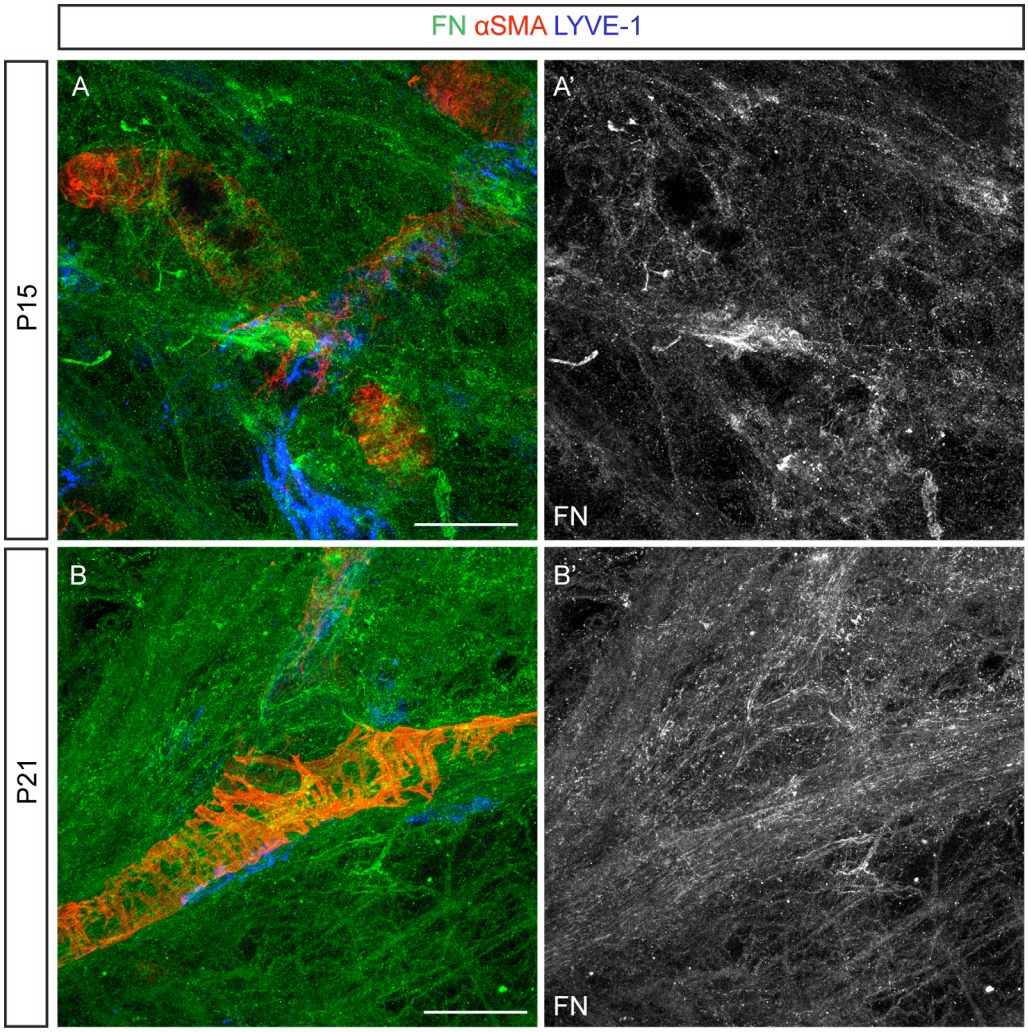

Figure 3.9 Fibronectin is not a useful marker of collecting lymphatic vessel development.
(A-B') Immunofluorescence of whole-mount ear-skin at indicated developmental stages using antibodies against Fibronectin (green), αSMA (red) and LYVE-1 (blue). Scale bars = 50μm.

Together, these data show that both LEC and SMC contribute to the formation of the basement membrane around lymphatic collecting vessels, and that extracellular matrix deposition may be one of the first signs of collecting vessel specification.

We have summarised these results into a timeline of events leading up to lymphatic collecting vessel differentiation (Figure 3.10).

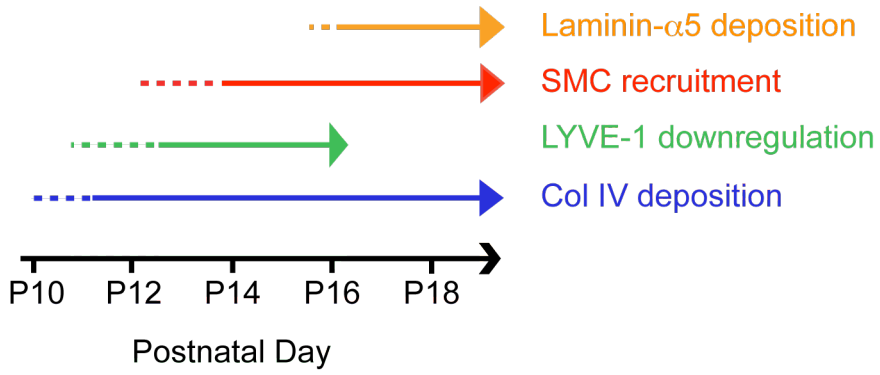

Figure 3.10 Timeline of collecting lymphatic vessel development.
Schematic, summarising the timing of dermal lymphatic collecting vessel differentiation events in the ear. Collagen IV deposition occurs just prior to LYVE-1 down-regulation, which in turn usually begins prior to SMC recruitment. Deposition of Laminin-α5 occurs after SMC are established around the collecting vessels.

3.3 Microarray analysis of lymphatic extracellular matrix

The composition of the lymphatic extracellular matrix and any differences to that of the blood vasculature has not been extensively studied. In order to better characterise the lymphatic extracellular matrix, we carried out a microarray study, using RNA samples extracted from mouse postnatal mesenteric lymphatic vessels, arteries and veins. Previous microarrays have compared the gene expression profiles of cultured primary LEC and BEC. However, using this approach, it is difficult to rule out the possibility of time in culture affecting gene expression. It is also impossible to distinguish between arterial and venous gene expression. Using whole vessels avoided these issues, and also allowed for the contribution of both SMC and EC to the lymphatic / vascular extracellular matrix. Furthermore, our *in vivo* approach allowed for the likelihood that the 3D environment and interactions between SMC and EC might affect deposition of vascular basement membrane and perhaps expression changes in the genes encoding extracellular matrix related proteins.

3.3.1 The Affymetrix GeneChip Array System

A microarray is an ideal tool for comparison of gene expression profiles from different samples. The Affymetrix system uses probes designed against exons from both established cDNA sequences and predicted gene structures, allowing a comprehensive profile of expression data to be generated. The probes are engineered onto a glass or silicone chip (an *Affy chip*) and then incubated with fluorophore-conjugated, sense-strand cDNA generated from the RNA samples we supplied. The cDNA binds to the complementary antisense strand of the probe, and after washing off non-specifically bound sequences, only strongly bound sequences remain. The amount of target sample bound to each probe will determine the strength of the signal from that spot. The Affymetrix system is a single-channel microarray, which provides intensity data for each probe on the dataset, giving a relative abundance compared to the other samples in the same experiment that have been processed using the same conditions. This can be expressed as a fold-change in expression for a gene in one sample, compared to the same gene in another sample (Figure 3.11). Further details about analysis of this data are given in materials and methods.

In this experiment, we used a Mouse Exon 1.0 Sense Target (ST) array (Affymetrix). This array uses around 4 probes per exon, or about 40 probes per gene, to allow either 'exon-level' or 'gene-level' analysis. The exon-level dataset allows detection and analysis of alternative splicing events and differential expression of each exon within a gene. For the purposes of this experiment however, we concentrated on 'gene-level' analysis. In this case, all the probes on different exons within a gene are collated into one data point, which represents expression of all the transcripts derived from that gene. Due to the high number of probes per gene, this array method allows a highly sensitive read-out of gene expression and generates statistically robust results.

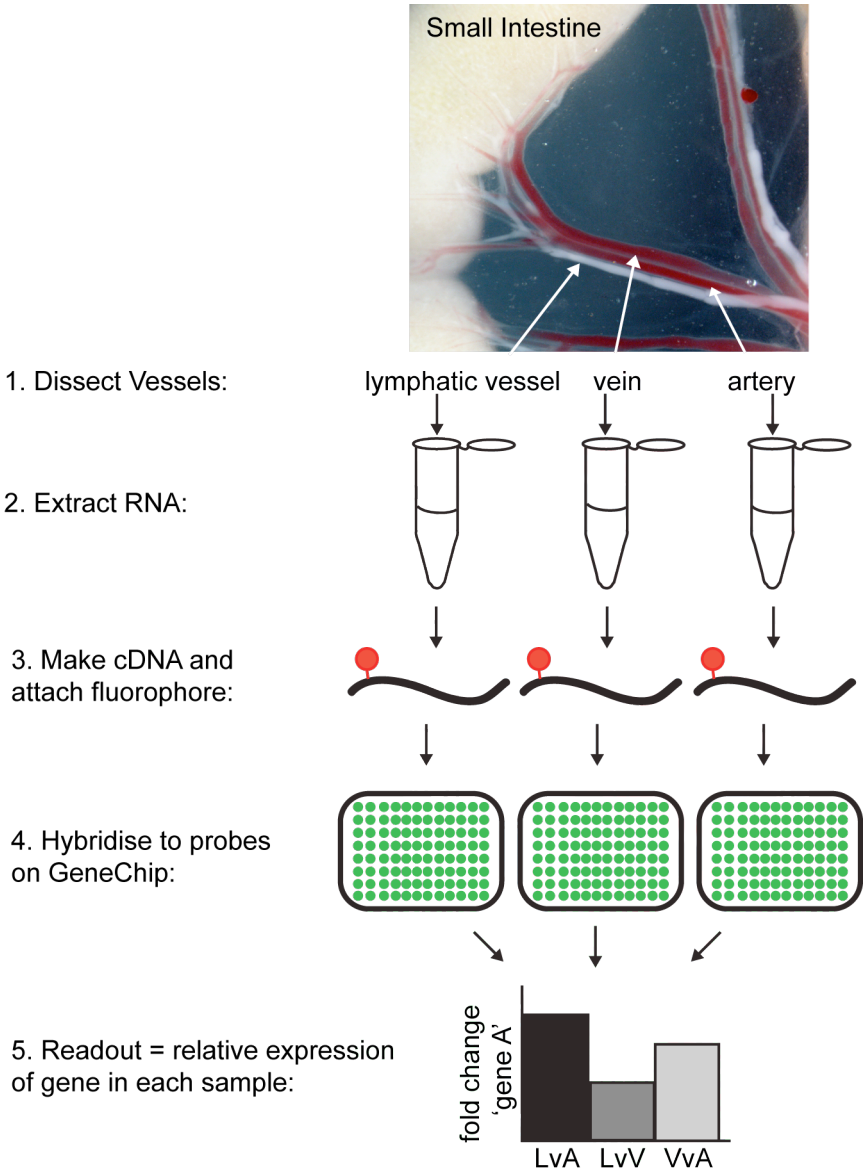

Figure 3.11 Microarray analysis of lymphatic vessels, arteries and veins.
Lymphatic vessels, arteries and veins were dissected from P6-7 wild type pups and the RNA extracted. Two independent samples of each vessel type were analysed using a Mouse Exon 1.0 ST Array (Affymetrix). Briefly, RNA is amplified, converted to cDNA, which is flourophore-conjugated and hybridised to an Affychip. Readout of the array is relative expression of a given gene in each vessel type.

3.3.2 Identification of lymphatic specific extracellular matrix related genes

Within our dataset we identified several known markers of lymphatic vessels, arteries and veins and confirmed that they were up- or downregulated in the expected pattern, thus confirming the reliability of our dataset (Table 3.1). However, since this array method does not provide absolute gene expression levels, we cannot rule out the possibility of slight cross-contamination across the samples, or from smaller blood capillaries and other tissue, such as nerves, which emphasises the importance of validating the specificity of target gene expression.

	Gene Symbol	Lymphatic v Vein	Lymphatic v Artery	Artery v Vein
Lymphatic markers	***Prox1***	**5.1**	**17.8**	-3.5
	Pdpn	**2.3**	**2.8**	-1.3
	Lyve1	**2.6**	**3.6**	-1.4
	Flt4 (Vegfr3)	**4.6**	**3.8**	1.2
	Stab1	**1.7**	**2.0**	-1.2
Blood vessel markers	***Vegfc***	**-3.8**	**-5.4**	1.4
	Figf (Vegfd)	**-3.3**	**-1.8**	-1.9
	Flt1 (Vegfr1)	**-2.7**	**-1.9**	-1.4
	Pdgfrb	**-2.0**	**-1.6**	-1.2
	Vwf	**-7.6**	**-4.3**	-1.8
Arterial markers	***Efnb2****	1.7	-1.1	**1.9**
	Hey1	1.2	-1.3	**1.6**
	Dll4	1.3	-1.4	**1.9**
Venous markers	***Ephb4****	-1.1	1.7	**-1.9**
	Nrp2*	1.5	3.5	**-2.4**

Table 3.1 Validation of microarray data: known markers of lymphatic vessels, arteries and veins show expected expression.
The fold change in expression of each gene in lymphatic vessels compared to veins and arteries, and arteries compared to veins. A number >0 indicates up-regulation and <0 indicates down-regulation. Known lymphatic, blood vessel, arterial and venous markers are up or down-regulated in the expected pattern. * indicates arterial/venous genes with known expression also in the lymphatics. Fold changes represent mean of two independent samples

To identify differential expression of extracellular matrix proteins between the lymphatic and blood vasculature, we selected all genes that were up- or down-regulated in lymphatic vessels compared to arteries and/or veins by a factor of 2 or more and carried out a Uniprot search on these genes to identify extracellular matrix proteins. We identified 14 genes involved in the formation, composition or degradation of the ECM that were expressed at least 2-fold higher in lymphatic vessels compared to arteries or veins (Table 3.2), and 15 genes of the same description that were expressed at least 2-fold higher in arteries and/or veins, compared to lymphatic vessels (Table 3.3).

Gene Symbol	Gene Name	Lymphatic v Vein	Lymphatic v Artery	Artery v Vein
Egfl6	EGF-like protein	**7.5**	**10.9**	**-1.4**
Reln	Reelin	**5.0**	**1.7**	**2.9**
Efemp1	Fibulin-3	**4.0**	**5.4**	**-1.4**
Prelp	Prolargin	**3.4**	**3.3**	**1.0**
Spock3	Osteonectin	**3.2**	**4.5**	**-1.4**
E330026B02Rik	Collagen, Type VI, alpha6	**2.9**	**3.5**	**-1.2**
Ltbp1	TGFbeta1 binding protein	**2.5**	**1.0**	**2.4**
Lgals3bp	Galectin-3 binding protein	**2.4**	**2.1**	**1.2**
Thsd4	Thrombospondin, type 1, domain containing 4	**2.2**	**-1.1**	**2.4**
Adamts19	ADAM metallopeptidase with thrombospondin type 1 motif, 19	**2.1**	**2.6**	**-1.2**
Nid2	Nidogen 2	**2.1**	**1.9**	**1.1**
Fras1	Extracellular matrix protein FRAS1	**1.9**	**3.1**	**-1.7**
Comp	Cartilage oligomeric matrix protein	**1.7**	**2.7**	**-1.6**
Mmp19	Matrix metalloproteinase 19	**1.5**	**2.1**	**-1.4**

Table 3.2 Extracellular matrix associated proteins that are up-regulated in lymphatic vessels compared to arteries and/or veins.
Genes associated with extracellular matrix structure, function, assembly or degradation that are up-regulated ≥2-fold in lymphatic vessels compared to veins or arteries in an Affymetrix GeneChip array. Fold change represents mean of two independent samples.

Gene Symbol	Gene Name	Lymphatic v Vein	Lymphatic v Artery	Artery v Vein
Ctgf*	Connective tissue growth factor	**-2.2**	**-4.4**	**2.0**
Spon1*	F-spondin	**-2.1**	**-3.6**	**1.7**
Col8a1	Collagen, type VIII, alpha 1	**1.4**	**-3.5**	**5.1**
Eln*	Tropoelastin	**-2.4**	**-3.2**	**1.4**
Adamts8	ADAM metallopeptidase with thrombospondin type 1 motif, 8	**-1.6**	**-2.7**	**1.2**
Mamdc2	Mamcan	**-2.3**	**-2.7**	**1.2**
Mmrn2	Emilin-3	**-1.8**	**-2.5**	**1.4**
Kazald1	Kazal-type serine protease inhibitor domain 1	**-1.2**	**-2.4**	**2.0**
Acan	Aggrecan	**1.0**	**-2.2**	**2.3**
Mia1*	Melanoma inhibitory activity protein	**-3.0**	**-2.2**	**-1.4**
Chad	Chondroadherin	**-5.0**	**-1.1**	**-4.5**
Adamts18	ADAM metallopeptidase with thrombospondin type 1 motif, 18	**-3.1**	**1.1**	**-3.3**
Tnc	Tenascin C	**-2.9**	**-1.9**	**-1.5**
Egflam	EGF-like, fibronectin type III and laminin G domains	**-2.1**	**-1.7**	**-1.3**
Adamts2	ADAM metallopeptidase with	**-2.1**	**-2.0**	**-1.1**

Table 3.3 Extracellular matrix associated proteins that are up-regulated in arteries or veins compared to lymphatic vessels.
Genes associated with extracellular matrix structure, function, assembly or degradation that are up-regulated ≥2-fold in veins or arteries compared to lymphatic vessels in an Affymetrix GeneChip array. * indicates genes that are up-regulated ≥2-fold in both arteries and veins compared to lymphatic vessels. Fold changes represent mean of two independent samples

We validated these results by examining lymphatic vs blood vascular expression by either immunostaining of whole-mount ear skin, or immunoblotting. Due to a lack of suitable antibodies, we were only able to obtain *in vivo* expression data for Efemp1. In corroboration of the microarray data that showed Efemp1 expression as 4-5 fold higher in lymphatic than blood vessels (Table 3.2), we observed Efemp1 expression specifically in the lymphatic vasculature (arrowhead, Figure 3.12 A-A'), while the blood vasculature remained negative (arrows, Figure 3.12 B-B'). We also confirmed preferential expression of Efemp1, Spock3 and Nid2 in LEC compared to BEC by immunoblotting (Figure 3.12 C-D), thus further validating the microarray results and strengthening the identification of new lymphatic specific basement membrane components, which may be of interest for future studies.

Our microarray results not only confirm that the lymphatic extracellular matrix is more complex than originally thought, but also identify several differences in gene expression between the extracellular matrices in the lymphatic and blood vasculature, allowing speculation that some of the genes highly expressed in the lymphatic extracellular matrix may be of specific functional importance.

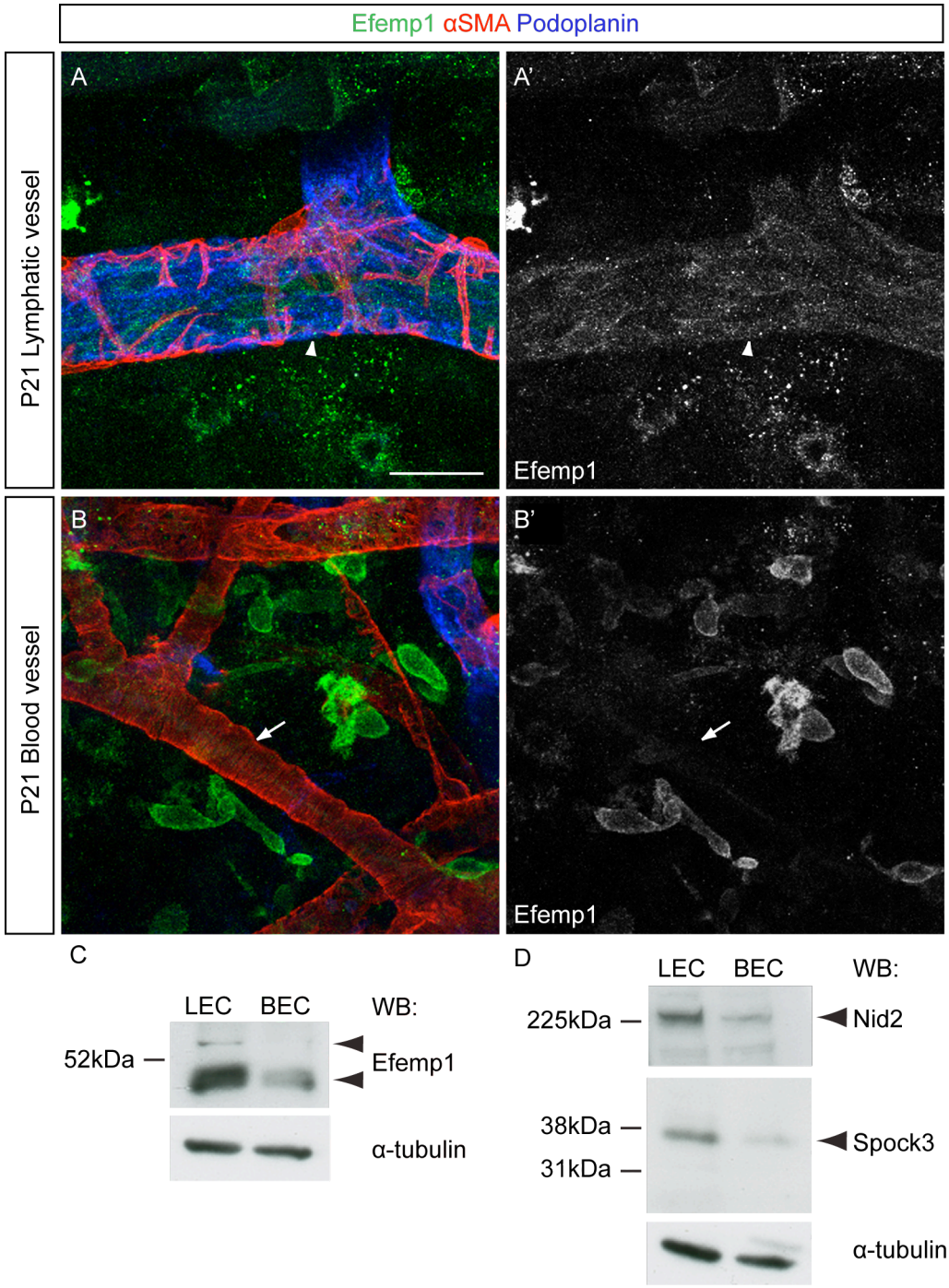

Figure 3.12 Validation of extracellular matrix genes identified as upregulated in lymphatic compared to blood vessels in the array.
(A-B') Immunofluorescence of whole-mount ear-skin at P21 with antibodies against Efemp-1 (green), αSMA (red) and podoplanin (blue). Arrowhead in A indicates Efemp1 positive lymphatic vessel, while arrow in B points to Efemp-1 negative blood vessel. (C-D) Immunoblot with indicated antibodies, showing increased expression of Efemp-1 (C), Nid2 and Spock3 (D) in cultured LEC compared to BEC. α-tubulin was used as a loading control in both cases.

Chapter 4. Reelin expression in the vasculature

4.1 Identification of Reelin as a lymphatic specific extracellular matrix protein

From our microarray, we identified *Reln* as a gene that was expressed 5-fold higher in lymphatic vessels than veins (Table 3.2). Reelin is a large extracellular matrix protein, whose expression and function has been extensively studied in the developing and mature central nervous system (Rice and Curran, 2001, Forster et al., 2010). The lymphatic-specific Reelin expression is consistent with *in vivo* data from rats and humans, where Reelin immunoreactivity was described in lymphatic, but not blood vessels (Samama and Boehm, 2005). However, despite its previous identification in non-neural tissues, little is known about Reelin function outside of the central nervous system. We decided that this would be an interesting candidate to follow up on, particularly since some human patients with a *RELN* mutation suffer from lymphoedema (Hong et al., 2000), which could potentially give our study clinical relevance.

4.1.1 Reelin expression in lymphatic development

We chose to analyse Reelin expression in the dermal lymphatic vasculature at three stages: embryonic, P14 and P21, so that we could clearly visualise expression in the immature plexus (E16), vessels that are actively undergoing remodelling (P14) and in the mature lymphatic vasculature (P21). The timing of development differs between tissues, so the developmental stage of the vasculature is not comparable between tissues at the same age; for example P0 in the dorsal skin is probably equivalent to P15 in the ear, and at P7 the mesenteric lymphatic vessels are fully mature, while the ear still

resembles the primitive plexus. For this reason, it is important to consider rather the developmental stage of the tissue of interest, rather than the age of the animal.

While Reelin immunoreactivity was readily detected from embryonic stages in the LYVE-1 positive, PECAM-1 positive lymphatic endothelium (arrowhead, Figure 4.1 A-A'), we could not identify any Reelin expression in LYVE-1 negative, PECAM-1 positive blood vessels (arrows, Figure 4.1 A-A').

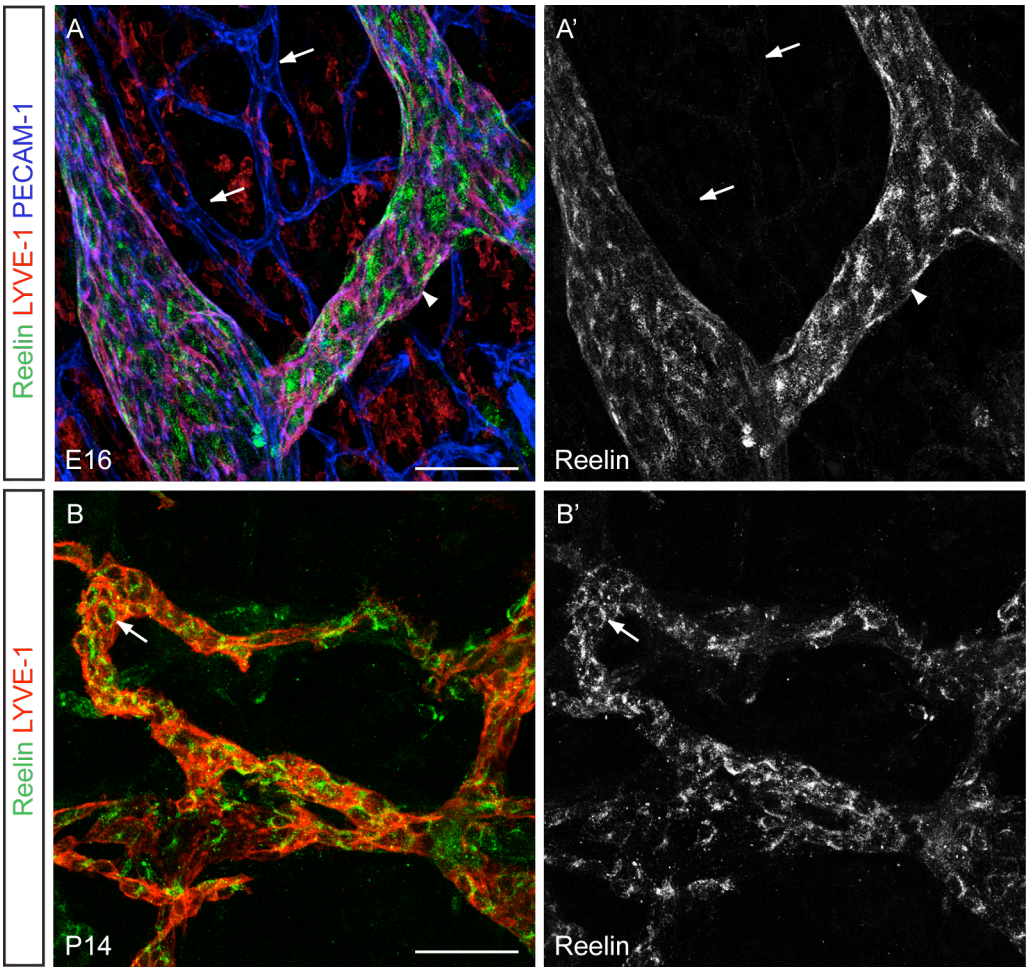

Figure 4.1 Reelin expression in the developing lymphatic vasculature.
Immunofluorescence of whole-mount dorsal skin (A-A') or ear-skin (B-B') at indicated developmental stages, using antibodies against Reelin (green), LYVE-1 (red) and PECAM-1 (blue; A). Scale bars = 50μm.

Reelin expression appeared intracellular in the immature lymphatic vasculature, even postnatally (arrow, Figure 4.1 B-B') and we confirmed its sub-cellular localisation by co-staining with Golgi and endoplasmic reticulum (ER) markers. Consistent with

reports that Reelin resides in the neuronal ER prior to secretion (Tinnes et al., 2011), we found that intracellular Reelin was mainly located in the ER (arrows, Figure 4.2 A-A''), and to a much lesser extent in the Golgi (arrows, Figure 4.2 B-B'').

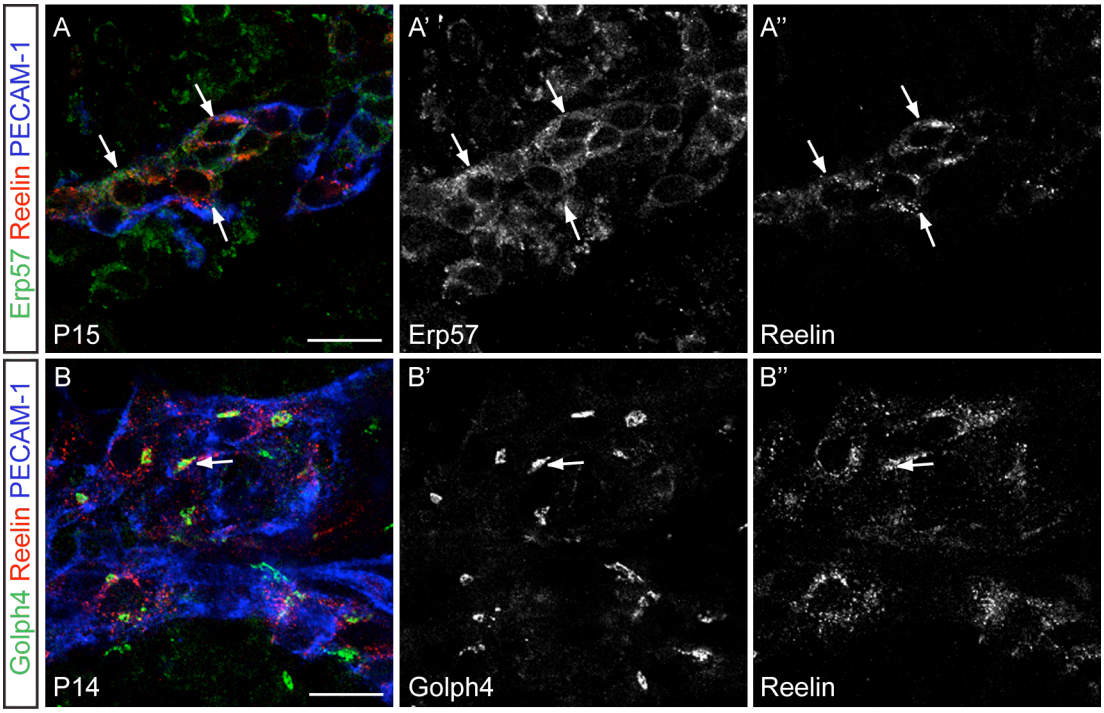

Figure 4.2 Sub-cellular Reelin localisation.
Immunofluorescence staining of whole-mount ear-skin at indicated developmental stages with antibodies against the ER marker, Erp57 (green; A-A'), the Golgi marker, Golph 4 (green, B-B'), Reelin (red) and PECAM-1 (blue). Images are single confocal z-stacks to show co-localisation. Arrows indicate areas of co-localisation. Scale bars = 15.87μm.

4.1.2 Reelin expression in the mature lymphatic vasculature

Amplification of Reelin immunostaining confirmed specific expression in the mature collecting lymphatic vessels and capillaries (Figure 4.3 A-B). We also observed positive staining in scattered single cells in these samples (asterisk Figure 4.3 B), but using the secondary antibody only revealed this to be a non-specific artefact of the amplification procedure (Figure 4.3 C-C').

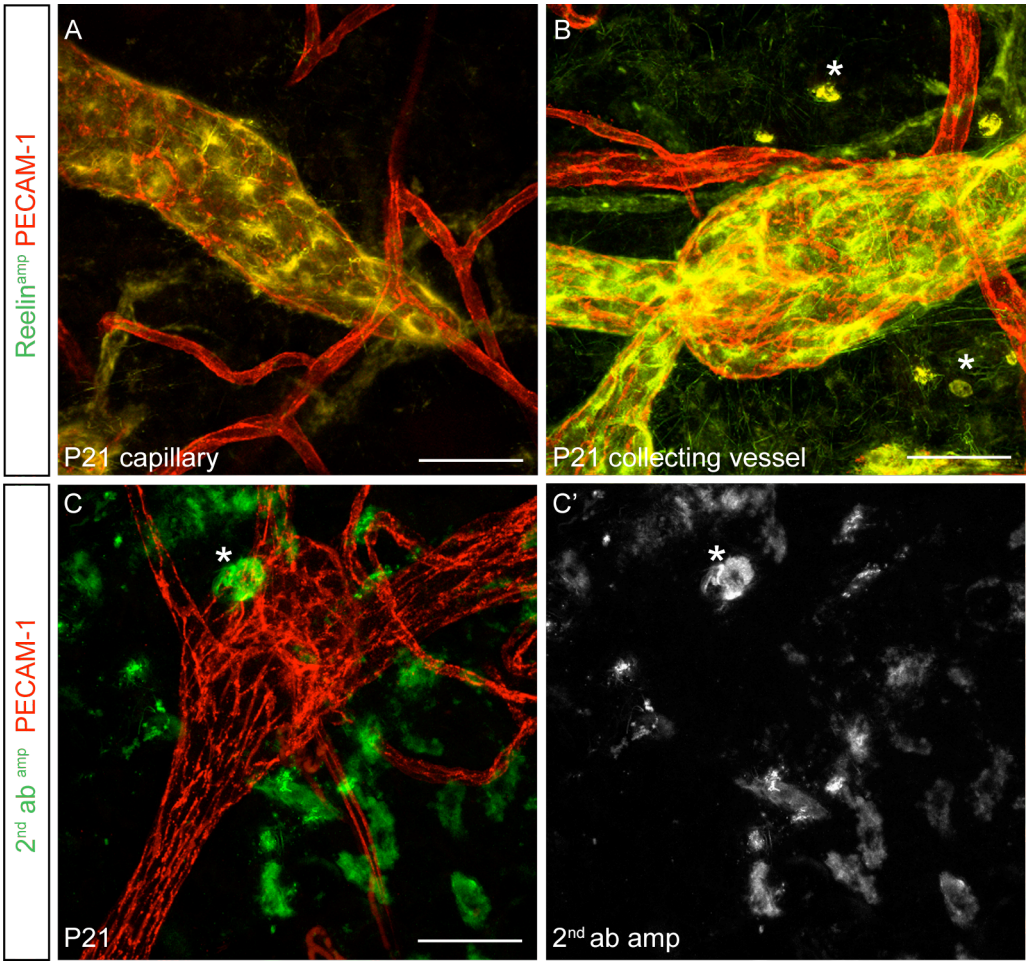

Figure 4.3 Reelin continues to be expressed in the mature lymphatic vasculature. Immunofluorescence staining of whole-mount ear-skin at P21 using antibodies against Reelin (amplified, green; A-B) or secondary antibody only (green; C) and PECAM-1 (red). Asterisks indicate non-specific signal amplification in scattered cells. Scale bars = 50μm.

Upon amplification, we also detected Reelin expression in the nerves (open arrowhead, Figure 4.4 A-A'), as well as low levels of Reelin expression in the veins (arrows, Figure 4.4 A-B'), but not in the arteries (closed arrowhead, Figure 4.4 A-B'). It is likely that the apparent arterial Reelin expression suggested by the microarray (Table 3.2) is in fact due to contamination of the arterial sample with Reelin positive nervous tissue, which is not visible without staining, but lies in close apposition to the blood vessels (Figure 4.4 A-A').

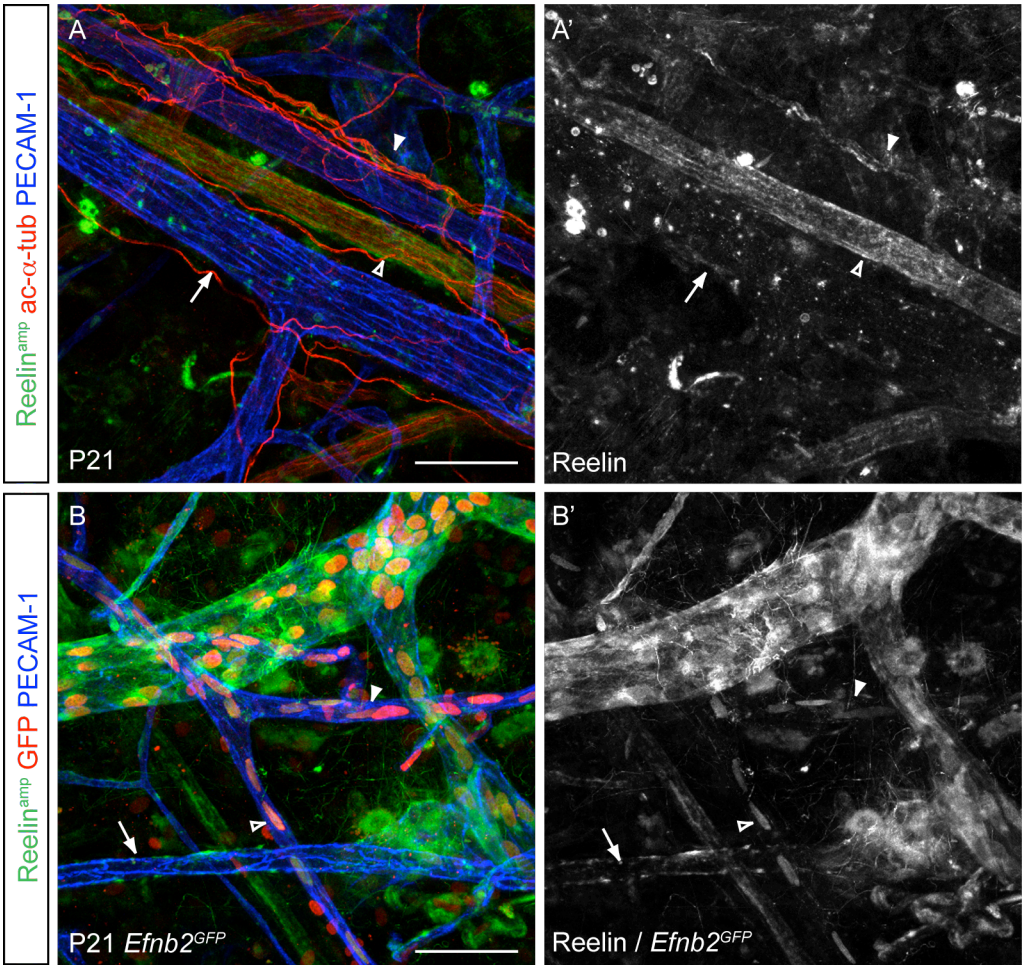

Figure 4.4 Amplification allows detection of weak Reelin signal in nerves and veins, but not arteries.
Immunofluorescence of whole-mount ear-skin in wildtype (A-A') or *Efnb2*^{GFP} (B-B') mice using antibodies against Reelin (amplified, green), acetylated α-tubulin (red, A-A'), GFP (red, B-B') and PECAM-1 (blue). Arrow in A indicates weakly Reelin-positive vein, empty arrowhead in A shows Reelin positive nerve and filled arrowhead shows close apposition of arteries and nerves. Arrow in A indicates weakly Reelin positive vein, filled arrowhead shows Reelin negative artery and empty arrowhead points to GFP-expressing arterial EC nuclei. Scale bars = 50μm.

Closer examination of endogenous Reelin expression in the mature lymphatic vasculature revealed interesting differences in Reelin localisation between collecting lymphatic vessels and capillaries. We observed intense punctuated, perinuclear Reelin staining in the capillaries (Figure 4.5 A-A'), whereas in the collecting vessels, Reelin immunoreactivity was weaker and more diffuse (Figure 4.5 B-B'). This suggested that

the lymphatic endothelial cells might secrete Reelin into the extracellular matrix of the collecting lymphatic vessels, while it is retained within the endothelium in capillaries.

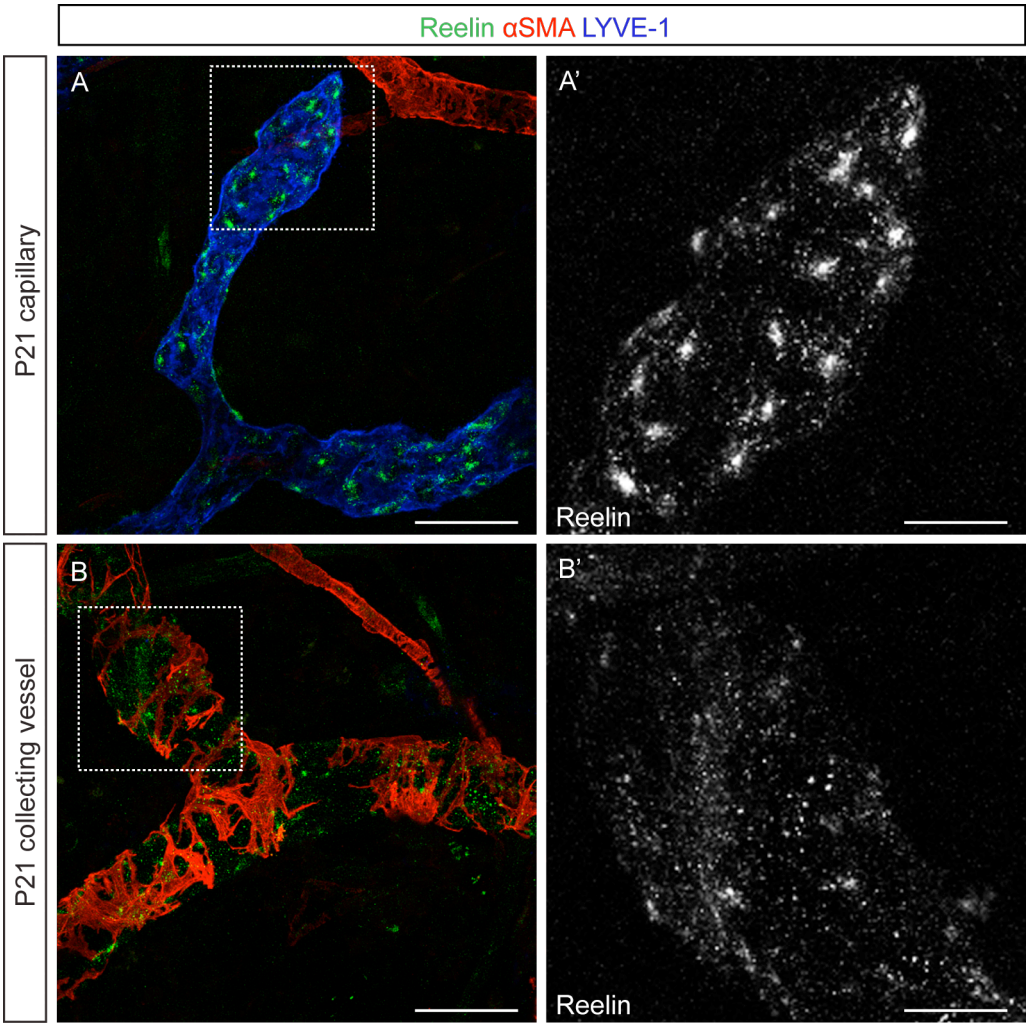

Figure 4.5 Reelin is localised differently in collecting vessels and capillaries. Immunofluorescence of whole-mount ear-skin at P21 using antibodies against Reelin (green), αSMA (red) and LYVE-1 (blue). Scale bars = 50μm (A,B) and 16.67μm (A', B') .

We tested this hypothesis by immunofluorescence and amplification of Reelin signal in non-permeabilised tissue, so that we only visualised extracellular Reelin. We observed very low Reelin staining around the lymphatic capillaries (arrow, Figure 4.6 A-A'), suggesting that the expression we had previously observed was indeed intracellular,

while much greater immunoreactivity was retained around the lymphatic collecting vessels (Figure 4.6 B-B'), which is indicative of secretion into the extracellular matrix.

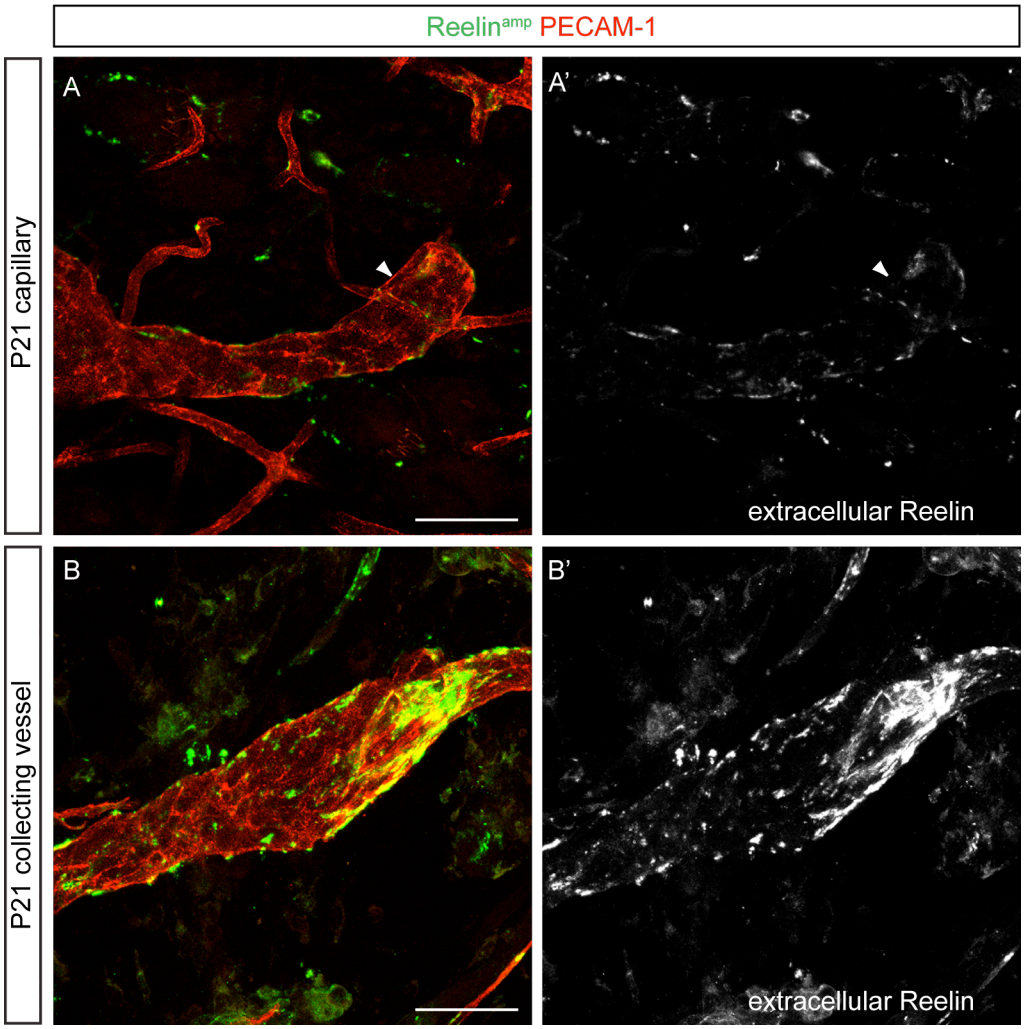

Figure 4.6 Reelin is secreted from the collecting vessels, but not the capillaries. Immunofluorescence of non-permeabilised whole-mount ear-skin using antibodies against Reelin (green, amplified) and PECAM-1 (red). Arrowhead indicates low-level of Reelin secretion from lymphatic capillaries. Scale bar = 50μm.

Taken together, these data indicate that Reelin expression is specific to the lymphatic endothelium in both the developing and mature dermal vasculature *in vivo*, but it is only efficiently secreted into the extracellular matrix of the collecting lymphatic vessels.

4.2 Interaction between LEC and SMC leads to release and processing of Reelin

We confirmed that lymphatic endothelial specific Reelin expression was maintained *in vitro* by qPCR analyses of RNA extracted from cultured primary human lymphatic endothelial cells (LEC), blood endothelial cells (BEC), umbilical vein- (HUV-) and aortic smooth muscle cells (HAoSMC) (Figure 4.7). This is consistent with the results of an earlier microarray, which identified *Reln* expression in cultured LEC, but not BEC (Petrova et al., 2002).

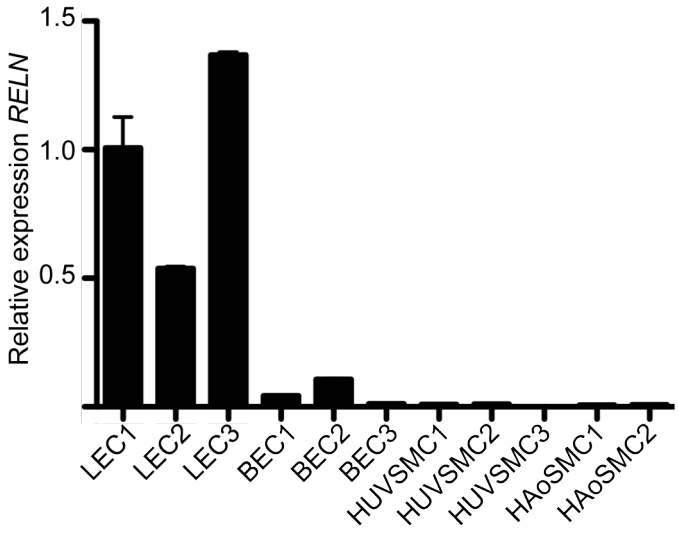

Figure 4.7 Lymphatic specificity of Reelin expression is maintained *in vitro*.
RT-PCR data showing *RELN* expression in 3 independent samples of LEC, BEC, HUVSMC and 2 of HAoSMC, relative to LEC1. Mean ± SEM is plotted.

Immunoprecipitation and Western blotting analysis of LEC and SMC using an antibody that recognises an epitope at the N-terminus of Reelin (Figure 4.8 A) also confirmed that Reelin protein is only produced by LEC *in vitro* (Figure 4.8 B).

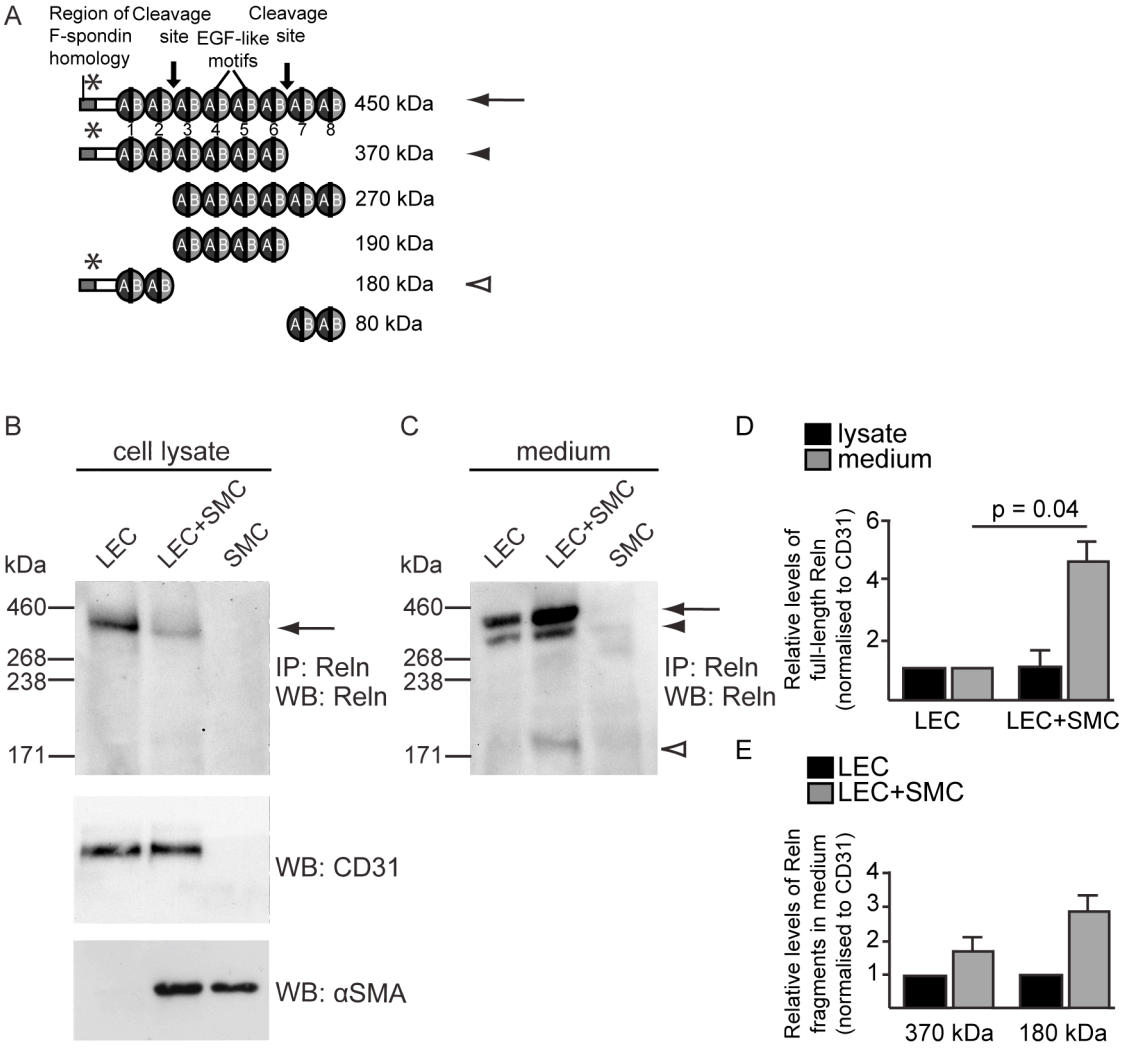

Figure 4.8 SMC enhance Reelin secretion from LEC and proteolytic processing. (A) Schematic of Reelin cleavage products, adapted from Jossin et al. (2007). Asterisk indicates antibody binding site. Arrow and arrowheads indicate cleavage products detected by the antibody. Analysis of whole cell lysate (B) and medium (C) of LEC and SMC cultured either alone or together, by immunoprecipitation and Western blot with antibodies to Reelin. Arrow indicates full length Reelin, arrowheads indicate cleavage products, eg 370 kDa and 180 kDa fragments in (C) . Analysis of whole cell lysate in (B) by Western blot with antibodies to CD31/PECAM-1 (for LEC) and aSMA (for SMC) show that equivalent numbers of cells were used. (D) Quantification of full-length Reelin protein levels, normalised to CD31/PECAM-1, in whole cell lysate (black bars) and culture medium (grey bars) of LEC cultured alone or together with SMC. Data represent mean (n= 3 experiments) ± SEM. (E) Quantification of Reelin N-terminal cleavage products, normalized to CD31/PECAM-1, secreted into the medium from LEC (black bars) and LEC+SMC co-cultures (grey bars). Data represent mean (n = 2 experiments) ± SEM.

We focussed on our observation that Reelin is secreted from the LEC of collecting vessels, but not the capillaries, as a way to investigate the mechanism of Reelin signalling in the lymphatic system. Since one of the main morphological differences between collecting vessels and capillaries is the presence of SMC around the former, we speculated that the release of Reelin into the extracellular matrix could be related to the recruitment of SMC. To test this, we analysed Reelin production and secretion by LEC that were cultured either alone or together with SMC. Examination of the whole cell lysate by immunoprecipitation and Western blot analysis revealed that LEC produced the full-length 450 kDa Reelin polypeptide (arrow, Figure 4.8 B). Analysis of the medium from LEC cultured alone showed that the full-length protein was secreted (arrow, Figure 4.8 C) and partially cleaved within the C-terminus, as described previously (Jossin et al., 2007), to give rise to another fragment of 370 kDa (closed arrowhead, Figure 4.8 C). Upon LEC co-culture with SMC, secretion of the full-length Reelin polypeptide was increased, with a corresponding increase in production of the 370 kDa fragment (Figure 4.8 C-E), although the production of Reelin was not affected (Figure 4.8 D). There is also a second processing event within the N-terminus, which gives rise to a 180 kDa fragment (open arrowhead, Figure 4.8 C, E), as well as the 190 kDa central Reelin fragment, which is capable of binding and activating the Reelin receptors ApoER2 and VLDLR (Jossin et al., 2007).

Incubation of SMC with LEC conditioned medium suggested that SMC can mediate the second N-terminal processing event (Figure 4.9 A). Although we sometimes also observed the 180kDa Reelin fragment in LEC cultured alone (Arrowhead, Figure 4.9 C), we were unable to determine whether LEC are also able to mediate this cleavage event in some cases, or whether this cleavage was due to the presence of contaminating BEC in our LEC culture, which may produce proteases that are not expressed in LEC. No increase in Reelin secretion or processing was seen when LEC were cultured in SMC conditioned medium (Figure 4.9 B) or on fibroblast-derived extracellular matrices (Figure 4.9 C), suggesting that the changes we observed upon LEC/SMC co-culture required the presence of SMC. Apparently lower Reelin levels in LEC cultured on a fibroblast matrix than on FN alone may reflect a reduced requirement for endogenous matrix protein secretion when a more complete matrix is provided exogenously, although this hypothesis would require further experimental evidence to confirm.

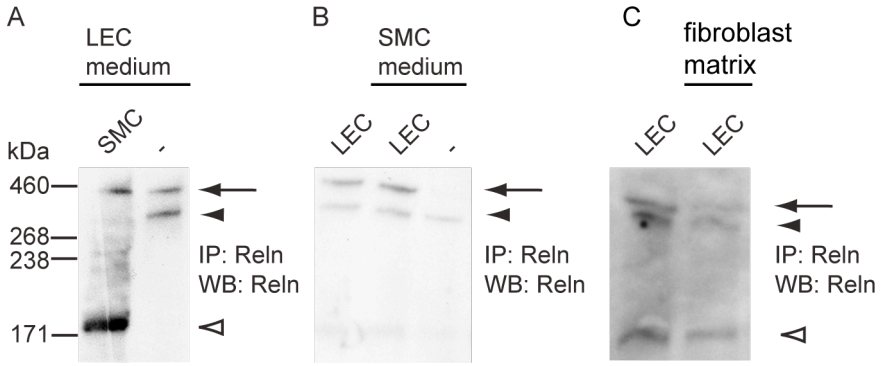

Figure 4.9 SMC can mediate Reelin processing.
(A) Analysis of LEC-conditioned medium alone or after incubation with SMC. (B) Analysis of medium from LEC cultured in normal medium, or SMC-conditioned medium. Note there is no change in Reelin secretion or processing. (C) Analysis of medium from LEC cultured in normal conditions or on a fibroblast-derived matrix. Note no change in Reelin secretion or processing.

Our results show that SMC can stimulate Reelin secretion from the LECs. Upon secretion, Reelin undergoes proteolytic processing and our experiments indicate that both SMC and LEC are involved in this process. Together these results suggest that SMC recruitment to the lymphatic collecting vessels activates Reelin signalling.

Chapter 5. Analysis of the *in vivo* function of Reelin in lymphatic vasculature

5.1 Collecting vessel development is impaired in *Reln* mutant mice

In order to assess the physiological function of Reelin in the lymphatic vasculature, we examined Reelin (encoded by *Reln*) deficient mice (D'Arcangelo et al., 1995). The *Reeler* mouse, which carries a spontaneous mutation in the *Reln* gene, was described long before the *Reln* gene was identified. *Reeler* mice are smaller than their wild-type siblings and suffer from severe ataxia, resulting in frequent trembling and falling over – a phenotype that when first described was likened to extreme inebriation (Falconer, 1951). *Reln* deficient mice initially develop normally, but neuronal defects become noticeable from approximately E14.5, once the first wave of post-mitotic neurons have migrated into the cortical plate in wild-type mice, but neurons in $Reln^{-/-}$ mice fail to reach their proper location (Tissir and Goffinet, 2003). Despite severe neurological defects, $Reln^{-/-}$ mice are initially grossly normal and are born in correct Mendelian ratios. The size difference between $Reln^{-/-}$ and wild-type siblings becomes apparent at about P10, and from approximately P14 onwards they start to display the characteristic ataxic gait, which becomes increasingly severe. Early reports indicate that some $Reln^{-/-}$ mice can surive to adulthood, although males are sterile. However, most *Reln* mutants die at around 3 weeks after birth, and they rarely survive weaning (even when this is delayed) (Falconer, 1951). We have not kept $Reln^{-/-}$ mice beyond 3 weeks of age in this study.

We studied the lymphatic vasculature of $Reln^{-/-}$ mice in the ear skin. In the ear, the vasculature develops by sprouting outwardly from proximal (near the head) to distal (outermost tip) regions of the ear. The characteristics of collecting vessels in this tissue vary along their length, for example in the degree of smooth muscle cell coverage,

which is generally denser at the proximal than distal end, where the collecting vessels terminate with the lymphatic capillaries. For this reason, detailed phenotypic analysis can be complicated by the necessity of comparing similar vessel regions between samples and the difficulties involved in achieving this in a reproducible manner, particularly when comparing samples of different sizes, as is the case for *Reln*$^{-/-}$ mice and their wild-type siblings. Therefore, to give us a detailed and reliable representation of the lymphatic phenotype of *Reln*$^{-/-}$ mice, we imaged along the entire length of individual vessels from proximal to distal ends of the ear. This approach revealed striking defects in *Reln* mutant (*Reeler*) collecting lymphatic vessels (Figure 5.1 A-B and see appendix, Figure 8.1 for original vessel images). In comparison to wild type vessels, *Reeler* collecting vessels retained abnormally high levels of LYVE-1 (Figure 5.1 A-C), and exhibited an irregular diameter, with abnormal constrictions and swellings along the length of the vessel (Figure 5.1 A-B, D). Vessel constrictions mainly seemed to occur at the sites of luminal valves, which developed normally in *Reeler* mutants (Figure 5.1 E-F), indicating that early stages of collecting vessel differentiation proceeded normally. *Reeler* mice also displayed reduced SMC coverage compared to wild type mice (Figure 5.2 A-C); by dividing the vessels into quarters from proximal (Q1) to distal (Q4) (Figure 5.1 A-B), we could quantify the degree of SMC coverage along the vessel. Despite maintaining a similar pattern of proximal to distal decrease, *Reln* mutants displayed significantly lower SMC coverage than wild type mice in each vessel quarter (Figure 5.2 C).

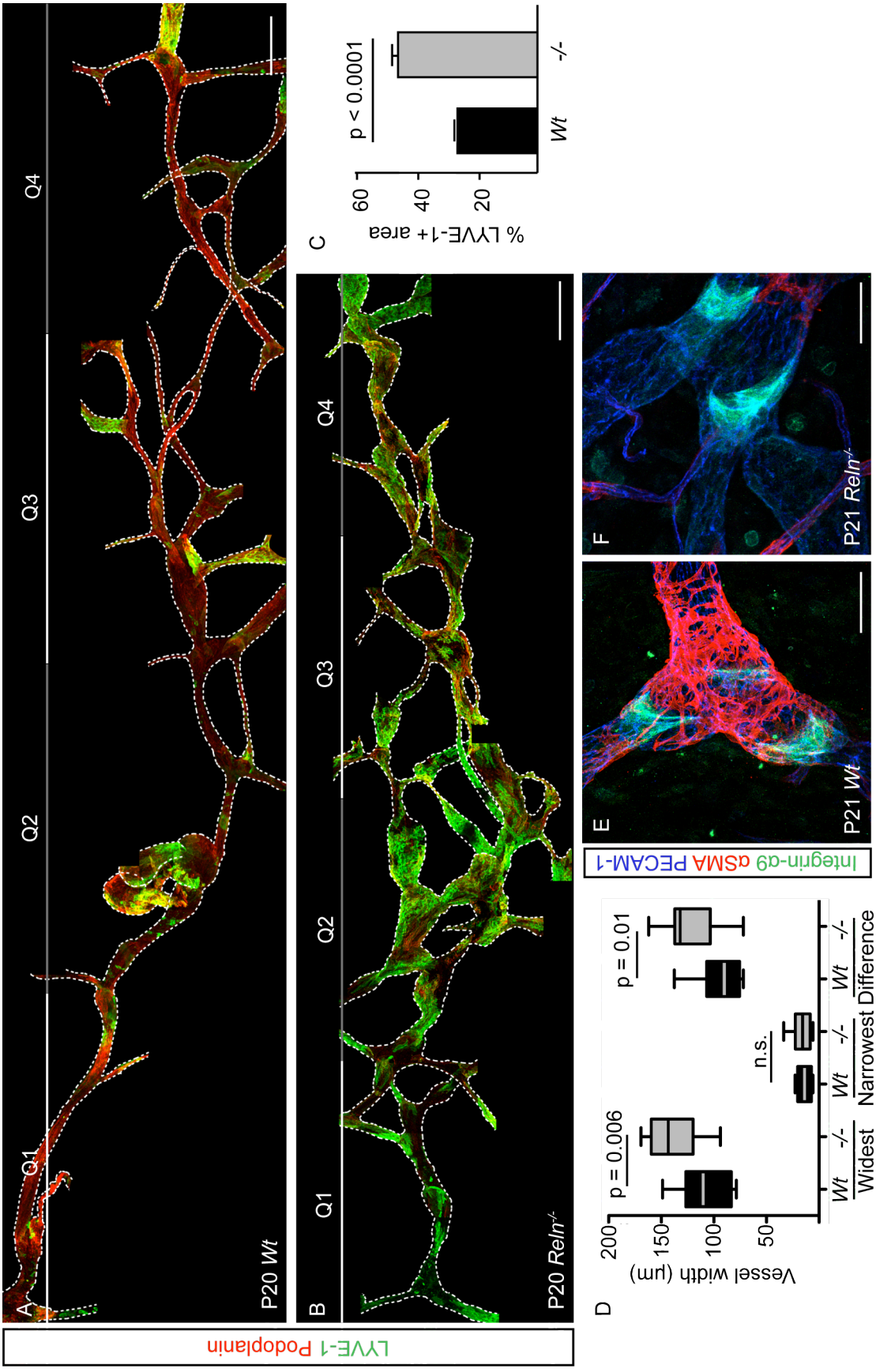
LYVE-1 Podoplanin
A
P20 Wt
Q1
Q2
Q3
Q4
B
P20 Reln-/-
C
% LYVE-1+ area
p < 0.0001
Wt
-/-
Integrin-α9 αSMA PECAM-1
E
P21 Wt
F
P21 Reln-/-
D
Vessel width (μm)
p = 0.006
p = 0.01
n.s.
Widest
Narrowest
Difference

Figure 5.1 *Reln* mutation leads to collecting vessel defects.
(A-B) Immunofluorescence of whole-mount ear-skin of wild-type (A) and *Reln*$^{-/-}$ (B) mice using antibodies against LYVE-1 (green) and podoplanin (red). Images (projections of confocal z-stacks) were aligned to trace the entire length of the vessel from proximal (Q1) to distal (Q4). Surrounding blood vasculature was removed for clarity (original images shown in appendix, Figure 8.1). (C) Quantification of LYVE-1 positive vessel area in wild-type and *Reln*$^{-/-}$ vessels. Data represent mean (n=6 vessels) ± SEM. (D) Quantification of widest and narrowest vessel points, and the difference between the two (n= 12 (*Wt*) and 15 (*Reln-/-*) vessels). Box represents interquartile range, line indicates mean and whiskers indicate minimum and maximum values. (E-F) Immunofluorescence of whole-mount ear-skin of wild-type (E) and *Reln*$^{-/-}$ (F) mice with antibodies against integrin-α9 (green), αSMA (red) and PECAM-1 (blue). Scale bars = 200μm (A-B), 50μm (E-F).

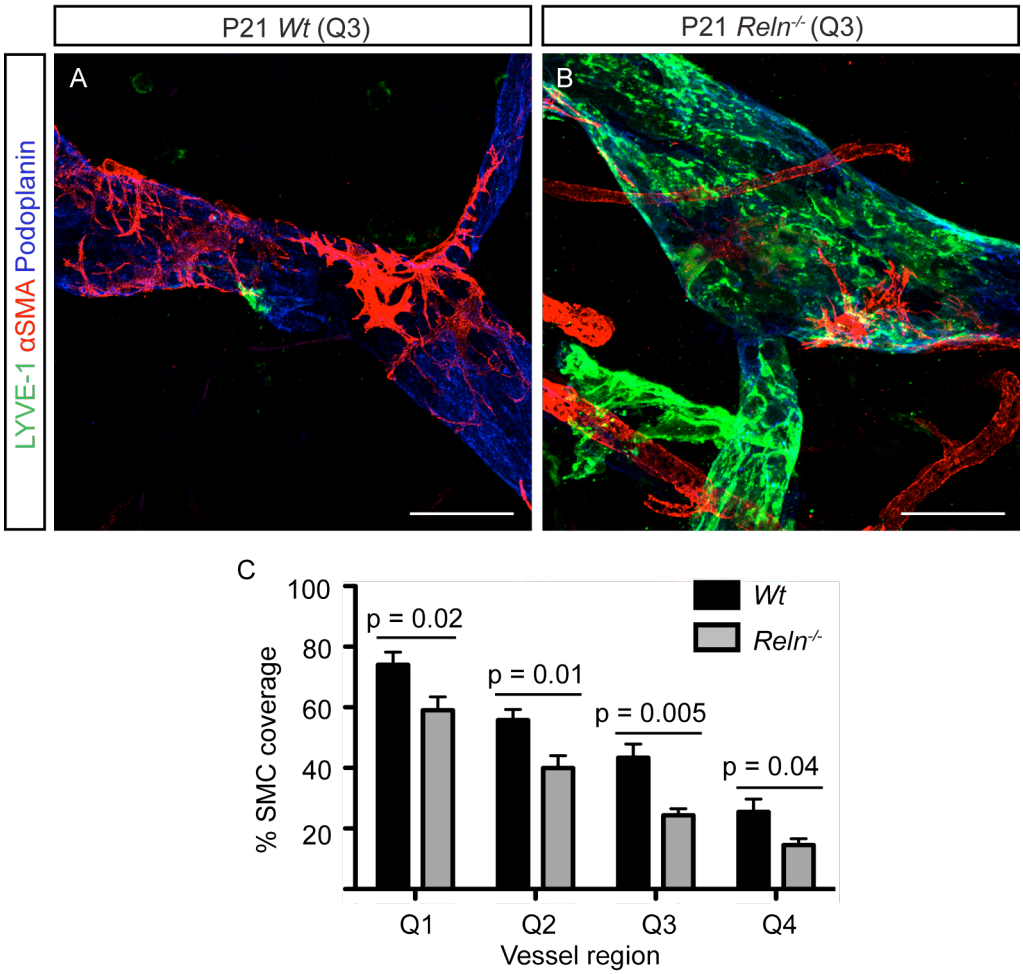

Figure 5.2 *Reln* mutation causes reduction in SMC coverage of collecting lymphatic vessels.
(A-B) Immunofluorescence staining of whole-mount ear-skin from wild-type (A) and *Reln*$^{-/-}$ (B) mice, taken from approximately the middle of the vessel (Q3). Note the reduction in SMC around the *Reln*$^{-/-}$ vessel, and SMC attachment to areas of high LYVE-1 expression, which is not seen in the wild-type. Scale bars = 50μm. (C) Quantification of smooth muscle cell coverage in vessel quarters. Data represent mean (n= 12 (*Wt*) and 15 (*Reln*$^{-/-}$) vessels) ± SEM.

We looked at deposition of other extracellular matrix proteins around *Reln*$^{-/-}$ collecting vessels to assess the impact of Reelin deficiency on the lymphatic basement membrane. We found that Collagen IV deposition occurred normally in *Reln* mutant mice (Figure 5.3 A-B'), another indication that early stages of collecting vessel differentiation occur normally in the absence of Reelin. Conversely, deposition of SMC-derived Laminin-α5 was strongly disrupted (Figure 5.3 C-D'), most likely as a consequence of reduced SMC coverage.

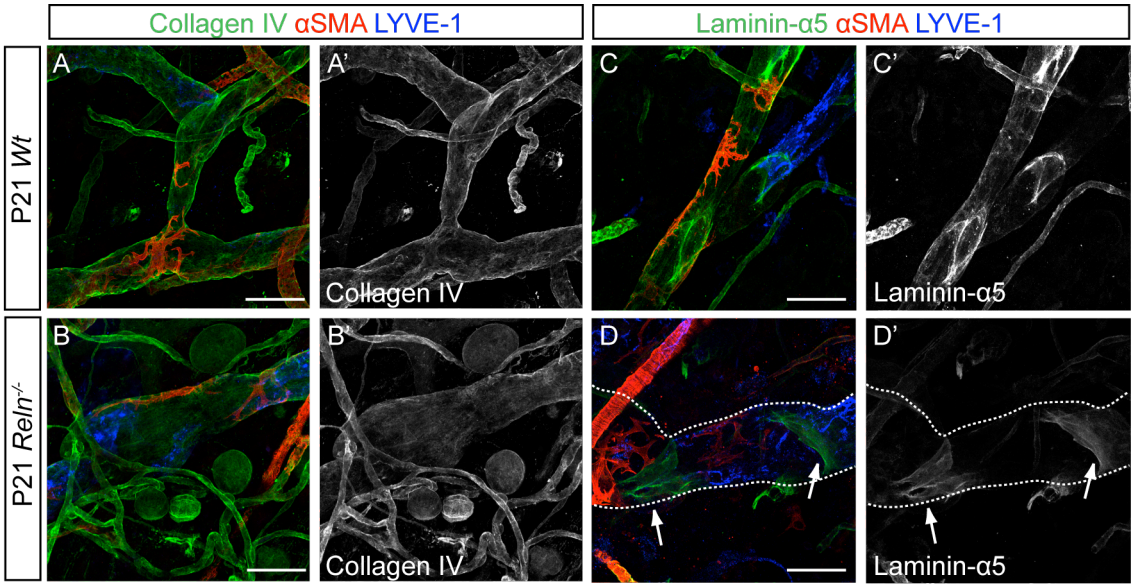

Figure 5.3 Collagen IV expression is not disrupted by *Reln* mutation, but less Laminin-α5 is deposited.
(A-D') Immunofluorescence staining of whole-mount wild-type (A-A', C-C') and *Reln* mutant (B-B', D-D') ear-skin using antibodies against Collagen IV, (green; A-B'), Laminin-α5 (green; C-D'), αSMA (red) and LYVE-1 (blue). Arrows indicate Laminin-α5 positive luminal valves. Scale bars = 50μm.

In addition to early collecting vessel differentiation events, the capillary beds also formed normally in *Reln* mutant mice (Figure 5.4 A-B), making it unlikely that the collecting vessel defects we observed were part of a general failure of lymphatic remodelling. These defects were also not secondary to nervous system defects, as we observed normal patterning of the nerves in *Reln* mutant mice (Figure 5.4 C-D). Together, these results demonstrate that Reelin deficiency leads to specific defects in collecting lymphatic vessel formation.

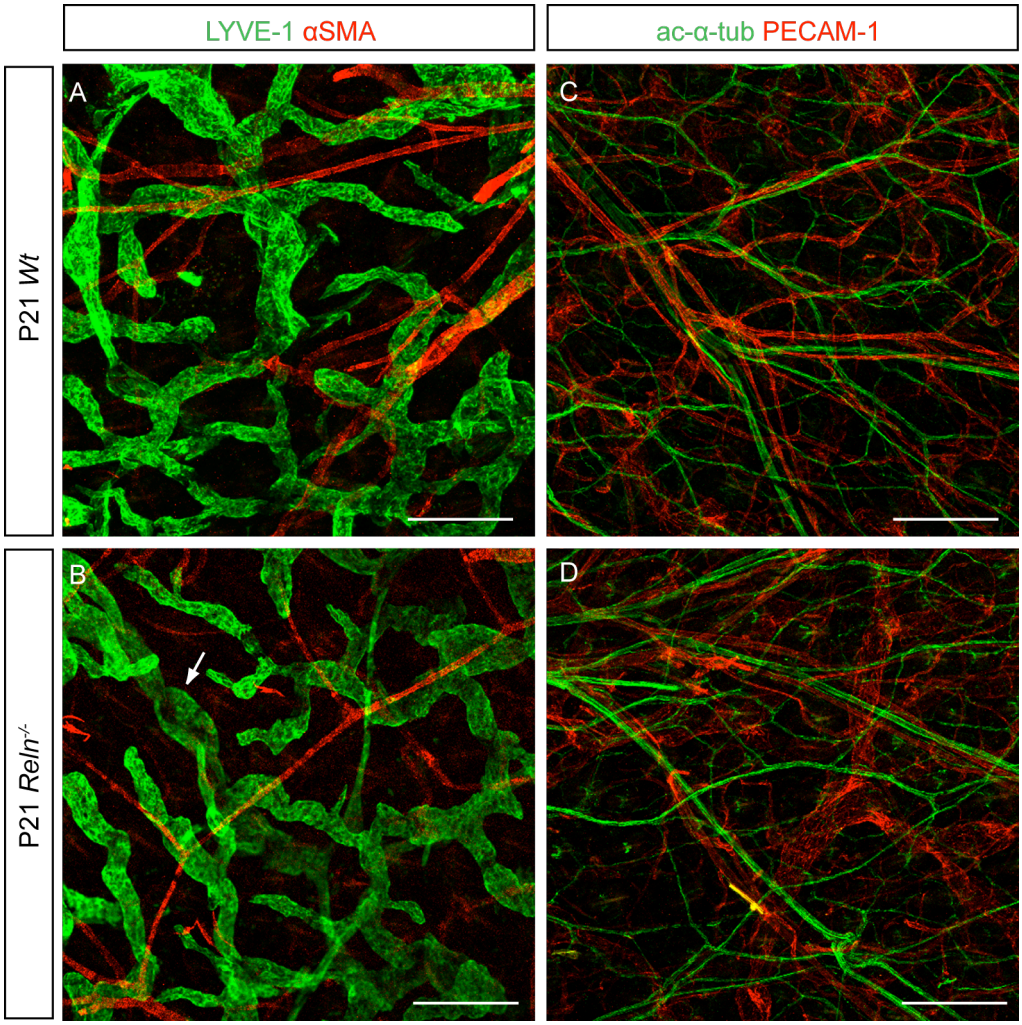

Figure 5.4 Capillary and nerve networks are not affected by *Reln* mutation.
(A-D) Immunofluorescence staining of whole-mount wild-type (A, C) and *Reln*$^{-/-}$ (B, D) ear-skin using antibodies against LYVE-1 (green; A-B), αSMA (red; A-B), acetylated α-tubulin (green; C-D) and PECAM-1 (red; C-D). Arrow in B points to LYVE-1 positive collecting vessel in *Reln*$^{-/-}$. Scale bars = 200μm.

5.2 Lymphatic flow is impaired in *Reln* mutant mice

Uptake of lymph occurs through the lymphatic capillaries, when changing pressure gradients between the vessel interior and the interstitium result in fluid influx. Lymph drains from the capillaries into the collecting lymphatic vessels, where SMC contractions aid lymph propulsion and forward movement, and luminal valves maintain unidirectionality.

To investigate whether the collecting vessel defects we observed had functional consequences, we injected FITC-Dextran intradermally into the ear. In this assay, Dextran injection into the interstitium increases interstitial pressure, leading to uptake of dye by the lymphatic capillaries. The high molecular weight of the Dextran means that it can only be absorbed by the lymphatic, and not the blood vasculature and visualising the fluorescent signal allows qualitative assessment of the subsequent movement of dye through the lymphatics, and efficiency of uptake/drainage, although dye that was free within the lumen is likely to be washed away during tissue fixation. In wild type mice, dye was efficiently taken up into the vessels surrounding the injection site (Arrow, Figure 5.5 A), and drained into LYVE-1 negative collecting lymphatic vessels (Arrowhead, Figure 5.5 B). Dye was rarely seen in LYVE-1 positive capillaries in wild type mice (Arrow Figure 5.5 B), with the exception of vessels in the immediate vicinity of the injection site. In contrast, in *Reln* mutant mice, we frequently observed no FITC-Dextran in vessels near the injection site (Arrow, Figure 5.5 C), while dye was retained in LYVE-1 positive vessels (Arrow, Figure 5.5 D), suggesting impaired lymphatic function. It is possible that the apparent retention of FITC-Dextran at the vessel edges in the $Reln^{-/-}$ ear (Figure 5.5 C) is indicative of dye leakage from the vessel and retention within the basement membrane, further suggesting functional deficiencies in the collecting vessels of these mice, but this would require further experimental confirmation.

In order to make a quantitative assessment of lymphatic function in $Reln^{-/-}$ mice, we looked at the larger collecting lymphatic vessels in the hindlimb. Earlier FITC-Dextran

injections into the footpad had revealed that although a minority (1 out of 5 mice injected) of *Reln* mutant mice showed morphological abnormalities in the hindlimb collecting lymphatic vessels (data not shown), after 15 minutes the dye is readily detectable in both wild type and mutant vessels and there is no evidence of vessel leakiness or backflow of dye, such as has been reported for mice with luminal valve deficiencies (Bazigou et al., 2009) (Figure 5.5 E-F). We were unable to carefully control the volume of dye that was injected in these experiments, which although kept as low as possible, was usually quite large. It is possible that this increases the pressure in the footpad and enhances lymph uptake beyond the physiological norm. Therefore to quantitatively assess efficiency of lymphatic function in *Reln* mutant mice, we needed to employ a more sensitive method of dye delivery and detection.

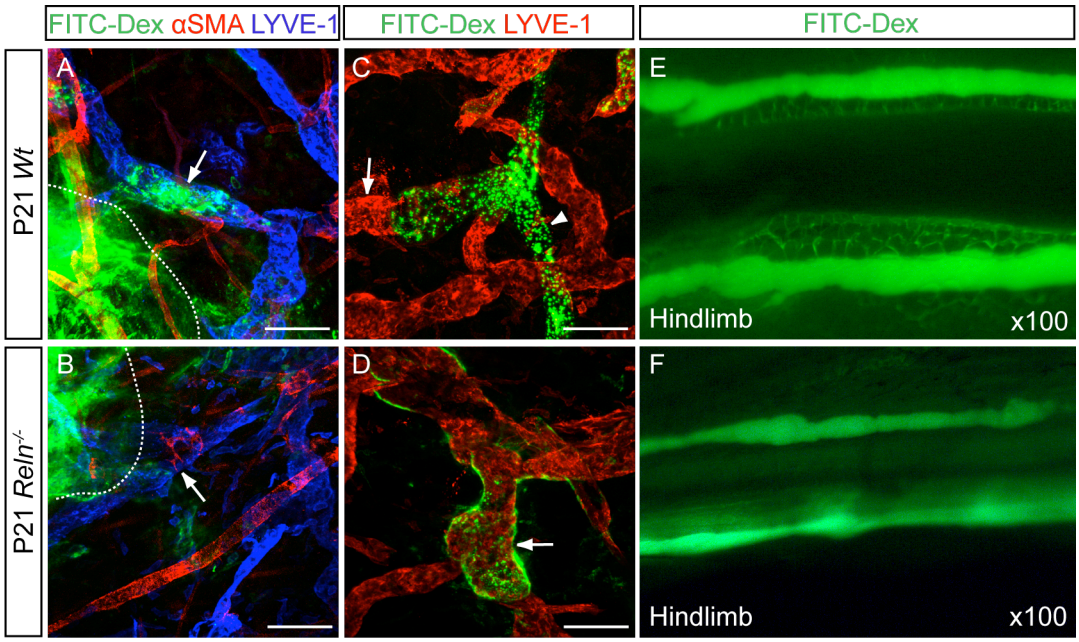

Figure 5.5 FITC-Dextran injection into *Reln* mutant ears suggests functional impairment of collecting lymphatic vessels.
(A-D) P21 wild-type (A, C) and *Reln*$^{-/-}$ (B, D) ear skin, injected with FITC-Dextran (green) and co-stained with antibodies against aSMA (red; A, B) and LYVE-1 (blue; A, B and red; C, D). Dashed line in (A, B) indicates the injection site, arrows point to adjacent collecting lymphatic vessels. Arrows in (C, D) point to LYVE-1 positive capillaries, arrowhead in (C) indicates LYVE-1 negative collecting vessel filled with FITC-dextran. Scale bars = 100μm. (E-F) Wild-type (E) and *Reln*$^{-/-}$ footpad injected with FITC-Dextran and collecting vessels imaged in the hindlimb. Dye is readily detectable in both wild-type and *Reln*$^{-/-}$ collecting vessels.

To this end, we injected 2ul of 1% ICG dye into the footpads of *Reln* mutant and control littermate mice using a Hamilton needle, followed by real-time imaging of uptake and measurement of fluorescent signal in a defined region of the vessel. We saw abnormal dye uptake in the *Reln*$^{-/-}$ compared to control mice (Figure 5.6 A). All but one *Reln* mutant mice showed decreased lymphatic function, while one showed abnormally fast dye uptake. In the wild type mice, the dye reached the inguinal lymph nodes within 5-6 seconds Figure 5.6 A'), but in most of the mutant mice, no dye was visible in the lymph node even at the end of 5 minutes of imaging (Figure 5.6 A''). In addition, measuring the dye content of the inguinal lymph nodes 5 minutes after Evan's blue injection into the footpad, revealed significantly more dye in control littermate than *Reln* mutant mice (Figure 5.6 B-B''), thus further confirming impaired lymphatic function in *Reeler* mice.

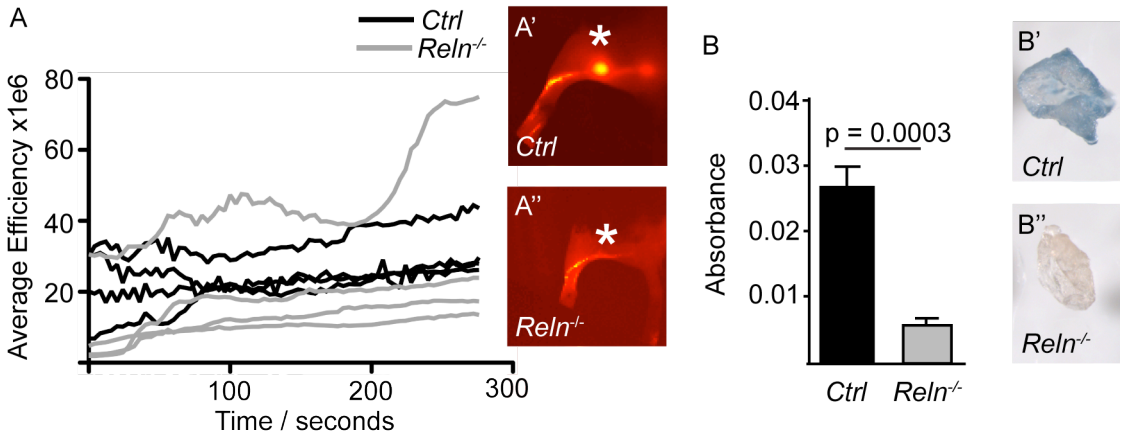

Figure 5.6 Impaired function in *Reln*$^{-/-}$ collecting lymphatic vessels.
(A-A'') Efficiency of fluorescent signal, representing efficiency of lymphatic function, in a defined region of a vessel after ICG injection into the hind limb footpad over time. After 5 minutes of injection, dye has reached inguinal lymph node (*) in wild type (A'), but not in *Reln*$^{-/-}$ mice (A''). (B) Quantification of Evan's blue dye content in inquinal lymph nodes of wild type and *Reln*$^{-/-}$ mice after 5 minutes of injection into the hind limb footpad. Mean and SEM are plotted (n= 4 (*Wt*) and 5 (*Reln*$^{-/-}$)). Insets show representative images of wild type (B') and *Reln*$^{-/-}$ (B'') lymph nodes before dye extraction.

Chapter 6. Reelin signalling in the lymphatic system

6.1 The canonical Reelin receptors, ApoER2 and VLDLR in the lymphatic system

6.1.1 Lymphatic expression of canonical Reelin receptors

In the nervous system, Reelin signals mainly via the low-density lipoprotein receptors, ApoER2 and VLDLR (Trommsdorff et al., 1999), which results in phosphorylation of the intracellular adapter protein Dab1 (Howell et al., 2000). We were interested to see whether this signalling pathway was conserved in the lymphatic vasculature. Our microarray data indicated that both *Apoer2* (also known as *Lrp8*) and *Vldlr* were expressed at similar levels in blood and lymphatic vessels *in vivo* (Figure 6.1 A), and RT-PCR analysis confirmed that LEC and SMC express both receptors *in vitro*, although *VLDLR* is expressed at a lower level in HUVSMC than LEC (Figure 6.1 B). In the absence of absolute expression data, we are unable to comment on the relative expression of each receptor compared to the other. We were also able to confirm VLDLR expression in the lymphatic endothelium *in vivo* by immunofluorescence (Figure 6.1 C), but unfortunately due to a lack of available antibodies, we could not use this technique to analyse ApoER2 expression *in vivo*.

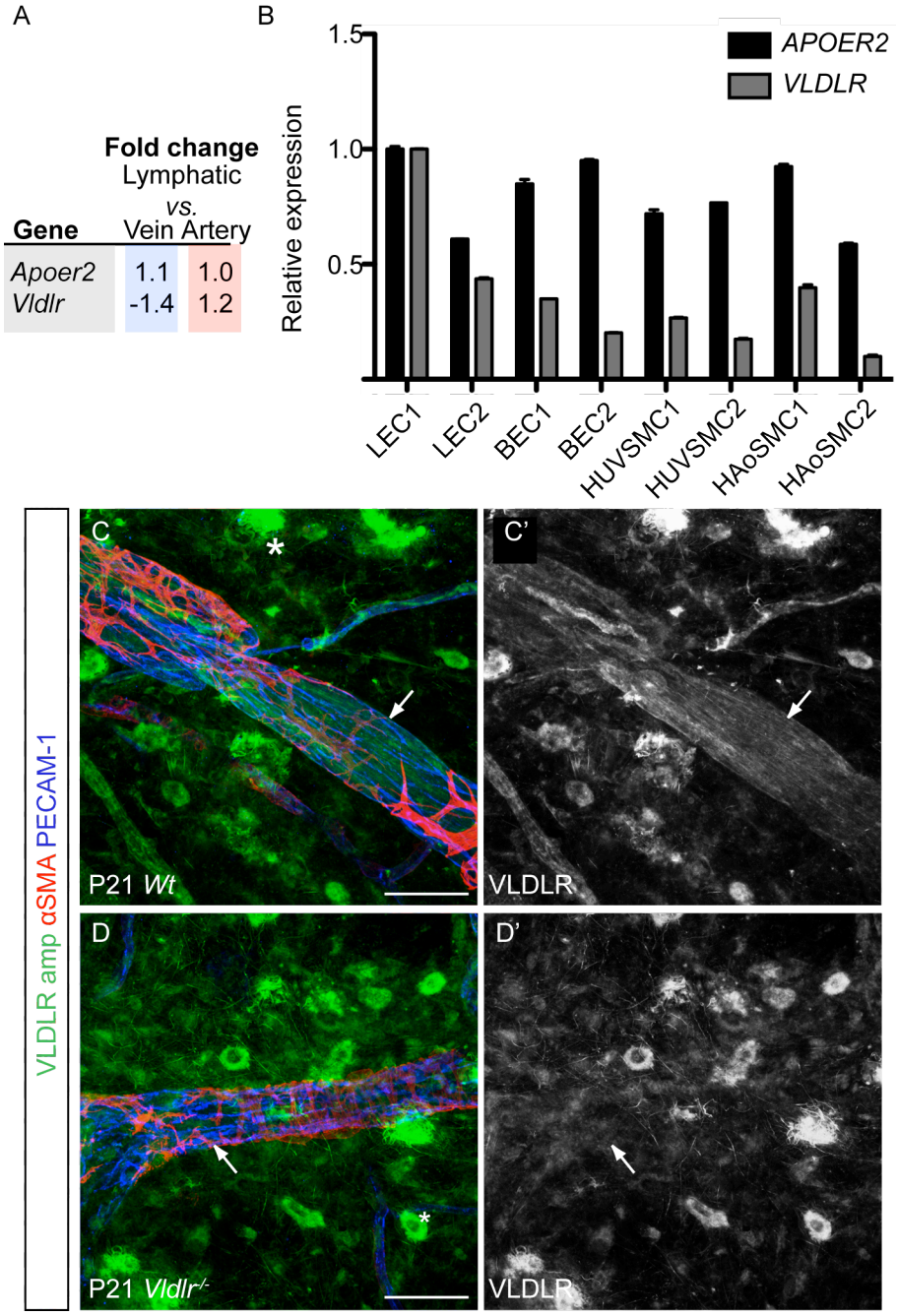

Figure 6.1 Lymphatic expression of canonical Reelin receptors, ApoER2 and VLDLR.
(A) Fold change in expression of *Apoer2* and *Vldlr* in lymphatic vessels versus veins and arteries in Affymetrix analysis. (B) Relative expression of *Apoer2* and *Vldlr* in 2 independent samples of LEC, BEC, HUVSMC and HAoSMC. Mean ± SEM is plotted. (C-D') Immunofluorescence staining of P21 ear skin in wild type (C, C') and *Vldlr*-/- (D, D') mice, using antibodies against VLDLR (green; signal amplified), aSMA (red) and PECAM-1 (blue). Absence of signal in (D, D'; arrow) demonstrates specificity of staining in (C, C'; arrow), (*) indicates non-specific staining in scattered cells.

6.1.2 *Apoer2$^{-/-}$;Vldlr$^{-/-}$* and *Dab1^{Scm}* mice do not recapitulate the *Reeler* phenotype in collecting lymphatic vessels

The gross phenotype of *Apoer2$^{-/-}$;Vldlr$^{-/-}$* mice is the same as that of *Reln$^{-/-}$* mice. The mutant mice are smaller than their wild-type siblings and suffer from severe ataxia, indicating that, as previously published, the neuronal phenotype is also the same as *Reln$^{-/-}$* mice (Trommsdorff et al., 1999). The neuronal phenotype of mice lacking *Dab1* is also reportedly identically to that of *Reln$^{-/-}$* mice (Howell et al., 1997, Sheldon et al., 1997). However, in the C3HeB/FeJ * DC/Le genetic background, the gross phenotype, and therefore presumably also the neuronal phenotype, is milder than that of *Reln$^{-/-}$* mice; in this background *Dab1^{Scm}* mice are still smaller than their wild-type siblings, but the ataxia is less pronounced.

Surprisingly, analysis of *Apoer2$^{-/-}$;Vldlr$^{-/-}$* mice revealed normal lymphatic collecting vessels (Figure 6.2 A-B and see appendix, Figure 8.2 for original vessels). Likewise, *Dab1^{Scm}* mice showed no demonstrable defects in collecting lymphatic vessel formation (Figure 6.2 A,C). In both cases, all parameters measured were normal (Figure 6.2 D-E and Figure 6.4 D), with the exception of a slight decrease in SMC coverage in *Apoer2$^{-/-}$;Vldlr$^{-/-}$* mice, particularly in the distal-most quarter, which could indicate a mild defect in SMC recruitment (Figure 6.2 D).

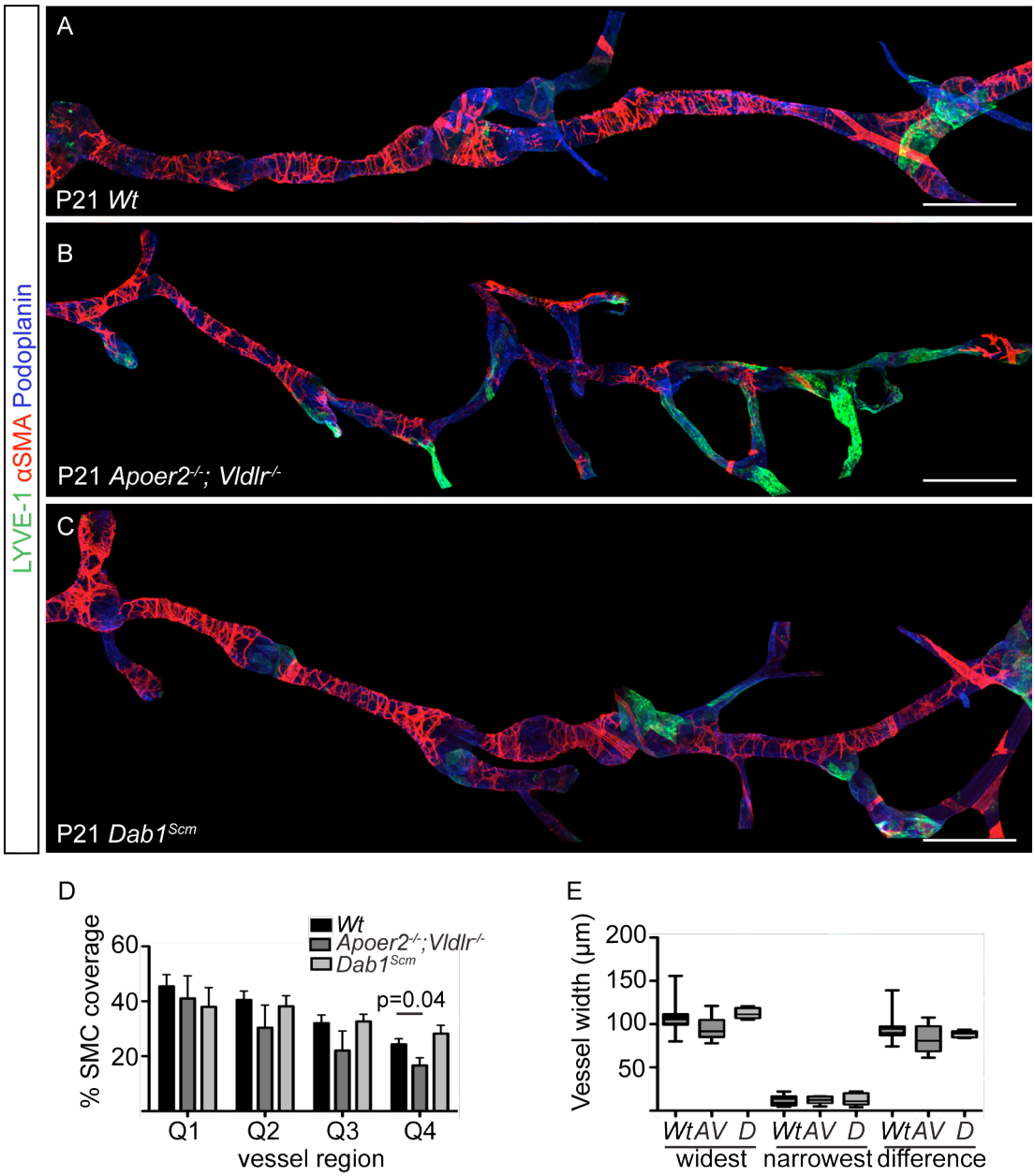

Figure 6.2 Normal lymphatic collecting vessels in *Apoer2$^{-/-}$;Vldlr$^{-/-}$* and *Dab1^{Scm}* mice.

(A-C) Immunofluorescence staining of P21 ear-skin from wild type (A), *Apoer2$^{-/-}$;Vldlr$^{-/-}$* (B) and *Dab1^{Scm}* (C) mice, using antibodies against LYVE-1 (green), aSMA (red) and Podoplanin (blue). Individual images (projections of confocal z-stacks) were aligned to trace the length of the vessel from proximal to distal end and the overlapping blood vasculature was blacked out for clarity. Segment from middle section of each vessel displayed (original images shown in Appendix, Figure 8.2) Scale bars = 200µm. (D) Smooth muscle cell coverage in vessel quarters. Data represent mean (n=12 (*Wt*) and n=6 (*Apoer2-/-;Vldlr-/-* and *Dab1Scm*) vessels) ± SEM. All differences were non-significant, except where indicated. (E) Quantification of widest and narrowest vessel points and the difference between the two in wild type (*W*), *Apoer2-/-;Vldlr-/- (AV)* and *Dab1Scm* (*D*) mice. Box represents interquartile range, line indicates mean and whiskers indicate minimum and maximum values. All differences were non-significant.

Overall, the absence of a similar lymphatic phenotype to that observed in *Reln*$^{-/-}$ mice in *Apoer2*$^{-/-}$*;Vldlr*$^{-/-}$ or *Dab1*^{Scm} mice was surprising, suggesting that this pathway is dispensable for normal lymphatic development, and furthermore implies the involvement of alternative receptor(s).

6.2 EphrinB2 as a putative Reelin receptor in the lymphatic system

6.2.1 Lymphatic expression of EphrinB2

EphrinBs have been recently suggested as novel Reelin receptors (Senturk et al., 2011). To investigate their potential involvement in mediating Reelin signalling in the lymphatic system, we first used *Efnb2*^{GFP} reporter mice to analyse expression of EphrinB2, the major EphrinB protein implicated in vascular development (Makinen et al., 2005, Foo et al., 2006, Wang et al., 2010). *Efnb2*^{GFP} mice have an H2B-GFP cDNA cassette inserted into exon 1 of the *Efnb2* gene, which results in nuclear GFP expression in *Efnb2* expressing cells (Davy and Soriano, 2007). We observed strong reporter expression in lymphatic and arterial endothelial cells (Figure 6.3 A, Ly), as well as in blood vascular SMC, as previously reported (Foo et al., 2006) (arrow, Figure 6.3 A'). However we could detect no GFP reporter activity in lymphatic SMC (arrowhead, Figure 6.1 A''). In addition, RT-PCR data demonstrated higher expression of *EFNB2* in cultured primary LEC than HUVSMC (Figure 6.3 B). Together, these data suggest that the target cell type responsive to Reelin signalling via Ephrin B2 in the lymphatic system is LEC.

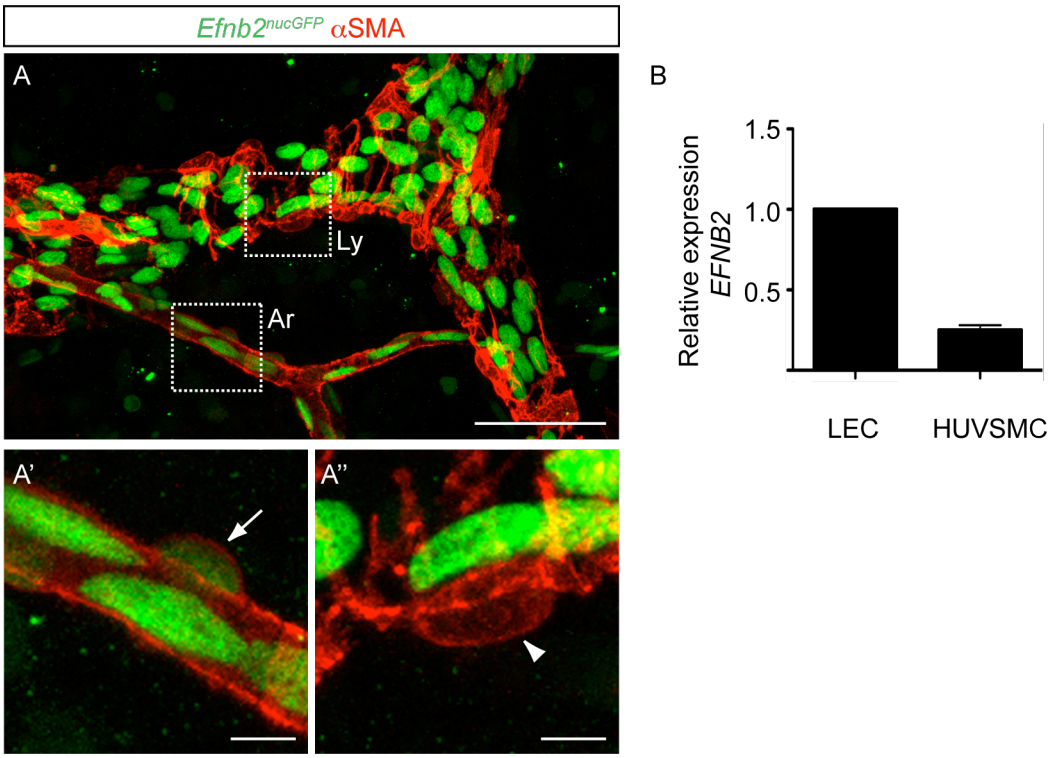

Figure 6.3 EphrinB2 is expressed in LEC, arterial EC and blood vascular SMC, but not lymphatic SMC.
(A-A'') Immunofluorescence staining of whole-mount *Efnb2*^{GFP} ear-skin with antibodies against GFP (green) and αSMA (red). Boxes indicate areas magnified in (A') and (A''). (A') shows *Efnb2*-GFP positive arterial (Ar) EC nuclei. Arrow points to *Efnb2* positive vascular SMC. (A'') shows *Efnb2*-GFP positive Lymphatic (Ly) EC nuclei. Arrowhead indicates *Efnb2* negative lymphatic SMC nuclei. Scale bars = 50μm (A) and 6.25μm (A'-A''). (B) Expression of *EFNB2* in HUVSMC relative to LEC. Mean fold change of 2 experiments is plotted ± SEM.

6.2.2 Lymphatic endothelial specific deletion of *Efnb2* resembles *Reeler* phenotype in collecting lymphatic vessels

Complete deletion of EphrinB2 results in embryonic lethality, due to failure of blood vascular development (Adams et al., 1999). Therefore, to allow for the requirement of EphrinB2 in early development and to ensure that any defects we observed were not secondary to a requirement for EphrinB2 in the vasculature, we specifically deleted EphrinB2 postnatally in the lymphatic endothelium. We crossed *Efnb2*^{lx} mice with a tamoxifen-inducible *Prox1-CreER*^{T2} line and induced *Efnb2* deletion just prior to the onset of collecting vessel development at P7, or at P12 by intraperitoneal injection of 4-OHT (Figure 6.4 A-B. See appendix, Figure 8.3 for original vessels), which lead to efficient Cre recombination (Figure 6.4 C and data not shown). Given the well documented role of Ephrin B2 in formation and maintenance of lymphatic valves (Makinen et al., 2005), (Wang et al., 2010), (Bazigou et al., 2011), the absence of valves in *Efnb2*$^{lx/lx}$*;Prox1-creER*^{T2} collecting vessels is strong evidence for efficient *Efnb2* deletion (Figure 6.4 A-B). However, in the absence of suitable antibodies, we were unable to confirm this at the protein level. In both cases, LEC-specific *Efnb2* deletion resulted in similar lymphatic defects to those observed in *Reln* mutants, including high LYVE-1 expression and a reduction in SMC coverage of the collecting vessels (Figure 6.4 A-B and D).

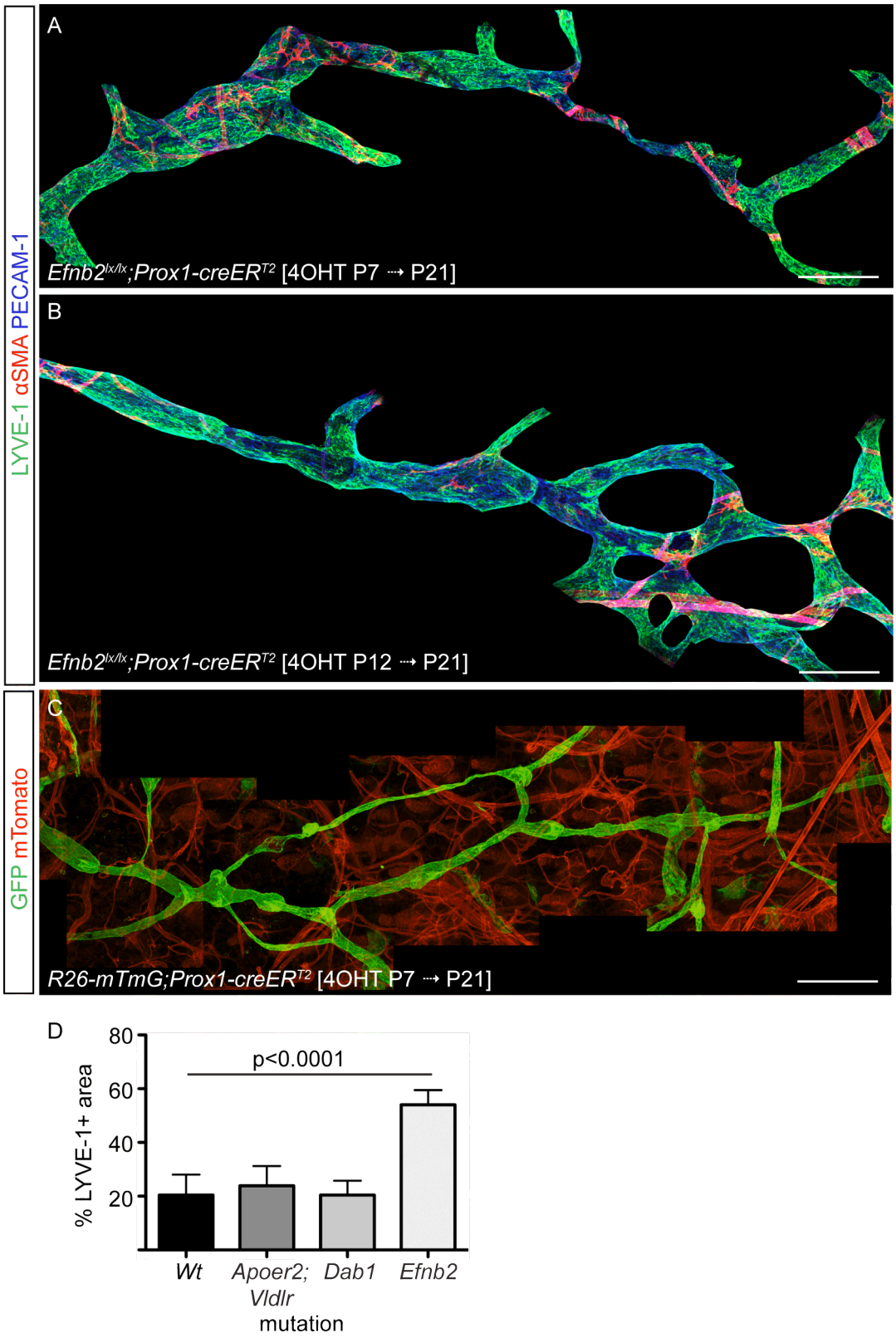
LYVE-1 αSMA PECAM-1
A
Efnb2lx/lx;Prox1-creERT2 [4OHT P7 ⇢ P21]
B
Efnb2lx/lx;Prox1-creERT2 [4OHT P12 ⇢ P21]
GFP mTomato
C
R26-mTmG;Prox1-creERT2 [4OHT P7 ⇢ P21]
D
% LYVE-1+ area
80
60
40
20
p<0.0001
Wt
Apoer2; Vldlr
Dab1
Efnb2
mutation

Figure 6.4 Collecting vessel defects following lymphatic-specific *Efnb2* deletion resemble those of *Reln*$^{-/-}$ mice.
(A-C) Immunofluorescence of P21 ear-skin from *Efnb2*$^{lx/lx}$*;Prox1-creER*^{T2} (A-B) or *R26-mTmG;Prox1-creER*^{T2} (C) mice, administered with 4-OHT at P7 (A, C) or P12 (B) and analysed at P21 using antibodies against LYVE-1 (green; A-B), αSMA (red; A-B), PECAM-1 (blue; A-B) and GFP (green; C). Individual images (projections of confocal z-stacks) were aligned to trace the entire length of the vessel. Middle segment of each vessel is shown, with surrounding blood vasculature blacked out for clarity in (A-B). Original vessels are shown in appendix, Figure 8.3. Scale bars = 200μm. (D) Quantification of LYVE-1 positive area in wild-type, *Apoer2*$^{-/-}$*;Vldlr*$^{-/-}$, *Dab1*^{Scm} and *Efnb2*$^{lx/lx}$*;Prox1-creER*^{T2} vessels. Data represent mean (n= 12 (*Wt*) and n= 6 (each mutant) vessels) ± SEM. Differences were non-significant except where indicated

SMC recruited to *Efnb2* deficient collecting vessels were often found around areas of the lymphatic endothelium that still expressed high levels of LYVE-1 (arrows, Figure 6.5 B, D), a situation that is rarely observed in wild type vessels, but is again reminiscent of *Reln*$^{-/-}$ collecting lymphatic vessels. It is also important to note that *Efnb2*$^{lx/lx}$ siblings appeared as wild-type (Figure 6.5 A, C), with regular SMC coverage and no LYVE-1 expression in collecting lymphatic vessels, thus ruling out the possibility that the *Efnb2*$^{lx/lx}$*;Prox1-creER*^{T2} phenotype was secondary to either tamoxifen injection, or homozygosity for the allele containing the LoxP flanked *Efnb2* exon.

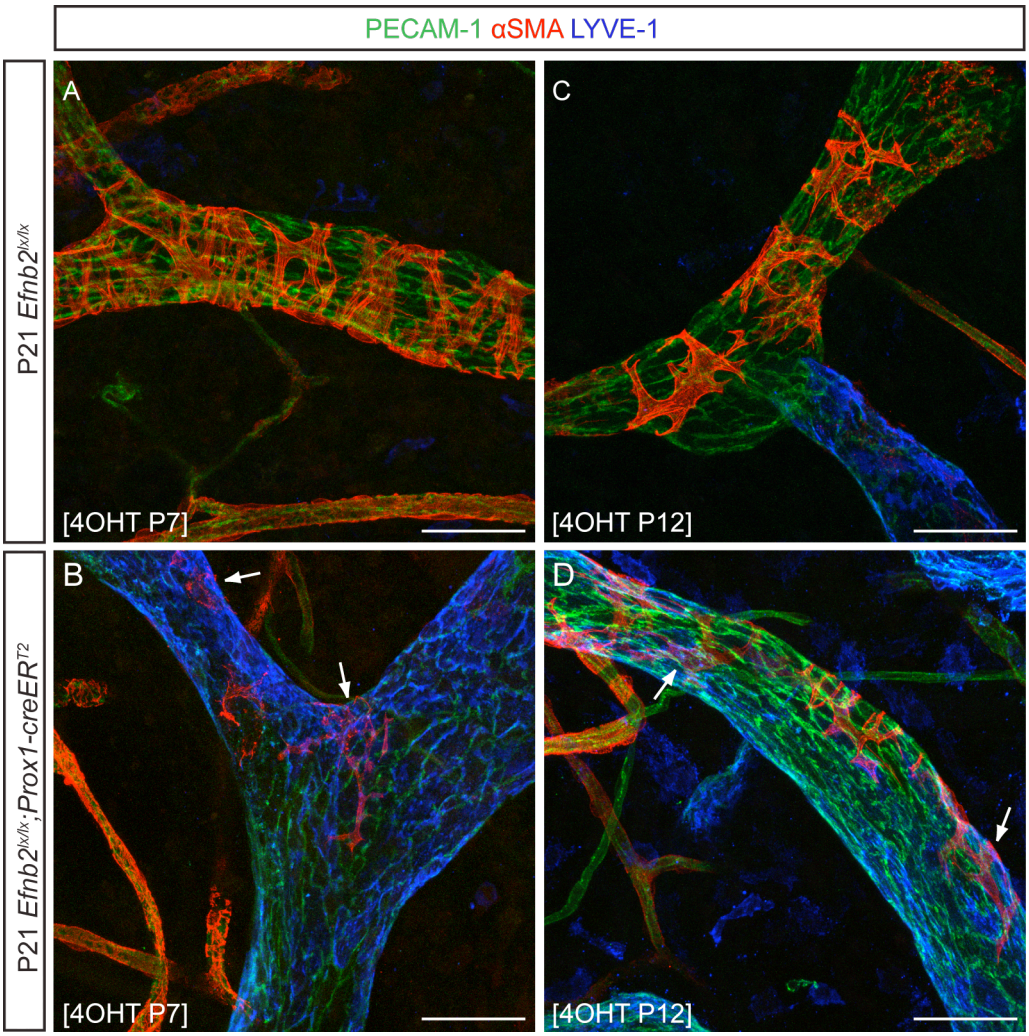

Figure 6.5 SMC are found at areas of high LYVE-1 expression in *Efnb2$^{lx/lx}$;Prox1-creER^{T2}* mice.
Immunofluorescence staining of whole-mount ear-skin from *Efnb2$^{lx/lx}$* (A-C) or *Efnb2$^{lx/lx}$;Prox1-creER^{T2}* mice (B-D), administered with 4-OHT at P7 (A-B) or P12 (C-D) and analysed at P21 using antibodies against PECAM-1 (green), αSMA (red) and LYVE-1 (blue). Note that *Efnb2$^{lx/lx}$* mice appear as wild-type; regular SMC coverage and no LYVE-1 expression in collecting lymphatic vessels. Arrows in (B) and (D) point to SMC that have attached in areas of high LYVE-1 expression. Scale bars = 50μm.

As in the case of *Reln* mutant mice, *Efnb2* deficient collecting lymphatic vessels generally appeared wider than wild type vessels. However they did not display the constrictions we observed in the *Reln$^{-/-}$* vessels, which is likely due to the absence of luminal valves in *Efnb2* deficient mice (Figure 6.4 and data not shown). The Reelin-independent requirement for *Efnb2* in formation and maintenance of luminal valves has been previously reported (Makinen et al., 2005)(Bazigou et al., 2011), and served as a useful marker of efficient Cre recombination in *Efnb2$^{lx/lx}$;Prox1-creER^{T2}* collecting

vessels. Another indication that EphrinB2 has Reelin-independent functions in the lymphatic endothelium was the observation that lymphatic capillaries in *Efnb2* deficient mice appeared abnormal and less branched, unlike the situation in *Reln*$^{-/-}$ mice (Figure 6.6 A-C). However, this phenotype would need to be quantified and investigated in more detail before being confirmed.

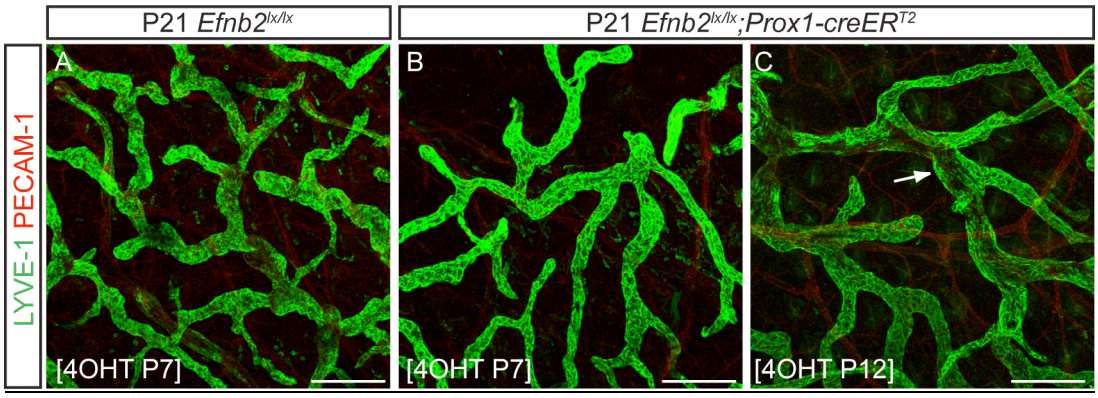

Figure 6.6 Abnormal lymphatic capillary network in *Efnb2*$^{lx/lx}$*;Prox1-creER*^{T2} mice.
(A-C) Immunofluorescence staining of whole-mount ear-skin from *Efnb2*$^{lx/lx}$*;Prox1-WT* (A) or *Efnb2*$^{lx/lx}$*;Prox1-creER*^{T2} (B-C), administered with 4-OHT at P7 (A-B) or P12 (C) and analysed at P21 using antibodies against LYVE-1 (green) and PECAM-1 (red). Arrow indicates LYVE-1 positive collecting vessel in *Efnb2*$^{lx/lx}$*;Prox1-creER*^{T2} mice. Scale bars = 200μm.

A preliminary observation suggested that Reelin remained intracellular in some *Efnb2* deficient collecting lymphatic vessels (Figure 6.7 B-B'), similar to the case in the developing lymphatic endothelium, while in the wild type siblings, Reelin expression in the collecting vessels was characteristically weak and diffuse (Figure 6.7 A-A'). This may be a result of either incomplete collecting vessel differentiation, or of the reduction in SMC coverage, although it would require further analysis to confirm and distinguish between these hypotheses.

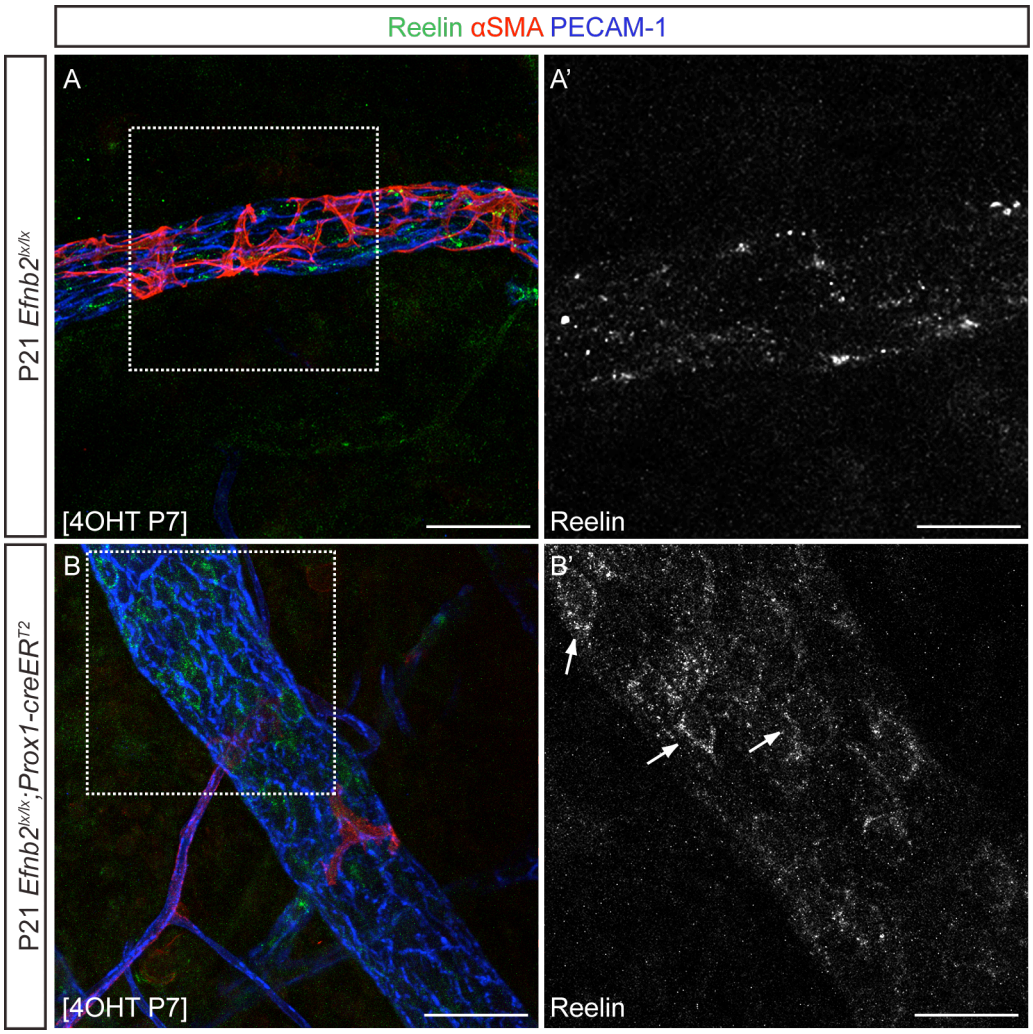

Figure 6.7 Reelin appears intra-cellular in *Efnb2$^{lx/lx}$;Prox1-creER^{T2}* collecting vessels.
Immunofluorescence staining of whole-mount ear-skin from *Efnb2$^{lx/lx}$* and *Efnb2$^{lx/lx}$;Prox1-creER^{T2}* mice, administered with 4-OHT at P7 and analysed at P21 using antibodies against Reelin (green), αSMA (red) and PECAM-1 (blue). Arrows indicate areas where Reelin signal appears intracellular. Scale bars = 50μm (A-B), 25μm (A'-B').

Overall, our *in vivo* data suggest EphrinB2 as a likely candidate for mediating Reelin signalling in the lymphatic endothelium.

6.3 Cellular mechanism of Reelin function in vascular cells

6.3.1 Reelin does not directly promote SMC adhesion or motility

The reduction in SMC coverage of *Reln*$^{-/-}$ collecting vessels suggested that Reelin might have a direct effect on SMC, for example by promoting SMC migration either towards or along the length of the vessel, which would be consistent with a role for Reelin in positively regulating neuronal migration (Jossin et al., 2004), (Sanada et al., 2004). Alternatively, Reelin might promote or secure SMC attachment to the vessel. Since we did not know which fragment of the protein may be active in the lymphatic system, we used Reelin secreted into the medium of HEK 293 cells, which contains predominantly full-length Reelin, but also its cleavage products in our *in vitro* experiments. We also used the commercially available Reelin central fragment. Application of only the central fragment of Reelin to cortical slice cultures is sufficient to rescue the neuronal phenotype of *Reeler* mice (Jossin et al., 2004), however it is important to note that we do not have a positive control for the efficacy of this fragment in the lymphatic system, and so were unable to confirm the functionality of the commercially available fragment prior to beginning experiments. Contrary to our hypothesis, *in vitro* investigations revealed no difference in the motility of untreated HUVSMC compared to those treated with either Reelin medium or the central Reelin fragment (Figure 6.8 A). Likewise, neither form of Reelin promoted SMC attachment to a non-adhesive surface (Figure 6.8 B).

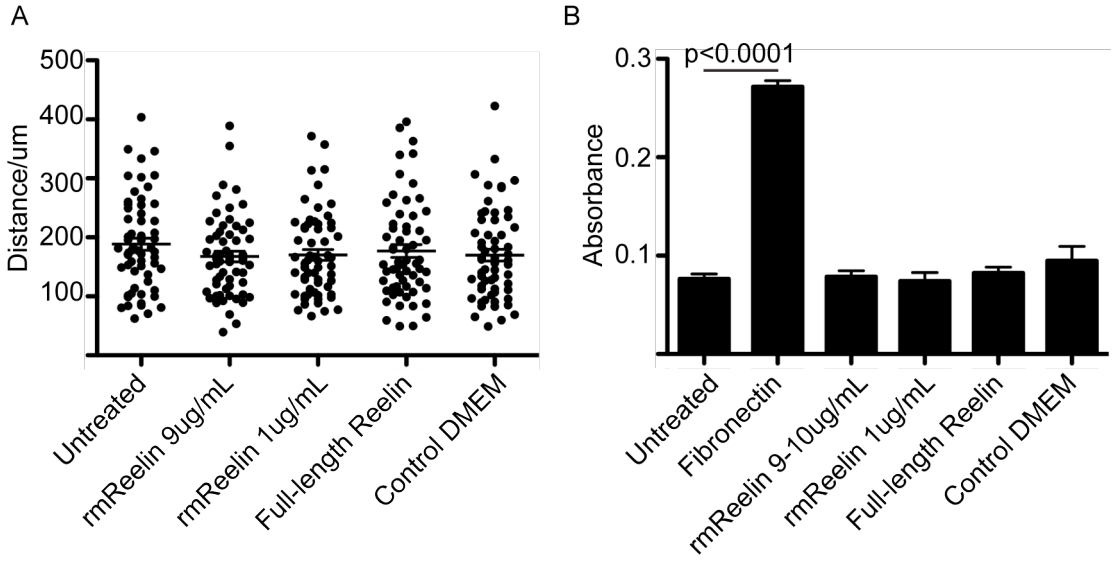

Figure 6.8 Reelin does not directly mediate HUVSMC adhesion or motility.
(A) Cell motility in each treatment condition. Each dot represents one cell (total 60 cells from 3 wells per condition). Bar represents mean distance ± SEM. (B) Absorbance reading, representing cell adhesion in each treatment condition. Mean ± SEM is plotted. N = 6 wells per condition.

We performed chemotaxis assays to determine whether Reelin could promote directional migration of SMC. We did not observe increased SMC migration in response to either Reelin medium, or the central fragment (data not shown), but consistent with previously published reports, we observed increased SMC migration towards LEC-conditioned medium (Veikkola et al., 2003) (Figure 6.9).

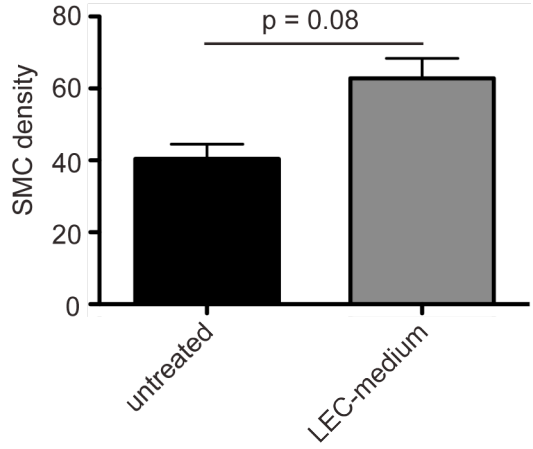

Figure 6.9 SMC migrate in response to LEC conditioned medium.
SMC density, representing number of cells migrated through Transwell membrane towards either untreated, or LEC-conditioned starvation medium. Mean ± SEM of 5 Regions of interest (ROI) per well (full description given in Materials and Methods) from 2 wells per condition is plotted. Graph is representative of 3 experiments.

6.3.2 Phospho-Kinase array did not reveal downstream components of the Reelin signalling pathway in vascular cells

In an attempt to determine which cell type was responsive to Reelin signalling and to identify downstream components of the Reelin signalling pathway in either LEC or HUVSMC to see if this gave us any mechanistic insights, we used Proteome Profiler Human Phospho-Kinase Array Kits (R&D Systems), in which antibodies against 46 different phosphorylated proteins are spotted onto a nitrocellulose membrane. Upon PDGF-BB stimulation of SMC, we saw increased phosphorylation of CREB (Nomiyama et al., 2006), Erk 1/2 (Hansmann et al., 2008), (Millette et al., 2005) and Akt (Millette et al., 2005), (Rauch et al., 2000), all known effectors of PDGF-BB signalling in SMC, indicating that the assay was working properly (Figure 6.10 A'-A''). However we saw no difference in phosphorylation levels of any proteins between untreated SMC and those stimulated with the central Reelin fragment (Figure 6.10 A''-A'''). We obtained a similar result with LEC. VEGF-C stimulation induced increased phosphorylation of CREB (Heckman et al., 2008), Akt (Lahdenranta et al., 2009), (Tvorogov et al., 2010) and Erk 1/2 (Cao et al., 2004, Tvorogov et al., 2010), again indicating that the assay had worked, since the phosphorylation levels of known

effectors of VEGF-C signalling in LEC were increased (Figure 6.10 B'-B''). However, once more we were unable to identify any differences in phosphorylation levels between untreated LEC and those treated with the central Reelin fragment (Figure 6.10 B''-B''').

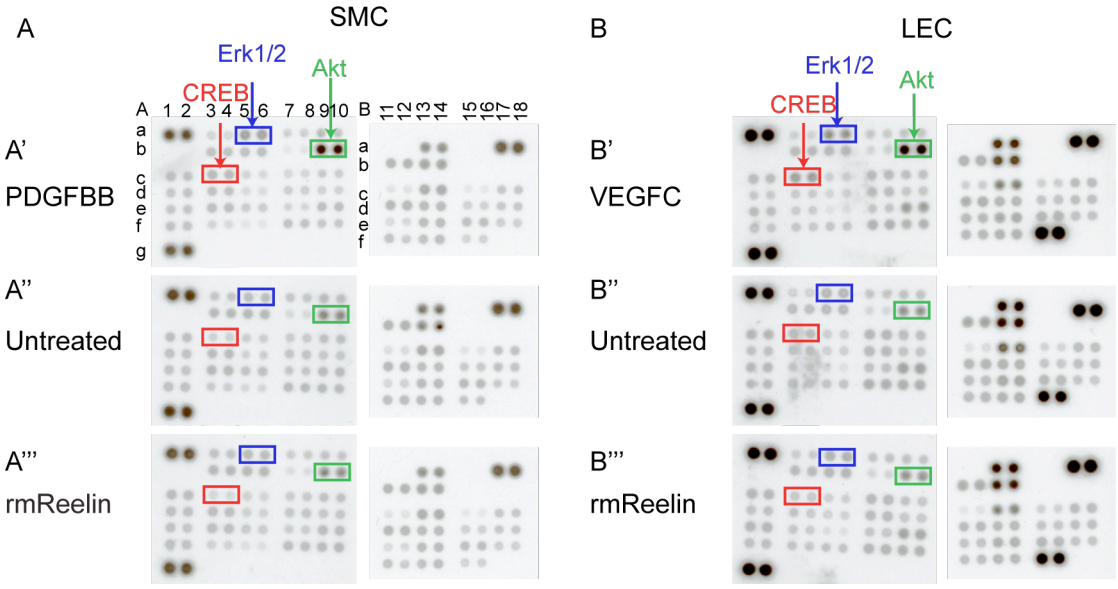

Figure 6.10 No change in phosphorylation levels of proteins after Reelin stimulation of LEC or SMC.
(A-B) Phospho-kinase array of HUVSMC (A) or LEC (B), stimulated with PDGF-BB (A'), VEGF-C (B'), un-stimulated (A'', B'') or stimulated with Reelin central fragment (A''', B'''). PDGF-BB stimulation of HUVSMC, or VEGF-C stimulation of LEC causes increased phosphorylation of CREB, Erk1/2 and Akt, as indicated, but there is no change after Reelin stimulation. Co-ordinates are marked only on (A') for clarity. See appendix, Figure 8.4 for array key.

6.3.3 Reelin stimulation of LEC increases production of SMC proliferation factor *MCP1* mRNA

Our earlier results indicated that Reelin signalling in the lymphatic vasculature may involve interaction between LEC and SMC, and since we were unable to detect a direct effect of Reelin on SMC motility or adhesion, but LEC-conditioned medium did promote SMC migration, we hypothesised that Reelin might stimulate LEC to produce

SMC-recruitment factors. While neither Reelin medium, nor the central Reelin fragment induced increased expression of *PDGFB, HBEGF, ANGPT2,* or *TGFβ1* mRNA, stimulation with Reelin medium induced a greater than 2 fold increase in *MCP1* production after both 4 and 8 hours, compared to control medium stimulated cells (Figure 6.11 A-B). After 24hr of Reelin stimulation, the difference in *MCP1* production by Reelin medium, compared to control medium stimulated, LEC was smaller, but still apparent (Figure 6.11 C). Interestingly, we did not see the same increase in *MCP1* expression in response to the central Reelin fragment, which together with our earlier negative results from the phosphoarray, may suggest that contrary to the case in the nervous system, the central fragment alone is not sufficient for activation of Reelin signalling in LEC.

Our results suggest that LEC can respond to Reelin by upregulating expression of *MCP1*, a known SMC recruitment and proliferation factor (Selzman et al., 2002), (Jay et al., 2010).

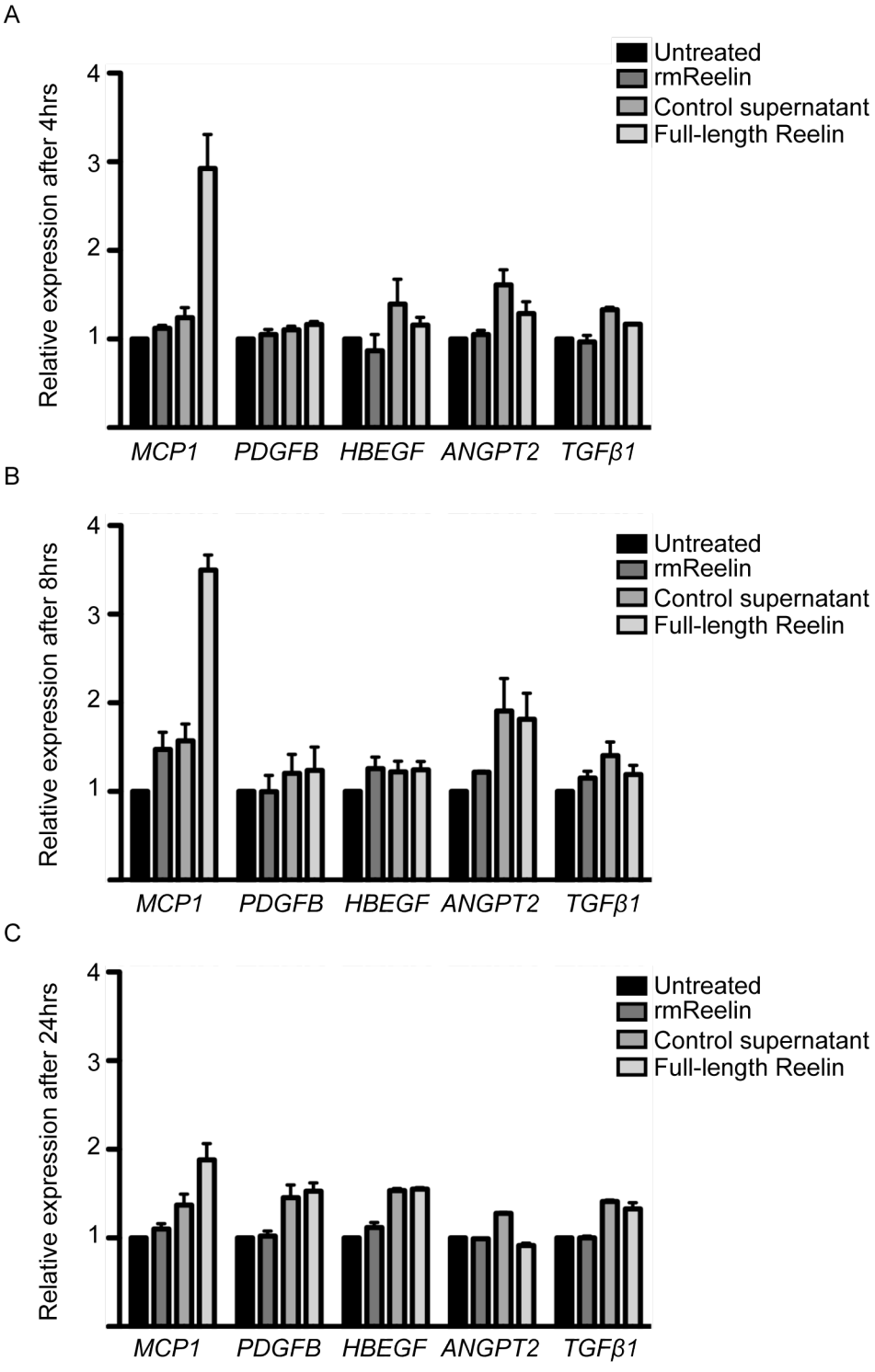

Figure 6.11 Reelin medium stimulates production of *MCP1* mRNA.
(A-C) Fold change in expression of SMC recruitment genes after 4 (A), 8 (B) or 24 (C) hours stimulation with either Reelin central fragment, Reelin medium or control medium, relative to expression in untreated LEC. Note strong increase in *MCP1* expression in Reelin medium stimulated compared to control-stimulated LEC after 4 and 8 hours, with no change in expression of any other SMC recruitment genes. Mean ± SEM of 2 experiments at each time point is plotted

6.4 Proposed model of Reelin action in the lymphatic vasculature

Our results suggest that initially all LEC express Reelin intracellularly, but upon differentiation of the collecting lymphatic vessels, SMC recruitment stimulates Reelin release and proteolytic processing. Secreted Reelin then increases endothelial *MCP1* expression, which leads to further SMC recruitment. The canonical Reelin receptors ApoER2 and VLDLR were not involved in this process, but *in vivo* data suggests the involvement of EphrinB2 in LEC in mediating Reelin signalling in lymphatic development, although the role of EphrinB2 requires further investigation (Figure 6.12).

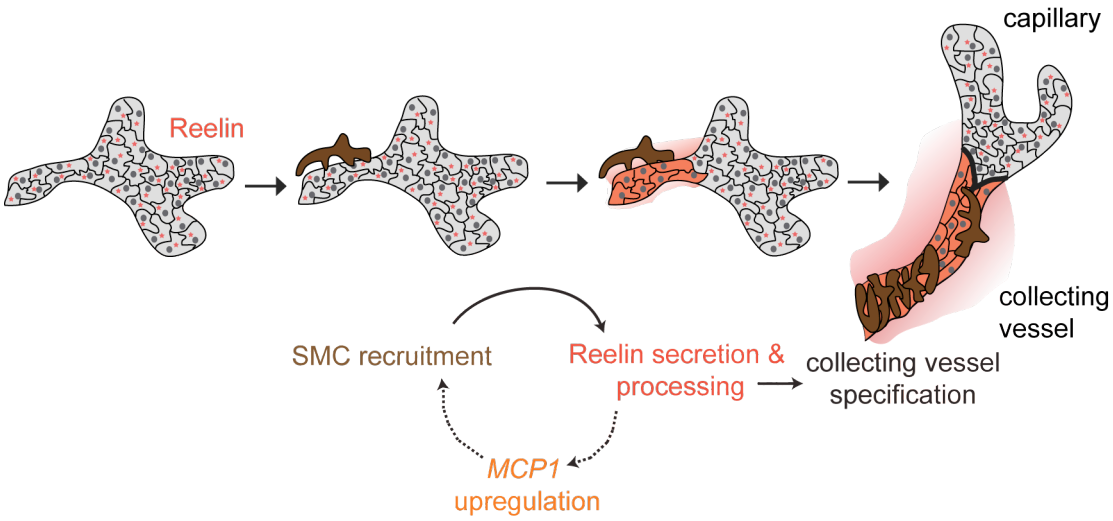

Figure 6.12 Proposed model of Reelin signalling during collecting lymphatic vessel formation.
Reelin (red star) is produced by LEC (grey cells). Upon SMC (brown cells) recruitment Reelin is secreted from LEC (red cells) and cleaved to release diffusible fragments (red gradient). Reelin can also up-regulate expression of *MCP1*, which encodes MCP-1 protein known to enhance SMC recruitment.

Chapter 7. Discussion

The initial aim of this work was to characterise the process of collecting lymphatic vessel remodelling in the ear-skin. To accomplish this, we used *in vivo* observations of wild-type tissue at differing postnatal stages and carried out microarray analysis to explore the largely un-investigated differences between the lymphatic and blood vascular basement membranes. We identified Reelin as a potentially interesting candidate for further study and so set about identifying its possible role in lymphatic vessel development. This was achieved by combining *in vivo* observations of *Reln*$^{-/-}$ *(Reeler)* mice with *in vitro* studies into the mechanism of Reelin activation and its cellular function within the lymphatic vasculature. Our findings are discussed in more detail below.

7.1 Dermal lymphatic collecting vessel differentiation

The gene expression and morphological changes involved in collecting vessel differentiation and maturation have been described in the embryonic mesenteric vessels, where it was found that *Foxc2* is a critical regulator of this process (Norrmen et al., 2009). Likewise, the development of luminal valves, an early step in collecting vessel differentiation, has also been described (Bazigou et al., 2009). However, the timing of lymphatic remodelling varies between tissues, and so determining the postnatal stage at which some of the processes involved in collecting vessel differentiation occur in the ear skin, for example LYVE-1 down-regulation, SMC recruitment and BM deposition, and the order in which these events occur, provided us with a useful tool for detailed assessment of this process in mutant mouse strains that might show a lymphatic phenotype.

7.1.1 SMC regulation of LYVE-1 down-regulation

While studying the timing of SMC recruitment to the lymphatic collecting vessels, we made some interesting observations concerning the relationship between SMC recruitment and LYVE-1 down-regulation. Our *in vivo* observations seemed contrary to previous suggestions that SMC recruitment leads to LYVE-1 down-regulation (Tammela et al., 2007), since we frequently saw areas of no LYVE-1 expression that were also devoid of SMC, suggesting that LYVE-1 down-regulation occurs prior to SMC recruitment. However, we also found that co-culturing LEC and SMC lead to down-regulation of *LYVE1* mRNA, which does suggest a role for SMC in regulation of LYVE-1 expression. LEC in direct contact with SMC *in vitro* still maintained LYVE-1 expression, which suggests that LYVE-1 down-regulation is not prerequisite for SMC/LEC contact, at least *in vitro*, and may indicate that LYVE-1 has a particularly long half-life, since protein expression was still maintained in co-culture while mRNA was down-regulated over the same period of time. Preliminary observations in *Lyve1*$^{-/-}$ mice indicated that the absence of LYVE-1 does not increase SMC recruitment to the collecting vessels, again suggesting that LYVE-1 does not normally inhibit SMC attachment.

Further evidence for a correlative relationship between LYVE-1 expression and SMC recruitment came from analysis of *Reln*$^{-/-}$ and *Efnb2*$^{lx/lx}$*;Prox1creER*^{T2} mice, which showed abnormally high levels of LYVE-1 expression in the collecting lymphatic vessels, concomitant with a reduction in SMC coverage. A similar phenomenon was reported in a mouse model of hypercholesterolemia in mice lacking the lipoprotein ApoE. Although *ApoE*$^{-/-}$ lymphatic collecting vessels initially formed normally, with regular SMC coverage and no LYVE-1 expression, after 16 weeks on a high-fat diet, they started to lose SMCs, which was accompanied by up-regulation of LYVE-1 (Lim et al., 2009). All of these data point to a relationship between SMC recruitment and LYVE-1 down-regulation, but this may not be a direct effect.

Since the function of LYVE-1 in the lymphatic vasculature is unknown, it might be interesting to explore this relationship further. Culturing LEC in conditioned medium

from SMC and examining LYVE-1 expression at both the protein and mRNA level might address the issue of whether a SMC-derived secreted factor is responsible for LYVE-1 down-regulation. It would also be interesting to take advantage of live imaging techniques, such as the explant cultures used by Pflicke et al. to image DC entry into the lymphatic vessels, in order to investigate SMC recruitment (Pflicke and Sixt, 2009). However, the tools do not yet exist that would enable real-time visualisation of LYVE-1 expression changes.

7.1.2 Composition and function of the lymphatic extracellular matrix

The deposition of BM proteins such as Collagen IV and Laminin-α5 proved useful indicators of collecting vessel maturation. However, in contrast to the situation in the blood vasculature, where the importance of the BM in maintenance of vessel structure and biological function is widely recognised, very little is known about the composition and function of the lymphatic basement membrane. Our microarray analysis revealed that a number of extra-cellular matrix related genes are specifically up-regulated in lymphatic vessels, compared to arteries or veins. This might suggest that the composition of the lymphatic basement membrane is more complex than previously suspected and may also indicate specific roles for these proteins in lymphatic development or function that would warrant further investigation. In one such example of this, we have identified Reelin as the first lymphatic specific extracellular matrix protein and a novel regulator of lymphatic collecting vessel development and function.

We identified Reelin expression in both the lymphatic capillaries and collecting vessels, but found that it was only secreted from the collecting vessels. Consistent with this, we found that lymphatic capillaries developed normally in the absence of Reelin, while there were specific defects in collecting lymphatic vessel formation. Together with our own and previously published observations of differential Collagen IV deposition between lymphatic collecting vessels and capillaries (Pflicke and Sixt, 2009), this suggests differences in the composition of lymphatic capillary and collecting vessel

BM. The differences in BM between different types of lymphatic vessel have been largely ignored to date, but are likely to be important given the functional differences between lymphatic capillaries and collecting vessels in mediating fluid uptake and transport respectively (Tammela and Alitalo, 2010). Further investigation into the differences between lymphatic capillary and collecting vessel BM may reveal whether ECM proteins have a part in regulating these distinct functions.

7.1.3 Role of smooth muscle cells in lymphatic function

To our knowledge, *Reln*$^{-/-}$ mice provide the first example of a mouse model with a lymphatic specific reduction in SMC coverage, without concomitant blood vascular, or other major lymphatic defects. The role of SMC and pericytes in maintenance of blood vessel stability has been well established by studies of mouse models lacking various elements required for proper mural cell recruitment (Hellstrom et al., 2001), (Abramsson et al., 2007), (Stenzel et al., 2009). However, severe vascular defects and embryonic lethality make these models unsuitable for examining the role of SMC in lymphatic collecting vessel development and function. As well as reduced SMC coverage, *Reln*$^{-/-}$ collecting vessels were enlarged, exhibited variable diameters, and expressed abnormally high levels of the lymphatic capillary marker LYVE-1. These defects are reminiscent of the blood vascular defects of *Pdgfb/Pdgfrβ* mutants, which fail to recruit pericytes to the blood vascular capillaries (Hellstrom et al., 2001), and may suggest that lymphatic SMC play a similar role to blood vascular mural cells in restricting the calibre and promoting the maturation of lymphatic collecting vessels. However, there are interesting functional differences between lymphatic and blood vascular smooth muscle, predominantly in their contractile properties. While the driving force for blood flow around the body comes from the heart, lymphatic vessels must act as both pump and conduit to regulate lymphatic flow (Quick et al., 2009). The forces driving lymph flow come from both extrinsic sources, such as skeletal muscle contractions or movement of the diaphragm during breathing, and intrinsic forces, generated by smooth muscle cell contractions (reviewed in (Zawieja, 2009)). In order

to achieve the force necessary for lymph propulsion, lymphatic SMC take on characteristics of both blood vascular and cardiac smooth muscle (reviewed in (Muthuchamy and Zawieja, 2008)). Tonic contractions that regulate vessel tone are similar to those seen in blood vascular SMC, but rapid phasic contractions, which swiftly decrease collecting vessel diameter and push the lymph through the downstream valve, more closely resemble cardiac muscle contractions. The impaired lymphatic function observed in *Reln*$^{-/-}$ mice may be indicative of a defect in SMC contractility or lymph pumping, which might have clinical significance, since some human patients with *RELN* mutations suffer from congenital lymphoedema (Hong et al., 2000). It would therefore be interesting to test lymphatic vessel contractility in *Reln*$^{-/-}$ mice directly. It would also be interesting to test the implications of reduced SMC coverage and impaired lymphatic function of *Reln*$^{-/-}$ mice in light of new insights into solute exchange in the lymphatic collecting vessels, and physiological levels of collecting vessel 'leakiness' (Scallan and Huxley, 2010). It is possible that the discontinuous coverage of SMC around collecting lymphatic vessels aids solute exchange, and therefore we might expect to see increased exchange or a corresponding increase in lymph protein concentration in *Reln*$^{-/-}$ vessels with reduced SMC coverage. This may be reflected in the possible FITC-Dextran leakage from *Reln*$^{-/-}$ vessels in Figure 5.5 C.

7.2 Reelin signalling in the lymphatic vasculature

The majority of Reelin research has pointed towards it signalling through the canonical receptors, ApoER2 and VLDLR, which leads to phosphorylation of the intracellular adaptor protein Dab1 and elicitation of the downstream response (reviewed in (Forster et al., 2010), (Frotscher et al., 2009)). Therefore, the development of normal collecting lymphatic vessels in *Apoer2*$^{-/-}$*;Vldlr*$^{-/-}$ and *Dab1*^{Scm} mice was very unexpected. The milder neuronal phenotype in *Dab1*^{Scm} mice in the C3HeB/FeJ * DC/Le background may indicate that any lymphatic phenotype would also be reduced. However, our negative data from the *Apoer2*$^{-/-}$*;Vldlr*$^{-/-}$ mice, which were in the same background as

the *Reeler* mice and showed a strong neuronal phenotype, but no lymphatic phenotype, makes this unlikely. A mild reduction in SMC coverage in *Apoer2*$^{-/-}$*;Vldlr*$^{-/-}$ mice means that a role for the canonical signalling pathway in SMC recruitment cannot be completely ruled out (especially since it is possible that we would have seen a similar reduction in *Dab1*^{Scm} mice had they been in the same genetic background), but a failure to recapitulate the *Reln*$^{-/-}$ phenotype makes the involvement of alternative receptors likely. A number of alternative Reelin receptors have been proposed, but the veracity of their Reelin binding properties is controversial, as will be discussed below.

7.2.1 CNR1

Cadherin related neuronal receptor 1 (CNR1) seemed to be expressed in a likely pattern to transmit Reelin signalling, with expression in the cortical plate, but not the marginal zone and binding assays demonstrated binding of the extracellular domain to the N-terminus of Reelin (Senzaki et al., 1999). This binding could be blocked by the CR-50 antibody, and seemed to identify an attractive candidate for a Reelin receptor, because Fyn also docked to the cytoplasmic tail of CNR1, thus identifying a mechanism whereby SFK could be brought into the Reelin signalling complex (Senzaki et al., 1999). However, this study used the extracellular domain of CNR1 purified from cell lysates and not secreted protein, raising the possibility that it may not have been folded into its proper structure. A second study reassessed CNR1 Reelin binding activity using both the entire extracellular domain of secreted CNR1, or just the first ectodomain, where Reelin binding is supposed to occur (Jossin et al., 2004). In this case, no Reelin binding to either form of CNR1 could be observed, while strong receptor binding to ApoER2 and VLDLR was observed in all constructs containing the Reelin central fragment (Jossin et al., 2004). This suggests that a conformational change upon CNR1 secretion leaves it unable to bind Reelin in a physiological setting and therefore means that CNR1 cannot be a Reelin receptor.

7.2.2 Integrin-α3

Integrin-α3β1 is co-expressed with Dab1 in migrating neurons and has also been proposed as a Reelin receptor following binding experiments where it was co-immunoprecipitated with both the CR-50 antibody and Reelin coated beads (Dulabon et al., 2000). Furthermore, loss of *Itgb1* in neuronal and glial precursors lead to a similar, but much less severe, disruption of the radial glial scaffold to that seen in *Reeler* mice (Forster et al., 2002). However, whether this is really due to Reelin-Integrin-α3β1 binding is again questionable. Dab1 phosphorylation is required for neuronal detachment from the glia, and in the process of detaching, neurons downregulate Integrin-α3 (Sanada et al., 2004). However, Dab1 phosphorylation is not induced by Reelin binding to Integrin-α3β1 (Dulabon et al., 2000), which suggested that while Integrin-α3β1 is likely important for the correct formation of the radial glial scaffold, and for neuronal detachment from glia, this is more likely to be a downstream effect of Reelin signalling via ApoER2/VLDLR than induced directly by Reelin-Integrin-α3β1 binding (Sanada et al., 2004). Perhaps the most convincing evidence against Integrin-α3β1 as a Reelin receptor comes from the lack of genetic data to support it. *Itgb1* deletion in migrating neurons has no effect on cortical patterning; the layers form correctly and there is no ectopic neuronal migration into the marginal zone (Belvindrah et al., 2007). This suggests that the requirement for Integrin-β1 for correct cortical development is in glia, rather than neurons. Furthermore, *Itga3*$^{-/-}$ mice also show no cortical patterning defects, or layer inversion, making it unlikely that in the absence of Integrin-β1, another β chain integrin substitutes for it and demonstrating that Integrin-α3 is not essential for Reelin signalling (Belvindrah et al., 2007).

7.2.3 EphrinBs

Recently, EphrinBs were also proposed as novel Reelin receptors (Senturk et al., 2011). Since EphrinB2 is highly expressed in the lymphatic vasculature, and known to be involved in lymphatic remodelling (Makinen et al., 2005), this seemed a likely candidate for a Reelin receptor in the lymphatic vasculature. Indeed, lymphatic endothelial specific deletion of *Efnb2* resulted in collecting vessel defects resembling those seen in *Reln*$^{-/-}$ mice, which was suggestive of a role for this protein in the Reelin signalling pathway.

However, given the controversy in the literature surrounding the existence of alternative Reelin receptors or co-receptors, it is important to have both strong genetic and biochemical data before drawing a firm conclusion. It will also be beneficial to confirm Reelin signalling through EphrinB2 in the lymphatic system by establishing whether Reelin can induce enhanced *MCP1* expression in LEC lacking EphrinB2, as we observed in wild-type LEC.

To this end, the current focus of this project is to confirm Reelin binding to EphrinB2 with binding assays. Preliminary data (not shown) suggests that EphrinB2 can bind to Reelin, as shown by Senturk et al., and furthermore that it binds to the N-terminal fragment. This has interesting implications in the context of our previous results, and perhaps tallies with our earlier conclusions that ApoER2 and VLDLR are not the major Reelin receptors in the lymphatic vasculature since, as discussed below, ApoER2 and VLDLR bind the central fragment of Reelin.

It should be noted that although an ApoER2/VLDLR and Dab1 independent function for Reelin is unusual, it is not unprecedented. Rossel and colleagues discovered a novel function for Reelin in neuronal migration in the hindbrain that was dependant on Dab1, but not on ApoER2/VLDLR (Rossel et al., 2005). Likewise, Cariboni and colleagues discovered an inhibitory function for Reelin in the migration of Gonadotropin-releasing hormone neurons that was independent of both ApoER2/VLDLR and Dab1 (Cariboni et al., 2005). Together with our data, this work suggests that Reelin signalling is more

complex than previously thought and that research to identify new Reelin binding proteins should consider not only the possibility of co-receptors for ApoER2/VLDLR, but also receptors that may function completely independently of the canonical signalling pathway. Greater diversity in Reelin signalling than previously imagined is also highlighted by our own work, and that of others, in identifying novel systems outside the CNS in which Reelin is functioning (Khialeeva et al., 2011).

7.3 Reelin activity in the lymphatic vasculature

In the developing cortex, Cajal Retzius cells in the marginal zone secrete Reelin, which signals to both the migrating neurons and closely apposed radial glial cells to direct correct cortical patterning (Tissir and Goffinet, 2003), (Sanada et al., 2004), (Hartfuss et al., 2003). Despite the close apposition between these cell types, it is not known whether cell-cell interactions are involved in activation or modulation of Reelin signalling in the developing nervous system. We confirmed *in vitro* that within the lymphatic system, Reelin was expressed specifically by LEC, but the presence of SMC enhanced its secretion and proteolytic processing. This suggests a previously un-described role for cell-cell interactions in activation of Reelin signalling.

While all reports seem to agree that proteolytic processing affects Reelin function, there is widespread controversy as to both the consequence of processing for Reelin signalling efficiency and the functional importance of the resulting fragments in mediating Reelin's biological actions.

7.3.1 The 'active' fragment in Reelin signalling

The central fragment of Reelin (repeats 3-6) binds to the canonical receptors, ApoER2 and VLDLR, is sufficient to activate Reelin signalling in both cultured neurons and

cortical explants and can even partially rescue neuronal migration defects in *Reeler* cortical slices (Jossin et al., 2004). Other reports suggest that the N-terminal fragment is necessary for the full efficacy of Reelin signalling, probably by mediating Reelin aggregation, and perhaps thus concentrating the signal (Utsunomiya-Tate et al., 2000). Further evidence for the importance of the N-terminal fragment for Reelin function comes from the fact that the CR-50 antibody, raised against an antigen in the N-terminus of Reelin, can inhibit Reelin function (Ogawa et al., 1995), (Zhao et al., 2004). This may even imply a signalling function for the N-terminus beyond protein aggregation. The highly basic C-terminus has also been implicated in Reelin function. There is 100% conservation in the C-terminus sequence at the amino acid level, and 92% conservation at the nucleotide level between all mammals whose sequences are obtainable, which is already suggestive of functional importance (Nakano et al., 2007). In the Orleans variant of *Reln* mutants ($Reln^{rl\text{-}Orl}$), a frameshift mutation results in production of a C-terminus truncated protein, which is produced, but not secreted, in homozygous mutants (de Bergeyck et al., 1997). $Reln^{rl\text{-}Orl}$ mice exhibit an identical phenotype to $Reln^{-/-}$ mice (Rice and Curran, 2001), demonstrating that Reelin secretion is essential for its function. The C-terminus is also reportedly necessary for efficient activation of the downstream signalling cascade of Reelin, and stable binding to the canonical receptors (Nakano et al., 2007). This may involve a conformational change in the protein, resulting in a close association between the C-terminus and the neighbouring eighth Reelin repeat, which then allows efficient signalling, or binding to a co-receptor (Kohno et al., 2009b).

Given this body of literature, it appears that the identity of the 'active' Reelin fragment is still open to debate, although the evidence for central fragment binding to ApoER2 and VLDLR and activating Reelin signalling in the nervous system is convincing (Jossin et al., 2007), (Jossin et al., 2004). However, even in this scenario there is room for additional, or alternative scenarios, as antibodies against ApoER2 or VLDLR were capable of binding their respective receptors and inducing Dab1 phosphorylation, but this was not sufficient to rescue the *Reeler* phenotype in cortical slice cultures (Jossin et al., 2004), suggesting that an additional Reelin signalling mechanism, independent of Dab1, may also be in play.

Overall, while one report suggests that Reelin cleavage at the N-terminus abolishes Reelin signalling capacity (Kohno et al., 2009a), most reports agree that Reelin processing is important for its function. For example, prevention of Reelin processing, either by application of MMP inhibitors, or as a result of epileptic activity, impairs Reelin signalling and results in cortical development defects or granule cell dispersion respectively, which are both characteristics of the *Reeler* phenotype (Jossin et al., 2007), (Duveau et al., 2010), (Tinnes et al., 2011).

7.3.2 Reelin processing in the lymphatic vasculature

In the nervous system, Reelin processing appears to be MMP-dependant (Lambert de Rouvroit et al., 1999), (Jossin et al., 2007), (Tinnes et al., 2011), and since the Reelin cleavage products we identified in LEC/SMC co-cultures were identical to those previously documented, it is likely that the same mechanism of processing occurs in the lymphatic vasculature.

We found that co-culture with SMC enhanced Reelin secretion, and presumably therefore signal activation. We also saw that following secretion, Reelin was proteolytically processed at both the N- and C-termini, likely by both LEC and SMC. We presume that this is again evidence of signal activation, possibly as proposed in the nervous system, by releasing the active fragment, although we do not know which part of the protein is active within the lymphatic system. Our results so far indicate that the central Reelin fragment alone is unlikely to be sufficient to activate Reelin signalling in the lymphatic vasculature. Since this is the fragment known to bind ApoER2 and VLDLR (Jossin et al., 2004), this seems compatible with our finding that lymphatic collecting vessels develop normally in *Apoer2*$^{-/-}$*;Vldlr*$^{-/-}$ mice and do not recapitulate the phenotype we observe in *Reln*$^{-/-}$ collecting vessels. Our recent preliminary observations that EphrinB2 binds the N-terminus of Reelin also support the suggestion that the central Reelin fragment may not be the major active fragment in Reelin signalling in the lymphatic vasculature.

Despite the possibility of a different active fragment being involved in the lymphatic vasculature, it is easy to envision how the model proposed by Jossin et al. could be applicable to this system: the authors suggest that full-length Reelin is secreted into, and likely anchored to, the ECM, but that its subsequent processing releases the smaller, diffusible active fragment, which signals to the target cells (Jossin et al., 2007). Although binding to any specific ECM protein is yet to be experimentally confirmed, immunofluorescence of neonatal cortical slices with antibodies against the individual Reelin fragments (N-terminus, C-terminus and central fragment) demonstrated that full-length Reelin remains in the MZ near the Cajal-Retzius cells from which it is secreted, thus suggesting that it may be anchored to the ECM. In contrast, the central and N-terminal fragments were detected in cortical plate at some distance from the MZ (Jossin et al., 2007). Our results suggest that in the lymphatic system, SMC recruitment to the collecting vessels enhances release of full-length Reelin, which is subsequently processed. The active fragment might then diffuse to signal either to migrating SMC, or further along the lymphatic vessels - perhaps further distally to locations that have not yet recruited SMC - and signal to other LEC, trigger increased production of factors involved in SMC recruitment and enhance SMC recruitment to distal parts of the vessel. Retention of full-length Reelin close to the cells from which it is secreted in the cortex (Jossin et al., 2007) may also be consistent with Reelin secretion from and signalling back to the lymphatic endothelium.

However, we cannot yet exclude the alternative hypothesis that Reelin cleavage is a mechanism of limiting Reelin function (Kohno et al., 2009a). In this situation, we might envision that the protein conformation of Reelin is critical for signalling and that cleavage at either one or both sites disrupts the protein structure and diminishes Reelin signalling capacity. Therefore, while secretion of full-length Reelin from the LEC upon SMC recruitment may lead to increased LEC-derived MCP-1 expression, and enhanced SMC recruitment, subsequent processing may limit this response and prevent over-migration of SMC to the collecting lymphatic vessels. Such a mechanism could contribute to the discontinuous SMC coverage of lymphatic collecting vessels, compared to the complete investment of SMC seen around arteries and veins.

Now that we have an assay with a positive read-out of Reelin activity, namely increased LEC *MCP1* expression, it will be interesting to distinguish between these hypotheses, by examining *MCP1* expression following LEC stimulation with either totally or partially cleaved Reelin fragments. Furin Inhibitor 1 could be used to block baseline processing by the HEK-293 cells (Kohno et al., 2009a). Alternatively, expression constructs encoding different Reelin fragments can be used (Jossin et al., 2004). If any fragment alone were capable of increasing *MCP1* expression, this would suggest it as the active fragment. Our preliminary results of EphrinB2 binding to the N-terminus suggest that this fragment will be particularly interesting in this regard. If the partially cleaved constructs that included this fragment were also able to increase *MCP1* expression, this might suggest that Reelin processing may release the fragment to allow increased signal diffusion, but doesn't 'activate' signalling. However, if only full-length, or partially cleaved, Reelin was able to induce *MCP1* expression, it would suggest that conformational changes to the protein structure caused by processing disrupted Reelin signalling capability.

7.3.3 Role of proteolytic processing in matrix biology

It is interesting to note that proteolytic processing has important implications for the biological function of many extracellular matrix molecules, in some cases even resulting in a cleavage product with an opposite function to that of the parent molecule, for example Endorepellin, generated by Perlecan cleavage, has anti-angiogenic properties, counter to the pro-angiogenic properties of its parent molecule (Mongiat et al., 2003), (Goyal et al., 2011). Many large extracellular matrix proteins, such as proteoglycans and Fibronectin bind growth factors, which enables them to either enhance growth factor signalling, perhaps by providing several binding sites and concentrating the signal, or inhibit signalling, by 'sequestering' growth factors (reviewed in (Hynes, 2009), (Kalluri, 2003)). In this case, proteolytic processing, perhaps upon angiogenic stimulus, can release the bound growth factors. Such a role for Reelin has not yet been explored, although its large size could indicate potential in

this respect and may provide a means by which Reelin could interact with other, as yet unidentified, signalling pathways (reviewed in (Tissir and Goffinet, 2003)). There is also interesting research suggesting that ECM proteins can directly signal through growth factor receptors (reviewed in (Hynes, 2009)). One such example is that of Laminin-5. Following proteolytic processing, EGF repeats in the cleavage product can bind to and activate the EGF receptor (Schenk et al., 2003).

7.4 Cellular mechanism of Reelin action

The mechanism of Reelin action is also highly complex, and in the developing nervous system it has been implicated in both facilitation of migration by somal translocation (Franco et al., 2011) and in preventing over-migration, perhaps by regulating detachment from the glial scaffold and stabilising the actin cytoskeleton (Sanada et al., 2004), (Chai et al., 2009). The reduction in SMC coverage around collecting lymphatic vessels of *Reln*$^{-/-}$ mice suggested that Reelin might be involved in directly promoting SMC migration, and consequently recruitment to the lymphatic vessels or in encouraging SMC attachment to the vessel once they had already migrated. However, a number of *in vitro* assays were unable to determine a direct effect of Reelin signalling on SMC behaviour. We used venous SMC in all our *in vitro* assays, as a method of obtaining a suitable number of pure lymphatic SMC, and maintaining them in culture, is not yet available, and our own preliminary attempts were unsuccessful (data not shown). Since there are genetic and functional differences between blood vascular and lymphatic smooth muscle (Muthuchamy et al., 2003), it remains a possibility that venous SMC may not respond the same way to Reelin that lymphatic SMC would. Moreover, while we examined the effect of Reelin stimulation on the production of LEC-derived SMC recruitment factors and found that Reelin treatment increased *MCP1* expression, we have not yet examined the effect of Reelin on SMC-derived *MCP1* mRNA. Since it is known that SMC express both MCP-1 and its receptor CCR2 (Potula et al., 2009), (Ma et al., 2007), it is possible that Reelin secretion from LEC

could enhance *MCP1* expression in both LEC and SMC to promote SMC recruitment to the vessels.

MCP-1 has been well documented to enhance SMC migration (Jay et al., 2010), (Ma et al., 2007), (Lo et al., 2005) and interestingly, endothelial cell expression of *MCP1* increased upon TGFβ stimulation and mediated the effect of TGFβ1 on SMC proliferation and migration (Ma et al., 2007). However, *TGFβ1* was not up-regulated in our experiment, suggesting that Reelin induces up-regulation of *MCP1* via an alternative pathway, which would require further investigation to elucidate. MCP-1 was originally identified and characterised based on its role in monocyte recruitment during inflammation (reviewed in (Deshmane et al., 2009)), and pro-inflammatory cytokines TNFα, IL-7β and IFNγ also up-regulate endothelial cell MCP-1 expression (Harkness et al., 2003). Reelin-induced up-regulation of *MCP1* by LEC is consistent with our observation of decreased SMC coverage of $Reln^{-/-}$ collecting lymphatic vessels, and suggests that Reelin may mediate SMC recruitment to the vessels via endothelial MCP-1 expression. Confirmation of this hypothesis might come from examination of the lymphatic phenotype of $Mcp1^{-/-}$ mice, which have a normal lifespan and so would be suitable for the same phenotypic analysis we conducted on $Reln^{-/-}$ mice (Lu et al., 1998). If similar lymphatic collecting vessel defects were observed in $Mcp1^{-/-}$ as $Reln^{-/-}$ mice, it would provide additional confirmation that Reelin mediates SMC recruitment via MCP-1.

7.5 Concluding remarks

Despite its importance in regulating tissue fluid homeostasis, absorbing dietary fat and assisting the immune response, understanding of lymphatic biology has been limited. However, great progress has been made in the last half-century in appreciation of the physiological and pathological functions of the lymphatic vasculature, and the mechanisms governing their regulation, as well as in the molecular regulation of lymphatic development. Importantly, with advancing knowledge of the genes and

proteins involved in regulating lymphatic vessel growth and function, is coming the development of therapeutic strategies to combat lymphoedema (Karkkainen et al., 2001), (Tammela et al., 2007) (reviewed in (Norrmen et al., 2011)). Although these have not yet progressed to the clinic, it gives an optimistic outlook for the future.

The 3D environment is important for regulating gene expression and cell behaviour both *in vitro* and *in vivo* and truly representative cellular responses can often not be generated in a 2D culture system (reviewed in (Griffith and Swartz, 2006)). Yet the contribution of the extracellular microenvironment to lymphatic development and function has remained largely unexplored. My project has begun to touch on this issue, with the identification of lymphatic specific extracellular matrix proteins, and in particular by identifying a role for Reelin in the correct development and function of collecting lymphatic vessels. Congenital lymphoedema in human patients with a *RELN* mutation emphasises the importance of the extracellular matrix in lymphatic vascular function and may give clinical relevance to this research (Hong et al., 2000). It is possible that further research into the functional importance of extracellular matrix proteins surrounding the lymphatic vasculature may identify other proteins whose loss results in lymphatic dysfunction, which could contribute to our understanding of lymphoedema and its causes, and potentially give rise to new therapeutic targets.

Chapter 8. Appendix

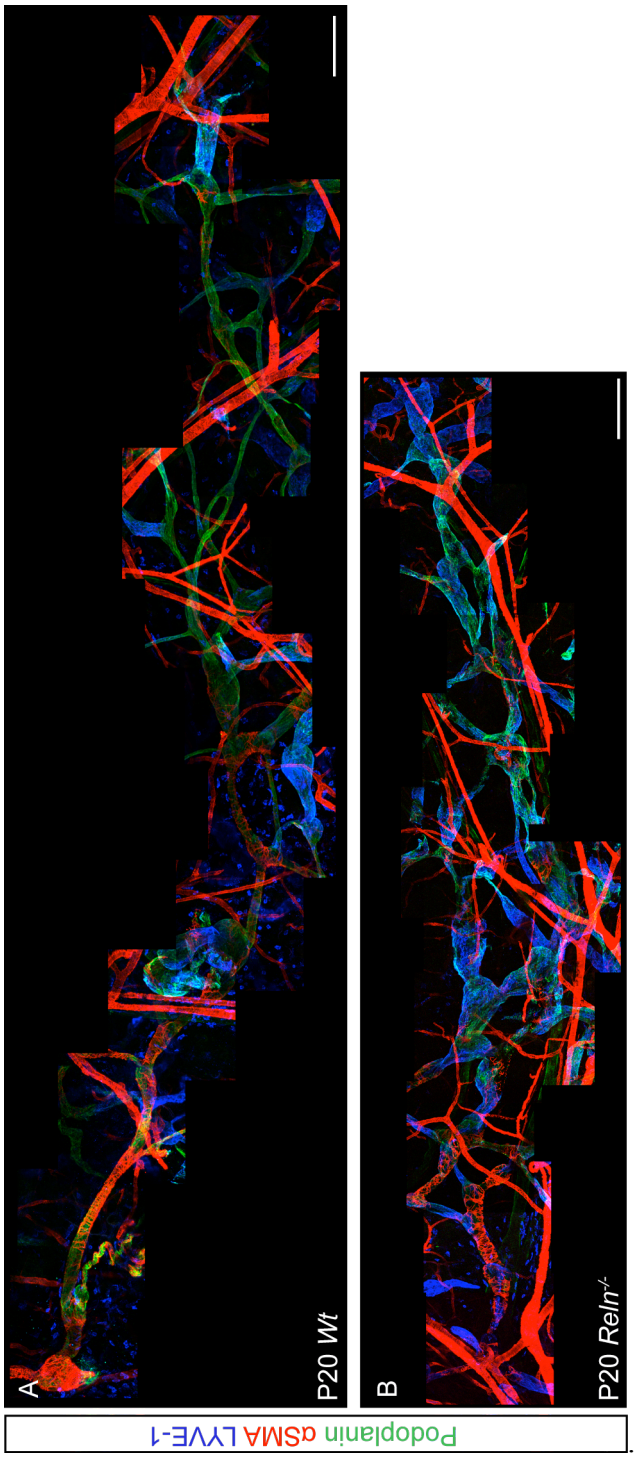

Figure 8.1 *Reln* mutation leads to collecting vessel defects: original vessel images
(A-B) Immunofluorescence staining of whole vessels shown in Figure 5.1, but without removing overlapping vasculature. Scale bars = 200µm.

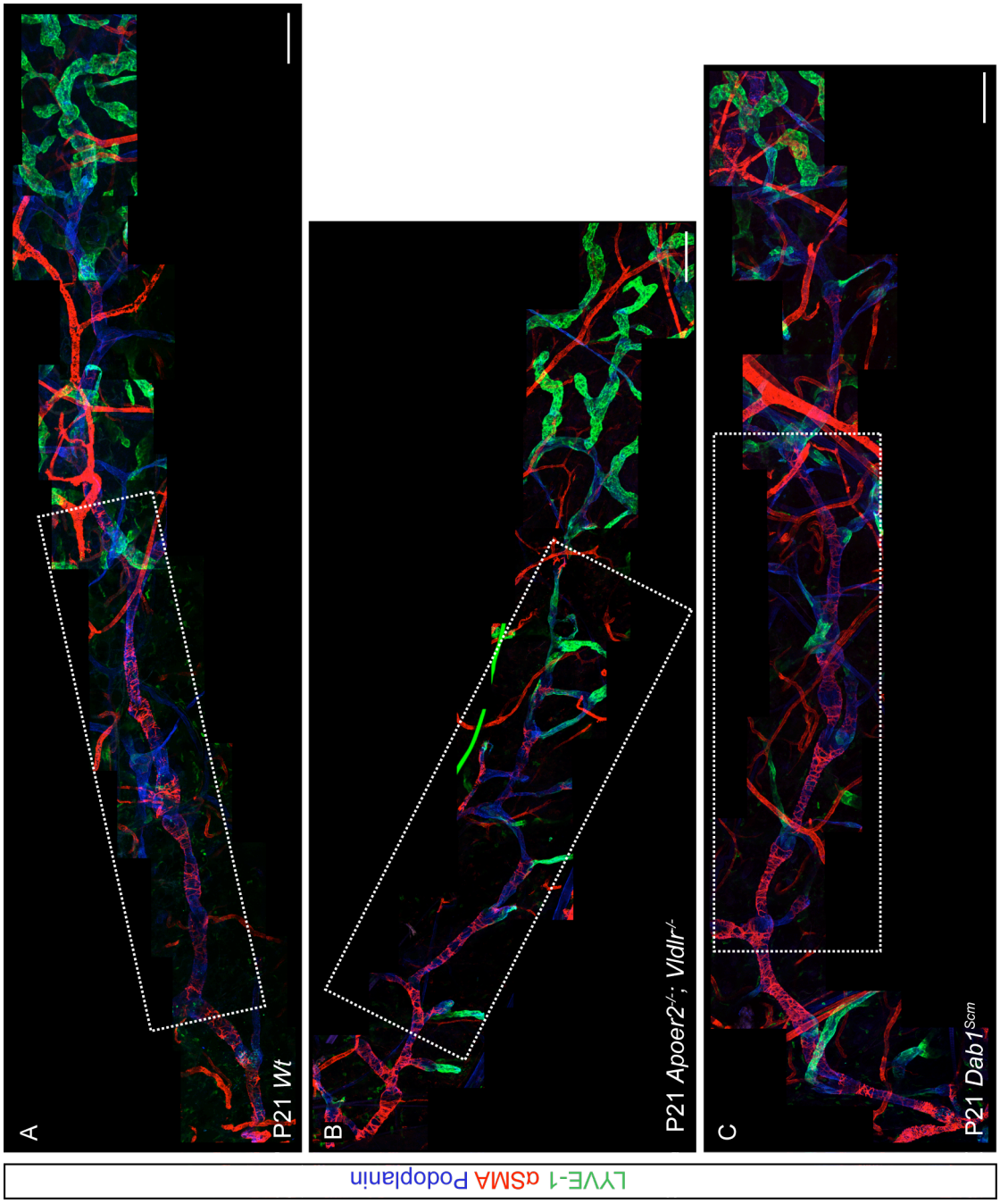
A
P21 Wt
B
P21 Apoer2-/-; Vldlr-/-
C
P21 Dab1Scm
LYVE-1 αSMA Podoplanin

Figure 8.2 Normal lymphatic collecting vessels in *Apoer2*$^{-/-}$;*Vldlr*$^{-/-}$ and *Dab1*^{Scm} mice: original vessel images.
Immunofluorescence staining of whole vessels shown in Figure 6.2; white boxes indicate areas magnified. Scale bars = 200μm.

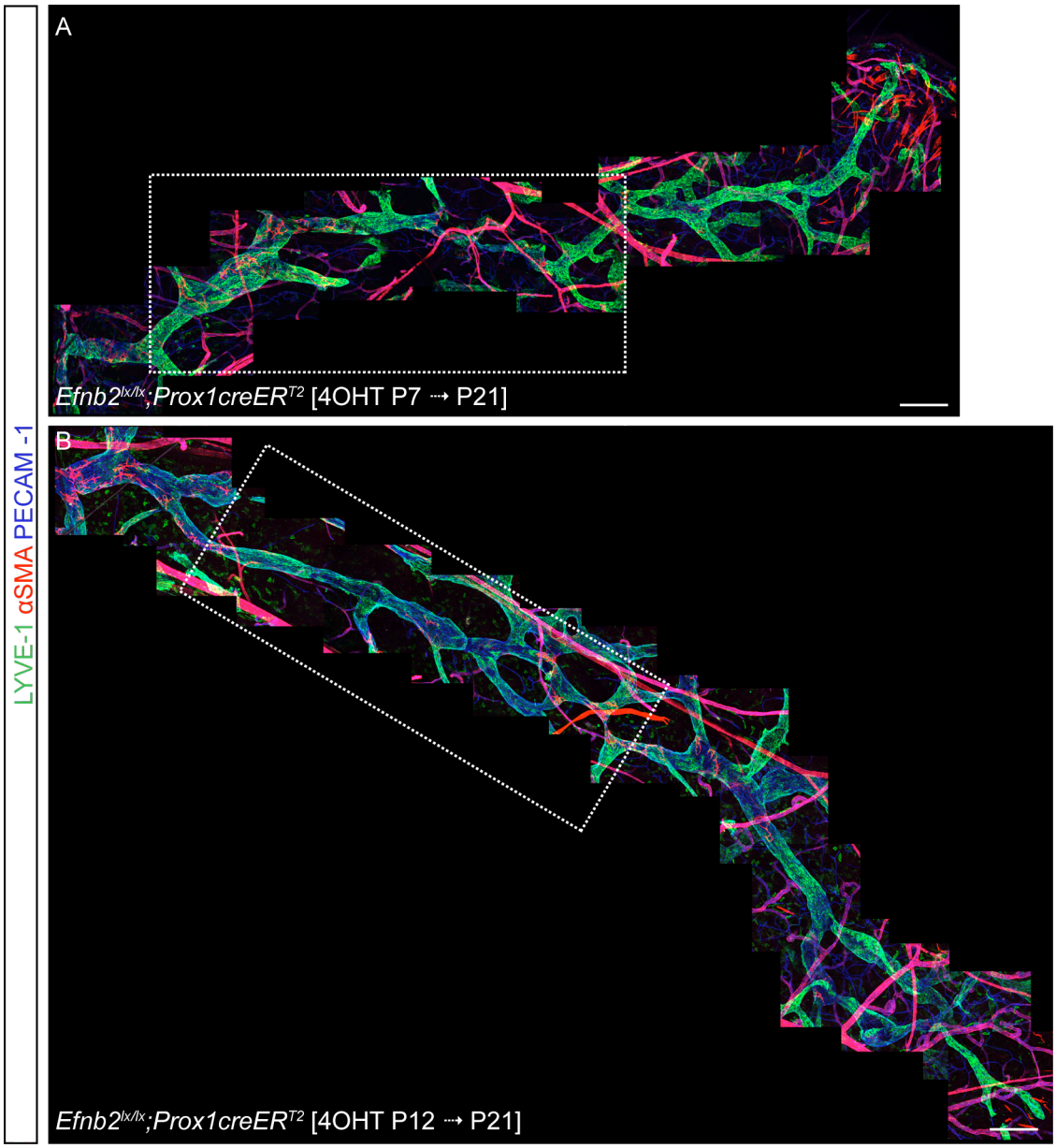

Figure 8.3 Collecting vessel defects following lymphatic-specific *Efnb2* deletion resemble those of *Reln*$^{-/-}$ mice: original vessel images.
(A-B) Immunofluorescence staining of *Efnb2*$^{lx/lx}$;*Prox1-creER*^{T2} vessels shown in Figure 6.4; white boxes indicate areas magnified. Scale bars = 200μm.

APPENDIX

Refer to the table below for the Human Phospho-Kinase Array coordinates.

Membrane/Coordinate	Target/Control	Phosphorylation Site	Cell Source/Treatment
A - A1, A2	Positive Control	—	—
A - A3, A4	p38α	T180/Y182	MCF-7/UV*
A - A5, A6	ERK1/2	T202/Y204, T185/Y187	HeLa/PMA*
A - A7, A8	JNK pan	T183/Y185, T221/Y223	MCF-7/UV*
A - A9, A10	GSK-3α/β	S21/S9	MCF-7/rhIGF-I
B - A13, A14	p53	S392	MCF-7/CPT*
B - A17, A18	Positive Control	—	—
A - B3, B4	MEK1/2	S218/S222, S222/S226	MCF-7/UV*
A - B5, B6	MSK1/2	S376/S360	HeLa/PMA*
A - B7, B8	AMPKα1	T174	Jurkat/H_2O_2*
A - B9, B10	Akt	S473	MCF-7/rhIGF-I*
B - B11, B12	Akt	T308	K562/Pervanadate
B - B13, B14	p53	S46	MCF-7/CPT*
A - C1, C2	TOR	S2448	MCF-7/UV*
A - C3, C4	CREB	S133	Jurkat/H_2O_2*
A - C5, C6	HSP27	S78/S82	HeLa/PMA*
A - C7, C8	AMPKα2	T172	HepG2/Metformin*
A - C9, C10	β-Catenin	—	HeLa/PMA*
B - C11, C12	p70 S6 Kinase	T389	MCF-7/CPT*
B - C13, C14	p53	S15	MCF-7/CPT*
B - C15, C16	p27	T198	Jurkat/H_2O_2*
B - C17, C18	Paxillin	Y118	K562/Pervanadate
A - D1, D2	Src	Y419	Colo205/SFM*
A - D3, D4	Lyn	Y397	Daudi/Pervanadate*
A - D5, D6	Lck	Y394	Jurkat/Pervanadate
A - D7, D8	STAT2	Y689	Daudi/rhIFN-α2A
A - D9, D10	STAT5a	Y699	U937/PMA + rhIL-4
B - D11, D12	p70 S6 Kinase	T421/S424	MCF-7/UV*
B - D13, D14	RSK1/2/3	S380	HeLa/PMA*
B - D15, D16	p27	T157	K562/Pervanadate
B - D17, D18	PLCγ-1	Y783	Jurkat/H_2O_2*

continued on next page...

Membrane/Coordinate	Target/Control	Phosphorylation Site	Cell Source/Treatment
A - E1, E2	Fyn	Y420	Daudi/Pervanadate*
A - E3, E4	Yes	Y426	K562/Pervanadate*
A - E5, E6	Fgr	Y412	K562/Pervanadate
A - E7, E8	STAT3	Y705	LNCap/rhIL-6
A - E9, E10	STAT5b	Y699	Daudi/rhIFN-α2A*
B - E11, E12	p70 S6 Kinase	T229	MCF-7/CPT*
B - E13, E14	RSK1/2	S221	U937/PMA + rhIL-4
B - E15, E16	c-Jun	S63	HeLa/PMA*
B - E17, E18	Pyk2	Y402	K562/Pervanadate*
A - F1, F2	Hck	Y411	Daudi/Pervanadate
A - F3, F4	Chk-2	T68	HeLa/CPT*
A - F5, F6	FAK	Y397	HepG2/Pervanadate
A - F7, F8	STAT6	Y641	U937/PMA + rhIL-4
A - F9, F10	STAT5a/b	Y699	Daudi/rhIFN-α2A
B - F11, F12	STAT1	Y701	Daudi/rhIFN-α2A
B - F13, F14	STAT4	Y693	NC-37/Pervanadate
B - F15, F16	eNOS	S1177	Jurkat/H_2O_2*
B - F17, F18	PBS (Negative Control)	—	—
A - G1, G2	Positive Control	—	—
A - G5, G6	PBS (Negative Control)	—	—

*A change in phosphorylation for this protein was detected in multiple cell sources.

Figure 8.4 Phospho-array key (R&D systems).
Details of phosphorylated proteins found at each membrane co-ordinate, together with phosphorylation site and cell source / treatment. Scan from Human proteome profiler kit handbook.

Chapter 9. Reference List

ABRAMSSON, A., KURUP, S., BUSSE, M., YAMADA, S., LINDBLOM, P., SCHALLMEINER, E., STENZEL, D., SAUVAGET, D., LEDIN, J., RINGVALL, M., LANDEGREN, U., KJELLEN, L., BONDJERS, G., LI, J. P., LINDAHL, U., SPILLMANN, D., BETSHOLTZ, C. & GERHARDT, H. 2007. Defective N-sulfation of heparan sulfate proteoglycans limits PDGF-BB binding and pericyte recruitment in vascular development. *Genes Dev,* 21, 316-31.

ABRAMSSON, A., LINDBLOM, P. & BETSHOLTZ, C. 2003. Endothelial and nonendothelial sources of PDGF-B regulate pericyte recruitment and influence vascular pattern formation in tumors. *J Clin Invest,* 112, 1142-51.

ABTAHIAN, F., GUERRIERO, A., SEBZDA, E., LU, M. M., ZHOU, R., MOCSAI, A., MYERS, E. E., HUANG, B., JACKSON, D. G., FERRARI, V. A., TYBULEWICZ, V., LOWELL, C. A., LEPORE, J. J., KORETZKY, G. A. & KAHN, M. L. 2003. Regulation of blood and lymphatic vascular separation by signaling proteins SLP-76 and Syk. *Science,* 299, 247-51.

ADAMS, R. H. & EICHMANN, A. 2010. Axon guidance molecules in vascular patterning. *Cold Spring Harb Perspect Biol,* 2, a001875.

ADAMS, R. H., WILKINSON, G. A., WEISS, C., DIELLA, F., GALE, N. W., DEUTSCH, U., RISAU, W. & KLEIN, R. 1999. Roles of ephrinB ligands and EphB receptors in cardiovascular development: demarcation of arterial/venous domains, vascular morphogenesis, and sprouting angiogenesis. *Genes Dev,* 13, 295-306.

ALDERS, M., HOGAN, B. M., GJINI, E., SALEHI, F., AL-GAZALI, L., HENNEKAM, E. A., HOLMBERG, E. E., MANNENS, M. M., MULDER, M. F., OFFERHAUS, G. J., PRESCOTT, T. E., SCHROOR, E. J., VERHEIJ, J. B., WITTE, M., ZWIJNENBURG, P. J., VIKKULA, M., SCHULTE-MERKER, S. & HENNEKAM, R. C. 2009. Mutations in CCBE1 cause generalized lymph vessel dysplasia in humans. *Nat Genet,* 41, 1272-4.

ALEXANDER, J. S., CHAITANYA, G. V., GRISHAM, M. B. & BOKTOR, M. 2010. Emerging roles of lymphatics in inflammatory bowel disease. *Ann N Y Acad Sci,* 1207 Suppl 1, E75-85.

ALITALO, K., TAMMELA, T. & PETROVA, T. V. 2005. Lymphangiogenesis in development and human disease. *Nature,* 438, 946-53.

ARMULIK, A., ABRAMSSON, A. & BETSHOLTZ, C. 2005. Endothelial/pericyte interactions. *Circ Res,* 97, 512-23.

ARNAUD, L., BALLIF, B. A., FORSTER, E. & COOPER, J. A. 2003. Fyn tyrosine kinase is a critical regulator of disabled-1 during brain development. *Curr Biol,* 13, 9-17.

ARROYO, A. G. & IRUELA-ARISPE, M. L. 2010. Extracellular matrix, inflammation, and the angiogenic response. *Cardiovasc Res,* 86, 226-35.

ASZODI, A., LEGATE, K. R., NAKCHBANDI, I. & FASSLER, R. 2006. What mouse mutants teach us about extracellular matrix function. *Annu Rev Cell Dev Biol,* 22, 591-621.

AUGUSTIN, H. G., KOH, G. Y., THURSTON, G. & ALITALO, K. 2009. Control of vascular morphogenesis and homeostasis through the angiopoietin-Tie system. *Nat Rev Mol Cell Biol,* 10, 165-77.

AVRAAMIDES, C. J., GARMY-SUSINI, B. & VARNER, J. A. 2008. Integrins in angiogenesis and lymphangiogenesis. *Nat Rev Cancer,* 8, 604-17.

BALUK, P., FUXE, J., HASHIZUME, H., ROMANO, T., LASHNITS, E., BUTZ, S., VESTWEBER, D., CORADA, M., MOLENDINI, C., DEJANA, E. & MCDONALD, D. M. 2007. Functionally specialized junctions between endothelial cells of lymphatic vessels. *J Exp Med,* 204, 2349-62.

BALUK, P., TAMMELA, T., ATOR, E., LYUBYNSKA, N., ACHEN, M. G., HICKLIN, D. J., JELTSCH, M., PETROVA, T. V., PYTOWSKI, B., STACKER, S. A., YLA-HERTTUALA, S., JACKSON, D. G., ALITALO, K. & MCDONALD, D. M. 2005. Pathogenesis of persistent lymphatic vessel hyperplasia in chronic airway inflammation. *J Clin Invest,* 115, 247-57.

BANERJI, S., NI, J., WANG, S. X., CLASPER, S., SU, J., TAMMI, R., JONES, M. & JACKSON, D. G. 1999. LYVE-1, a new homologue of the CD44 glycoprotein, is a lymph-specific receptor for hyaluronan. *J Cell Biol,* 144, 789-801.

BASTIN, G. & HEXIMER, S. P. 2011. Intracellular regulation of heterotrimeric G-protein signaling modulates vascular smooth muscle cell contraction. *Arch Biochem Biophys,* 510, 182-9.

BAZIGOU, E., XIE, S., CHEN, C., WESTON, A., MIURA, N., SOROKIN, L., ADAMS, R., MURO, A. F., SHEPPARD, D. & MAKINEN, T. 2009. Integrin-alpha9 is required for fibronectin matrix assembly during lymphatic valve morphogenesis. *Dev Cell,* 17, 175-86.

BAZIGOU, E., LYONS, O. T., SMITH A., VENN, G. E., COPE, C., BROWN, N. A. & MAKINEN, T. 2011. Genes regulating lymphangiogenesis control venous valve formation and maintenance in mice. *J Clin Invest,* 121, 2984-92

BEFFERT, U., MORFINI, G., BOCK, H. H., REYNA, H., BRADY, S. T. & HERZ, J. 2002. Reelin-mediated signaling locally regulates protein kinase B/Akt and glycogen synthase kinase 3beta. *J Biol Chem,* 277, 49958-64.

BEFFERT, U., WEEBER, E. J., DURUDAS, A., QIU, S., MASIULIS, I., SWEATT, J. D., LI, W. P., ADELMANN, G., FROTSCHER, M., HAMMER, R. E. & HERZ, J. 2005. Modulation of synaptic plasticity and memory by Reelin involves differential splicing of the lipoprotein receptor Apoer2. *Neuron,* 47, 567-79.

BELVINDRAH, R., GRAUS-PORTA, D., GOEBBELS, S., NAVE, K. A. & MULLER, U. 2007. Beta1 integrins in radial glia but not in migrating neurons are essential for the formation of cell layers in the cerebral cortex. *J Neurosci,* 27, 13854-65.

BENJAMIN, L. E., HEMO, I. & KESHET, E. 1998. A plasticity window for blood vessel remodelling is defined by pericyte coverage of the preformed endothelial network and is regulated by PDGF-B and VEGF. *Development,* 125, 1591-8.

BERGERS, G. & SONG, S. 2005. The role of pericytes in blood-vessel formation and maintenance. *Neuro Oncol,* 7, 452-64.

BERTOZZI, C. C., SCHMAIER, A. A., MERICKO, P., HESS, P. R., ZOU, Z., CHEN, M., CHEN, C. Y., XU, B., LU, M. M., ZHOU, D., SEBZDA, E., SANTORE, M. T., MERIANOS, D. J., STADTFELD, M., FLAKE, A. W., GRAF, T., SKODA, R., MALTZMAN, J. S., KORETZKY, G. A. & KAHN, M. L. 2010. Platelets regulate lymphatic vascular development through CLEC-2-SLP-76 signaling. *Blood,* 116, 661-70.

BOARDMAN, K. C. & SWARTZ, M. A. 2003. Interstitial flow as a guide for lymphangiogenesis. *Circ Res,* 92, 801-8.

BOCK, H. H. & HERZ, J. 2003. Reelin activates SRC family tyrosine kinases in neurons. *Curr Biol,* 13, 18-26.

BOCK, H. H., JOSSIN, Y., LIU, P., FORSTER, E., MAY, P., GOFFINET, A. M. & HERZ, J. 2003. Phosphatidylinositol 3-kinase interacts with the adaptor protein Dab1 in response to Reelin signaling and is required for normal cortical lamination. *J Biol Chem,* 278, 38772-9.

BRORSON, H., OHLIN, K., OLSSON, G. & NILSSON, M. 2006. Adipose tissue dominates chronic arm lymphedema following breast cancer: an analysis using volume rendered CT images. *Lymphat Res Biol,* 4, 199-210.

BRUYERE, F., MELEN-LAMALLE, L., BLACHER, S., ROLAND, G., THIRY, M., MOONS, L., FRANKENNE, F., CARMELIET, P., ALITALO, K., LIBERT, C., SLEEMAN, J. P., FOIDART, J. M. & NOEL, A. 2008. Modeling lymphangiogenesis in a three-dimensional culture system. *Nat Methods,* 5, 431-7.

CAI, J., KEHOE, O., SMITH, G. M., HYKIN, P. & BOULTON, M. E. 2008. The angiopoietin/Tie-2 system regulates pericyte survival and recruitment in diabetic retinopathy. *Invest Ophthalmol Vis Sci,* 49, 2163-71.

CAO, R., BJORNDAHL, M. A., RELIGA, P., CLASPER, S., GARVIN, S., GALTER, D., MEISTER, B., IKOMI, F., TRITSARIS, K., DISSING, S., OHHASHI, T., JACKSON, D. G. & CAO, Y. 2004. PDGF-BB induces intratumoral lymphangiogenesis and promotes lymphatic metastasis. *Cancer Cell,* 6, 333-45.

CARIBONI, A., RAKIC, S., LIAPI, A., MAGGI, R., GOFFINET, A. & PARNAVELAS, J. G. 2005. Reelin provides an inhibitory signal in the migration of gonadotropin-releasing hormone neurons. *Development,* 132, 4709-18.

CARRAMOLINO, L., FUENTES, J., GARCIA-ANDRES, C., AZCOITIA, V., RIETHMACHER, D. & TORRES, M. 2010. Platelets play an essential role in separating the blood and lymphatic vasculatures during embryonic angiogenesis. *Circ Res,* 106, 1197-201.

CHAI, X., FORSTER, E., ZHAO, S., BOCK, H. H. & FROTSCHER, M. 2009. Reelin stabilizes the actin cytoskeleton of neuronal processes by inducing n-cofilin phosphorylation at serine3. *J Neurosci,* 29, 288-99.

CHEN, Y., BEFFERT, U., ERTUNC, M., TANG, T. S., KAVALALI, E. T., BEZPROZVANNY, I. & HERZ, J. 2005. Reelin modulates NMDA receptor activity in cortical neurons. *J Neurosci,* 25, 8209-16.

CLAVIN, N. W., AVRAHAM, T., FERNANDEZ, J., DALUVOY, S. V., SOARES, M. A., CHAUDHRY, A. & MEHRARA, B. J. 2008. TGF-beta1 is a negative regulator of lymphatic regeneration during wound repair. *Am J Physiol Heart Circ Physiol,* 295, H2113-27.

COSTELL, M., GUSTAFSSON, E., ASZODI, A., MORGELIN, M., BLOCH, W., HUNZIKER, E., ADDICKS, K., TIMPL, R. & FASSLER, R. 1999. Perlecan maintains the integrity of cartilage and some basement membranes. *J Cell Biol,* 147, 1109-22.

COURTES, S., VERNEREY, J., PUJADAS, L., MAGALON, K., CREMER, H., SORIANO, E., DURBEC, P. & CAYRE, M. 2011. Reelin controls progenitor cell migration in the healthy and pathological adult mouse brain. *PLoS One,* 6, e20430.

COX, T. R. & ERLER, J. T. 2011. Remodeling and homeostasis of the extracellular matrix: implications for fibrotic diseases and cancer. *Dis Model Mech,* 4, 165-78.

D'AMICO, G., KORHONEN, E. A., WALTARI, M., SAHARINEN, P., LAAKKONEN, P. & ALITALO, K. 2010. Loss of endothelial Tie1 receptor impairs lymphatic vessel development-brief report. *Arterioscler Thromb Vasc Biol,* 30, 207-9.

D'ARCANGELO, G., MIAO, G. G., CHEN, S. C., SOARES, H. D., MORGAN, J. I. & CURRAN, T. 1995. A protein related to extracellular matrix proteins deleted in the mouse mutant reeler. *Nature,* 374, 719-23.

DANUSSI, C., SPESSOTTO, P., PETRUCCO, A., WASSERMANN, B., SABATELLI, P., MONTESI, M., DOLIANA, R., BRESSAN, G. M. & COLOMBATTI, A. 2008. Emilin1 deficiency causes structural and functional defects of lymphatic vasculature. *Mol Cell Biol,* 28, 4026-39.

DAVIS, G. E. & SENGER, D. R. 2005. Endothelial extracellular matrix: biosynthesis, remodeling, and functions during vascular morphogenesis and neovessel stabilization. *Circ Res,* 97, 1093-107.

DAVIS, G. E. & SENGER, D. R. 2008. Extracellular matrix mediates a molecular balance between vascular morphogenesis and regression. *Curr Opin Hematol,* 15, 197-203.

DAVY, A. & SORIANO, P. 2007. Ephrin-B2 forward signaling regulates somite patterning and neural crest cell development. *Dev Biol,* 304, 182-93.

DE BERGEYCK, V., NAKAJIMA, K., LAMBERT DE ROUVROIT, C., NAERHUYZEN, B., GOFFINET, A. M., MIYATA, T., OGAWA, M. & MIKOSHIBA, K. 1997. A truncated Reelin protein is produced but not secreted in the 'Orleans' reeler mutation (Reln[rl-Orl]). *Brain Res Mol Brain Res,* 50, 85-90.

DELLINGER, M., HUNTER, R., BERNAS, M., GALE, N., YANCOPOULOS, G., ERICKSON, R. & WITTE, M. 2008. Defective remodeling and maturation of the lymphatic vasculature in Angiopoietin-2 deficient mice. *Dev Biol,* 319, 309-20.

DESHMANE, S. L., KREMLEV, S., AMINI, S. & SAWAYA, B. E. 2009. Monocyte chemoattractant protein-1 (MCP-1): an overview. *J Interferon Cytokine Res,* 29, 313-26.

DHAVAN, R. & TSAI, L. H. 2001. A decade of CDK5. *Nat Rev Mol Cell Biol,* 2, 749-59.

DIETRICH, T., ONDERKA, J., BOCK, F., KRUSE, F. E., VOSSMEYER, D., STRAGIES, R., ZAHN, G. & CURSIEFEN, C. 2007. Inhibition of inflammatory lymphangiogenesis by integrin alpha5 blockade. *Am J Pathol,* 171, 361-72.

DIXON, J. B., GREINER, S. T., GASHEV, A. A., COTE, G. L., MOORE, J. E. & ZAWIEJA, D. C. 2006. Lymph flow, shear stress, and lymphocyte velocity in rat mesenteric prenodal lymphatics. *Microcirculation,* 13, 597-610.

DUIT, S., MAYER, H., BLAKE, S. M., SCHNEIDER, W. J. & NIMPF, J. 2010. Differential functions of ApoER2 and very low density lipoprotein receptor in Reelin signaling depend on differential sorting of the receptors. *J Biol Chem,* 285, 4896-908.

DULABON, L., OLSON, E. C., TAGLIENTI, M. G., EISENHUTH, S., MCGRATH, B., WALSH, C. A., KREIDBERG, J. A. & ANTON, E. S. 2000. Reelin binds alpha3beta1 integrin and inhibits neuronal migration. *Neuron,* 27, 33-44.

DUMONT, D. J., JUSSILA, L., TAIPALE, J., LYMBOUSSAKI, A., MUSTONEN, T., PAJUSOLA, K., BREITMAN, M. & ALITALO, K. 1998. Cardiovascular failure in mouse embryos deficient in VEGF receptor-3. *Science,* 282, 946-9.

DUVEAU, V., MADHUSUDAN, A., CALEO, M., KNUESEL, I. & FRITSCHY, J. M. 2010. Impaired reelin processing and secretion by Cajal-Retzius cells contributes to granule cell dispersion in a mouse model of temporal lobe epilepsy. *Hippocampus*.

EILKEN, H. M. & ADAMS, R. H. 2010. Dynamics of endothelial cell behavior in sprouting angiogenesis. *Curr Opin Cell Biol,* 22, 617-25.

ENGE, M., BJARNEGARD, M., GERHARDT, H., GUSTAFSSON, E., KALEN, M., ASKER, N., HAMMES, H. P., SHANI, M., FASSLER, R. & BETSHOLTZ, C. 2002. Endothelium-specific platelet-derived growth factor-B ablation mimics diabetic retinopathy. *EMBO J,* 21, 4307-16.

ETCHEVERS, H. C., VINCENT, C., LE DOUARIN, N. M. & COULY, G. F. 2001. The cephalic neural crest provides pericytes and smooth muscle cells to all blood vessels of the face and forebrain. *Development,* 128, 1059-68.

FALCONER, D. 1951. Two new mutants, 'Trembler' and 'Reeler', with neurological actions in the house mouse (Mus Musculus L.). *J Genet,* 50, 192-201.

FANG, J., DAGENAIS, S. L., ERICKSON, R. P., ARLT, M. F., GLYNN, M. W., GORSKI, J. L., SEAVER, L. H. & GLOVER, T. W. 2000. Mutations in FOXC2 (MFH-1), a forkhead family transcription factor, are responsible for the hereditary lymphedema-distichiasis syndrome. *Am J Hum Genet,* 67, 1382-8.

FENG, L., ALLEN, N. S., SIMO, S. & COOPER, J. A. 2007. Cullin 5 regulates Dab1 protein levels and neuron positioning during cortical development. *Genes Dev,* 21, 2717-30.

FENG, Y., WANG, W., HU, J., MA, J., ZHANG, Y. & ZHANG, J. 2010. Expression of VEGF-C and VEGF-D as significant markers for assessment of lymphangiogenesis and lymph node metastasis in non-small cell lung cancer. *Anat Rec (Hoboken),* 293, 802-12.

FERRARA, N. 2010. Binding to the extracellular matrix and proteolytic processing: two key mechanisms regulating vascular endothelial growth factor action. *Mol Biol Cell,* 21, 687-90.

FERRELL, R. E., BATY, C. J., KIMAK, M. A., KARLSSON, J. M., LAWRENCE, E. C., FRANKE-SNYDER, M., MERINEY, S. D., FEINGOLD, E. & FINEGOLD, D. N. 2010. GJC2 missense mutations cause human lymphedema. *Am J Hum Genet,* 86, 943-8.

FIGUEROA, J. E., OUBRE, J. & VIJAYAGOPAL, P. 2004. Modulation of vascular smooth muscle cells proteoglycan synthesis by the extracellular matrix. *J Cell Physiol,* 198, 302-9.

FOO, S. S., TURNER, C. J., ADAMS, S., COMPAGNI, A., AUBYN, D., KOGATA, N., LINDBLOM, P., SHANI, M., ZICHA, D. & ADAMS, R. H. 2006. Ephrin-B2 controls cell motility and adhesion during blood-vessel-wall assembly. *Cell,* 124, 161-73.

FORSTER, E., BOCK, H. H., HERZ, J., CHAI, X., FROTSCHER, M. & ZHAO, S. 2010. Emerging topics in Reelin function. *Eur J Neurosci,* 31, 1511-8.

FORSTER, E., TIELSCH, A., SAUM, B., WEISS, K. H., JOHANSSEN, C., GRAUS-PORTA, D., MULLER, U. & FROTSCHER, M. 2002. Reelin, Disabled 1, and beta 1 integrins are required for the formation of the radial glial scaffold in the hippocampus. *Proc Natl Acad Sci U S A,* 99, 13178-83.

FRANCO, S. J., MARTINEZ-GARAY, I., GIL-SANZ, C., HARKINS-PERRY, S. R. & MULLER, U. 2011. Reelin regulates cadherin function via Dab1/Rap1 to control neuronal migration and lamination in the neocortex. *Neuron,* 69, 482-97.

FRANCOIS, M., CAPRINI, A., HOSKING, B., ORSENIGO, F., WILHELM, D., BROWNE, C., PAAVONEN, K., KARNEZIS, T., SHAYAN, R., DOWNES, M., DAVIDSON, T., TUTT, D., CHEAH, K. S., STACKER, S. A., MUSCAT, G. E., ACHEN, M. G., DEJANA, E. & KOOPMAN, P. 2008. Sox18 induces development of the lymphatic vasculature in mice. *Nature,* 456, 643-7.

FROTSCHER, M. 2010. Role for Reelin in stabilizing cortical architecture. *Trends Neurosci,* 33, 407-14.

FROTSCHER, M., CHAI, X., BOCK, H. H., HAAS, C. A., FORSTER, E. & ZHAO, S. 2009. Role of Reelin in the development and maintenance of cortical lamination. *J Neural Transm,* 116, 1451-5.

FRYKMAN, P. K., BROWN, M. S., YAMAMOTO, T., GOLDSTEIN, J. L. & HERZ, J. 1995. Normal plasma lipoproteins and fertility in gene-targeted mice homozygous for a disruption in the gene encoding very low density lipoprotein receptor. *Proc Natl Acad Sci U S A,* 92, 8453-7.

FUXE, J., TABRUYN, S., COLTON, K., ZAID, H., ADAMS, A., BALUK, P., LASHNITS, E., MORISADA, T., LE, T., O'BRIEN, S., EPSTEIN, D. M., KOH, G. Y. & MCDONALD, D. M. 2011. Pericyte requirement for anti-leak action of angiopoietin-1 and vascular remodeling in sustained inflammation. *Am J Pathol,* 178, 2897-909.

GAENGEL, K., GENOVE, G., ARMULIK, A. & BETSHOLTZ, C. 2009. Endothelial-mural cell signaling in vascular development and angiogenesis. *Arterioscler Thromb Vasc Biol,* 29, 630-8.

GALE, N. W., PREVO, R., ESPINOSA, J., FERGUSON, D. J., DOMINGUEZ, M. G., YANCOPOULOS, G. D., THURSTON, G. & JACKSON, D. G. 2007. Normal lymphatic development and function in mice deficient for the lymphatic hyaluronan receptor LYVE-1. *Mol Cell Biol,* 27, 595-604.

GALE, N. W., THURSTON, G., HACKETT, S. F., RENARD, R., WANG, Q., MCCLAIN, J., MARTIN, C., WITTE, C., WITTE, M. H., JACKSON, D., SURI, C., CAMPOCHIARO, P. A., WIEGAND, S. J. & YANCOPOULOS, G. D. 2002. Angiopoietin-2 is required for postnatal angiogenesis and lymphatic patterning, and only the latter role is rescued by Angiopoietin-1. *Dev Cell,* 3, 411-23.

GARMY-SUSINI, B., AVRAAMIDES, C. J., SCHMID, M. C., FOUBERT, P., ELLIES, L. G., BARNES, L., FERAL, C., PAPAYANNOPOULOU, T., LOWY, A., BLAIR, S. L., CHERESH, D., GINSBERG, M. & VARNER, J. A. 2010. Integrin alpha4beta1 signaling is required for lymphangiogenesis and tumor metastasis. *Cancer Res,* 70, 3042-51.

GASHEV, A. A., DAVIS, M. J., DELP, M. D. & ZAWIEJA, D. C. 2004. Regional variations of contractile activity in isolated rat lymphatics. *Microcirculation,* 11, 477-92.

GASHEV, A. A., DAVIS, M. J. & ZAWIEJA, D. C. 2002. Inhibition of the active lymph pump by flow in rat mesenteric lymphatics and thoracic duct. *J Physiol,* 540, 1023-37.

GENTLEMAN, R. C., CAREY, V. J., BATES, D. M., BOLSTAD, B., DETTLING, M., DUDOIT, S., ELLIS, B., GAUTIER, L., Ge, Y., GENTRY, J et al., 2004. Bioconductor: open software development for computational biology and bioinformatics. *Genome Biol,* 5, R80.

GEORGE, E. L., GEORGES-LABOUESSE, E. N., PATEL-KING, R. S., RAYBURN, H. & HYNES, R. O. 1993. Defects in mesoderm, neural tube and vascular development in mouse embryos lacking fibronectin. *Development,* 119, 1079-91.

GERHARDT, H. & BETSHOLTZ, C. 2003. Endothelial-pericyte interactions in angiogenesis. *Cell Tissue Res,* 314, 15-23.

GIAMPIERI, S., MANNING, C., HOOPER, S., JONES, L., HILL, C. S. & SAHAI, E. 2009. Localized and reversible TGFbeta signalling switches breast cancer cells from cohesive to single cell motility. *Nat Cell Biol,* 11, 1287-96.

GORDON, E. J., RAO, S., POLLARD, J. W., NUTT, S. L., LANG, R. A. & HARVEY, N. L. 2010. Macrophages define dermal lymphatic vessel calibre during development by regulating lymphatic endothelial cell proliferation. *Development,* 137, 3899-910.

GOTSCH, U., BORGES, E., BOSSE, R., BOGGEMEYER, E., SIMON, M., MOSSMANN, H. & VESTWEBER, D. 1997. VE-cadherin antibody accelerates neutrophil recruitment in vivo. *J Cell Sci,* 110 (Pt 5), 583-8.

GOYAL, A., PAL, N., CONCANNON, M., PAUL, M., DORAN, M., POLUZZI, C., SEKIGUCHI, K., WHITELOCK, J. M., NEILL, T. & IOZZO, R. V. 2011. Endorepellin, perlecan angiostatic module, interacts with both the [alpha]2[beta]1 integrin and VEGFreceptor 2: A dual receptor antagonism. *J Biol Chem*.

GRIFFITH, L. G. & SWARTZ, M. A. 2006. Capturing complex 3D tissue physiology in vitro. *Nat Rev Mol Cell Biol,* 7, 211-24.

GRUNWALD, I. C., KORTE, M., ADELMANN, G., PLUECK, A., KULLANDER, K., ADAMS, R. H., FROTSCHER, M., BONHOEFFER, T. & KLEIN, R. 2004. Hippocampal plasticity requires postsynaptic ephrinBs. *Nat Neurosci,* 7, 33-40.

HACK, I., BANCILA, M., LOULIER, K., CARROLL, P. & CREMER, H. 2002. Reelin is a detachment signal in tangential chain-migration during postnatal neurogenesis. *Nat Neurosci,* 5, 939-45.

HACK, I., HELLWIG, S., JUNGHANS, D., BRUNNE, B., BOCK, H. H., ZHAO, S. & FROTSCHER, M. 2007. Divergent roles of ApoER2 and Vldlr in the migration of cortical neurons. *Development,* 134, 3883-91.

HAIKO, P., MAKINEN, T., KESKITALO, S., TAIPALE, J., KARKKAINEN, M. J., BALDWIN, M. E., STACKER, S. A., ACHEN, M. G. & ALITALO, K. 2008. Deletion of vascular endothelial growth factor C (VEGF-C) and VEGF-D is not equivalent to VEGF receptor 3 deletion in mouse embryos. *Mol Cell Biol,* 28, 4843-50.

HALIN, C., FAHRNGRUBER, H., MEINGASSNER, J. G., BOLD, G., LITTLEWOOD-EVANS, A., STUETZ, A. & DETMAR, M. 2008. Inhibition of chronic and acute skin inflammation by treatment with a vascular endothelial growth factor receptor tyrosine kinase inhibitor. *Am J Pathol,* 173, 265-77.

HANSMANN, G., DE JESUS PEREZ, V. A., ALASTALO, T. P., ALVIRA, C. M., GUIGNABERT, C., BEKKER, J. M., SCHELLONG, S., URASHIMA, T., WANG, L., MORRELL, N. W. & RABINOVITCH, M. 2008. An antiproliferative BMP-2/PPARgamma/apoE axis in human and murine SMCs and its role in pulmonary hypertension. *J Clin Invest,* 118, 1846-57.

HARKNESS, K. A., SUSSMAN, J. D., DAVIES-JONES, G. A., GREENWOOD, J. & WOODROOFE, M. N. 2003. Cytokine regulation of MCP-1 expression in brain and retinal microvascular endothelial cells. *J Neuroimmunol,* 142, 1-9.

HARTFUSS, E., FORSTER, E., BOCK, H. H., HACK, M. A., LEPRINCE, P., LUQUE, J. M., HERZ, J., FROTSCHER, M. & GOTZ, M. 2003. Reelin signaling directly affects radial glia morphology and biochemical maturation. *Development,* 130, 4597-609.

HARVEY, N. L., SRINIVASAN, R. S., DILLARD, M. E., JOHNSON, N. C., WITTE, M. H., BOYD, K., SLEEMAN, M. W. & OLIVER, G. 2005. Lymphatic vascular

defects promoted by Prox1 haploinsufficiency cause adult-onset obesity. *Nat Genet,* 37, 1072-81.

HE, Y., KOZAKI, K., KARPANEN, T., KOSHIKAWA, K., YLA-HERTTUALA, S., TAKAHASHI, T. & ALITALO, K. 2002. Suppression of tumor lymphangiogenesis and lymph node metastasis by blocking vascular endothelial growth factor receptor 3 signaling. *J Natl Cancer Inst,* 94, 819-25.

HE, Y., RAJANTIE, I., ILMONEN, M., MAKINEN, T., KARKKAINEN, M. J., HAIKO, P., SALVEN, P. & ALITALO, K. 2004. Preexisting lymphatic endothelium but not endothelial progenitor cells are essential for tumor lymphangiogenesis and lymphatic metastasis. *Cancer Res,* 64, 3737-40.

HECKMAN, C. A., HOLOPAINEN, T., WIRZENIUS, M., KESKITALO, S., JELTSCH, M., YLA-HERTTUALA, S., WEDGE, S. R., JURGENSMEIER, J. M. & ALITALO, K. 2008. The tyrosine kinase inhibitor cediranib blocks ligand-induced vascular endothelial growth factor receptor-3 activity and lymphangiogenesis. *Cancer Res,* 68, 4754-62.

HEINRICH, C., NITTA, N., FLUBACHER, A., MULLER, M., FAHRNER, A., KIRSCH, M., FREIMAN, T., SUZUKI, F., DEPAULIS, A., FROTSCHER, M. & HAAS, C. A. 2006. Reelin deficiency and displacement of mature neurons, but not neurogenesis, underlie the formation of granule cell dispersion in the epileptic hippocampus. *J Neurosci,* 26, 4701-13.

HELLSTROM, M., GERHARDT, H., KALEN, M., LI, X., ERIKSSON, U., WOLBURG, H. & BETSHOLTZ, C. 2001. Lack of pericytes leads to endothelial hyperplasia and abnormal vascular morphogenesis. *J Cell Biol,* 153, 543-53.

HELLSTROM, M., KALEN, M., LINDAHL, P., ABRAMSSON, A. & BETSHOLTZ, C. 1999. Role of PDGF-B and PDGFR-beta in recruitment of vascular smooth muscle cells and pericytes during embryonic blood vessel formation in the mouse. *Development,* 126, 3047-55.

HERZ, J. & CHEN, Y. 2006. Reelin, lipoprotein receptors and synaptic plasticity. *Nat Rev Neurosci,* 7, 850-9.

HIESBERGER, T., TROMMSDORFF, M., HOWELL, B. W., GOFFINET, A., MUMBY, M. C., COOPER, J. A. & HERZ, J. 1999. Direct binding of Reelin to VLDL receptor and ApoE receptor 2 induces tyrosine phosphorylation of disabled-1 and modulates tau phosphorylation. *Neuron,* 24, 481-9.

HIRAKAWA, S., BROWN, L. F., KODAMA, S., PAAVONEN, K., ALITALO, K. & DETMAR, M. 2007. VEGF-C-induced lymphangiogenesis in sentinel lymph nodes promotes tumor metastasis to distant sites. *Blood,* 109, 1010-7.

HIRSCHI, K. K., ROHOVSKY, S. A. & D'AMORE, P. A. 1998. PDGF, TGF-beta, and heterotypic cell-cell interactions mediate endothelial cell-induced recruitment of 10T1/2 cells and their differentiation to a smooth muscle fate. *J Cell Biol,* 141, 805-14.

HOGAN, B. M., BOS, F. L., BUSSMANN, J., WITTE, M., CHI, N. C., DUCKERS, H. J. & SCHULTE-MERKER, S. 2009. Ccbe1 is required for embryonic lymphangiogenesis and venous sprouting. *Nat Genet,* 41, 396-8.

HONG, S. E., SHUGART, Y. Y., HUANG, D. T., SHAHWAN, S. A., GRANT, P. E., HOURIHANE, J. O., MARTIN, N. D. & WALSH, C. A. 2000. Autosomal recessive lissencephaly with cerebellar hypoplasia is associated with human RELN mutations. *Nat Genet,* 26, 93-6.

HOUCK, K. A., LEUNG, D. W., ROWLAND, A. M., WINER, J. & FERRARA, N. 1992. Dual regulation of vascular endothelial growth factor bioavailability by genetic and proteolytic mechanisms. *J Biol Chem,* 267, 26031-7.

HOWELL, B. W., HAWKES, R., SORIANO, P. & COOPER, J. A. 1997. Neuronal position in the developing brain is regulated by mouse disabled-1. *Nature,* 389, 733-7.

HOWELL, B. W., HERRICK, T. M. & COOPER, J. A. 1999. Reelin-induced tyrosine [corrected] phosphorylation of disabled 1 during neuronal positioning. *Genes Dev,* 13, 643-8.

HOWELL, B. W., HERRICK, T. M., HILDEBRAND, J. D., ZHANG, Y. & COOPER, J. A. 2000. Dab1 tyrosine phosphorylation sites relay positional signals during mouse brain development. *Curr Biol,* 10, 877-85.

HUANG, S. S., LIU, I. H., SMITH, T., SHAH, M. R., JOHNSON, F. E. & HUANG, J. S. 2006. CRSBP-1/LYVE-l-null mice exhibit identifiable morphological and functional alterations of lymphatic capillary vessels. *FEBS Lett,* 580, 6259-68.

HUANG, X. Z., WU, J. F., FERRANDO, R., LEE, J. H., WANG, Y. L., FARESE, R. V., JR. & SHEPPARD, D. 2000. Fatal bilateral chylothorax in mice lacking the integrin alpha9beta1. *Mol Cell Biol,* 20, 5208-15.

HUGHES, S. & CHAN-LING, T. 2004. Characterization of smooth muscle cell and pericyte differentiation in the rat retina in vivo. *Invest Ophthalmol Vis Sci,* 45, 2795-806.

HUNTINGTON, G. S. & MCCLURE, C. F. 1910. The anatomy and development of the jugular lymph sacs in the domestic cat *(Felis domestica). Am J Anat,* 10, 177-311.

HYNES, R. O. 2009. The extracellular matrix: not just pretty fibrils. *Science,* 326, 1216-9.

INAI, T., MANCUSO, M., HASHIZUME, H., BAFFERT, F., HASKELL, A., BALUK, P., HU-LOWE, D. D., SHALINSKY, D. R., THURSTON, G., YANCOPOULOS, G.

D. & MCDONALD, D. M. 2004. Inhibition of vascular endothelial growth factor (VEGF) signaling in cancer causes loss of endothelial fenestrations, regression of tumor vessels, and appearance of basement membrane ghosts. *Am J Pathol,* 165, 35-52.

IRIZARRY, R. A., BOLSTAD, B. M., COLLIN, F., COPE, L. M., HOBBS, B. & SPEED, T. P. 2003. Summaries of Affymetrix GeneChip probe level data. *Nucleic Acids Res,* 31, e15.

IRRTHUM, A., DEVRIENDT, K., CHITAYAT, D., MATTHIJS, G., GLADE, C., STEIJLEN, P. M., FRYNS, J. P., VAN STEENSEL, M. A. & VIKKULA, M. 2003. Mutations in the transcription factor gene SOX18 underlie recessive and dominant forms of hypotrichosis-lymphedema-telangiectasia. *Am J Hum Genet,* 72, 1470-8.

ISSA, A., LE, T. X., SHOUSHTARI, A. N., SHIELDS, J. D. & SWARTZ, M. A. 2009. Vascular endothelial growth factor-C and C-C chemokine receptor 7 in tumor cell-lymphatic cross-talk promote invasive phenotype. *Cancer Res,* 69, 349-57.

JAY, S. M., SHEPHERD, B. R., ANDREJECSK, J. W., KYRIAKIDES, T. R., POBER, J. S. & SALTZMAN, W. M. 2010. Dual delivery of VEGF and MCP-1 to support endothelial cell transplantation for therapeutic vascularization. *Biomaterials,* 31, 3054-62.

JEANSSON, M., GAWLIK, A., ANDERSON, G., LI, C., KERJASCHKI, D., HENKELMAN, M. & QUAGGIN, S. E. 2011. Angiopoietin-1 is essential in mouse vasculature during development and in response to injury. *J Clin Invest,* 121, 2278-89.

JI, R. C. 2006. Lymphatic endothelial cells, lymphangiogenesis, and extracellular matrix. *Lymphat Res Biol,* 4, 83-100.

JOSSIN, Y., GUI, L. & GOFFINET, A. M. 2007. Processing of Reelin by embryonic neurons is important for function in tissue but not in dissociated cultured neurons. *J Neurosci,* 27, 4243-52.

JOSSIN, Y., IGNATOVA, N., HIESBERGER, T., HERZ, J., LAMBERT DE ROUVROIT, C. & GOFFINET, A. M. 2004. The central fragment of Reelin, generated by proteolytic processing in vivo, is critical to its function during cortical plate development. *J Neurosci,* 24, 514-21.

JURISIC, G. & DETMAR, M. 2009. Lymphatic endothelium in health and disease. *Cell Tissue Res,* 335, 97-108.

KAIPAINEN, A., KORHONEN, J., MUSTONEN, T., VAN HINSBERGH, V. W., FANG, G. H., DUMONT, D., BREITMAN, M. & ALITALO, K. 1995. Expression of the fms-like tyrosine kinase 4 gene becomes restricted to lymphatic endothelium during development. *Proc Natl Acad Sci U S A,* 92, 3566-70.

KALLURI, R. 2003. Basement membranes: structure, assembly and role in tumour angiogenesis. *Nat Rev Cancer,* 3, 422-33.

KANADY, J. D., DELLINGER, M. T., MUNGER, S. J., WITTE, M. H. & SIMON, A. M. 2011. Connexin37 and Connexin43 deficiencies in mice disrupt lymphatic valve development and result in lymphatic disorders including lymphedema and chylothorax. *Dev Biol,* 354, 253-66.

KARKKAINEN, M. J., FERRELL, R. E., LAWRENCE, E. C., KIMAK, M. A., LEVINSON, K. L., MCTIGUE, M. A., ALITALO, K. & FINEGOLD, D. N. 2000. Missense mutations interfere with VEGFR-3 signalling in primary lymphoedema. *Nat Genet,* 25, 153-9.

KARKKAINEN, M. J., HAIKO, P., SAINIO, K., PARTANEN, J., TAIPALE, J., PETROVA, T. V., JELTSCH, M., JACKSON, D. G., TALIKKA, M., RAUVALA, H., BETSHOLTZ, C. & ALITALO, K. 2004. Vascular endothelial growth factor C is required for sprouting of the first lymphatic vessels from embryonic veins. *Nat Immunol,* 5, 74-80.

KARKKAINEN, M. J., SAARISTO, A., JUSSILA, L., KARILA, K. A., LAWRENCE, E. C., PAJUSOLA, K., BUELER, H., EICHMANN, A., KAUPPINEN, R., KETTUNEN, M. I., YLA-HERTTUALA, S., FINEGOLD, D. N., FERRELL, R. E. & ALITALO, K. 2001. A model for gene therapy of human hereditary lymphedema. *Proc Natl Acad Sci U S A,* 98, 12677-82.

KARPANEN, T., EGEBLAD, M., KARKKAINEN, M. J., KUBO, H., YLA-HERTTUALA, S., JAATTELA, M. & ALITALO, K. 2001. Vascular endothelial growth factor C promotes tumor lymphangiogenesis and intralymphatic tumor growth. *Cancer Res,* 61, 1786-90.

KARPANEN, T., HECKMAN, C. A., KESKITALO, S., JELTSCH, M., OLLILA, H., NEUFELD, G., TAMAGNONE, L. & ALITALO, K. 2006a. Functional interaction of VEGF-C and VEGF-D with neuropilin receptors. *FASEB J,* 20, 1462-72.

KARPANEN, T. & MAKINEN, T. 2006. Regulation of lymphangiogenesis--from cell fate determination to vessel remodeling. *Exp Cell Res,* 312, 575-83.

KARPANEN, T., WIRZENIUS, M., MAKINEN, T., VEIKKOLA, T., HAISMA, H. J., ACHEN, M. G., STACKER, S. A., PYTOWSKI, B., YLA-HERTTUALA, S. & ALITALO, K. 2006b. Lymphangiogenic growth factor responsiveness is modulated by postnatal lymphatic vessel maturation. *Am J Pathol,* 169, 708-18.

KERJASCHKI, D., HUTTARY, N., RAAB, I., REGELE, H., BOJARSKI-NAGY, K., BARTEL, G., KROBER, S. M., GREINIX, H., ROSENMAIER, A., KARLHOFER, F., WICK, N. & MAZAL, P. R. 2006. Lymphatic endothelial progenitor cells contribute to de novo lymphangiogenesis in human renal transplants. *Nat Med,* 12, 230-4.

KERJASCHKI, D., REGELE, H. M., MOOSBERGER, I., NAGY-BOJARSKI, K., WATSCHINGER, B., SOLEIMAN, A., BIRNER, P., KRIEGER, S., HOVORKA, A., SILBERHUMER, G., LAAKKONEN, P., PETROVA, T., LANGER, B. & RAAB, I.

2004. Lymphatic neoangiogenesis in human kidney transplants is associated with immunologically active lymphocytic infiltrates. *J Am Soc Nephrol,* 15, 603-12.

KHIALEEVA, E., LANE, T. F. & CARPENTER, E. M. 2011. Disruption of reelin signaling alters mammary gland morphogenesis. *Development,* 138, 767-76.

KOHNO, S., KOHNO, T., NAKANO, Y., SUZUKI, K., ISHII, M., TAGAMI, H., BABA, A. & HATTORI, M. 2009a. Mechanism and significance of specific proteolytic cleavage of Reelin. *Biochem Biophys Res Commun,* 380, 93-7.

KOHNO, T., NAKANO, Y., KITOH, N., YAGI, H., KATO, K., BABA, A. & HATTORI, M. 2009b. C-terminal region-dependent change of antibody-binding to the Eighth Reelin repeat reflects the signaling activity of Reelin. *J Neurosci Res,* 87, 3043-53.

KOJIMA, T., AZAR, D. T. & CHANG, J. H. 2008. Neostatin-7 regulates bFGF-induced corneal lymphangiogenesis. *FEBS Lett,* 582, 2515-20.

KRUEGEL, J., MIOSGE, N. 2010. Basement membrane components are key players in specialized extracellular matrices. *Cell Mol Life Sci*, 67, 2879-95.

LAHDENRANTA, J., HAGENDOORN, J., PADERA, T. P., HOSHIDA, T., NELSON, G., KASHIWAGI, S., JAIN, R. K. & FUKUMURA, D. 2009. Endothelial nitric oxide synthase mediates lymphangiogenesis and lymphatic metastasis. *Cancer Res,* 69, 2801-8.

LAMBERT DE ROUVROIT, C., DE BERGEYCK, V., CORTVRINDT, C., BAR, I., EECKHOUT, Y. & GOFFINET, A. M. 1999. Reelin, the extracellular matrix protein deficient in reeler mutant mice, is processed by a metalloproteinase. *Exp Neurol,* 156, 214-7.

LEE, J. Y., PARK, C., CHO, Y. P., LEE, E., KIM, H., KIM, P., YUN, S. H. & YOON, Y. S. 2010. Podoplanin-expressing cells derived from bone marrow play a crucial role in postnatal lymphatic neovascularization. *Circulation,* 122, 1413-25.

LEE, S., JILANI, S. M., NIKOLOVA, G. V., CARPIZO, D. & IRUELA-ARISPE, M. L. 2005. Processing of VEGF-A by matrix metalloproteinases regulates bioavailability and vascular patterning in tumors. *J Cell Biol,* 169, 681-91.

LEVICK, J. R. & MICHEL, C. C. 2010. Microvascular fluid exchange and the revised Starling principle. *Cardiovasc Res,* 87, 198-210.

LIM, H. Y., RUTKOWSKI, J. M., HELFT, J., REDDY, S. T., SWARTZ, M. A., RANDOLPH, G. J. & ANGELI, V. 2009. Hypercholesterolemic mice exhibit lymphatic vessel dysfunction and degeneration. *Am J Pathol,* 175, 1328-37.

LIN, F. J., CHEN, X., QIN, J., HONG, Y. K., TSAI, M. J. & TSAI, S. Y. 2010. Direct transcriptional regulation of neuropilin-2 by COUP-TFII modulates multiple steps in murine lymphatic vessel development. *J Clin Invest,* 120, 1694-707.

LINDAHL, P., JOHANSSON, B. R., LEVEEN, P. & BETSHOLTZ, C. 1997. Pericyte loss and microaneurysm formation in PDGF-B-deficient mice. *Science,* 277, 242-5.

LIU, B., MA, J., WANG, X., SU, F., LI, X., YANG, S., MA, W. & ZHANG, Y. 2008. Lymphangiogenesis and its relationship with lymphatic metastasis and prognosis in malignant melanoma. *Anat Rec (Hoboken),* 291, 1227-35.

LO, I. C., SHIH, J. M. & JIANG, M. J. 2005. Reactive oxygen species and ERK 1/2 mediate monocyte chemotactic protein-1-stimulated smooth muscle cell migration. *J Biomed Sci,* 12, 377-88.

LU, B., RUTLEDGE, B. J., GU, L., FIORILLO, J., LUKACS, N. W., KUNKEL, S. L., NORTH, R., GERARD, C. & ROLLINS, B. J. 1998. Abnormalities in monocyte recruitment and cytokine expression in monocyte chemoattractant protein 1-deficient mice. *J Exp Med,* 187, 601-8.

MA, J., WANG, Q., FEI, T., HAN, J. D. & CHEN, Y. G. 2007. MCP-1 mediates TGF-beta-induced angiogenesis by stimulating vascular smooth muscle cell migration. *Blood,* 109, 987-94.

MACHNIK, A., NEUHOFER, W., JANTSCH, J., DAHLMANN, A., TAMMELA, T., MACHURA, K., PARK, J. K., BECK, F. X., MULLER, D. N., DERER, W., GOSS, J., ZIOMBER, A., DIETSCH, P., WAGNER, H., VAN ROOIJEN, N., KURTZ, A., HILGERS, K. F., ALITALO, K., ECKARDT, K. U., LUFT, F. C., KERJASCHKI, D. & TITZE, J. 2009. Macrophages regulate salt-dependent volume and blood pressure by a vascular endothelial growth factor-C-dependent buffering mechanism. *Nat Med,* 15, 545-52.

MAGDALENO, S., KESHVARA, L. & CURRAN, T. 2002. Rescue of ataxia and preplate splitting by ectopic expression of Reelin in reeler mice. *Neuron,* 33, 573-86.

MAJESKY, M. W. 2007. Developmental basis of vascular smooth muscle diversity. *Arterioscler Thromb Vasc Biol,* 27, 1248-58.

MAJESKY, M. W., DONG, X. R., REGAN, J. N. & HOGLUND, V. J. 2011. Vascular smooth muscle progenitor cells: building and repairing blood vessels. *Circ Res,* 108, 365-77.

MAKINEN, T., ADAMS, R. H., BAILEY, J., LU, Q., ZIEMIECKI, A., ALITALO, K., KLEIN, R. & WILKINSON, G. A. 2005. PDZ interaction site in ephrinB2 is required for the remodeling of lymphatic vasculature. *Genes Dev,* 19, 397-410.

MAKINEN, T., JUSSILA, L., VEIKKOLA, T., KARPANEN, T., KETTUNEN, M. I., PULKKANEN, K. J., KAUPPINEN, R., JACKSON, D. G., KUBO, H., NISHIKAWA,

S., YLA-HERTTUALA, S. & ALITALO, K. 2001a. Inhibition of lymphangiogenesis with resulting lymphedema in transgenic mice expressing soluble VEGF receptor-3. *Nat Med,* 7, 199-205.

MAKINEN, T., NORRMEN, C. & PETROVA, T. V. 2007. Molecular mechanisms of lymphatic vascular development. *Cell Mol Life Sci,* 64, 1915-29.

MAKINEN, T., VEIKKOLA, T., MUSTJOKI, S., KARPANEN, T., CATIMEL, B., NICE, E. C., WISE, L., MERCER, A., KOWALSKI, H., KERJASCHKI, D., STACKER, S. A., ACHEN, M. G. & ALITALO, K. 2001b. Isolated lymphatic endothelial cells transduce growth, survival and migratory signals via the VEGF-C/D receptor VEGFR-3. *EMBO J,* 20, 4762-73.

MANDRIOTA, S. J., JUSSILA, L., JELTSCH, M., COMPAGNI, A., BAETENS, D., PREVO, R., BANERJI, S., HUARTE, J., MONTESANO, R., JACKSON, D. G., ORCI, L., ALITALO, K., CHRISTOFORI, G. & PEPPER, M. S. 2001. Vascular endothelial growth factor-C-mediated lymphangiogenesis promotes tumour metastasis. *EMBO J,* 20, 672-82.

MARUYAMA, K., II, M., CURSIEFEN, C., JACKSON, D. G., KEINO, H., TOMITA, M., VAN ROOIJEN, N., TAKENAKA, H., D'AMORE, P. A., STEIN-STREILEIN, J., LOSORDO, D. W. & STREILEIN, J. W. 2005. Inflammation-induced lymphangiogenesis in the cornea arises from CD11b-positive macrophages. *J Clin Invest,* 115, 2363-72.

MCCLOSKEY, K. D., HOLLYWOOD, M. A., THORNBURY, K. D., WARD, S. M. & MCHALE, N. G. 2002. Kit-like immunopositive cells in sheep mesenteric lymphatic vessels. *Cell Tissue Res,* 310, 77-84.

MELLOR, R. H., HUBERT, C. E., STANTON, A. W., TATE, N., AKHRAS, V., SMITH, A., BURNAND, K. G., JEFFERY, S., MAKINEN, T., LEVICK, J. R. & MORTIMER, P. S. 2010. Lymphatic dysfunction, not aplasia, underlies Milroy disease. *Microcirculation,* 17, 281-96.

MELLOR, R. H., TATE, N., STANTON, A. W., HUBERT, C., MAKINEN, T., SMITH, A., BURNAND, K. G., JEFFERY, S., LEVICK, J. R. & MORTIMER, P. S. 2011. Mutations in FOXC2 in Humans (Lymphoedema Distichiasis Syndrome) Cause Lymphatic Dysfunction on Dependency. *J Vasc Res,* 48, 397-407.

MILLETTE, E., RAUCH, B. H., DEFAWE, O., KENAGY, R. D., DAUM, G. & CLOWES, A. W. 2005. Platelet-derived growth factor-BB-induced human smooth muscle cell proliferation depends on basic FGF release and FGFR-1 activation. *Circ Res,* 96, 172-9.

MINER, J. H., CUNNINGHAM, J. & SANES, J. R. 1998. Roles for laminin in embryogenesis: exencephaly, syndactyly, and placentopathy in mice lacking the laminin alpha5 chain. *J Cell Biol,* 143, 1713-23.

MINER, J. H., LI, C., MUDD, J. L., GO, G. & SUTHERLAND, A. E. 2004. Compositional and structural requirements for laminin and basement membranes during mouse embryo implantation and gastrulation. *Development,* 131, 2247-56.

MISHIMA, K., WATABE, T., SAITO, A., YOSHIMATSU, Y., IMAIZUMI, N., MASUI, S., HIRASHIMA, M., MORISADA, T., OIKE, Y., ARAIE, M., NIWA, H., KUBO, H., SUDA, T. & MIYAZONO, K. 2007. Prox1 induces lymphatic endothelial differentiation via integrin alpha9 and other signaling cascades. *Mol Biol Cell,* 18, 1421-9.

MITEVA, D. O., RUTKOWSKI, J. M., DIXON, J. B., KILARSKI, W., SHIELDS, J. D. & SWARTZ, M. A. 2010. Transmural flow modulates cell and fluid transport functions of lymphatic endothelium. *Circ Res,* 106, 920-31.

MONGIAT, M., SWEENEY, S. M., SAN ANTONIO, J. D., FU, J. & IOZZO, R. V. 2003. Endorepellin, a novel inhibitor of angiogenesis derived from the C terminus of perlecan. *J Biol Chem,* 278, 4238-49.

MULLER, M. C., OSSWALD, M., TINNES, S., HAUSSLER, U., JACOBI, A., FORSTER, E., FROTSCHER, M. & HAAS, C. A. 2009. Exogenous reelin prevents granule cell dispersion in experimental epilepsy. *Exp Neurol,* 216, 390-7.

MUTHUCHAMY, M., GASHEV, A., BOSWELL, N., DAWSON, N. & ZAWIEJA, D. 2003. Molecular and functional analyses of the contractile apparatus in lymphatic muscle. *FASEB J,* 17, 920-2.

MUTHUCHAMY, M. & ZAWIEJA, D. 2008. Molecular regulation of lymphatic contractility. *Ann N Y Acad Sci,* 1131, 89-99.

MUZUMDAR, M. D., TASIC, B., MIYAMICHI, K., LI, L. & LUO, L. 2007. A global double-fluorescent Cre reporter mouse. *Genesis,* 45, 593-605.

NAKANO, Y., KOHNO, T., HIBI, T., KOHNO, S., BABA, A., MIKOSHIBA, K., NAKAJIMA, K. & HATTORI, M. 2007. The extremely conserved C-terminal region of Reelin is not necessary for secretion but is required for efficient activation of downstream signaling. *J Biol Chem,* 282, 20544-52.

NOMIYAMA, T., NAKAMACHI, T., GIZARD, F., HEYWOOD, E. B., JONES, K. L., OHKURA, N., KAWAMORI, R., CONNEELY, O. M. & BRUEMMER, D. 2006. The NR4A orphan nuclear receptor NOR1 is induced by platelet-derived growth factor and mediates vascular smooth muscle cell proliferation. *J Biol Chem,* 281, 33467-76.

NORRMEN, C., IVANOV, K. I., CHENG, J., ZANGGER, N., DELORENZI, M., JAQUET, M., MIURA, N., PUOLAKKAINEN, P., HORSLEY, V., HU, J., AUGUSTIN, H. G., YLA-HERTTUALA, S., ALITALO, K. & PETROVA, T. V. 2009. FOXC2 controls formation and maturation of lymphatic collecting vessels through cooperation with NFATc1. *J Cell Biol,* 185, 439-57.

NORRMEN, C., TAMMELA, T., PETROVA, T. V. & ALITALO, K. 2011. Biological basis of therapeutic lymphangiogenesis. *Circulation,* 123, 1335-51.

NY, A., KOCH, M., SCHNEIDER, M., NEVEN, E., TONG, R. T., MAITY, S., FISCHER, C., PLAISANCE, S., LAMBRECHTS, D., HELIGON, C., TERCLAVERS, S., CIESIOLKA, M., KALIN, R., MAN, W. Y., SENN, I., WYNS, S., LUPU, F., BRANDLI, A., VLEMINCKX, K., COLLEN, D., DEWERCHIN, M., CONWAY, E. M., MOONS, L., JAIN, R. K. & CARMELIET, P. 2005. A genetic Xenopus laevis tadpole model to study lymphangiogenesis. *Nat Med,* 11, 998-1004.

OGAWA, M., MIYATA, T., NAKAJIMA, K., YAGYU, K., SEIKE, M., IKENAKA, K., YAMAMOTO, H. & MIKOSHIBA, K. 1995. The reeler gene-associated antigen on Cajal-Retzius neurons is a crucial molecule for laminar organization of cortical neurons. *Neuron,* 14, 899-912.

OHL, L., MOHAUPT, M., CZELOTH, N., HINTZEN, G., KIAFARD, Z., ZWIRNER, J., BLANKENSTEIN, T., HENNING, G. & FORSTER, R. 2004. CCR7 governs skin dendritic cell migration under inflammatory and steady-state conditions. *Immunity,* 21, 279-88.

OHTANI, Y. & OHTANI, O. 2001. Postnatal development of lymphatic vessels and their smooth muscle cells in the rat diaphragm: a confocal microscopic study. *Arch Histol Cytol,* 64, 513-22.

OLSON, E. C., KIM, S. & WALSH, C. A. 2006. Impaired neuronal positioning and dendritogenesis in the neocortex after cell-autonomous Dab1 suppression. *J Neurosci,* 26, 1767-75.

OU, J. J., WU, F. & LIANG, H. J. 2010. Colorectal tumor derived fibronectin alternatively spliced EDA domain exserts lymphangiogenic effect on human lymphatic endothelial cells. *Cancer Biol Ther,* 9, 186-91.

PADERA, T. P., KUO, A. H., HOSHIDA, T., LIAO, S., LOBO, J., KOZAK, K. R., FUKUMURA, D. & JAIN, R. K. 2008. Differential response of primary tumor versus lymphatic metastasis to VEGFR-2 and VEGFR-3 kinase inhibitors cediranib and vandetanib. *Mol Cancer Ther,* 7, 2272-9.

PARK, T. J. & CURRAN, T. 2008. Crk and Crk-like play essential overlapping roles downstream of disabled-1 in the Reelin pathway. *J Neurosci,* 28, 13551-62.

PAUPERT, J., SOUNNI, N. E. & NOEL, A. 2011. Lymphangiogenesis in post-natal tissue remodeling: Lymphatic endothelial cell connection with its environment. *Mol Aspects Med,* 32, 146-58.

PETROVA, T. V., KARPANEN, T., NORRMEN, C., MELLOR, R., TAMAKOSHI, T., FINEGOLD, D., FERRELL, R., KERJASCHKI, D., MORTIMER, P., YLA-HERTTUALA, S., MIURA, N. & ALITALO, K. 2004. Defective valves and abnormal

mural cell recruitment underlie lymphatic vascular failure in lymphedema distichiasis. *Nat Med,* 10, 974-81.

PETROVA, T. V., MAKINEN, T., MAKELA, T. P., SAARELA, J., VIRTANEN, I., FERRELL, R. E., FINEGOLD, D. N., KERJASCHKI, D., YLA-HERTTUALA, S. & ALITALO, K. 2002. Lymphatic endothelial reprogramming of vascular endothelial cells by the Prox-1 homeobox transcription factor. *EMBO J,* 21, 4593-9.

PFLICKE, H. & SIXT, M. 2009. Preformed portals facilitate dendritic cell entry into afferent lymphatic vessels. *J Exp Med,* 206, 2925-35.

POSCHL, E., SCHLOTZER-SCHREHARDT, U., BRACHVOGEL, B., SAITO, K., NINOMIYA, Y. & MAYER, U. 2004. Collagen IV is essential for basement membrane stability but dispensable for initiation of its assembly during early development. *Development,* 131, 1619-28.

POTULA, H. S., WANG, D., QUYEN, D. V., SINGH, N. K., KUNDUMANI-SRIDHARAN, V., KARPURAPU, M., PARK, E. A., GLASGOW, W. C. & RAO, G. N. 2009. Src-dependent STAT-3-mediated expression of monocyte chemoattractant protein-1 is required for 15(S)-hydroxyeicosatetraenoic acid-induced vascular smooth muscle cell migration. *J Biol Chem,* 284, 31142-55.

PRINCE, R. N., SCHREITER, E. R., ZOU, P., WILEY, H. S., TING, A. Y., LEE, R. T. & LAUFFENBURGER, D. A. 2010. The heparin-binding domain of HB-EGF mediates localization to sites of cell-cell contact and prevents HB-EGF proteolytic release. *J Cell Sci,* 123, 2308-18.

PYTOWSKI, B., GOLDMAN, J., PERSAUD, K., WU, Y., WITTE, L., HICKLIN, D. J., SKOBE, M., BOARDMAN, K. C. & SWARTZ, M. A. 2005. Complete and specific inhibition of adult lymphatic regeneration by a novel VEGFR-3 neutralizing antibody. *J Natl Cancer Inst,* 97, 14-21.

QIU, S., KORWEK, K. M., PRATT-DAVIS, A. R., PETERS, M., BERGMAN, M. Y. & WEEBER, E. J. 2006. Cognitive disruption and altered hippocampus synaptic function in Reelin haploinsufficient mice. *Neurobiol Learn Mem,* 85, 228-42.

QUICK, C. M., NGO, B. L., VENUGOPAL, A. M. & STEWART, R. H. 2009. Lymphatic pump-conduit duality: contraction of postnodal lymphatic vessels inhibits passive flow. *Am J Physiol Heart Circ Physiol,* 296, H662-8.

QUICK, C. M., VENUGOPAL, A. M., GASHEV, A. A., ZAWIEJA, D. C. & STEWART, R. H. 2007. Intrinsic pump-conduit behavior of lymphangions. *Am J Physiol Regul Integr Comp Physiol,* 292, R1510-8.

RAHIER, J. F., DE BEAUCE, S., DUBUQUOY, L., ERDUAL, E., COLOMBEL, J. F., JOURET-MOURIN, A., GEBOES, K. & DESREUMAUX, P. 2011. Increased lymphatic vessel density and lymphangiogenesis in inflammatory bowel disease. *Aliment Pharmacol Ther*.

RANDOLPH, G. J., ANGELI, V. & SWARTZ, M. A. 2005. Dendritic-cell trafficking to lymph nodes through lymphatic vessels. *Nat Rev Immunol,* 5, 617-28.

RAUCH, B. H., WEBER, A., BRAUN, M., ZIMMERMANN, N. & SCHROR, K. 2000. PDGF-induced Akt phosphorylation does not activate NF-kappa B in human vascular smooth muscle cells and fibroblasts. *FEBS Lett,* 481, 3-7.

RICE, D. S. & CURRAN, T. 2001. Role of the reelin signaling pathway in central nervous system development. *Annu Rev Neurosci,* 24, 1005-39.

RINGELMANN, B., RODER, C., HALLMANN, R., MALEY, M., DAVIES, M., GROUNDS, M. & SOROKIN, L. 1999. Expression of laminin alpha1, alpha2, alpha4, and alpha5 chains, fibronectin, and tenascin-C in skeletal muscle of dystrophic 129ReJ dy/dy mice. *Exp Cell Res,* 246, 165-82.

RISEBRO, C. A., SEARLES, R. G., MELVILLE, A. A., EHLER, E., JINA, N., SHAH, S., PALLAS, J., HUBANK, M., DILLARD, M., HARVEY, N. L., SCHWARTZ, R. J., CHIEN, K. R., OLIVER, G. & RILEY, P. R. 2009. Prox1 maintains muscle structure and growth in the developing heart. *Development,* 136, 495-505.

ROCKSON, S. G. 2001. Lymphedema. *Am J Med,* 110, 288-95.

ROSSEL, M., LOULIER, K., FEUILLET, C., ALONSO, S. & CARROLL, P. 2005. Reelin signaling is necessary for a specific step in the migration of hindbrain efferent neurons. *Development,* 132, 1175-85.

RUCKER, H. K., WYNDER, H. J. & THOMAS, W. E. 2000. Cellular mechanisms of CNS pericytes. *Brain Res Bull,* 51, 363-9.

RUHRBERG, C., GERHARDT, H., GOLDING, M., WATSON, R., IOANNIDOU, S., FUJISAWA, H., BETSHOLTZ, C. & SHIMA, D. T. 2002. Spatially restricted patterning cues provided by heparin-binding VEGF-A control blood vessel branching morphogenesis. *Genes Dev,* 16, 2684-98.

RUTKOWSKI, J. M., BOARDMAN, K. C. & SWARTZ, M. A. 2006. Characterization of lymphangiogenesis in a model of adult skin regeneration. *Am J Physiol Heart Circ Physiol,* 291, H1402-10.

SABIN, F. R. 1902. On the Origin of the Lymphatic System from the Veins and the Development of the Lymph Hearts and Thoracic Duct in the Pig. *American Journal of Anatomy,* 1, 23.

SAITO, N., HAMADA, J., FURUKAWA, H., TSUTSUMIDA, A., OYAMA, A., FUNAYAMA, E., SAITO, A., TSUJI, T., TADA, M., MORIUCHI, T. & YAMAMOTO, Y. 2009. Laminin-421 produced by lymphatic endothelial cells induces chemotaxis for human melanoma cells. *Pigment Cell Melanoma Res,* 22, 601-10.

SAMAMA, B. & BOEHM, N. 2005. Reelin immunoreactivity in lymphatics and liver during development and adult life. *Anat Rec A Discov Mol Cell Evol Biol,* 285, 595-9.

SANADA, K., GUPTA, A. & TSAI, L. H. 2004. Disabled-1-regulated adhesion of migrating neurons to radial glial fiber contributes to neuronal positioning during early corticogenesis. *Neuron,* 42, 197-211.

SASAKI, T., FASSLER, R. & HOHENESTER, E. 2004. Laminin: the crux of basement membrane assembly. *J Cell Biol,* 164, 959-63.

SATO, T. N., TOZAWA, Y., DEUTSCH, U., WOLBURG-BUCHHOLZ, K., FUJIWARA, Y., GENDRON-MAGUIRE, M., GRIDLEY, T., WOLBURG, H., RISAU, W. & QIN, Y. 1995. Distinct roles of the receptor tyrosine kinases Tie-1 and Tie-2 in blood vessel formation. *Nature,* 376, 70-4.

SAUNDERS, W. B., BOHNSACK, B. L., FASKE, J. B., ANTHIS, N. J., BAYLESS, K. J., HIRSCHI, K. K. & DAVIS, G. E. 2006. Coregulation of vascular tube stabilization by endothelial cell TIMP-2 and pericyte TIMP-3. *J Cell Biol,* 175, 179-91.

SCALLAN, J. P. & HUXLEY, V. H. 2010. In vivo determination of collecting lymphatic vessel permeability to albumin: a role for lymphatics in exchange. *J Physiol*, 588, 243-54.

SCHENK, S., HINTERMANN, E., BILBAN, M., KOSHIKAWA, N., HOJILLA, C., KHOKHA, R. & QUARANTA, V. 2003. Binding to EGF receptor of a laminin-5 EGF-like fragment liberated during MMP-dependent mammary gland involution. *J Cell Biol,* 161, 197-209.

SCHULTE-MERKER, S., SABINE, A. & PETROVA, T. V. 2011. Lymphatic vascular morphogenesis in development, physiology, and disease. *J Cell Biol,* 193, 607-18.

SELZMAN, C. H., MILLER, S. A., ZIMMERMAN, M. A., GAMBONI-ROBERTSON, F., HARKEN, A. H. & BANERJEE, A. 2002. Monocyte chemotactic protein-1 directly induces human vascular smooth muscle proliferation. *Am J Physiol Heart Circ Physiol,* 283, H1455-61.

SENTURK, A., PFENNIG, S., WEISS, A., BURK, K. & ACKER-PALMER, A. 2011. Ephrin Bs are essential components of the Reelin pathway to regulate neuronal migration. *Nature,* 472, 356-60.

SENZAKI, K., OGAWA, M. & YAGI, T. 1999. Proteins of the CNR family are multiple receptors for Reelin. *Cell,* 99, 635-47.

SHELDON, M., RICE, D. S., D'ARCANGELO, G., YONESHIMA, H., NAKAJIMA, K., MIKOSHIBA, K., HOWELL, B. W., COOPER, J. A., GOLDOWITZ, D. & CURRAN, T. 1997. Scrambler and yotari disrupt the disabled gene and produce a reeler-like phenotype in mice. *Nature,* 389, 730-3.

SHIELDS, J. D., FLEURY, M. E., YONG, C., TOMEI, A. A., RANDOLPH, G. J. & SWARTZ, M. A. 2007. Autologous chemotaxis as a mechanism of tumor cell homing to lymphatics via interstitial flow and autocrine CCR7 signaling. *Cancer Cell,* 11, 526-38.

SKOBE, M. & DETMAR, M. 2000. Structure, function, and molecular control of the skin lymphatic system. *J Investig Dermatol Symp Proc,* 5, 14-9.

SKOBE, M., HAWIGHORST, T., JACKSON, D. G., PREVO, R., JANES, L., VELASCO, P., RICCARDI, L., ALITALO, K., CLAFFEY, K. & DETMAR, M. 2001. Induction of tumor lymphangiogenesis by VEGF-C promotes breast cancer metastasis. *Nat Med,* 7, 192-8.

SRINIVASAN, R. S., DILLARD, M. E., LAGUTIN, O. V., LIN, F. J., TSAI, S., TSAI, M. J., SAMOKHVALOV, I. M. & OLIVER, G. 2007. Lineage tracing demonstrates the venous origin of the mammalian lymphatic vasculature. *Genes Dev,* 21, 2422-32.

SRINIVASAN, R. S., GENG, X., YANG, Y., WANG, Y., MUKATIRA, S., STUDER, M., PORTO, M. P., LAGUTIN, O. & OLIVER, G. 2010. The nuclear hormone receptor Coup-TFII is required for the initiation and early maintenance of Prox1 expression in lymphatic endothelial cells. *Genes Dev,* 24, 696-707.

STENZEL, D., NYE, E., NISANCIOGLU, M., ADAMS, R. H., YAMAGUCHI, Y. & GERHARDT, H. 2009. Peripheral mural cell recruitment requires cell-autonomous heparan sulfate. *Blood,* 114, 915-24.

STRATMAN, A. N., MALOTTE, K. M., MAHAN, R. D., DAVIS, M. J. & DAVIS, G. E. 2009a. Pericyte recruitment during vasculogenic tube assembly stimulates endothelial basement membrane matrix formation. *Blood,* 114, 5091-101.

STRATMAN, A. N., SAUNDERS, W. B., SACHARIDOU, A., KOH, W., FISHER, K. E., ZAWIEJA, D. C., DAVIS, M. J. & DAVIS, G. E. 2009b. Endothelial cell lumen and vascular guidance tunnel formation requires MT1-MMP-dependent proteolysis in 3-dimensional collagen matrices. *Blood,* 114, 237-47.

STRATMAN, A. N., SCHWINDT, A. E., MALOTTE, K. M. & DAVIS, G. E. 2010. Endothelial-derived PDGF-BB and HB-EGF coordinately regulate pericyte recruitment during vasculogenic tube assembly and stabilization. *Blood,* 116, 4720-30.

SURI, C., JONES, P. F., PATAN, S., BARTUNKOVA, S., MAISONPIERRE, P. C., DAVIS, S., SATO, T. N. & YANCOPOULOS, G. D. 1996. Requisite role of angiopoietin-1, a ligand for the TIE2 receptor, during embryonic angiogenesis. *Cell,* 87, 1171-80.

SUZUKI-INOUE, K., FULLER, G. L., GARCIA, A., EBLE, J. A., POHLMANN, S., INOUE, O., GARTNER, T. K., HUGHAN, S. C., PEARCE, A. C., LAING, G. D., THEAKSTON, R. D., SCHWEIGHOFFER, E., ZITZMANN, N., MORITA, T., TYBULEWICZ, V. L., OZAKI, Y. & WATSON, S. P. 2006. A novel Syk-dependent

mechanism of platelet activation by the C-type lectin receptor CLEC-2. *Blood,* 107, 542-9.

SUZUKI-INOUE, K., INOUE, O., DING, G., NISHIMURA, S., HOKAMURA, K., ETO, K., KASHIWAGI, H., TOMIYAMA, Y., YATOMI, Y., UMEMURA, K., SHIN, Y., HIRASHIMA, M. & OZAKI, Y. 2010. Essential in vivo roles of the C-type lectin receptor CLEC-2: embryonic/neonatal lethality of CLEC-2-deficient mice by blood/lymphatic misconnections and impaired thrombus formation of CLEC-2-deficient platelets. *J Biol Chem,* 285, 24494-507.

TAKAMATSU, H., TAKEGAHARA, N., NAKAGAWA, Y., TOMURA, M., TANIGUCHI, M., FRIEDEL, R. H., RAYBURN, H., TESSIER-LAVIGNE, M., YOSHIDA, Y., OKUNO, T., MIZUI, M., KANG, S., NOJIMA, S., TSUJIMURA, T., NAKATSUJI, Y., KATAYAMA, I., TOYOFUKU, T., KIKUTANI, H. & KUMANOGOH, A. 2010. Semaphorins guide the entry of dendritic cells into the lymphatics by activating myosin II. *Nat Immunol,* 11, 594-600.

TAMMELA, T. & ALITALO, K. 2010. Lymphangiogenesis: Molecular mechanisms and future promise. *Cell,* 140, 460-76.

TAMMELA, T., SAARISTO, A., HOLOPAINEN, T., LYYTIKKA, J., KOTRONEN, A., PITKONEN, M., ABO-RAMADAN, U., YLA-HERTTUALA, S., PETROVA, T. V. & ALITALO, K. 2007. Therapeutic differentiation and maturation of lymphatic vessels after lymph node dissection and transplantation. *Nat Med,* 13, 1458-66.

TAMMELA, T., SAARISTO, A., LOHELA, M., MORISADA, T., TORNBERG, J., NORRMEN, C., OIKE, Y., PAJUSOLA, K., THURSTON, G., SUDA, T., YLA-HERTTUALA, S. & ALITALO, K. 2005. Angiopoietin-1 promotes lymphatic sprouting and hyperplasia. *Blood,* 105, 4642-8.

THYBOLL, J., KORTESMAA, J., CAO, R., SOININEN, R., WANG, L., IIVANAINEN, A., SOROKIN, L., RISLING, M., CAO, Y. & TRYGGVASON, K. 2002. Deletion of the laminin alpha4 chain leads to impaired microvessel maturation. *Mol Cell Biol,* 22, 1194-202.

TINNES, S., SCHAFER, M. K., FLUBACHER, A., MUNZNER, G., FROTSCHER, M. & HAAS, C. A. 2011. Epileptiform activity interferes with proteolytic processing of Reelin required for dentate granule cell positioning. *FASEB J,* 25, 1002-13.

TISSIR, F. & GOFFINET, A. M. 2003. Reelin and brain development. *Nat Rev Neurosci,* 4, 496-505.

TOBLER, N. E. & DETMAR, M. 2006. Tumor and lymph node lymphangiogenesis--impact on cancer metastasis. *J Leukoc Biol,* 80, 691-6.

TROMMSDORFF, M., GOTTHARDT, M., HIESBERGER, T., SHELTON, J., STOCKINGER, W., NIMPF, J., HAMMER, R. E., RICHARDSON, J. A. & HERZ, J.

1999. Reeler/Disabled-like disruption of neuronal migration in knockout mice lacking the VLDL receptor and ApoE receptor 2. *Cell,* 97, 689-701.

TVOROGOV, D., ANISIMOV, A., ZHENG, W., LEPPANEN, V. M., TAMMELA, T., LAURINAVICIUS, S., HOLNTHONER, W., HELOTERA, H., HOLOPAINEN, T., JELTSCH, M., KALKKINEN, N., LANKINEN, H., OJALA, P. M. & ALITALO, K. 2010. Effective suppression of vascular network formation by combination of antibodies blocking VEGFR ligand binding and receptor dimerization. *Cancer Cell,* 18, 630-40.

UHRIN, P., ZAUJEC, J., BREUSS, J. M., OLCAYDU, D., CHRENEK, P., STOCKINGER, H., FUERTBAUER, E., MOSER, M., HAIKO, P., FASSLER, R., ALITALO, K., BINDER, B. R. & KERJASCHKI, D. 2010. Novel function for blood platelets and podoplanin in developmental separation of blood and lymphatic circulation. *Blood,* 115, 3997-4005.

UTSUNOMIYA-TATE, N., KUBO, K., TATE, S., KAINOSHO, M., KATAYAMA, E., NAKAJIMA, K. & MIKOSHIBA, K. 2000. Reelin molecules assemble together to form a large protein complex, which is inhibited by the function-blocking CR-50 antibody. *Proc Natl Acad Sci U S A,* 97, 9729-34.

VAINIONPAA, N., BUTZOW, R., HUKKANEN, M., JACKSON, D. G., PIHLAJANIEMI, T., SAKAI, L. Y. & VIRTANEN, I. 2007. Basement membrane protein distribution in LYVE-1-immunoreactive lymphatic vessels of normal tissues and ovarian carcinomas. *Cell Tissue Res,* 328, 317-28.

VAN AGTMAEL, T., BAILEY, M. A., SCHLOTZER-SCHREHARDT, U., CRAIGIE, E., JACKSON, I. J., BROWNSTEIN, D. G., MEGSON, I. L. & MULLINS, J. J. 2010. Col4a1 mutation in mice causes defects in vascular function and low blood pressure associated with reduced red blood cell volume. *Hum Mol Genet,* 19, 1119-28.

VAN HELDEN, D. F. 1993. Pacemaker potentials in lymphatic smooth muscle of the guinea-pig mesentery. *J Physiol,* 471, 465-79.

VEIKKOLA, T., LOHELA, M., IKENBERG, K., MAKINEN, T., KORFF, T., SAARISTO, A., PETROVA, T., JELTSCH, M., AUGUSTIN, H. G. & ALITALO, K. 2003. Intrinsic versus microenvironmental regulation of lymphatic endothelial cell phenotype and function. *FASEB J,* 17, 2006-13.

VENTRUTI, A., KAZDOBA, T. M., NIU, S. & D'ARCANGELO, G. 2011. Reelin deficiency causes specific defects in the molecular composition of the synapses in the adult brain. *Neuroscience*.

VON DER WEID, P. Y. & ZAWIEJA, D. C. 2004. Lymphatic smooth muscle: the motor unit of lymph drainage. *Int J Biochem Cell Biol,* 36, 1147-53.

VON TELL, D., ARMULIK, A. & BETSHOLTZ, C. 2006. Pericytes and vascular stability. *Exp Cell Res,* 312, 623-9.

WANG, Y., NAKAYAMA, M., PITULESCU, M. E., SCHMIDT, T. S., BOCHENEK, M. L., SAKAKIBARA, A., ADAMS, S., DAVY, A., DEUTSCH, U., LUTHI, U., BARBERIS, A., BENJAMIN, L. E., MAKINEN, T., NOBES, C. D. & ADAMS, R. H. 2010. Ephrin-B2 controls VEGF-induced angiogenesis and lymphangiogenesis. *Nature,* 465, 483-6.

WANG, Y. & OLIVER, G. 2010. Current views on the function of the lymphatic vasculature in health and disease. *Genes Dev,* 24, 2115-26.

WARE, M. L., FOX, J. W., GONZALEZ, J. L., DAVIS, N. M., LAMBERT DE ROUVROIT, C., RUSSO, C. J., CHUA, S. C., JR., GOFFINET, A. M. & WALSH, C. A. 1997. Aberrant splicing of a mouse disabled homolog, mdab1, in the scrambler mouse. *Neuron,* 19, 239-49.

WEEBER, E. J., BEFFERT, U., JONES, C., CHRISTIAN, J. M., FORSTER, E., SWEATT, J. D. & HERZ, J. 2002. Reelin and ApoE receptors cooperate to enhance hippocampal synaptic plasticity and learning. *J Biol Chem,* 277, 39944-52.

WIGLE, J. T. & OLIVER, G. 1999. Prox1 function is required for the development of the murine lymphatic system. *Cell,* 98, 769-78.

WIIG, H., KESKIN, D. & KALLURI, R. 2010. Interaction between the extracellular matrix and lymphatics: consequences for lymphangiogenesis and lymphatic function. *Matrix Biol,* 29, 645-56.

WIJELATH, E. S., RAHMAN, S., NAMEKATA, M., MURRAY, J., NISHIMURA, T., MOSTAFAVI-POUR, Z., PATEL, Y., SUDA, Y., HUMPHRIES, M. J. & SOBEL, M. 2006. Heparin-II domain of fibronectin is a vascular endothelial growth factor-binding domain: enhancement of VEGF biological activity by a singular growth factor/matrix protein synergism. *Circ Res,* 99, 853-60.

WILTING, J., PAPOUTSI, M., SCHNEIDER, M. & CHRIST, B. 2000. The lymphatic endothelium of the avian wing is of somitic origin. *Dev Dyn,* 217, 271-8.

WITTE, M. H., WAY, D. L., WITTE, C. L. & BERNAS, M. 1997. Lymphangiogenesis: mechanisms, significance and clinical implications. *EXS,* 79, 65-112.

XU, Y., YUAN, L., MAK, J., PARDANAUD, L., CAUNT, M., KASMAN, I., LARRIVEE, B., DEL TORO, R., SUCHTING, S., MEDVINSKY, A., SILVA, J., YANG, J., THOMAS, J. L., KOCH, A. W., ALITALO, K., EICHMANN, A. & BAGRI, A. 2010. Neuropilin-2 mediates VEGF-C-induced lymphatic sprouting together with VEGFR3. *J Cell Biol,* 188, 115-30.

YANG, H., KIM, C., KIM, M. J., SCHWENDENER, R. A., ALITALO, K., HESTON, W., KIM, I., KIM, W. J. & KOH, G. Y. 2011. Soluble vascular endothelial growth factor receptor-3 suppresses lymphangiogenesis and lymphatic metastasis in bladder cancer. *Mol Cancer,* 10, 36.

YUAN, L., MOYON, D., PARDANAUD, L., BREANT, C., KARKKAINEN, M. J., ALITALO, K. & EICHMANN, A. 2002. Abnormal lymphatic vessel development in neuropilin 2 mutant mice. *Development,* 129, 4797-806.

ZAWIEJA, D. C. 2009. Contractile physiology of lymphatics. *Lymphat Res Biol,* 7, 87-96.

ZHANG, D., LI, B., SHI, J., ZHAO, L., ZHANG, X., WANG, C., HOU, S., QIAN, W., KOU, G., WANG, H. & GUO, Y. 2010a. Suppression of tumor growth and metastasis by simultaneously blocking vascular endothelial growth factor (VEGF)-A and VEGF-C with a receptor-immunoglobulin fusion protein. *Cancer Res,* 70, 2495-503.

ZHANG, L., ZHOU, F., HAN, W., SHEN, B., LUO, J., SHIBUYA, M. & HE, Y. 2010b. VEGFR-3 ligand-binding and kinase activity are required for lymphangiogenesis but not for angiogenesis. *Cell Res,* 20, 1319-31.

ZHAO, S., CHAI, X., FORSTER, E. & FROTSCHER, M. 2004. Reelin is a positional signal for the lamination of dentate granule cells. *Development,* 131, 5117-25.

ZHAO, S. & FROTSCHER, M. 2010. Go or stop? Divergent roles of Reelin in radial neuronal migration. *Neuroscientist,* 16, 421-34.

ZHOU, Z., APTE, S. S., SOININEN, R., CAO, R., BAAKLINI, G. Y., RAUSER, R. W., WANG, J., CAO, Y. & TRYGGVASON, K. 2000. Impaired endochondral ossification and angiogenesis in mice deficient in membrane-type matrix metalloproteinase I. *Proc Natl Acad Sci U S A,* 97, 4052-7.